

**MODIFICATION, CHARACTERISATION AND APPLICATION OF
COCONUT WASTES AS FILLERS IN RUBBER COMPOUNDING**

BY

FRIDAY PATRICK MOMOH

**HND Polymer Technology (Auchi Polytechnic, Auchi), 1996; PGD Industrial
Chemistry (FUTA), 2006; M.TECH Industrial Chemistry (FUTA), 2011**

P14SCCH 9020

A Thesis Submitted to the School of Postgraduate Studies,
Ahmadu Bello University, Zaria In Partial Fulfillment of the Requirements for the
Award of the Degree of Doctor of Philosophy (Ph.D) in Polymer Science and
Technology

Department of Chemistry,
Faculty of Physical Sciences,
Ahmadu Bello University,
Zaria, Nigeria

October, 2017

DECLARATION

I hereby declare that this thesis titled “Modification, Characterisation and Application of Coconut Wastes as Fillers in Rubber Compounding” has been written by me, and it is a record of my own research work.

As far as I know, no part of this thesis has been presented in any previous application for a higher degree at this or any other University. The information derived from the literature has been duly acknowledged in the text and a list of references provided.

Name of Student

Signature

Date

CERTIFICATION

This thesis entitled “Modification, Characterisation and Application of Coconut Wastes as Fillers in Rubber Compounding” by Friday Patrick Momoh meets the regulations governing the award of the degree of Doctor of Philosophy (Ph.D) of Ahmadu Bello University, Zaria, Nigeria, and is approved for its contribution to knowledge and literary presentation.

Prof. P.A.P. Mamza
Chairman, Supervisory Committee

Date

Prof. C.E. Gimba
Member, Supervisory Committee

Date

Prof. P. Nkeonye
Member, Supervisory Committee

Date

Prof. A.O. Oyewale
Head of Department

Date

Prof. A.Z. Abubakar
Dean, School of Postgraduate Studies

Date

DEDICATION

This piece is dedicated to all my teachers right from my foundational training to the accomplishment of this task. They helped to ignite and fan the embers of continuous and persistent academic pursuit in my life.

ACKNOWLEDGEMENTS

Completing this thesis has been thoroughly fascinating, at times tasking. I could not have executed a thorough research work without key persons who have played crucial and primary parts in my studies. Therefore, I would humbly like to acknowledge those personalities who contributed to the success documented here.

Firstly, I would like to thank the Chairman of Committee, my most esteemed Major Supervisor, Prof. Paul Andrew Mamza for his thoroughness, doggedness, guidance, reassurance, immense support and untiring commitments despite his schedules as the President, Polymer Institute of Nigeria. I fully appreciate my other Supervisors; Prof. Casimir Emmanuel Gimba and Prof. Peter Nkeonye for their invaluable and immeasurable supports, and for giving me the opportunity to begin and conclude my research.

I specially thank the staff of the Department of Chemistry, Ahmadu Bello University, Zaria for providing academic and research friendly environment to ease my research findings. I wish to express my heartfelt gratitude to the following persons and agencies: The Head of Department of Chemistry, Ahmadu Bello University, Zaria, Prof. A.O. Oyewale, the Departmental Postgraduate Coordinator, who coincidentally is my Major and erudite Supervisor, Prof. P.A.P. Mamza and the Departmental Seminar Coordinator, the ever meticulous Dr. I. Abdulkadir. My appreciation equally go to the Laboratory technical staff of Chemistry and Chemical Engineering Departments at Ahmadu Bello University, Zaria, Nigeria; Polymer Technology Department, Auchi Polytechnic, Auchi, Nigeria; Nigerian Institute of Leather Science and Technology (NILEST), Zaria, Nigeria; Chemical Sciences Department, Obafemi Awolowo University, Ife, Nigeria; Polymer Testing Department, Rubber Research Institute of Nigeria, Iyanomo (RRIN), Benin City, Nigeria; Chemistry Department, Federal University of Technology, Minna, Nigeria; Chemical Sciences Department, Redeemer's University, Ede, Nigeria; Steel Raw Materials Exploration Agency (National Steel Council) Malali, Kaduna, Nigeria; Polymer and Materials Testing Laboratory, Federal Institute of Industrial Research, Oshodi (FIIRO), Lagos, Nigeria; Smiles Consult Statistical Data Analyst, Auchi, Nigeria; my research friend (Ajekwene Kingsley Kema) at Cochin University of Science and Technology, India, for knowledge exchange and interactions; and my dear

friend, Abdul-Wahab Okele for his accommodative nature throughout my stay at Ahmadu Bello University, Zaria.

My special thanks go to the management team of Auchi Polytechnic, Auchi, for its approval of my study and for official permission towards the incessant field trips, analyses tour, and job security while the training/research lasted.

My colleagues and inner circle of friends at the Department of Polymer Technology, Auchi Polytechnic, Auchi, are highly appreciated for exchange of professional ideas and advice. Thank you all for your motivational talks and encouragement to finish in record time.

Special thanks to my family for their foundational supports in my previous trainings and undertakings. I really appreciate all your sacrifices, as words could not describe the love and dedication you have shown throughout my life.

I sincerely thank all my Spiritual Fathers, Colleagues and Subordinates in the Vineyard of God (The Redeemed Christian Church of God) for their prayers and moral supports. They kept urging me until this victory became a reality.

I owe my deepest gratitude to my dear wife, *Kehinde Joy Momoh*, for her love, prayers, care and encouragement. She is the most wonderful woman I have ever met in my life. She is the one to receive credit for each and every single achievement I have made since the union of hearts. I also thank the wonderful seeds of the union: *Eveshosename, Eveshoyan and Eveshoyaname* for their sacrifices, good wishes and being there to bear the brunt of my frequent absence from the family.

Finally, I most heartedly owe it all to the Almighty God who kept me in all my journeys and ensured that I found favour for accomplishment in all I committed to His trust. All glory belongs to Him the highest God forever.

ABSTRACT

In this study, coconut palm wastes were obtained, washed to remove sands and debris and then dried at 95°C for 1 hr to remove surface moisture. Filler modifications through carbonisation were done at varying temperatures of 300°C, 400°C, 500°C, 600°C and 700°C. Both raw fillers and carbonised fillers were ground to achieve 100 µm particle sizes, after which they were characterised. Formulations were appropriately drawn for the mixing and compounding process. Rheological determination and flow properties were evaluated. Physico-mechanical measurement of hardness, abrasion resistance index, compressive strength, tensile strength, flexural strength, modulus and elongation at break to ascertain composites reinforcement levels were also carried out. All measurements were according to American Society for Testing and Materials (ASTM) standards. Furthermore, qualitative assessments of modification levels were estimated using Fourier infrared spectroscopic studies (FTIR), X-ray diffraction analysis (XRD), X-ray fluorescence (XRF) of elemental oxides presence, scanning electron microscopic analysis (SEM), thermal gravimetric analysis (TGA) and chemical resistance measurements through sorption inference and analysis. Carbonisation strengthened the polymer-carbon bond and therefore increased reinforcements of the composite matrix effectively at 500°C for the coconut shell and 600°C for the coconut fibre. Optimum formulations of 500°C for the shell and 600°C for the fibre were technically utilised in the engineering design and manufacture of vibration dampeners for motor cycle hub and industrial oil seals for bambury mixers employed in the mixing and mastication of rubbers. Qualitative comparisons in properties such as resilience/rebound study, hysteresis, dynamic flex cracking, flex fatigue, weathering/ozone resistance and chemical resistance showed a comparatively good products when functionally and aesthetically compared to available commercial grades. The formulated products were

of high performance quality. Modification through carbonisation therefore created a positive effect and improvements on the morphology, degree of crystallisation/crystallite formations, physico-mechanical properties, chemical resistance, weathering/ozone resistance, and development in resilience/rebound properties, thermal gravimetric degradation/stability, and improvement in active elemental oxides and depletion of lignocelluloses of the coconut shell and fibre through infrared spectroscopic study. The results of mechanical and chemical sorption properties that gave the optimised formulation for the fibre and shell composites used in the modeled products were further theoretically evaluated through predictive and statistical analysis of variance (ANOVA). The new Duncan's multiple range test (DMRT) was used to verify the significance differences between subject factors of mechanical properties and samples (modification temperatures) at 95% probability and deterministic levels. A great proportion of the properties and samples satisfied the significant measurement levels and therefore positive agreements between theoretical and experimental results were established as a contribution to reinforcements. All these noticed improvements resulted in better filler-rubber adhesion and interactions and specifically leading to the reinforcement of the resulting composites and therefore present the composites as useful materials for predictive product development in engineering designs and applications.

TABLE OF CONTENTS

	Page
Title - - - - -	i
Declaration - - - - -	ii
Certification - - - - -	iii
Dedication - - - - -	iv
Acknowledgments - - - - -	v
Abstract - - - - -	vii
Table of Contents - - - - -	ix
List of Tables - - - - -	xxiii
List of Figures - - - - -	xxv
List of Plates - - - - -	xxix
List of Appendices - - - - -	xxxii
List of Symbols and Abbreviations - - - - -	xxxiii
CHAPTER ONE: INTRODUCTION	
1.1 Preamble - - - - -	1
1.2 Polymer Modification - - - - -	2
1.2.1 Fillers - - - - -	4
1.2.2 Application of Fillers - - - - -	5

1.3 Agricultural By-Products	-	-	-	-	-	-	-	8
1.4 Natural Fibres in Composites	-	-	-	-	-	-	-	8
1.5 Coconut Powder as Fillers in Composites	-	-	-	-	-	-	-	11
1.6 Natural Rubber	-	-	-	-	-	-	-	12
1.7 Chemistry and Development of Natural Rubber	-	-	-	-	-	-	-	13
1.8 Processing Techniques of Natural Rubber Latex	-	-	-	-	-	-	-	22
1.8.1 Preserved Field Latex	-	-	-	-	-	-	-	23
1.8.2 Ribbed Smoked Sheet (RSS)	-	-	-	-	-	-	-	23
1.8.3 Coagulation	-	-	-	-	-	-	-	24
1.9 Types of Natural Rubber	-	-	-	-	-	-	-	25
1.9.1 White and Pale Crepe	-	-	-	-	-	-	-	25
1.9.2 Crepe Rubber	-	-	-	-	-	-	-	26
1.9.3 Thin Brown Rubber	-	-	-	-	-	-	-	26
1.9.4 Technically Specified Rubber (TSR)	-	-	-	-	-	-	-	26
1.9.5 Superior Processing Rubber	-	-	-	-	-	-	-	27
1.9.6 Hevea Crumb Rubber	-	-	-	-	-	-	-	27
1.10 Modifications of Natural Rubber	-	-	-	-	-	-	-	27
1.10.1 Filler Incorporation	-	-	-	-	-	-	-	27

1.10.2 Halogenation	-	-	-	-	-	-	-	28
1.10.3 Cyclisation	-	-	-	-	-	-	-	28
1.10.4 Resinous Addition	-	-	-	-	-	-	-	28
1.10.5 Epoxidisation	-	-	-	-	-	-	-	29
1.10.6 Grafting Process		-	-	-	-	-	-	29
1.10.7 Degraded Inclusion	-	-	-	-	-	-	-	29
1.10.8 Blending	-	-	-	-	-	-	-	29
1.11 Basic Properties of Natural Rubber	-	-	-	-	-	-	-	29
1.11.1 Comparison between Raw Natural Rubber and Vulcanised Natural Rubber								30
1.11.2 Hardening of Natural Rubber	-	-	-	-	-	-	-	31
1.12 Application of Natural Rubber	-	-	-	-	-	-	-	32
1.13 Statement of Research Problem	-	-	-	-	-	-	-	32
1.14 Aims of the Research	-	-	-	-	-	-	-	33
1.15 Research Objectives of the Study	-	-	-	-	-	-	-	34
1.16 Scope/Limitations of the Study	-	-	-	-	-	-	-	34
1.17 Justification/Significance of the Study	-	-	-	-	-	-	-	36
1.18 Potential Contributions to Knowledge	-	-	-	-	-	-	-	37
CHAPTER TWO: LITERATURE REVIEW								
2.1 Previous Works	-	-	-	-	-	-	-	40

2.2 Classification of Fillers	-	-	-	-	-	-	-	44
2.2.1 Black Fillers and Classification by Manufacturing Process	-	-						45
2.2.1 (a) Furnace Black Process	-	-	-	-	-	-	-	45
2.2.1 (b) Channel Process	-	-	-	-	-	-	-	45
2.2.1 (c) Acetylene Black Process	-	-	-	-	-	-	-	46
2.2.1 (d) Lamp Black Process	-	-	-	-	-	-	-	46
2.2.2 Non-Black Fillers for Rubber	-	-	-	-	-	-	-	46
2.2.3 Principal Characteristics of Rubber Filler					-	-	-	47
2.2.4 Stretch Resistance Characteristics	-	-	-	-	-	-	-	48
2.2.5 Resilience and Hysteresis Characteristics			-	-	-	-	-	50
2.2.6 Abrasion Resistance Characteristics	-	-	-	-	-	-	-	50
2.2.7 Tear Resistance Characteristics	-	-	-	-	-	-	-	51
2.3 Lignocellulose Biomass Nature of Coconut Shell and Fibre	-	-						51
2.4 Filler-Polymer Interaction-	-	-	-	-	-	-	-	53
2.5 Filler Carbonisation	-	-	-	-	-	-	-	54
2.6 Compounding and Mixing Process	-	-	-	-	-	-	-	55
2.6.1 Compound Design	-	-	-	-	-	-	-	57
2.6.2 Composites Formations Using Fibres, Fillers and Selective Additives	-							57
2.6.3 Additives in Compounding	-	-	-	-	-	-	-	58

2.6.3 (a) Fillers	-	-	-	-	-	-	-	-	58
2.6.3 (b) Plasticisers	-	-	-	-	-	-	-	-	59
2.6.3 (c) Vulcanisation Chemicals	-	-	-	-	-	-	-	-	60
2.6.3 (d) Acceleration Agents	-	-	-	-	-	-	-	-	62
2.6.3 (e) Activators	-	-	-	-	-	-	-	-	62
2.6.3 (f) Anti-Degrading Agents	-	-	-	-	-	-	-	-	63
2.6.3 (g) Processing Aids	-	-	-	-	-	-	-	-	64
2.6.3 (h) Pigments	-	-	-	-	-	-	-	-	64
2.6.4 Mechanism of Mixing	-	-	-	-	-	-	-	-	64
2.6.5 Mastication Process of Rubber	-	-	-	-	-	-	-	-	66
2.6.6 Principle of Compounding	-	-	-	-	-	-	-	-	67
2.6.7 Rheological Determination	-	-	-	-	-	-	-	-	68
2.6.8 Rubber Degradation Processes	-	-	-	-	-	-	-	-	70
2.6.8 (a) Non-Chain-Scission Reactions	-	-	-	-	-	-	-	-	70
2.6.8 (b) Chain-Scission Reactions	-	-	-	-	-	-	-	-	71
2.6.8 (c) Oxidative Degradation	-	-	-	-	-	-	-	-	72
2.6.8 (d) Ozone Cracking	-	-	-	-	-	-	-	-	73
2.6.8 (e) Stages of Ozone Cracking	-	-	-	-	-	-	-	-	74
2.7 Physico-Mechanical Properties of Rubber	-	-	-	-	-	-	-	-	74

2.7.1 Hardness	-	-	-	-	-	-	-	-	74
2.7.2 Abrasion Resistance Index	-	-	-	-	-	-	-	-	75
2.7.3 Compression Set, Strength and Deflection	-	-	-	-	-	-	-	-	76
2.7.3 (a) Measuring Compression Set	-	-	-	-	-	-	-	-	76
2.7.3 (b) Compression-Deflection	-	-	-	-	-	-	-	-	77
2.7.3 (c) Measuring Compression-Deflection	-	-	-	-	-	-	-	-	77
2.7.4 Tensile Strength and Tensile Set	-	-	-	-	-	-	-	-	78
2.7.4 (a) Measuring Tensile Strength	-	-	-	-	-	-	-	-	78
2.7.4 (b) Tensile Set	-	-	-	-	-	-	-	-	78
2.7.4 (c) Measuring Tensile Set	-	-	-	-	-	-	-	-	79
2.7.5 Elongation at Break	-	-	-	-	-	-	-	-	79
2.7.5 (a) Measuring Elongation	-	-	-	-	-	-	-	-	79
2.7.6 Young's Modulus	-	-	-	-	-	-	-	-	79
2.7.6 (a) Measuring Young's Modulus	-	-	-	-	-	-	-	-	80
2.7.6 (b) Yield Point	-	-	-	-	-	-	-	-	80
2.7.7 Tear Strength/Resistance	-	-	-	-	-	-	-	-	81
2.7.7 (a) Measuring Tear Resistance	-	-	-	-	-	-	-	-	81
2.7.8 Weathering/Ozone Resistance	-	-	-	-	-	-	-	-	82
2.7.8 (a) Measuring Weathering/Ozone Resistance	-	-	-	-	-	-	-	-	82

2.7.9 Flexural Testing -	-	-	-	-	-	-	-	-	82
2.8 Qualitative Parameters Study	-	-	-	-	-	-	-	-	83
2.8.1 Fourier Transforms Infrared Spectroscopy (FTIR)	-	-	-	-	-	-	-	-	83
2.8.2 Scanning Electron Microscopy (SEM)	-	-	-	-	-	-	-	-	85
2.8.2 (a) Application	-	-	-	-	-	-	-	-	86
2.8.2 (b) Sample Preparation	-	-	-	-	-	-	-	-	87
2.8.3 X-ray Diffraction Study (XRD)-	-	-	-	-	-	-	-	-	88
2.8.3 (a) X-ray Powder Diffraction	-	-	-	-	-	-	-	-	88
2.8.4 Thermal Gravimetric Analysis (TGA)	-	-	-	-	-	-	-	-	90
2.8.4 (a) Mechanism of Weight Change in TGA	-	-	-	-	-	-	-	-	90
2.8.4 (b) Resolution Enhancement in TGA	-	-	-	-	-	-	-	-	91
2.8.5 X-ray Fluorescence Analysis (XRF)	-	-	-	-	-	-	-	-	92
2.8.5 (a) Underlying Physics	-	-	-	-	-	-	-	-	92
2.8.5 (b) Characteristics Radiation	-	-	-	-	-	-	-	-	93
2.8.5 (c) Crystals	-	-	-	-	-	-	-	-	93
2.8.5 (d) Applications	-	-	-	-	-	-	-	-	94
2.9 Predicting the Performance of Products/Processes Using Mathematical Models	-	-	-	-	-	-	-	-	95
2.9.1 Analysis of Variance (ANOVA)	-	-	-	-	-	-	-	-	97
2.9.2 T-Test	-	-	-	-	-	-	-	-	98

CHAPTER THREE: MATERIALS AND METHODS

3.1 Collection, Treatment of Materials and Reagents-	-	-	-	100
3.2 Characterisation of the Raw and Carbonised Fillers	-	-	-	101
3.2.1 Determination of Loss on Ignition	-	-	-	101
3.2.2 Measurement of pH	-	-	-	102
3.2.3 Determination of Bulk Density	-	-	-	102
3.2.4 Determination of Iodine Adsorption Number	-	-	-	102
3.2.5 Determination of Moisture Content	-	-	-	103
3.2.6 Determination of Oil Absorption	-	-	-	103
3.2.7 Determination of Ash Content	-	-	-	103
3.2.8 Determination of Particle Dimensions and Lumen	-	-	-	104
3.3 Formulation Design, Mastication and Mixing	-	-	-	104
3.4 Determination of Cure Characteristics	-	-	-	105
3.5 Physico-Mechanical Testing/Measurements	-	-	-	106
3.5.1 Hardness Test	-	-	-	106
3.5.2 Abrasion Resistance Index Test	-	-	-	106
3.5.2 (a) Calculation of Abrasion Resistance Index (ARI_A)	-	-	-	107
3.5.3 Compressive Strength Measurements	-	-	-	107
3.5.4 Tensile Strength/Modulus/Elongation at Break Measurements	-	-	-	108

3.5.5 Flexural Strength/Modulus Measurements	-	-	-	-	-	108
3.5.5 (a) Test Sample	-	-	-	-	-	109
3.6 Qualitative/Quantitative Analysis	-	-	-	-	-	109
3.6.1 Fourier Transforms Infra-red Spectroscopy (FTIR)	-	-	-	-	-	109
3.6.2 Scanning Electron Microscopy (SEM)	-	-	-	-	-	110
3.6.3 X-ray Diffraction Analysis (XRD)	-	-	-	-	-	110
3.6.3 (a) Setting of the XRD Equipment	-	-	-	-	-	111
3.6.3 (b) Bulk Analysis	-	-	-	-	-	112
3.6.3 (c) Generation of Raw Data	-	-	-	-	-	111
3.6.4 X-ray Fluorescence Analysis (XRF)	-	-	-	-	-	112
3.6.4 (a) Pelletisation of Samples	-	-	-	-	-	112
3.6.4 (b) Setting of the XRF Equipment	-	-	-	-	-	113
3.6.4 (c) Loading and Running of Sample	-	-	-	-	-	113
3.6.4 (d) Generation of Raw Data	-	-	-	-	-	113
3.6.5 Thermal Gravimetric Analysis (TGA)	-	-	-	-	-	113
3.6.6 Sorption Measurements	-	-	-	-	-	113
3.7 Production of Vibration Dampener for Motor Cycle Hub and Industrial Oil Seal for Bambury Mixer	-	-	-	-	-	114
3.7.1 Mould Design for the Vibration Dampener	-	-	-	-	-	114
3.7.2 Compound Mixing Process for the Vibration Dampener	-	-	-	-	-	115

3.7.3 Moulding Process for the Vibration Dampener	-	-	-	-	-	-	115
3.7.4 Product Evaluative Measurement (Vibration Dampener)	-	-	-	-	-	-	116
3.8 Production Process Condition for the Oil Seal	-	-	-	-	-	-	116
3.8.1 Mould Design for the Oil Seal	-	-	-	-	-	-	116
3.8.2 Formulation Design for the Oil Seal	-	-	-	-	-	-	117
3.8.3 Compounding for the Oil Seal	-	-	-	-	-	-	117
3.8.4 Evaluative Measurement for the Oil Seal	-	-	-	-	-	-	117
3.8.5 Chemical Resistance Evaluation for the Oil Seal	-	-	-	-	-	-	118
3.8.6 Weathering/Ozone Resistance Measurement of the Oil Seal	-	-	-	-	-	-	118
3.9 Predicting the Performance of the Optimised Coconut Fibre and Shell Filled Composites	-	-	-	-	-	-	118

CHAPTER FOUR: RESULTS

4.1 Characterisation	-	-	-	-	-	-	120
4.2 Hardness Properties	-	-	-	-	-	-	120
4.3 Abrasion Resistance Index	-	-	-	-	-	-	121
4.4 Compression Set Results	-	-	-	-	-	-	121
4.5 Compressive Stress-Strain Relationship	-	-	-	-	-	-	122
4.6 Results of Tensile Strength/Modulus/EAB	-	-	-	-	-	-	123

4.7 Tensile Stress-Strain Relationship	-	-	-	-	-	124
4.8 Results of Flexural Strength	-	-	-	-	-	125
4.9 Flexure Stress-Strain Relationship	-	-	-	-	-	125
4.10 3-D Plots Presentation of Mechanical Analysis	-	-	-	-	-	126
4.11 Sorption Tests Results and Plots-	-	-	-	-	-	129
4.12 Infrared Spectroscopic Analysis	-	-	-	-	-	130
4.13 Scanning Electron Microscopy Results and Plates	-	-	-	-	-	136
4.14 X-Ray Diffractograms Results and Evaluation of the Degree of Crystallisation	-	-	-	-	-	143
4.15 X-Ray Fluorescence Analysis of Elemental Oxides	-	-	-	-	-	150
4.16 Thermal Gravimetric Results and Evaluation	-	-	-	-	-	151
4.17 Motor Cycle Vibration Dampener Evaluation Study	-	-	-	-	-	153
4.17.1 Dynamic Fatigue Evaluation Test for the Vibration Dampener	-	-	-	-	-	153
4.17.2 Resilience Evaluation by Vertical Rebound of the Vibration Dampener	-	-	-	-	-	153
4.17.3 Comparative Evaluation of the Produced Vibration Dampener with Commercial Type	-	-	-	-	-	154
4.18.1 Chemical Evaluative Measurement for the Oil Seal	-	-	-	-	-	154
4.18.2 Flex Fatigue Evaluation for the Oil Seal	-	-	-	-	-	154
4.19 Statistical Modelling on Performance Prediction	-	-	-	-	-	155
4.20 Pictorial Presentation Stages of Experimental Sampling	-	-	-	-	-	155

CHAPTER FIVE: DISCUSSION

5.1 Characterisation	-	-	-	-	-	-	-	-	162
5.2 Hardness Properties	-	-	-	-	-	-	-	-	163
5.3 Abrasion Resistance	-	-	-	-	-	-	-	-	164
5.4 Compressive Strength	-	-	-	-	-	-	-	-	164
5.5 Compressive Stress-Strain Relationship	-	-	-	-	-	-	-	-	164
5.6 Tensile Strength/Modulus/EAB	-	-	-	-	-	-	-	-	165
5.7 Tensile Stress-Strain Relationship	-	-	-	-	-	-	-	-	167
5.8 Flexure Strength	-	-	-	-	-	-	-	-	167
5.9 Flexure Stress-Strain Relationship	-	-	-	-	-	-	-	-	168
5.10 Mechanical Analysis Using 3-D Plots	-	-	-	-	-	-	-	-	168
5.11 Sorption Evaluation	-	-	-	-	-	-	-	-	169
5.12 Infrared Spectroscopic Evaluation	-	-	-	-	-	-	-	-	169
5.13 Scanning Electron Microscope	-	-	-	-	-	-	-	-	170
5.14 X-Ray Diffractograms Evaluation	-	-	-	-	-	-	-	-	171
5.15 Elemental Oxides Evaluation	-	-	-	-	-	-	-	-	173
5.16 Thermal Gravimetric Evaluation	-	-	-	-	-	-	-	-	174
5.17 Dynamic Fatigue of Vibration Dampener	-	-	-	-	-	-	-	-	175
5.18 Resilience by Vertical Rebound Evaluation for Vibration Dampener	-	-	-	-	-	-	-	-	175

5.19 Comparative Evaluation Study of Vibration Dampener	-	-	-	-	-	-	-	-	176
5.20 Chemical Evaluation of Oil Seal	-	-	-	-	-	-	-	-	177
5.21 Flex Fatigue Evaluation of Oil Seal	-	-	-	-	-	-	-	-	177
5.22 Performance Prediction Using Modelling via ANOVA	-	-	-	-	-	-	-	-	178

CHAPTER SIX: SUMMARY, CONCLUSION AND RECOMMENDATIONS

6.1 Summary	-	-	-	-	-	-	-	-	-	184
6.2 Conclusion	-	-	-	-	-	-	-	-	-	186
6.3 Recommendations for Further Studies	-	-	-	-	-	-	-	-	-	189
References	-	-	-	-	-	-	-	-	-	190
Appendices	-	-	-	-	-	-	-	-	-	217
Publications	-	-	-	-	-	-	-	-	-	279

LIST OF TABLES

Table	Title	Page
1.1	Basic Characteristics of Natural Rubber - - - -	13
1.2	Percentage Composition of Natural Rubber Latex - - -	23
1.3	Comparison of Raw Natural Rubber (NR) with Vulcanised Natural Rubber (VNR) - - - - - - - - - -	31
3.1	Properties of Standard African Rubber (SAR) - - -	100
3.2	Compound Design/Formulation Table - - - -	105
3.3	Formulation for the Oil Seal Production - - - -	117
4.1	Characterisation of Raw Coconut Shell and Fibre, Carbonised Coconut Shell and Fibre - - - - - - - - - -	120
4.2	Results of Hardness Test (\AA) - - - - - - - - - -	120
4.3	Results of Abrasion Resistance Indices (ARI_A) - - - - -	121
4.4	Results of Compression Set - - - - - - - - - -	121
4.5	Results of Tensile, Modulus and Elongation at Break - - -	123
4.6	Results of Flexural Strength - - - - - - - - - -	125
4.7	Sorption Test Results - - - - - - - - - -	129
4.8	Particle Properties of SEM Weighted by Volume - - - -	142
4.9	Particle Properties of SEM Weighted by Count - - - -	142
4.10	Crystalline Parameters for Coconut Shell - - - - -	143

4.11	Crystalline Parameters for Coconut Fibre	-	-	-	-	143
4.12	Crack Initiation Time and Revolution of the Motor Cycle Dampener	-				153
4.13	Resilience/Rebound Percentage Evaluation of the Motor Cycle Dampener	-	-	-	-	153
4.14	Comparative Study of the Produced Vibration Dampener and “Dampener A” (Commercial Type)	-	-	-	-	154
4.15	Chemical Evaluative Measurement Results for the Oil Seal	-				154
4.16	Crack Initiation Time after Weathering/Ozone Exposure of the Oil Seal					154

LIST OF FIGURES

Figure	Title	Page
1.1	Poly-Cis-1, 4-Isoprene - - - - -	20
4.1	Compressive Stress versus Compressive Strain Curves for 300°C, 400°C, 500°C, 600°C and 700°C Carbonisation Treatment For Coconut Shell - - - - -	122
4.2	Compressive Stress versus Compressive Strain Curves for 300°C, 400°C, 500°C, 600°C and 700°C Carbonisation Treatment For Coconut Fibre - - - - -	122
4.3	Compressive Stress versus Compressive Strain Curves for Raw Coconut Fibre and Raw Coconut Shell - - - - -	123
4.4	Tensile Stress versus Tensile Strain Curves for 300°C, 400°C, 500°C, 600°C and 700°C Carbonisation Treatment for Coconut Shell - - - - -	124
4.5	Tensile Stress versus Tensile Strain Curves for 300°C, 400°C, 500°C, 600°C and 700°C Carbonisation Treatment for Coconut Fibre - - - - -	124
4.6	Tensile Stress versus Tensile Strain Curves for Raw Coconut Shell and Raw Coconut Fibre - - - - -	124
4.7	Flexure Stress versus Flexure Strain Curves for 300°C, 400°C, 500°C, 600°C and 700°C Carbonisation Treatment for Coconut Shell - - - - -	125
4.8	Flexure Stress versus Flexure Strain Curves for 300°C, 400°C, 500°C, 600°C and 700°C Carbonisation Treatment for Coconut Fibre - - - - -	126
4.9	Flexure Stress versus Flexure Strain Curves for Raw Coconut	

	Fibre and Raw Coconut Shell -	-	-	-	-	-	126
4.10	3-D Plots of Hardness, Abrasion and Compression Strength Versus Carbonisation Temperature for Fibre Filled Composites	-					126
4.11	3-D Plot of Elongation at Break versus Carbonisation Temperature for Fibre Filled Composites	-	-	-	-	-	127
4.12	3-D Plots of Tensile Strength, Modulus and Flexure Strength Versus Carbonisation Temperature for Fibre Filled Composites	-					127
4.13	3-D Plots of Hardness, Abrasion and Compression Strength Versus Carbonisation Temperature for Shell Filled Composites	-					128
4.14	3-D Plot of Elongation at Break versus Carbonisation Temperature for Shell Filled Composites	-	-	-	-	-	128
4.15	3-D Plots of Tensile Strength, Modulus and Flexure Strength Versus Carbonisation Temperature for Shell Filled Composites	-					129
4.16	FTIR Spectrum for Raw Coconut Shell	-	-	-	-		130
4.17	FTIR Spectrum for Coconut Shell at 300°C	-	-	-	-		130
4.18	FTIR Spectrum for Coconut Shell at 400°C	-	-	-	-		131
4.19	FTIR Spectrum for Coconut Shell at 500°C	-	-	-	-		131
4.20	FTIR Spectrum for Coconut Shell at 600°C	-	-	-	-		132
4.21	FTIR Spectrum for Coconut Shell at 700°C	-	-	-	-		132
4.22	FTIR Spectrum for Raw Coconut Fibre	-	-	-	-		133
4.23	FTIR Spectrum for Coconut Fibre at 300°C	-	-	-	-		133

4.24	FTIR Spectrum for Coconut Fibre at 400°C	-	-	-	-	134
4.25	FTIR Spectrum for Coconut Fibre at 500°C	-	-	-	-	134
4.26	FTIR Spectrum for Coconut Fibre at 600°C	-	-	-	-	135
4.27	FTIR Spectrum for Coconut Fibre at 700°C	-	-	-	-	135
4.28	Graphs of Cumulative SEM Properties weighted by Volume and by Count	-	-	-	-	143
4.29	X-Ray Diffractogram of Raw Coconut Shell Filler	-	-	-	-	144
4.30	X-Ray Diffractogram of Coconut Shell Filler at 300°C	-	-	-	-	144
4.31	X-Ray Diffractogram of Coconut Shell Filler at 400°C	-	-	-	-	145
4.32	X-Ray Diffractogram of Coconut Shell Filler at 500°C	-	-	-	-	145
4.33	X-Ray Diffractogram of Coconut Shell Filler at 600°C	-	-	-	-	146
4.34	X-Ray Diffractogram of Coconut Shell Filler at 700°C	-	-	-	-	146
4.35	X-Ray Diffractogram of Raw Coconut Fibre Filler	-	-	-	-	147
4.36	X-Ray Diffractogram of Coconut Fibre Filler at 300°C	-	-	-	-	147
4.37	X-Ray Diffractogram of Coconut Fibre Filler at 400°C	-	-	-	-	148
4.38	X-Ray Diffractogram of Coconut Fibre Filler at 500°C	-	-	-	-	148
4.39	X-Ray Diffractogram of Coconut Fibre Filler at 600°C	-	-	-	-	149
4.40	X-Ray Diffractogram of Coconut Fibre Filler at 700°C	-	-	-	-	149
4.41	Compositional Chart of Major Elemental Oxides of Coconut Shell as a Function of Carbonisation Temperature	-	-	-	-	150

4.42	Compositional Chart of Major Elemental Oxides of Coconut Fibre as a Function of Carbonisation Temperature	-	-	-	-	150
4.43	TGA Plot Showing Percentages of Weight Loss (Lignocelluloses of Coconut Shell)	-	-	-	-	151
4.44	TGA Plot Showing Percentages of Weight Loss (Lignocelluloses of Coconut Fibre)	-	-	-	-	152

LIST OF PLATES

Plate	Title	Page
4.1	SEM Monograph of Composite with Raw Coconut Fibre - -	136
4.2	SEM Monograph of Composite with Coconut Fibre at 300°C -	136
4.3	SEM Monograph of Composite with Coconut Fibre at 400°C -	137
4.4	SEM Monograph of Composite with Coconut Fibre at 500°C -	137
4.5	SEM Monograph of Composite with Coconut Fibre at 600°C -	138
4.6	SEM Monograph of Composite with Coconut Fibre at 700°C -	138
4.7	SEM Monograph of Composite with Raw Coconut Shell - -	139
4.8	SEM Monograph of Composite with Coconut Shell at 300°C -	139
4.9	SEM Monograph of Composite with Coconut Shell at 400°C -	140
4.10	SEM Monograph of Composite with Coconut Shell at 500°C -	140
4.11	SEM Monograph of Composite with Coconut Shell at 600°C -	141
4.12	SEM Monograph of Composite with Coconut Shell at 700°C -	141
4.13	Sample of Collected Coconut Shell Waste - - - -	155
4.14	Sample of Collected Coconut Fibre Waste - - - -	155
4.15	Sample of Ground Coconut Fibre Waste and Sieved to 100 µm -	156
4.16	Sample of Ground Coconut Shell Waste and Sieved to 100 µm -	156
4.17	Samples of Ground Coconut Shell and Fibre Treated at Various Temperatures	

	Of 300°C, 400°C, 500°C, 600°C, 700°C and Sieved to 100 µm	-	157
4.18	Sheeted Samples and Test Pieces of Composites Compound from Raw And Treated Coconut Shell and Fibre	- - - -	157
4.19	Samples of Raw and Treated Shell and Fibre Prepared for the Various Quantitative/Qualitative Analysis and Evaluative Study	-	158
4.20	Vibration Dampeners for Motor Cycle Hubs from Raw Coconut Shell, Raw Coconut Fibre, Carbonised Shell at 500°C and Carbonised Fibre at 600°C	- - - - - - - -	159
4.21	Oil Seals for Bambury Mixers from Raw Coconut Shell, Raw Coconut Fibre, Carbonised Shell at 500°C and Carbonised Fibre at 600°C	- -	160
4.22	Designed and Constructed Mould Consisting of the Male and Female Parts used for the Compression Moulding Process of Vibration Dampeners Of Motor Cycle Hub	- - - - - - -	161
4.23	Designed and Constructed Mould Consisting of the Male and Female Parts used for the Compression Moulding Process of Industrial Oil Seals useful in Bambury Mixers (Two Roll Mills)	- -	161

LIST OF APPENDICES

Appendix	Title	Page
I	Data Points for Tensile, Compression and Flexural Stress-Strain Relationship in Fibre and Shell - - - -	217
II	Data for FTIR Values of Raw Coconut Shell - -	222
III	Data for FTIR Values of Carbonised Coconut Shell at 300°C -	222
IV	Data for FTIR Values of Carbonised Coconut Shell at 400°C -	223
V	Data for FTIR Values of Carbonised Coconut Shell at 500°C -	223
VI	Data for FTIR Values of Carbonised Coconut Shell at 600°C -	224
VII	Data for FTIR Values of Carbonised Coconut Shell at 700°C -	224
VIII	Data for FTIR Values of Raw Coconut Fibre - - -	225
IX	Data for FTIR Values of Carbonised Coconut Fibre at 300°C -	225
X	Data for FTIR Values of Carbonised Coconut Fibre at 400°C -	226
XI	Data for FTIR Values of Carbonised Coconut Fibre at 500°C -	226
XII	Data for FTIR Values of Carbonised Coconut Fibre at 600°C -	227
XIII	Data for FTIR Values of Carbonised Coconut Fibre at 700°C -	227
XIV	Generated XRD Data for Raw Coconut Shell - - -	228
XV	Generated XRD Data for Carbonised Coconut Shell at 300°C -	229
XVI	Generated XRD Data for Carbonised Coconut Shell at 400°C -	230

XXVII	Generated XRD Data for Carbonised Coconut Shell at 500°C -	231
XXVIII	Generated XRD Data for Carbonised Coconut Shell at 600°C -	232
XIX	Generated XRD Data for Carbonised Coconut Shell at 700°C -	233
XX	Generated XRD Data for Raw Coconut Fibre - - -	234
XXI	Generated XRD Data for Carbonised Coconut Fibre at 300°C -	235
XXII	Generated XRD Data for Carbonised Coconut Fibre at 400°C -	236
XXIII	Generated XRD Data for Carbonised Coconut Fibre at 500°C -	237
XXIV	Generated XRD Data for Carbonised Coconut Fibre at 600°C -	238
XXV	Generated XRD Data for Carbonised Coconut Fibre at 700°C -	239
XXVI	X-Ray Fluorescence Analysis of Major and Minor Elemental Oxides Composition of Coconut Shell and Fibre - - -	240
XXVII	Predictive Analysis and Statistical Modeling Chart for the Mechanical and Chemical Sorption Properties of the Optimised Coconut Fibre Composites used in Model Productions - -	241
XXVIII	Predictive Analysis and Statistical Modeling Chart for the Mechanical and Chemical Sorption Properties of the Optimised Coconut Shell Composites used in Model Productions - -	259

LIST OF SYMBOLS AND ABBREVIATIONS

μm	Milimicron
2θ	2 Theta (Bragg's Angle)
ACD	Average Crystalline Dimensions
ANOVA	Analysis of Variance
ARI	Abrasion Resistance Index
ASTM	American Society for Testing and Materials
BHT	Butylated Hydroxyl Toluol
BSE	Back Scattered Electron
J/g	Jules per Grams
J/sec/cm ^o C	Jules per Second per Centimetres per Degree Celsius
CDP	Construction Products Directive
CFP	Coconut Fibre Powder
CL	Cathode Luminescence
CSP	Coconut Shell Powder
CV	Constant Viscosity Rubber
DF	Degrees of Freedom
DMRT	Duncan's Multiple Range Test
DRC	Dry Rubber Content

Ea	Activation Energy
EAB	Elongation at Break
EBSD	Diffacted Back Scattered Electron
EDS	Energy Dispersive X-Ray Spectroscopy
ENR	Epoxidised Natural Rubber
EPMA	Electron Probe Micro Analysis
FTIR	Fourier Transforms Infra-Red Spectroscopy
FWHM	Full Width at Half Maximum
G	Shear Modulus
GFRP	Glass Fibre Reinforced Polymer
GPa	Giga Pascal
HDPE	High Density Polyethylene
kg	Kilograms
LATZ	Low Ammonia-TMTD-Zinc
LOD	Loss on Drying
LSD	Least Significance Difference
MAPP	Maleic Anhydride-Grafted Polypropylene
MBTS	Mercaptobenzothiazole Disulphide
MDR	Moving Die Rheometer

M_n	Number Average Molecular Weight
MPa	Mega Pascal
MS	Mean Square
M_w	Weight Average Molecular Weight
NBR	Acrylonitrile Butadiene Rubber
NR	Natural Rubber
ODR	Oscillating Disk Rheometer
PBNA	Phenyl Betanaphthyl Amine
PCC	Pearson Correlation Coefficient
pH	Potential of Hydrogen
PKK	Peeks Constant
PNP	Paranitrophenol
Post Hoc	Latin Word for: “After this”
PP	Polypropylene
PPHR	Parts per Hundred Rubbers
PRI	Plasticity Retention Index
Kg/cm	Kilogrammes per centimetre
PVAc	Poly (Vinyl Acetate)
RNP	Recycled News Paper

RNR	Raw Natural Rubber
RPM	Revolution per Minutes
RSS	Ribbed Smoked Sheet
SAR	Standard African Rubber
SBR	Styrene Butadiene Rubber
SEM	Scanning Electron Microscopy
SMR	Standard Malaysian Rubber
SMRCV	Standard Malaysian Rubber-Constant Viscosity
SMRLV	Standard Malaysian Rubber-Low Viscosity
SPR	Superior Processing Rubber
SS	Sum of Squares
T _g	Glass Transition Temperature
TGA	Thermal Gravimetric Analysis
TMQ	Trimethyl Quinoline
TMTD	Tetramethylthiuram Disulphide
TSR	Technically Specified Rubber
UTM	Universal Testing Machine
UV	Ultra-Violet
V/mm	Volts per Millimetres

VNR	Vulcanized Natural Rubber
XRD	X-Ray Diffractogram
XRF	X-Ray Fluorescence
Ω/cm	Ohms per Centimeter
σ	Flexural Stress
τ	Tensile Stress

CHAPTER ONE

INTRODUCTION

1.1 Preamble

Product modification has become a current trend in the utilisation of modern materials especially in achieving better vulcanisate properties as applied to rubber compounding. Prominent additives for rubber product modification are a wide range of filler materials – both natural and synthetic in origin. Carbon black filler has often taken the lead when it comes to the use of fillers for improvement in reinforcement properties despite its short comings such as its non-renewable petroleum origin, dark colour, contamination and pollution, because of its proven reinforcing ability (Agunsoye *et al.*, 2012).

Fillers have marked effect on the physical and chemical properties of vulcanisates. Tensile and modulus properties could be modified using appropriate fillers (Ahmedna *et al.*, 1997; and Ahmedna *et al.*, 2000).

Owing to environmental awareness and economic considerations, biological/agricultural materials-reinforced polymer composites are seen to present a viable alternative to synthetic material-reinforced polymer composites as finding natural filler that will bond properly with the rubber is a challenge. However, merely substituting synthetic with natural fillers only solves part of the problem. Therefore selecting a suitable material for the matrix is a key consideration (Akay, 1993; Akinlabi *et al.*, 2011).

Coconut palm waste is an abundant agro-by-product in southern part of Nigeria is considered promising in this regard. Various works on the application of natural fillers in composites like pineapple, sisal, jute, cotton, rice husks and bamboo as the reinforcements in composites have been reported in the literatures. Using natural fillers

to reinforce the composed materials offers the following potential benefits in comparison with mineral fillers: strong and rigid due to cellulosic nature, light weight, environmentally friendly, economical, renewable and abundant resource (Sapuan *et al.*, 2003; Jain *et al.*, 2012; Alok *et al.*, 2013; Momoh *et al.*, 2017a, b).

Coconut palm waste is a potential candidate for the development of new composites because of its high strength and modulus properties (Michael and Wolcott, 1999; Momoh *et al.*, 2016a). Composites of high strength coconut filler can be used in a broad range of applications as, building materials, marine cordage, fishnets, and other household appliances. However, it should be noted that coconut palm waste filler like all other natural fillers suffer the following disadvantages: (i) degradation by moisture (ii) poor surface adhesion to hydrophobic polymers (iii) non-uniform filler sizes (iv) unsuitable for high temperature applications due to low ignition point (v) susceptibility to fungal and insect attack (Sapuan *et al.*, 2003; Mishra and Shimpi, 2005; Megiatto *et al.*, 2008; Md. Rezaur *et al.*, 2010).

This work therefore emphasises the modification of coconut palm waste through carbonisation in an attempt at combating these shortcomings. Extensive carbonised powder characterisation and evaluation will be carried out in an attempt to establish the filler properties under different carbonisation conditions.

1.2 Polymer Modification

Typically, commercial plastics are mixtures of one or more polymers and a variety of additives such as plasticisers, flame retardants, processing lubricants, stabilizers, and fillers. The exact formulation will depend upon the specific application or processing requirement (Jae *et al.*, 2010; Jacob *et al.*, 2014). Additives are materials added to polymers to alter their properties in order to make them suitable for certain identified

functions. The exact character of these additives will depend on the method of processing to be used and the desired properties required in the finished product (Additives, 2004). Different additives can influence the same polymer to have such varying characteristics and therefore applications. For example, poly(vinyl chloride) is a thermally unstable polymer having high modulus of elasticity, or stiffness, typical of other glassy polymers at room temperature. In order to obtain a flexible-graded resin for use as packaging film or for wire insulation, the polymer must be blended with a plasticiser to reduce its glass transition temperature (T_g) and with a small amount of an additive to improve its thermal stability at the required processing temperature (Ansarifar and Nijahwan, 2000; Ansarifar *et al.*, 2004; Ansarifar *et al.*, 2005; Andrzej and Abdullah, 2010).

Polymeric composites are physical mixtures of a polymer (the matrix) and a reinforcing filler (the dispersed phase) that serves to improve some mechanical properties such as modulus of rigidity or abrasion resistance. Fillers may be inorganic (e.g. calcium carbonate, graphite fibre) or organic (aromatic polyamide such as Kevlar) (Ansarifar *et al.*, 2005). Virtually, any material can be used as the composite matrix, including ceramic, carbon, and polymeric materials. Typically, matrices for polymeric composites are thermoset such as rubber or polyester resins; however, some engineering thermoplastics with high T_g and good impact strength, such as thermoplastic Polysulfones, have been used for composites. Principal applications for composites are in construction and transportation. Similarly, by using suitable additives, a range of products such as tyres, battery cases, elastic bands and erasers, can be obtained from rubber. Different additives perform different functions and the major ones can be grouped as follows: Fillers, plasticisers, blowing agents, processing aids/lubricants, anti-

ageing agents such as anti-degradants and anti-oxidant, flame retardants/inhibitors, cross linking agents, activating agents and colourants (Ansarifar *et al.*, 2004).

Generally, additives must be cheap and stable both under processing and service conditions (Arayapranee *et al.*, 2005; Arayapranee and Rempel, 2008; Araùjo *et al.*, 2008; Arayapranee and Rempel, 2009). The focus of this present work will be mainly on fillers as the main additive of interest for the modification process.

1.2.1 Fillers

The original use of fillers was to reduce the volume cost of the polymer in which case they are called extenders. Apart from cost reduction, fillers perform other functions such as improvement in tensile properties, improvement in tear resistance, nerve strength, impact resistance and improved resistance to solvent porosity. The physical properties of polymers can be modified by incorporation of fillers, which comes in various forms and types. Fillers in general can sometimes have adverse effects on properties e.g. products with fillers usually have less glossy finish. Fillers can either be particulate, rubbery or fibrous in nature, and each of these impact some characteristic to the polymer. For instance particulate fillers in general affect many properties of the polymer, such as:

- (i) Substantial reduction in cost by volume
- (ii) Corresponding increase in moduli properties and hardness
- (iii) Reduction in extrudate die swell
- (iv) Improved electrical insulation
- (v) Corresponding adjustments in tensile strength, elongation at break and flexural properties (Arroyo *et al.*, 2003).

Fillers are particles added to material (plastics, rubbers, composite material, and concrete) to lower the consumption of more expensive binder material or to better some properties of the mixture material. Worldwide, more than 53 million tons of fillers with a total sum of approximately EUR 16 billion are used every year in different application areas, such as paper, plastics, rubber, paints, coatings, adhesives and sealants. As such, fillers, produced by more than 700 companies, rank among the world's major raw materials and are contained in a variety of goods for daily consumer needs (Arroyo *et al.*, 2003; Aribike *et al.*, 2007; Awatefe *et al.*, 2014; Awatefe *et al.*, 2016).

1.2.2 Applications of fillers

Additives, fillers, and reinforcements are used to change and improve the physical and mechanical properties of plastics and rubbers. In general, reinforcing fibres increase the mechanical properties of polymer composites while particular fillers of various types increase modulus. Examples are baron, carbon, fibrous mineral, glass and Kevlar (Ayeni *et al.*, 2013a, b). Electrical properties can be affected by many types of filler. For example, by adding conductive fillers, an electromagnetic shielding property can be built into plastics, which are normally poor electrical conductors (Ayeni *et al.*, 2014). Anti-static agents can be used to attract moisture, reducing the build-up of static charge. Examples are aluminium powders and carbon fibre graphite (Ayeni *et al.*, 2014). Different fillers are employed widely as extenders to lower the cost of composite materials e.g., are calcium carbonate, silica and clay (Ayeni *et al.*, 2013a, b; Ayeni *et al.*, 2014).

Fillers also enhance properties of the products, for example, in composites. In such cases, a beneficial chemical interaction develops between the host material and the

filler. As a result, a number of optimised types of fillers, nano-fillers or surface treated goods have been developed (Ayo *et al.*, 2011).

Low-aspect fillers could modify the properties and moulding of the compound to which they are added. If the fillers are characterised with a low aspect ratio between the longest and the shortest dimensions, the basic properties will be less changed from those of the unfilled polymer (Ayo *et al.*, 2011 and Momoh *et al.*, 2016). Fillers at such level will benefit the composites in the following ways:

- (i) Shrinkage of parts will be less
- (ii) Thermal resistance may be improved
- (iii) Strength, especially compressive strength, will be improved
- (iv) Impact resistance will often be lower than for the unfilled polymer
- (v) Solvent resistance will often be improved (Arayapranee *et al.*, 2005; Ayo *et al.*, 2011).

High-aspect fillers: fibres may modify the properties when the aspect ratio between the longest and the shortest dimension of the filler is large, for example, greater than 25, the filler can be characterised as a fibre. Fibre reinforcements will significantly affect the properties of the compounds to which they are added. Example, the following characteristic nature will be pronounced:

- (i) Fibres Impact Strength: Assuming good bonding between the fibre and the polymer matrix, the strength in the fibre direction will be significantly increased. If many fibres are oriented in the same direction, large differences will be noted between the modulus in the orientation direction and in the direction

perpendicular to the orientation. The latter will be very close to that for the unfilled polymer (Ayo *et al.*, 2011).

(ii) Fibres Affect Shrinkage: The fibres will also have a significant effect on the shrinkage properties of the compounds: Shrinkage in the orientation direction will be much less than the shrinkage in the cross direction (Brahma *et al.*, 2005 and Momoh *et al.*, 2016a, b).

(iii) Importance of Predicting Fibre Orientation: Because the fibre orientation varies with the flow direction, in the thickness direction, and at weld line locations, it is important to be able to predict these orientations, in order to predict the properties of the moulded article (Belmars *et al.*, 1983; Bledzki and Gassan, 1999; Brahma *et al.*, 2005).

The typical fibre contents of a polymer composite may range from 20% to 80% of the total weight. The most common form of fibre fillers is E-glass, typically used to reinforce thermosets, such as polyester and epoxy resins. E-glass is a boron-alumina-silicate glass having low alkali-metal content and containing small percentages of calcium oxide (CaO) and magnesium oxide (MgO) (Hafsat *et al.*, 2016). For special application, such as in the manufacture of aerospace materials, fibres of boron, kevlar and especially carbon or graphite, are preferred (Dhakal *et al.*, 2007; Habibi *et al.*, 2008; Hafsat *et al.*, 2016).

For highly demanding applications, microfibrils or whiskers (synthetically-grown single crystals) of alumina or silicon carbide may be used. Whiskers can have tensile strength as high as 27.6 GPa and modulus as high as 690 GPa (Han *et al.*, 2012). Other composite fillers recently being considered include Buckminsterfullerene, C₆₀, that has been found to increase both T_g and thermal stability (Han-Seung *et al.*, 2006).

1.3 Agricultural By-Products

The various sources of filler available can either be natural or synthetic, that is, the filler can occur naturally either as agricultural waste such as coconut palm which forms the basis of this research study. Other sources include: Palm kernel shell, rice husk, groundnut shell, palm kernel bunch, coconut palm frond, etc. Generally, agricultural by-products are major constituent of environmental menace. Although they replenish the soil, but the environmental pollution they usually emanate over-rides the agricultural advantages derived.

In rubber compounding, the choice of suitable compounding ingredients are always determined by the properties required, the processing procedures and the cost of production. The search for renewable fillers from natural source becomes imminent so that they can act as substitute for the non-renewable fillers (Larbig *et al.*, 1998; Lou *et al.*, 2007; Lee *et al.*, 2009).

1.4 Natural Fibres in Composites

The increasing demand for greener and biodegradable materials leading to the satisfaction of society requires a compelling towards the advancement of nano-materials science. Natural fibres will take a major role in the emerging “green” economy based on energy efficiency, the use of renewable materials in polymer products, industrial processes that reduce carbon emissions and recyclable materials that minimise waste. Natural fibres are a kind of renewable resources, which have been renewed by nature and human ingenuity for thousands of years. They are also carbon neutral; they absorb the equal amount of carbon dioxide they produce. These fibres are completely renewable, environmentally friendly, high specific strength, non-abrasive, low cost, and bio-degradability (Madhukiran *et al.*, 2013). Due to these characteristics, natural fibres

have recently become attractive to researchers and scientists as an alternative method for fibres reinforced composites (Lovely *et al.*, 2006; Lopattananon *et al.*, 2006; Madhukiran *et al.*, 2013).

Natural fibres now dominated the automotive, construction and sporting industries by its superior mechanical properties. These natural fibres include flax, hemp, jute, sisal, kenaf, coir and many others. The various advantages of natural fibres are low density, low cost, low energy inputs and comparable mechanical properties and also better elasticity of polymer composites reinforced with natural fibres, especially when modified with crushed fibres, embroidered and 3-D weaved fibres. Glass fibre reinforced polymer (GFRP) is a fibre reinforced polymer made of a plastic matrix reinforced by fine fibres of glass (Mandal and Alam, 2012). Fibre glass is lightweight, strong, and robust material used in different industries due to its excellent properties. Although strength properties are somewhat lower than carbon fibre and it is less stiff, the material is typically less brittle in nature, and the raw materials are much less expensive. Its bulk strength and weight properties are very favourable when compared to metals, and it can be easily formed using moulding processes (Mark, 1964; Lin *et al.*, 2002; Lin *et al.*, 2006., Mandal and Alam, 2012).

In modern times, natural fibres such as sisal and jute fibre composite materials are replacing the glass and carbon fibres owing to their easy availability and cost. The use of natural fibres is improved remarkably due to the fact that field of application is improved day by day especially in automotive industries (Mohanty *et al.*, 2002). Natural fibre composites have gained increasing interest due to their eco-friendly properties. A lot of work has been done by researchers based on these natural fibres. Natural fibres such as jute, sisal, silk and coir are inexpensive, abundant and renewable, lightweight, with low density, high toughness, and biodegradable. Natural fibres such as jute have

the potential to be used as a replacement for traditional reinforcement materials in composites for application which require high strength to weight ratio and further weight reduction (Móczó and Pukónszky, 2008; Mohanty *et al.*, 2000; Mohanty *et al.*, 2002).

The performance of the natural fibre polymer composites is influenced by several factors, such as fibres micro-fibrillar angle, defects, structure, physical properties, chemical composition, cell dimensions, mechanical properties and the interaction of a fibre with the polymer matrix. Thus, to understand the properties of natural fibre-reinforced composite materials, it is essential to recognise the mechanics, physical, and chemical composition/properties of natural fibres. The most important matters in the development of natural fibre reinforced composites are (Maulida *et al.*, 2000):

- i. Surface adhesion characteristics of the fibres,
- ii. Thermal stability of the fibres, and
- iii. Dispersion of the fibres in the case of thermoplastic composites (Mod *et al.*, 1981; Maulida *et al.*, 2000; Morreale *et al.*, 2008).

The polarity characteristic of the natural fibre process leads to incompatibility difficulties with many polymers. Hydrophilic or polar characters of natural fibres produced composites with weak interface. Several chemical modifications or pretreatment of surface are being made to improve and enhance the adhesion or interfacial bonding between polymers and natural fibres (Morton, 1987; Mueller and Krobjilowski, 2003; Nurdina *et al.*, 2009).

The pretreatments of the natural fibre are usually done to clean and remove pollution from the fibre surface, to modify chemically the surface, decreases the rate of moisture

absorption tendency, and to increase the external unevenness (Momoh *et al.*, 2016a, b). The incorporation of natural fibres as filler or reinforcement produces significant changes in thermal stability of polymeric matrix. The manufacturing and the processing of these composites involves the collaboration of fibres and matrix at sufficiently high temperatures, hence, can lead to degradation of the bio-material, which results in unfavourable effects on the final properties (Park *et al.*, 2003; Osabohien *et al.*, 2006; Onyeagoro, 2012a, b).

1.5 Coconut Powder as Fillers in Composites

Coconut shell is one of the most important natural fillers produced in tropical countries like Malaysia, Nigeria, Thailand and India. Coconut shell filler is a potential candidate for the development of new composites because of its high strength and modulus properties. The coconut particles have remarkable interest in the automotive industry owing to its hard-wearing quality and high hardness, good acoustic resistance, moth-proof, non-toxic, resistant to microbial and fungi degradation, and not easily combustible (Pradhan *et al.*, 2004; Pothan *et al.*, 2006; Poletto *et al.*, 2011; Onyeagoro, 2012a, b).

Composites of high strength coconut filler can be used in broad range of application as: building materials, marine cordage, fishnets, furniture and other house hold appliances. Their availability, renewability, low density, and price as well as satisfactory mechanical properties make them attractive and an ecological alternative to glass, carbon and man-made fibres used for the manufacturing of composites (Premlal *et al.*, 2002; Pino *et al.*, 2006; Park *et al.*, 2008).

Coconut shells are available in abundance in Nigeria as a waste product after consumption of coconut water and meat. Such abundance can fulfill the demand of filler

based composites while reducing waste procurement and processing of coconut shell powder is cost effective than other artificial fillers.

The morphology and mechanical properties of coconut shell reinforced composites such as polyethylene have been evaluated to establish the possibility of using it as new material for engineering applications. The result showed that the hardness of the composites increases with increase in coconut shell content though the tensile strength, modulus of elasticity; impact energy and ductility of the composites decreased with increase in the particle content (Poh *et al.*, 2002; Poletto *et al.*, 2010; Agunsoye *et al.*, 2012).

1.6 Natural Rubber

Natural rubber (NR) is a high molecular weight polymeric substance with viscoelastic properties. Structurally it is Cis-1, 4 – polyisoprene. Isoprene is a diene and 1, 4 addition leaves a double bond in each of the isoprene unit in the polymer. Because of this, natural rubber shows all the reactions of an unsaturated polymer. It gives addition compound with halogens, ozone, hydrogen chloride and several other reactants that react with olefins. An interesting reaction of natural rubber is its combination with sulphur. This is known as vulcanisation. This reaction converts the plastic and viscous nature of raw rubber into elastic. Vulcanised rubber will have very high tensile strength and comparatively low elongation. Its hardness and abrasion resistance also will be high when compared to raw rubber. Because of the unique combination of these properties, natural rubber finds application in the manufacture of a variety of products (Patternman, 1986; Okieimen *et al.*, 2003; Osabohien and Egboh, 2007).

The main use of natural rubber is in automobile. In developed countries nearly sixty percent of all rubber consumed are for automobile tyres and tubes. In heavy duty tyres,

the major portion of the rubber used is NR (Osabohien and Egboh, 2007). In addition to tyres a modern automobile has more than 300 components made out of rubber. Many of these are processed from NR. Uses of NR in hoses, footwear, battery boxes, foam mattresses, balloons, toys etc. are well known. In addition to this, NR now finds extensive use in soil stabilisation, in vibration absorption and in road making. A variety of NR based engineering products are developed for use in these fields (Rivin, 1963; Pandey *et al.*, 2003; Prakash, 2009) Some basic characteristic of NR are represented in Table 1.1

Table 1.1: Basic Characteristics of Natural Rubber

Property	Value/Unit
Specific gravity	0.92
Refractive index	1.52
Coefficient of cubical expansion	0.00062/ ⁰ C
Cohesive energy density	63.7 J/cc
Heat of combustion	10547.084 J/g
Thermal conductivity	0.00032 J/sec/cm/ ⁰ C
Dielectric constant	2.37
Power factor (at 1000 cycles)	0.15 – 0.2
Volume resistivity	1015Ω/cm
Dielectric strength	3937V/mm

Source: Professional Association of Natural Rubber in Africa, Standard African Rubber (SAR) Manual, 1998

1.7 Chemistry and Development of Natural Rubber

Natural rubber of commerce is obtained from the latex of *Hevea brasiliensis*, a native of Brazil but widely grown on plantations in tropical Africa (Nigeria) and Asia. The composition of the Hevea latex varies between quite wide limits in composition (Brydson, 1978).

The non-rubber components not only have a biological function but also influence both the methods of coagulation to form dry rubber and also the techniques of latex technology. The empirical formula for the natural rubber molecule appears to have been first determined by Faraday who reported his findings in 1826. He calculated that carbon and hydrogen were the only elements present and his results correspond to the formula C_5H_8 (Blow and Hepburn, 1971; Boonstra, 1975; Boonstra, 1979).

The possibility showed that the NR molecules might contain a mixture of cis- and trans-groups was considered to be unlikely because such a mixed polymer would have an irregular structure and be unable to crystallise in the manner of natural rubber. Infra-red studies have subsequently confirmed that NR was the cis-polymer. Infra-red studies have indeed shown for a long while that natural rubber was at least 95% cis – 1, 4 – polyisoprene. The absence of any peak corresponding to a vinyl group precluded the presence of measurable amounts of 1, 2-material but an infra-red band at 890cm^{-1} was at one time thought to be due possibly to the products of a 3, 4 – structure (Blow and Hepburn, 1971; Boyle *et al.*, 2004; Matador, 2007).

Time-averaging techniques using high resolution nuclei magnetic resonance (NMR) which are capable of detecting 3, 4 – groups at concentrations of less than 0.3% have however failed to establish the existence of any such moiety and have also failed to show up any trace of trans-material (Golub *et al.*, 1962; Chen, 1966; Chen and Porter, 1994). The conclusion must therefore be that the molecule is more than 99% cis–1, 4-polyisoprene. Since all the evidence points to the conclusion that the NR molecule is not obtained in nature by the polymerisation of isoprene the absence of detectable pendant groups as would be produced by 1, 2 – and 3, 4 – addition is hardly surprising (Brydson, 1978; Burfield *et al.*, 1984; Matador, 2007).

Macromolecules of NR are long, regular, flexible and practically linear, thus it has very good elastic properties ($T_g \cong -70^{\circ}\text{C}$) and spontaneously crystallises (maximum crystallisation rate is approximately at -25°C) also under influence of deformation forces already at relative prolongation of more than 80%. It has also excellent strength characteristics and keeps them also in form of vulcanisates Matador, 2007). Tensile strength of NR vulcanisates filled with active fillers may be also more than 30 MPa. Its molecular weight M_w varies the most often in between $10^4 - 10^7$ and polymolecularity M_w/M_n approximately from 2.5 to 10. In non-vulcanised status it is reversibly prolonged under high deformation rates already to (800 – 1000) %. It belongs to highly deformation rates already to commercial types of NR rubber must be masticated prior to compounding. NR types with regulated constant viscosity (CV) practically do not need mastication and they have good processing properties (Da Dosta *et al.*, 2002; Dailatos, 2009; Matador, 2007; Daniel *et al.*, 2009).

NR belongs to highly non-saturated rubbers, because each of their structural unit contains one double link. Also reactive α – methylene hydrogen are related with its presence. Both types of these function groups may take part in different addition or substitution Polymeranalogical (e.g. during hydrohalogenation). They are utilised for chemical modification of the rubber itself as well as for its vulcanisation. In general, the NR rubbers are vulcanised by means of sulphur systems, but also other vulcanising agents can be used (Phenol formaldehyde resins, urethanes, peroxides and others). Ozone and oxygen react very easily with NR function groups, which cause its very low aging resistance (Colthup *et al.*, 1990; Dick, 2001; Matador, 2007; Ciolacu *et al.*, 2011).

Rubbers and elastomers are polymer materials that are characterised by ability of reversible deformation under influence of external deformation forces. Extent of deformation depends on the structure and molecular weight of deformed rubber and also

on external conditions of deformation; it can achieve some (100 up to 1000) % already at low stress (Matador, 2007). This property, marked as elastic, eventually highly elastic deformation, has entropy character. It rests in ability of the rubber macromolecules to occupy more ordered forms under stress, and on removal of stress to return to their ideal statistically random conformation, under ideal conditions without deformation of chemical bond distances or their angles (only non-combinatorial entropy is changed). The entropy reduction (ΔS) at unchanged free energy of the stressed system ($\Delta G = \Delta H - T\Delta S = 0$) must be connected with enthalpy reduction (ΔH), which becomes evident externally by heat buildup of the deformed sample. In ideal case the macromolecules may return to original position after elimination of stress and the stressed samples cooled down to original temperature (Matador, 2007).

The rubbers have usually long and regular macromolecule chains without large substituent, with partially oriented structural units. Thus their segments are moveable and also at low temperatures they can freely rotate around simple chemical bonds. It is related to their low glass transition temperature, T_g . Typical examples of such rubbers are poly-cis-1, 4-butadiene and poly-cis-1, 4-isoprene. They have T_g around -110 , eventually -70°C . With increasing of the content of irregularities in polymer chain (trans-1, 4; 1, 2; and 3, 4 structural units) or under presence of large substituent (styrene-butadiene rubbers) their T_g is increasing. Under glass transition temperature or crystallisation temperature (when rubber crystallises) the rubbers are solid polymers similar to plastomers. During heating they changed from elastic, eventually high elastic state to viscoelastic state above softening temperature they are plastic and they flow. It is advantageous when rubbers at normal temperature crystallise only under stress and their T_g is significantly lower than their usage temperature (Gilman *et al.*, 2005; Matador, 2007).

The rubbers gain optimum properties of engineering materials only in form of vulcanisates. It is possible to transfer them into this form by means of vulcanisation. Basis is in creating of chemical and physical cross-links among rubber macromolecules, consequence of that three-dimensional network is created and material obtains unique properties. In most cases this cannot be achieved only by cross-linking itself, but also some other additives must be added to rubbers. Except of cross-linking agents and antidegradants (they reduce ageing process) those are mainly fillers (they are making rubbers not only cheaper but they positively influence also some of their commercial properties) and also additives allowing compounding of all necessary powder or liquid ingredients to the rubbers, very often marked as auxiliary processing additives (Matador, 2007).

Presently, a lot of rubber types are on the market that can be divided into more groups in accordance with different criterion (e.g. saturated and unsaturated, natural and synthetic, polar and non-polar, crystallising and non-crystallising, etc.). From view of their usage and basic properties these can be also divided into (Momoh et al., 2016a, b):

- (i) Rubbers for general use-they have properties complying with requirements of more products, often also with different properties, they are relatively cheap, produced and consumed in big volume.
- (ii) Special rubbers- except of basic elastic properties, they have at least one special property, e.g. Ageing resistance, resistance against chemicals, resistance against swelling in non-polar oils, resistance against high or low temperatures etc. Normally, they are produced and consumed in lower volume than general rubbers and they are significantly more expensive.

In professional literature and also in practice the rubbers are named besides commercial names also with abbreviations. The abbreviation consists of a number of capital letters. The last letter of appropriate abbreviation characterises typical atom or group that is present in the rubber macromolecule (Gilman et al., 2005):

M – Rubbers with saturated hydrocarbon chain of methylene type

N – Rubbers containing nitrogen in polymer chain

O – Rubbers containing oxygen in polymer chain

Q – Rubbers containing oxygen and silica in polymer chain

R – Rubbers with unsaturated hydrocarbon polymer chain (diene)

T – Rubbers containing sulphur in polymer chain

U – Rubbers containing carbon, oxygen and nitrogen in polymer chain

Z – Rubbers containing phosphor and nitrogen in polymer chain.

Other letters of the abbreviation characterise monomers, the rubber was produced from. For example, in accordance with that, the SBR abbreviation means butadiene-styrene rubber, CR is chloroprene rubber, EPM is ethylene-propylene rubber, BR is butadiene rubber etc. Also some other letters can create a part of abbreviation, and these closer characterise appropriate rubber, e.g. OE-SBR is oil extended styrene-butadiene rubber, L-SBR means styrene-butadiene rubber produced by polymerisation in solution, H-NBR is hydrogenated acrylonitrile-butadiene rubber, CIIR is chlorinated isobutene-isoprene rubber, etc. (Gilman *et al.*, 2005; Matador, 2007).

Natural rubber has vegetable origin. It is created by enzymatic processes in many plants, belonging mainly to families of Euphorbiacea, Compositea, Moracea and Apocynacea.

It is industrially achieved mainly from the tree called *Hevea brasiliensis* belonging to *Euphorbiaceae* family. It is grown in plantation way in warm (average monthly temperature of 25-28°C) and humid (humidity around 80%) climate of South-Eastern Asia (Malaysia, India, China, Sri Lanka, Vietnam), in western Africa (Nigeria, Cambodia) and in north part of South America (Brazil, Guatemala). Annual production of rubber is presently varying around 3000-3500kg per 1ha and it depends on weather, soil quality, used stimulation means, age of trees and other external factors. The first source of rubber is sucrose that is created from carbon dioxide and water during photosynthesis process. In the first biosynthesis stage the acetyl-coenzyme A is created from it and this is changed into isopentenyl-pyrophosphate through mevalonate acid and the rubber in form of latex is generated by polymerisation. The rubber is achieved from it by means of coagulation (Matador, 2007; Daniel *et al.*, 2009).

Natural rubber obtained from *Hevea brasiliensis* is practically pure poly-cis-1, 4 isoprene (contains more than 99.9% of cis-1, 4 structural units) from chemical view. At the end of its macromolecules there may be bonded also non-isoprene structural units, mainly proteins, amino acids and phospholipids, in macromolecules backbone those may be also epoxide, ester, aldehydes, eventually and lactone groups. Also part of non-rubber additives that are present in latex is remaining in rubber. Their content may be different but generally it is varying in range 5-10%. In spite of their small amount in rubber they have significant influence on its properties and they represent one reason of different properties of natural rubber and its synthetic equivalent (IR) (Daniel *et al.*, 2009).

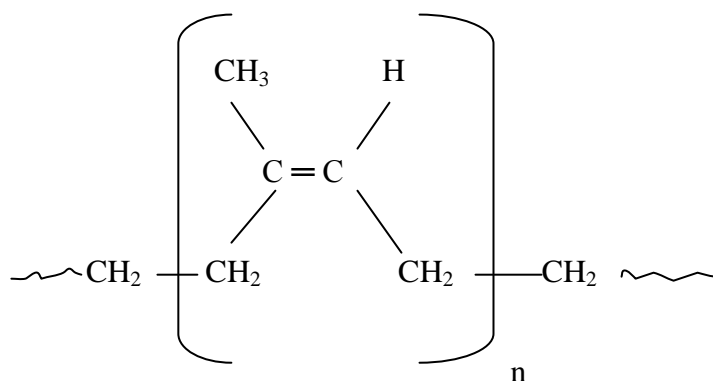


Figure. 1.1 Poly-cis-1, 4-isoprene

Natural rubber achieved from fresh latex and immediately dried-out after coagulation contain small portion of gel, too. Gel-rubber has higher content of nitrogen and minerals in comparison with sol-rubber, which leads to vision that rubber chains are more branched in gel-rubber and they are mutually connected with proteins through hydrogen bridges. This assumption is approved also by discovery that content of gel-rubber in deproteinised rubber is much lower. Average amount of side branches per one rubber macromolecule is varying approximately from 1 to 6 and it is higher in macromolecules with higher molecular weight. Accompaniment of the natural rubber storing is gradual increasing of its viscosity that is externally shown by its hardening. Reason of this phenomenon is not well known, but it is accredited to cross-linking reactions of non-rubber groups present in its macromolecules (Ansarifar *et al.*, 2005).

NR latex in *Hevea brasiliensis* is located in latex vessels to be founded in various parts of the tree. The lowest occurring is in the wood and the highest in the secondary phloem. There are the vessels aligned to spirals in concentric circles close to cambium. It is obtained from them by tapping based on cutting of the tree bark by special knife under approximate angle of 30°. Latex spontaneously flows out of this slot, because it occurs in spurses under hydrostatic pressure of 1-1.9 MPa. It is collected into special bowls (Daniel *et al.*, 2009; De Rosa *et al.*, 2010).

Natural rubber latex is a colloid system having the rubber particles dispersed in water. Latex particle size is varying approximately from 0.05 to 3 μ m. In fresh latex they have mainly spherical shape that is under their aggregation gradually changed to pear shape (section through rubber particles). Besides these also small amounts of proteins, resinous matters (including lipids), hydrocarbons and mineral substances are present in NR latex. Part of these non-rubbery matters, mainly proteins and lipids, is surrounded by a surface of rubbery particles and gives them negative charge, which assures the latex stability (Dhakal *et al.*, 2007; Matador, 2007).

Specific weight of fresh NR latex is 0.96 -0.98g/cm³ and its pH is varying within 6.5-7.0. It coagulates by standing on the air, and for this reason it must be stabilised. The most often used item for this stabilisation is ammonia (HA latex- maximum 0.7% NH₃) or its combinations (LA latex – 0.2% NH₃) with secondary stabilizers, such as dithiocarbamates, combination of Tetramethylthiuram disulphide and ZnO, Lauric or boric acid. These are added to latex only in very small amounts, normally 0.01 -0.05%. Some rubber products (e.g. foam rubber, gloves, condoms, glues) are produced directly from latex. The latex is modified for these reasons to have higher dry rubber content (DRC) values (minimum 60- 65% of rubber). It is performed by means of its concentrations, the most often by centrifugation and sedimentation, but also water evaporation, thickening and electro-decantation is used. During these operations also eventual dirtiness and non-rubbery additives are removed from rubber besides increase of the dry rubber content in latex (Matador, 2007; Daniel *et al.*, 2009).

Mastication is a process during which the elastic rubber achieves plastic properties. During mastication breaking of chemical bonds in its macromolecules take place by means of high shear forces. This process results in the decreasing of molecular weight and viscosity of rubber and consequently it becomes treatable. Mastication of NR is

performed either at low temperature on mills or at higher temperature in closed mixers, often in the presence of peptisers (they act as donors of electrons or hydrogen), that increase its efficiency. Besides mechanical degradation of rubbery macromolecules also their oxidation degradation occurs in this process and its rate is upgraded with mastication temperature increasing. Mastication of the NR is the most efficient at temperatures below 60-70°C and above 120-130°C, its efficiency is low in interval between these temperatures (Gilman *et al.*, 2005).

Mastication of synthetic rubber is much less efficient, and thus they are either produced with the molecular weight and viscosity suitable for their processing or they are modified in final production stages by means of suitable oils (e.g. SBR extended by oil). Advantage of such modification is in possibility to keep the high molecular weights, that normally afford better physical-mechanical and dynamic properties to vulcanisates and also processing of rubbers is good (Matador, 2007).

1.8 Processing Techniques of Natural Rubber from Latex

Latex is a white or slightly yellowish opaque liquid with a specific gravity, which varies between 0.974 and 0.986. It is a weak lyophilic colloidal system of spherical or pear shaped rubber globules suspended in an aqueous serum. The rubber globule is surrounded by a protective layer of proteins and phospholipids, which impart the lyophilic nature to latex. The stability of latex is due to the negative charge present on the protective layer. Also it contains a variety of non-rubber constituents both organic and inorganic, in addition to rubber (Flory and Rehner, 1943; Flory, 1953; Hosler, 1999). The proportion of these constituents may vary with clone, soil nutrition, climate etc. Latex composition could be represented as shown in the Table 1.2

Table 1.2: Percentage Composition of Natural Rubber Latex

Composition	Percent (%)
Rubber	30– 40
Proteins	2– 2.5
Ash	0.7– 0.9
Resins	1– 2.0
Sugars	1– 1.5
Water	55– 65

Fresh latex, as it comes out from the tree is slightly alkaline or neutral. It becomes acidic rapidly due to bacterial action. The formation of organic acids neutralizes the negative charge on rubber particles and the latex gradually gets coagulated on keeping. Therefore, fresh latex cannot be kept for long without preservative treatment. Latex can be processed into any of the following forms: Preserved field latex and latex concentrate, sheet rubber, block rubber, crepe rubber. Field coagulum can be processed only into crepe rubber or block rubber (Helge, 2000; Roger, 2002; Rowel, 2005)

1.8.1 Preserved field latex

Field latex is preserved using suitable preservative for long term storage. The processing of preserved field latex consists essentially of adding the preservative (usually ammonia, minimum 1%) to the sieved latex, bulking, settling, blending and packing. Field latex can also be preserved with LATZ (low ammonia – TMTD – zinc oxide) system (Zhang, 2004a).

1.8.2 Ribbed smoked sheet (RSS)

Latex is coagulated in suitable containers into thin slabs of coagulum and rolled through a set of smooth rollers followed by a grooved set and dried to obtain sheet rubber. Depending upon the drying method, sheet rubbers are classified into two: Ribbed

Smoked Sheets (RSS) and Air Dried Sheets (Pale Amber Unsmoked Sheets) (Chotirat *et al.*, 2007; Daniel *et al.*, 2009).

For processing latex into sheet rubber, it is important that the latex collected is brought to the processing centre before pre-coagulation sets in. In cases where the latex is found to be prone to pre-coagulation, an anticoagulant is used. Latex brought to the centre is strained through 40 and 60 mesh stainless steel sieves. The volume of latex is measured with a standard vessel and a calibrated rod. The DRC is estimated with a metrolac, which is a special type of hydrometer calibrated to directly read the DRC. However, laboratory methods are employed for accurate determinations (Eiras and Pessan, 2009).

Latex is diluted in bulking tanks to a standard consistency of $\frac{1}{2}$ kg of dry rubber for every 4 litres of the diluted latex (12.5% DRC). The diluted latex is allowed to stand in the bulking tank for a fixed time (usually 15 to 20 minutes) for the heavy dirt particles to sediment. The diluted latex is drawn out from the bulking tank without disturbing the sediment layer of impurities into the coagulation pans or tanks. Four litres of latex is usually transferred to each pan (Daniel *et al.*, 2009; Eiras and Pessan, 2009).

1.8.3 Coagulation

Formic acid or acetic is generally used for coagulation. The quantity of acid required for satisfactory coagulation depends on various factors like the amount and type of anticoagulant used the duration of coagulation, the season and the nature of the latex. The acid requirement may slightly change under varying conditions and can be fixed up by experience. Only diluted acid should be used for coagulation and should be thoroughly mixed with latex (Daniel *et al.*, 2009). Catalyst AC and Sulphuric acid are also used by growers. Catalyst AC is a dry powder and comparatively a safe coagulant.

Normally, 100cm³ of a 5 percent solution of this chemical is enough for making a ½kg sheet (Nasir and Choo, 1989).

Since sulphuric acid is highly corrosive, care should be taken in its handling and dilution. 300 ml of a 0.5% solution of the acid is required for same day sheeting and 250 ml for next day sheeting. Coagulum from latex often shows a tendency for surface darkening. To prevent this, a small quantity of sodium bisulphate (1.2g per kg DRC), dissolved in water may be added to the diluted latex before coagulation. After coagulation, the coagulum is removed from the pan or tank and thoroughly washed in running water (Daniel *et al.*, 2009). They are rolled either in a sheeting battery or smooth rollers to a thickness of 3 mm and finally passed through the grooved roller. White sheeting, the coagulum is continuously washed. The sheets are again washed in running water in a tank. Mould growth on sheet rubber can be prevented by treating freshly machined sheet in a dilute solution of paranitrophenol (PNP). The concentration of PNP is 0.05 to 0.1% in water. 100 litres of the solution will be sufficient for treating 100 sheets. The wet sheets are allowed to drip on reapers arranged in a well-ventilated dripping shed (Nasir and Choo, 1989; Daniel *et al.*, 2009).

1.9 Types of Natural Rubber

Apart from ribbed smoked sheet (RSS), which forms a major group type of natural rubber as described above; other six (6) types are described thus: Ribbed smoked sheet (RSS), white and pale crepe, crepe rubber, thin brown rubber, technically specified rubber, superior processing rubber, Hevea crumb rubber (Daniel *et al.*, 2009).

1.9.1 White and pale crepe

Selected field latex is treated with sodium bisulphate and then strained several times. The latex is diluted with water to 25% weight of DRC. A dilute solution of acetic acid is

added. Reflection rich in pigments floats-off the surface, which is removed and bleached. Formic acid is added to the bleach portion to reduce the pH to 4.5. It is then poured into aluminum partitioned batteries to coagulate into slabs. The slabs are processed in mills under water and are converted into thick blankets which are transferred to macerator mills. It undergoes shearing and mastication. The slabs are then reduced to 1–3 mm thickness. On smoother finishing mills, the sheets are dried at (31–34)⁰C for several days. This is graded in the basis of colour, smell, dust, specs, sand and foreign materials (El-Tayeb and Nasir, 2007; George *et al.*, 2001).

1.9.2 Crepe rubber

The latex is coagulated and washed in washing mills; (16–20) % latex yields a soft, cohesive coagulate which on standing gives a clear serum. The residue is washed with water on closely spaced rollers. The thin sheets are dried at 17⁰C for two hours in vacuum driers. It is then cooled to a brownish colour. Initial concentrated rubber is obtained from undiluted latex. This is graded according to colour, purity and strength (Golub *et al.*, 1962; George, 2000; Ghosh, 2007).

1.9.3 Thin brown rubber

The raw materials used are fresh cup lump, wet slab, unsmoked sheets or high-grade scraps. These are milled with water on grooved wash mills. Then they are dried for three weeks in large open drying sheds. The resultant sheets may be thin brown or thick brown. These are graded according to colour and contamination (Ghosh, 2007).

1.9.4 Technically specified rubber (TSR)

The coagulum is milled in series of wash mills to obtain clear and homogenised rubber. The wet crumbs are dried in air-circulating ovens at 100⁰C (Gent and Pulford, 1983).

1.9.5 Superior processing rubber

This is a mixture of cross-linked (SPR) rubber and unmodified rubber. It is processed as RSS, Pale crepe, brown crepe and air dried sheets. These rubbers are used as processing aids in mixture with regular grade NR to give low die swell, smoother and faster extrusion and improved calendaring (Gent, 1989).

1.9.6 Hevea crumb rubber

In Standard Malaysian Rubber (SMR) castor oil is added to field latex prior to coagulation. It is then milled with castor oil, which acts as a crumbling agent. SMR is then converted to fine crumbs. These are washed with water and dried at $(80 - 100)^{\circ}\text{C}$ for 3 hours. This is known as Hevea crumbs and consists of SMRCV, SMRLV, SMRWF, SMR 5, SMR 10, SMR 20, SMR 50 and SMRGD grades (James and Burak, 2005).

1.10 Modification of natural rubber

There are various forms of NR rubber modification which may include the following techniques: Filler Incorporation, hydrogenation, halogenations, cyclisation, resinous addition, epoxidisation, grafting process, degraded inclusion, blending.

1.10.1 Filler incorporation

Fillers are most widely used additives in polymer compositions. They are used in all plastics, natural and synthetic rubber and in coatings. Filler is an inert material added to a polymer composition to improve its properties and/or to reduce its cost. On being mixed with the resin, it forms a heterogeneous mixture which can be moulded under the influence of heat or pressure or both. There are reinforcing fillers, active fillers and

inactive fillers which may be black or non-black in colour; organic or inorganic in nature (Iyasele and Okieimen, 2004).

1.10.2 Halogenation

NR can be chlorinated in a solution in latex and in solid state. Glass transition temperature of chlorinated NR increases with increasing chlorine content. These are light, cream coloured and thermoplastic products. It is used as adhesive and for textile wafting, and sometimes in black coloured paint. NR undergoes reaction with hydrogen halides. With hydrogen chloride (HCl) it produces a very hard white product $(C_5H_4Cl)_n$; which gives a transparent film (Kabir *et al.*, 2006).

1.10.3 Cyclisation

NR on treatment with Sulphuric acid gives a hard brittle product. NR can be reacted with sulphuric acid, sulphonyl chloride and other sulphur compounds. It can also be cyclised with $ZnCl_2$ and Chlorostanic acid. These are of two types, brown black similar to balata and light and low molecular weight resins soluble in many solvents and compatible with resins, oils and plasticizers (Kandem *et al.*, 2004; Jurkowska *et al.*, 2006).

1.10.4 Resinous addition

Phenol formaldehyde resins are added during vulcanisation. These have low compression set, excellent dynamic stability and good aging properties. Mooney viscosity does not increase (Joseph *et al.*, 2002; Joseph *et al.*, 2003a, b).

1.10.5 Epoxidisation

Trialkyl ethylene double bond in NR reacts with per acids to produce the epoxidised product in high yields. A mixture of H₂O₂ and formic acid has been found to give satisfactory results. Glass transition temperature increases by 1°C per mole of epoxidation per mole of NR. Epoxidised natural rubber (ENR) has T_g near room temperature. These are used as anti-skidding agents (Kim *et al.*, 2006; Kim *et al.*, 2007).

1.10.6 Grafting process

Styrene, vinyl acetate, acrylonitrile and methyl methacrylate can graft NR. Peroxides and hydroperoxides initiate the reaction. These grafted products are used for reinforcing vulcanisates and adhesives (Karmakar *et al.*, 2007; Liang, 2011).

1.10.7 Degraded inclusion

Liquid NR on oxidation gives a dark viscous material, to be used in rubber processing as a binder and processing aid (Guo, 2009).

1.10.8 Blending

This could be binary or ternary blending; where NR can be blended with polyolefin or polystyrenes. This gives a thermoplastic rubber (Chand *et al.*, 1987).

1.11 Basic Properties of Natural Rubber

- (i) Crude rubber is a tough and elastic solid. It becomes soft and sticky as the temperature rises.
- (ii) Its specific gravity is 0.92.
- (iii) The most important property of natural rubber is its elasticity. When stretched, it expands and attains its original state, when released. This is

due to its coil-like structure. The molecules straighten out when stretched and when released, they coil up again. Therefore applying a stress can easily deform rubber. Note that when this stress is removed, it retains its original shape (Ekebafé *et al.*, 2009).

- (iv) Raw natural rubber has elasticity over a narrow range of temperature from 10 to 60 degrees centigrade. Because of this, articles made of raw natural rubber do not work well in hot weather.
- (v) Raw natural rubber has low tensile strength and abrasion resistant.
- (vi) It absorbs large quantities of water.
- (vii) It is insoluble in water, alcohol, acetone, dilute acids and alkalis.
- (viii) It is insoluble in ether, carbon disulphide, carbon tetrachloride, petrol and turpentine when vulcanized.
- (ix) Pure rubber is a transparent, amorphous solid, which on stretching or prolonged cooling becomes crystalline (Choi *et al.*, 2003; Egwaikhide *et al.*, 2007a,b; Ekebafé *et al.*, 2009)

1.11.1 Comparison between raw natural rubber and vulcanised natural rubber

Most of the shortcomings/weakness of raw natural rubber has its corrections in the vulcanised rubber as indicated in Table 1.3 (Hull and Clyne, 1996):

Table 1.3: Comparison of Raw Natural Rubber (RNR) with Vulcanised Natural Rubber (VNR)

Raw Natural Rubber (RNR)	Vulcanised Natural Rubber (VNR)
Soft and sticky	Comparatively hard and non-sticky
Low tensile strength and not very Strong	High tensile strength and very Strong
Low elasticity	High elasticity
Can be used over a narrow range of Temperature from (10 - 60) ⁰ C	Can be used over a wide range of Temperature from (40 - 100) ⁰ C
Low abrasion resistance	High abrasion resistance
Absorbs a large amount of water	Absorbs a small amount of water
Soluble in solvents like ether, carbon disulphide, carbon tetrachloride, petrol and turpentine.	Insoluble in all the usual solvents.

1.11.2 Hardening of natural rubber

Rubber can be hardened by adding carbon black as filler (solid substance added for strength and to reduce cost) to it during the vulcanisation process. This increases the strength and abrasion resistance of natural rubber. Carbon black when mixed with rubber in rubber tyres makes them more durable and cuts the cost. The vulcanised and hardened rubber is used to make tyres and tubes of automobiles and conveyor belts for industrial use. Vulcanised natural rubber could also be useful for rubber bands, football bladders and gloves (Ishak and Bakar, 1995; Igwe and Ejim, 2011; Husseinsyah and Mostapha, 2011).

1.12 Application of Natural Rubber

Rubber is versatile and finds a wide range of application in the production of the following:

- (i) Pneumatic tyres and tubes
- (ii) Belting-conveyors, transmissions and V-belts
- (iii) Hose-hand made and braided
- (iv) Footwear sole-micro-cellular, unit, resin rubber, DVP/DIP
- (v) Cable-insulation and sheath
- (vi) Coated fabric and calendared sheeting
- (vii) Moulded items like seats, gaskets, auto components
- (viii) Rubber to metal bonded components
- (ix) Rubber rollers
- (x) Extruded items like tubing, weather strips
- (xi) Adhesives
- (xii) Latex products – dipped goods, threads and foams (Honday, 1966; Hon and Shiraishi, 2001).

1.13 Statement of Research Problem

The increasing health challenges in the use of carbon black with its high nitrosamines contents in rubber compounding have become worrisome in recent times. An attempt at finding and developing alternative filler materials to combat all major disadvantages of carbon black in rubber reinforcement is a major focus of this work. A polymeric matrix

material with better filler/matrix interaction together especially from natural and renewable agro-byproducts is a promising venture in compound design because of larger surface area, and greater aspect ratio, with fascinating properties (Cao *et al.*, 2009; Momoh *et al.*, 2016b and Momoh *et al.*, 2017 a, b).

Being environmentally friendly, applications of coconut palm wastes offer new technology and entrepreneurial opportunities for several sectors, such as aerospace, automotive, electronics, and agro-technology industries. Hybrid agro-based composites that exploit the synergy between natural materials in a reinforced rubber can lead to improved properties along with maintaining environmental appeal.

1.14 Aims of the Research

- (i) This research work is intended to present workable and applicative information about coconut palm wastes which include the shells and fibres composites with specific concern to harnessing them, removing them away from the environment as wastes, moving them from waste to wealth, characterising them, evaluating their potentials and appropriately modifying them to extend the frontiers and modern technological advancements through the scientific exploitation of renewably abundant and available materials.
- (ii) The far reaching implication is geared towards products development especially in automobile, engineering and specialty applications. The target will be to eradicate modern challenges in the utilisation of composites by appropriate formulation designs and product optimisation.

1.15 Research Objectives of the Study

- (i) This research work seeks to broaden the horizon for rubber product development through reinforcement of composites from renewable agricultural wastes.
- (ii) This work also sort the use of carbonisation as an appropriate modification method for morphological re-orientation of coconut palm waste to alleviate certain inherent weaknesses as stated in the Justification.
- (iii) The health implication of the use of non-renewable mineral fillers like carbon black for rubber reinforcements was a major driving force for this research study.
- (iv) This work seek to utilised modern and high-tech analytical laboratory equipment to analyse and evaluate the possible extent of modification attained through carbonisation using standard measurement test methods.

1.16 Scope/Limitations of the Study

In order to fulfill the stated aim and objectives, the scope of the research will cover the following studies:

- (i) Sourcing and gathering of coconut palm shells and fibres. Thorough washing in water to remove sands and debris. Oven drying to remove moisture retained during the washing operations.
- (ii) Physical modification of the coconut shell and fibre by carbonisation process.
- (iii) Grounding of both raw and treated shell/fibre. Particle filtering and sizing operations to achieve 100 μm .

- (iv) Characterisation of the raw and treated fillers in terms of pH value, iodine adsorption number to determine surface area reactivity, loss on ignition, bulk density, ash content, fibre dimensions, moisture content, oil absorption and particle size determination.
- (v) Formulation design, mixing and compounding in a two roll mill to achieve a compounded mix in the form of sheets.
- (vi) Rheological determination using oscillating disk rheometer, (ODR Model 2000). This will enable the determination of processing/cure characteristics parameters such as temperature of cure, press pressure, time of cure, optimum cure determination; scorch time, modulus control and reversion cure as well as mix viscosity of melt.
- (vii) Press curing to stabilise crosslink formation.
- (viii) Mechanical evaluation of hardness, abrasion resistance index measurements, compressive strength determination, tensile strength, modulus, elongation at break and flexural strength analysis.
- (ix) Chemical sorption evaluation to determine extent of crosslink interaction between filler and rubber matrix.
- (x) Qualitative evaluative analysis on composites using Fourier transform infra-red spectroscopy (FTIR), scanning electron microscope (SEM), X-ray diffraction study (XRD), X-ray fluorescence analysis (XRF), thermal degradation and stability measurement using thermogravimetric analysis (TGA).
- (xi) Development of an engineering product from achieved best formulation using the modified coconut shell and fibre.

- (xii) Property comparison between formulated and manufactured engineering product with such standard product in the commercial market and usage by evaluative field/product analysis.
- (xiii) Mathematical modelling using analysis of variance (ANOVA) for between subject factors of mechanical and chemical sorption properties with sample modification through carbonisation temperature.

1.17 Justification/Significance of the Study

- (a) The possible advantages, such as reduced tool wear, low cost, and low density per unit volume and acceptable specific strength, along with their sustainable renewable and degradable features are some of the important properties of the coconut palm wastes, which make them suitable to use as filler in rubber composites (Egwaikhide *et al.*, 2007).
- (b) Synthetic filler materials, such as carbon black, carbon fibres, glass fibres create severe ecological, and health hazard problems in their use in rubber compounding. A suitable replacement from natural alternatives like coconut palm wastes is necessitated (Okieimen *et al.*, 2003a,b).
- (c) Easy approaches and schemes are readily established to supplement and appropriately modify certain inherent deficiencies such as; poor fibre/matrix interactions, water resistance, and relatively lower durability. Although weaker interfacial bonds between highly hydrophilic natural fillers and hydrophobic, non-polar organophilic rubber matrix, often leads to considerable decrease in the properties of the composites and, thus, significantly obstructs their industrial utilisation and production. However, the surface of the natural coconut filler can be easily modified and this can be achieved by physical, mechanical and/or chemical means via carbonisation (Nemour, 1999; Newman, 2008).

- (d) A perfect substitutes to traditional or conventional automobile and bridge bearing materials are the fibre reinforced rubber composites due to a number of factors which include: higher strength and stiffness with reference to specific gravity; better resistance to corrosion, natural hazardous environments, no conductivity, non-toxicity and lower life-cycle costs; and higher fatigue strength and impact energy absorption capacity (Myhre and Mackillop, 2002; Osman *et al.*, 2010).
- (e) When coconut palm wastes, especially the fibres are used to prepare construction or building modules, then, under developed or developing countries, with rural regions, will tend to enforce the cultivation of required manufacturing crops and this would be empowering to address their own housing, poverty and financial issues without any outsider support. They become a way of contributing to the economic growth, entrepreneurial development and job creation.
- (f) An attempt is being made for the utilisation of locally manufactured starting materials, goods and Nigerian service companies in production operations, projects and well engineering.

1.18 Potential Contributions to Knowledge

The purpose of scientific research is to add to the body of knowledge. Results obtained from this thesis will precisely address:

- (a) Further information on polymer network structure via filler modification will be contributed to existing and inadequate literature.
- (b) The carbonisation process for the modification of the coconut palm wastes which is a novel approach is intended to show that the removal/depletion of

lignocellulose components and moisture which are prominent features that hinders the use of most agricultural wastes and by-products in polymer matrix reinforcements could be readily dealt with giving a better interactions between agro-based fillers and polymer matrix of composites.

- (c) The elemental compositional analysis has shown that at least eighteen (18) metal oxides are present both at trace and macro levels in the coconut palm wastes; and carbonisation increased the potassium oxide (K_2O) component in preference to all other minor and major participating metal oxides.
- (d) Modification of the coconut palm waste through carbonisation clearly showed a direct impact on the molecular re-orientation of the shell and the fibre as seen in the particle aggregations, glassy-like strands depicted by SEM and the increase in crystalline index shown by X-ray diffractions evaluated.
- (e) The optimised formulation design has been proven to be effective and efficient in imparting appropriate reinforcements to certain engineering wares such as the produced motor cycle vibration dampener and industrial oil seals for bambury mixers, popularly called two-roll mill used in rubber mastication and mixing. Needed mechanical properties were greatly improved upon by good filler-matrix interactions in the composites.
- (f) The viability of coconut palm wastes, otherwise seen as environmental nuisance would be validated and profitably converted from waste to wealth through the appropriate techniques to be exploited this thesis.
- (g) Statistical predictions and modelling of mechanical and chemical sorption properties in response to product modification through filler carbonisation shall be made available. Levels of significance and non-significance by means of

ANOVA evaluative studies could encourage further mathematical modelling using other means.

CHAPTER TWO

LITERATURE REVIEW

2.1 Previous Works

The tensile and flexural properties of composites made from coconut shell filler particles and epoxy resin have been studied by Sapuan *et al.*, 2003. They performed several characterisation studies on composites prepared from coconut shell filler particles at three different filler contents of 5%, 10% and 15% by weight. Their experimental results showed that tensile and flexural properties of the composites increased with the increase in the filler particle content. The composite materials demonstrated somewhat linear behaviour and sharp fracture for tensile and slight non-linear behaviour and sharp fracture for flexural testing.

Jacob *et al.*, (2014), worked on the evaluation of mechanical properties of coconut shell fibres as reinforcement material in epoxy matrix. The morphology and mechanical properties of coconut shell reinforced with epoxy resin composite was evaluated to establish the possibility of using it as a new material for engineering applications.

Satyanarayana *et al.*, (1982), reported the structure property studies of fibres from various parts of the coconut tree. Fibres from different structural parts of the coconut palm tree (*Cocos nucifera, linn*) was examined for properties such as size, density, electrical resistivity, ultimate tensile strength, initial modulus and percentage elongation. The stress-strain diagrams fracture made microfibrillar angle as well as cellulose and lignin contents of these fibres were determined. They conclude that the physical and mechanical properties exhibited by the different fibres from coconut tree can be used for various applications, especially as composites.

Husseinsyah and Mostapha (2011), worked on the effect of filler content on properties of coconut shell filled polyester composites and found out that the tensile strength, Young's modulus and water absorption of polyester/CS composites increased with increasing CS content but elongation at break decreased. Morphological study indicates that the tendency of filler-matrix interaction improved with the increasing filler in polyester matrix.

Onyeagoro (2012a, b) carried out a research on cure characteristics and physico-mechanical properties of carbonised bamboo fibre filled natural rubber vulcanisates. The cure characteristics and physico-mechanical properties of carbonised bamboo fibre filled natural rubber vulcanisates were studied as a function of filler loading, filler particle size and compatibiliser. The scorch time, t_2 and cure time, t_{90} of carbonised bamboo fibre filled natural rubber vulcanisates decreased with increased in filler loading and the presence of compatibiliser.

Osman *et al.*, (2010) studied the effect of maleic anhydride-grafted polypropylene (MAPP) on the properties of recycled newspaper (RNP) filled polypropylene (PP)/natural rubber (NR) composites. The authors found that the incorporation of MAPP reduced the water uptakes of the composites.

In another study by Ansarifer *et al.*, (2005), on the properties of natural rubber reinforced with synthetic precipitated amorphous white silica nano-filler, it was reported that compression set, tensile strength and hardness were improved on addition of filler into the rubber, while elongation at break, tear strength and cyclic fatigue were adversely affected. Yang *et al.*, (2006) studied the influence of graphite particle size, and shape on the properties of acrylonitrile butadiene rubber (NBR) and found that graphite with the smallest particle size possessed the best reinforcing ability, while the

largest graphite particles exhibited the lowest function coefficient of the composites among four fillers investigated.

The reinforcing effects of coal shale based fillers on natural rubber on the basis of filler particle size have been investigated by Zhao and Xiang in 2004. The authors reported that the ultra-micro coal-shale powder exhibited excellent filler properties.

Egwaikhide *et al.*, 2007 studied the effect of coconut fibre on the cure characteristics, physico-mechanical and swelling properties of natural rubber vulcanisates. The results showed that coconut fibre could be potential reinforcing filler for natural rubber compounds. The study indicates that the potential of coconut fibre and other agricultural by-products can be exploited further by controlling particle size and particle distribution, improving filler dispersion and also its surface functionality.

The mechanism of reinforcement of elastomers by filler was reviewed by Brahma *et al.*, 2005. They considered that the filler increased the number of chains, which shared the load of a broken polymer chain. It is known that in the case of filled vulcanisates, the efficiency of reinforcement depends on a complex interaction of several filler related parameters. These include particle size, particle shape, particle dispersion, surface area, surface reactivity, structure of the filler and the bonding quality between the filler and the rubber matrix.

Bhaskar and Singh (2013) studied physical and mechanical properties of coconut shell particle reinforced-epoxy composite. Experimental results showed that density, strength, modulus of elasticity and percent elongation decreased with percent weight of shell particles within the range of (20-35) % of reinforcement.

Alok *et al.*, (2013) studied the mechanical properties and absorption behavior of coconut shell powder epoxy composite in different particle size and reinforcement in

different volumes. Tests evaluated showed that tensile strength, flexural property and hydrophilic behaviour along with engineering application of resulting composites were of highly appreciated values in automobile reinforcements.

The morphology and mechanical properties of coconut shell reinforced polyethylene composite have been evaluated to establish the possibility of using it as a new material for engineering application. The coconut shell reinforced composites were prepared by compaction low density polyethylene matrix with 5% - 25% fractional volume of coconut shell particles. The effects of particles on the mechanical properties of the composites produced were investigated. The result showed that the hardness of the composites increased with increase in coconut shell content though the tensile strength, modulus of elasticity; impact energy and ductility of the composite decreased with increase in the particle content (Agunsoye *et al.*, 2012).

Han-Seung Yang *et al.*, (2006) reported that the tensile strength of the bio-composites decreased slightly as the filler loading increased. However the composites retained an acceptable level of strength. As the filler loading increased, the poor interfacial bonding between the filler and matrix of polymer caused the tensile strength and izod impact strength of the composites to be reduced. This poor interfacial bonding resulted to an increase in the number of micro voids causing increased water absorption. With the addition of compatibilising agent, the interfacial bonding between the filler and the matrix polymer was greatly improved, resulting in improved dimensional stabilities and water absorption behaviour.

Ayo *et al.*, (2011) worked on the effect of filler carbonisation temperature on the mechanical properties of natural rubber composites. The effect of carbonisation temperature on the mechanical properties of groundnut shell filled natural rubber

composite was studied. It was found that some mechanical properties such as tensile strength, modulus, hardness and abrasion resistance increased with filler carbonisation temperatures and loading while other properties such as compression set, flex fatigue and elongation decreased with filler carbonisation temperature and loading. The percentage swelling in benzene, toluene and xylene also decreased with carbonisation.

The present work focused on the modification of coconut palm wastes - both shell and fibre through carbonisation at various temperatures of 300⁰C - 700⁰C. Characterisation and analytical evaluations will be done to conceptualise its usefulness in natural rubber development in the areas of engineering and commodity applications.

2.2 Classification of Fillers

Fillers are of various types and are classified according to their sources. Using source classification, they could be described as organic, inorganic or mineral and fibrous fillers. Fillers could also be widely classified primarily on their colour; such as black and non-black fillers. Fillers could even further be classified as: reinforcing, non-reinforcing and semi-reinforcing (Blow and Hepburn, 1971).

Reinforced fillers are those with increased in tensile strength, tear strength, modulus, hardness and abrasion resistance of rubber vulcanisates in which they are incorporated and dispersed. The most important black existing filler is carbon black, which are used both on tyre and non-tyre applications. Different types of carbon blacks are used and their differences lie in their particle sizes, surface areas and structures Blow and Hepburn, 1971).

2.2.1 Black fillers and classification by manufacturing process

Carbon black could be produced through thermal decomposition method or the partial combustion method using hydrocarbons such as oil or natural gas as raw material. The characteristics of carbon black vary depending on manufacturing process, and as such carbon black is classified by manufacturing process. Carbon black produced with the furnace process, which is the most commonly used method now, is called “furnace black”, distinguishing it from carbon black, which is manufactured with other processes (Blow and Hepburn, 1971).

2.2.1 (a) Furnace black process

This method forms carbon black by blowing petroleum oil or coal oil as raw material (feedstock oil) into high temperature gases to combust them partially (Boonstra, 1975). This method is suitable for mass production due to its high yield, and allows wide control over its properties such as particle size or structure. It is currently the most common method used for manufacturing carbon black for various applications from rubber reinforcement to colouring (Boonstra, 1975).

2.2.1 (b) Channel process

This method forms carbon black by bringing partially combusted fuel, which is generated with natural gas as raw material, into contact with channel steel (H-shaped steel) and then collecting the carbon black which results (Boonstra, 1975). There are yield and environmental issues around this method, and therefore has lost the leading role as the mass production process to the furnace process. This method, however, provides carbon black with many functional groups on the surface, being used in some painting applications.

2.2.1 (c) Acetylene black process

This process obtains carbon by thermally decomposing acetylene gas. It provides carbon black with higher structures and high crystallinity, and is mainly used for electric conductive agents (Boonstra, 1975).

2.2.1 (d) Lamp black process

This method obtains carbon black by collecting soot from fumes generated by burning oils or pine wood (Blow and Hepburn, 1971). This method has been used since the days before Christ, and is not suitable for mass production. However, it is used as raw material for ink sticks as it provides carbon black with specific colour.

2.2.2 Non-black fillers for rubber

The non-black fillers for rubber are calcium carbonate, kaolin clay, precipitated silica, talc, barite, wollastonite, mica, precipitated silicates, fumed silica, diatomite and a host of biological/agricultural by-products. The three most widely used, by volume and by functionality, are calcium carbonate, kaolin clay and precipitated silica.

A rubber compound contains, on the average, less than 5 Kg/cm of chemical additives per 100 Kg/cm of elastomer; while filler loading is typically 10-15 times higher. Amongst the ingredients used to modify the properties of rubber products, the filler often plays a significant role. Most of the rubber fillers used today offer some functional benefit that contributes to the processability or utility of the rubber product. Styrene butadiene rubber, for example, has virtually no commercial use as an unfilled compound (Boonstra, 1979).

2.2.3 Principal characteristics of rubber filler

The characteristics which determine the properties filler will impart to a rubber compound are: Particle Size, particle surface area, particle surface activity and, particle shape.

Surface activity relates to the compatibility of the filler with a specific elastomer and the ability of the elastomer to adhere to the filler. Functional fillers transfer applied stress from the rubber matrix to the strong and stiff mineral. It seems reasonable then that this stress transfer will be better affected if the mineral particles are smaller, because greater surface is thereby exposed for a given mineral concentration. And if these particles are needle-like, fibrous or plaity in shape, they will better intercept the stress propagation through the matrix (Herrara-Franco *et al.*, 1997).

A compound's physical/mechanical properties can be strongly influenced by the matrix. For instance, an air gap between a filler particle and the matrix represents a point of zero strength. If the size of the filler particle greatly exceeds the polymer inter-chain distance, it introduces an area of localized stress. This can contribute to elastomer chain rupture on flexing or stretching. Fillers with particle size greater than 100,000 nm (100 µm) are therefore generally avoided because they can reduce performance rather than extend or reinforce (Herrara-Franco *et al.*, 1997).

The principal characteristics of rubber fillers-particle size, shape, surface area and surface activity - are inter-dependent in improving rubber properties (Herrara-Franco *et al.*, 2004). In considering fillers of adequately small particle size to provide some level of reinforcement, the general influence of each of the other three filler characteristics on rubber properties can be generalised as follows:

- (i) Increasing surface area (decreasing particle size) gives; higher Mooney viscosity, tensile strength, abrasion resistance, tear resistance, and hysteresis; lower resilience.
- (ii) Increasing surface activity (better filler-rubber bond) gives; higher abrasion resistance, chemical adsorption or reaction, modulus, and hysteresis (except silated fillers).
- (iii) Increasing surface activity (including surface treatment) gives; higher abrasion resistance, chemical adsorption or reaction, modulus, and hysteresis (except for silane-treated fillers).
- (iv) Increasing aspect ratio/structure gives; higher Mooney viscosity, modulus, and hysteresis. This will lower the resilience and extrusion shrinkage; longer incorporation time.

2.2.4 Stretch resistance characteristics

The introduction of filler into the vulcanisates provides additional resistance to elongation. A filler with low surface activity will increase resistance to elongation by the viscous drag its surface provides to the polymer trying to stretch and slide around it (Jikan *et al.*, 2008). Higher surface area, greater aspect ratio, and higher loading (the latter two effectively increasing the surface area exposed to the elastomer) will all increase the modulus. Fillers with strong chain attachments, through active sites or coupling agents, provide the most resistance to the chain extension and separation required for elongation.

The effect of filler particles on the ability of the compound to stretch can be pictured as shown in the following steps (Jikan *et al.*, 2008):

- (i) Step 1 – Before stretching, the elastomer chains are in random configuration. The existing chain will have multiple points of attachment to the filler particles, some loosely held by weak bonds, others strongly held by active sites under tension.
- (ii) Steps 2 and 3 – Resistance is the energy required to detach the chain segments from these active sites. The amount of energy required to attain maximum elongation, and then required to cleave chain-chain and chain-filler attachments, accounts for the tensile strength of a filled system of this type.
- (iii) Step 4 – After the stretching force has been removed, the elastomer chains return to their preferred random orientation, except that now they have the minimum number of points of attachment to the filler as a consequence of having been extended in Step 3. Less force would now be required to return these chains to ultimate extension, because the intermediate points of attachment that existed in Steps 1 and 2 have been eliminated.

This explains the phenomenon known as stress softening. With repeated stress-relaxation cycling, a decrease in modulus from the initial maximum is obtained. Stress softening as a temporary effect. After a period without strain, the rubber will recover most of its original modulus can be permanently lost, however, due to irrecoverable chain and bond cleavage, calcium carbonates for rubber, often referred to as “whiting”, fall into two general classifications. The first is wet or dry ground natural limestone, spanning average particle sizes of 5000 nm down to about 700 nm. The second is precipitated particle size range down to 40 nm (Jikan *et al.*, 2008).

2.2.5 Resilience and hysteresis characteristics

Resilience is essentially a measure of rubber elasticity – the ability to quickly return to the original shape following deformation. Unfilled elastomers are at their peak resilience because there is no obstacle to elastomer chain extension and contraction. The introduction of filler creates such an obstacle in proportion to the strength of the particle – polymer interaction. A compound resilience is therefore generally in inverse proportion to filler loading and reinforcement. Resilience can be considered the ratio of energy release on recovery to the energy impressed on deformation (Additives, 2004).

Hysteresis can be considered as the amount of impressed energy that is converted to heat instead of mechanical energy as elastic rebound. In unfilled rubber the conversion to heat energy is related to the friction of elastomer chains sliding past each other. Fillers increase hysteresis from polymer filler friction and the dislodging of polymer segments from filler surfaces (Additives, 2004).

Reinforcing fillers, which adhere more strongly to the elastomer chains, usually provide the greatest increase in hysteresis. Notable exceptions are silane-treated kaolin and precipitated silica.

2.2.6 Abrasion resistance characteristics

Filler particles are considerably harder than the surrounding matrix and can thus insulate the rubber against wear. Filler size, shape and matrix adhesion therefore also affect abrasion resistance. Loss of large or poorly bound filler particles by abrasion exposes the relatively soft surrounding elastomer matrix to wear. The effect is acute on the edge of the depression left by the dislodged particle. This is the area most susceptible to elongation, crack initiation and ultimate loss (Ismail *et al.*, 2002; Hong *et al.*, 2007).

2.2.7 Tear resistance characteristics

Tear resistance is essentially a measure of resistance to the propagation of a crack or slit under tension. Large or poorly bound fillers will act as flaws and initiate or propagate cracks under test conditions. Small particle size, high surface area, high surface activity and high aspect ratio allow the filler particles to act as barriers to the propagation of micro cracks, in addition to providing the higher tensile strength required to resist failure (John and Samuel, 2010).

2.3 Lignocellulose Biomass Nature of Coconut Shell and Fibre

Lignocelluloses mainly consist of cellulose, hemicelluloses, and lignin which are bonded together by covalent bonding various intermolecular bridges, and Van der Waal's forces forming a complex structure, making it resistant to enzymatic hydrolysis and insoluble in water (Sullivan, 1997). Lignocellulosic biomass includes all plants and plant derived materials, including agricultural crops and trees, wood and wood residues, municipal residues, and other residue materials (Ayeni *et al.*, 2013).

The cellulose (40 – 55% of total feedstock dry matter) is a glucose polymer linked by β – 1, 4 glycosidic bonds with the degree of polymerisation from 10,000 in native wood to 1,000 in bleached kraft pulps. The basic building block of this linear polymer is cellobiose, a glucose-glucose dimer. Cellulose has a tendency to form intra – and inter – molecular hydrogen bonds by the hydroxyl groups on the linear cellulose chains, which stiffen the straight chain and promote aggregation into a crystalline structure and give cellulose a multitude of partially crystalline fibre structures and morphology. Hydrolysis of cellulose results in individual glucose monomer. This process is also known as saccharification. Its density and complexity resist hydrolysis without preliminary chemical or mechanical degradation or swelling.

In nature, cellulose is usually associated with other polysaccharides such as hemicellulose (xylan)/or lignin. It is the skeletal basis of plant cell walls (Ademark *et al.*, 1981). It contains both crystalline (70%) and non-crystalline or amorphous (30%) structure. Hemicellulose (24 – 40% of total feedstock dry matter) is a short, highly branched polymer of five carbon (C₅) and six carbon (C₆) sugars. Specifically hemicellulose contain xylose (xylose has acidic group glucuronic acid which makes it more resistant to enzymatic hydrolysis) and arabinose (C₅) and galactose, glucose, and mannose (C₆). It is more readily hydrolysed compared to cellulose because of the branched amorphous structure. A major product of hemicellulose hydrolysis is the C₅ sugar. The monosaccharides released upon hemicellulose hydrolysis include a large fraction of pentose (Mod *et al.*, 1981).

Lignin is a highly cross-linked phenyl propylene polymer and the largest non-carbohydrate fraction of lignocelluloses. It's the third major component of lignocellulosic biomass. In wood biomass it makes up 25- 36% depending on the type of wood. It plays an important role in cell wall structure as a permanent bonding agent among plant cells. Unlike cellulose, lignin cannot be de-polymerized to its original monomers. Lignin and hemicellulose form a sheath that surrounds the cellulosic portion of the biomass. Lignin protects lignocelluloses against insect attack. This complexity has made it as resistant to detailed chemical characterisation as it is to microbial degradation, which greatly impedes the understanding of its effects. Cellulose, hemicellulose, lignin and the other components are ordered in varying composition in the different parts of the fibre wall depending on the species of biomass. Extractives include non-structural components that are non-chemically bound components of biomass such as sucrose, nitrate/nitrite, protein, ash, chlorophyll, waxes. The extractives are removed because they potentially interfere with downstream analysis of biomass

sample. Gravimetric analysis describes a set of methods for the quantitative determination of a sample or material based on the mass of a solid (Ayeni *et al.*, 2013 and Ayeni *et al.*, 2014).

2.4 Filler–Polymer Interactions

Filled vulcanisates compared with pure gum vulcanisates, of otherwise, of otherwise identical formulation and cured to their optimum, shows two important characteristics differences: the modulus at 300% strain is greatly increased, and the swelling of the elastomer in solvents is reduced. Both modulus and swelling are used to determine crosslink density. The modulus is related to crosslink density by the well-known formula from the kinetic theory of elasticity (Flory, 1953).

Swelling involves diffusion of relatively small, mobile molecules into a system of chain segment. The chain segments are considerably larger than the diffusing molecules, compatible with them, but bound by strong valence links to an insoluble three-dimensional network. At the start of the process, the rubber at the surface of a component has a high liquid concentration while the liquid concentration in the bulk of the component is zero. Subsequently, the liquid molecule diffuses into the rubber just below the surface and eventually into the bulk of the rubber. As the diffusion process proceeds, the dimension of the rubber component increases until the concentration of the liquid is uniform throughout the component and equilibrium swelling is achieved (Boonstra, 1975).

Evidently, for a given solvent, the higher the crosslink density of the rubber the lower the swelling, and conversely, for a given degree of crosslink density, a more powerful solvent will give a higher degree of swelling. The relationship is quantitatively expressed by the Flory–Rehner equation (Flory and Rehner, 1943):

$$V = [\ln(1 - V_r) + V_r + XV_r^2] / [V_s X (V_r^{1/3} - V_r/2)] \quad 2.1$$

Eqn. (1) is used frequently to calculate V_r , the crosslink density, from swelling measurements. In this equation, V_s is the molar volume of the solvent, and V_r is the volume fraction of rubber in the swollen gel; X is the interaction parameter – for natural rubber. It is usually of the order of 0.4 in good solvents. The x -parameter can be determined from the cohesive energy density of solvent and polymer (Boonstra, 1975).

If this equation is applied to rubbers containing reinforcing fillers, one finds that V_{rf} of the rubber phase in the swollen gel (corrected for the volume of filler, since the filler is assumed not to swell) is always much higher than in the pure gum, V_{ro} , so that the ratio V_{ro}/V_{rf} decreases with increase of filler loading. This ratio represents the degree of restriction of the rubber matrix swelling due to interaction of the polymer with the filler (Boonstra, 1979).

2.5 Filler Carbonisation

Carbonisation is the term for the conversion of an organic substance into carbon or a carbon – containing residue through pyrolysis or destructive distillation. It is often used in organic chemistry with reference to the generation of coal gas and coal tar from raw coal. Fossil fuels generally are the products of the carbonisation of vegetable matter. The term carbonisation is also applied to the pyrolysis of coal to produce coke. Carbonisation is also a stage in the charcoal making process, and is considered the most important step of all since it has such power to influence the whole process from the growing tree to the final distribution of charcoal to various sources (Myhre and Mackillop, 2002).

In the wool processing industry, carbonisation is the name for a chemical process by which vegetable matter is removed from wool; it is part of the wool sourcing process

(Additives, 2004). Since carbonisation is a pyrolytic reaction, it is considered a complex process in which many reactions take place concurrently such as dehydrogenation, condensation, hydrogen transfer and isomerisation. Carbonisation differs from coalification in that it occurs much faster, due to its reaction rate being faster by many orders of magnitude. For the final pyrolysis temperature, the amount of heat applied controls the degree of carbonisation and the residual content of foreign elements. Carbonisation is often exothermic, which means that it could in principle be made self-sustaining and be used as source of energy that does not produce carbon dioxide (Helge *et al.*, 2000).

Carbonisation produces substances which can prove harmful and simple precautions should be taken to reduce risks. The gas produced by carbonisation has a high content of carbon monoxide which is poisonous when breathed. Therefore, when working around the kiln or pit during operation and when the kiln is opened for unloading, care must be taken that proper ventilation is provided to allow the carbon monoxide, which is also produced during unloading through spontaneous ignition of the hot fuel, to be dispersed. The tars and smoke produced from carbonisation, although not directly poisonous may have long-term damaging effects on the respiratory system. Housing areas should, where possible, be located so that prevailing winds carrying smoke from charcoal operations away from them and batteries of Kilns should not be located in close proximity to housing areas (Helge *et al.*, 2000).

2.6 Compounding and Mixing Process

The need to meet exacting end-use requirements and at the same time reduce costs is stimulating a broad spectrum of product development involving the use of fillers and reinforcements to upgrade product performance rather than the development of new and

usually more expensive resins. For example, because of their advantageous light weight, high strength, fatigue life, and corrosion resistance, structural composites have been used successfully and admirably in aircraft and in numerous industrial and consumer applications in place of conventional materials like metals (Helge *et al.*, 2000). Fibre-reinforced materials have moved within a short time from being a curiosity to having a central role in engineering materials development. Polymers, thermoplastics, and thermosets can be reinforced to produce quite frequently a completely new kind of structural materials.

Different types of fillers are employed in resin formulation; the most common are calcium carbonate, talc, silica, wollastonite, clay, calcium sulphate, mica, glass structures, and alumina trihydrate. Fillers serve a number of purposes. Inert materials like wood flour, clay, and talc serve to reduce resin costs and to a certain extent, improve processability and heat dissipation in thermosetting resins. Both alumina trihydrate and talc improve flame retardance. Mica is used to modify the electrical and heat-insulating properties of a polymer. Parts moulded from composites containing phlogopite mica as a reinforcement exhibit little or no warpage on demoulding or subjection to elevated temperature (Helge *et al.*, 2000). A variety of fillers, e.g. particulate fillers such as carbon black, aluminum flakes, and metal or metal-coated fibres may be used to reduce mould shrinkage as well as to produce statically conductive polymers, shielding of electromagnetic interference/radio frequency interference. Particulate fillers such as carbon black or silica are used as reinforcing fillers to improve the strength and abrasion resistance of commercial elastomers. Fibres such as asbestos, glass, carbon, cellulose, and aramid are used principally to improve some mechanical property/properties such as modulus, tensile strength, tear strength,

abrasion resistance, notched impact strength, and fatigue strength as well as enhance the heat-deflection temperature (Helge *et al.*, 2000).

2.6.1 Compound design

For a rubber to be useful, it must be able to function properly in given applications. The performance of a rubber is determined primarily by the composition and structure of the rubber molecules after an appropriate compound design. These control the physical, chemical, and other characteristics of the rubber material (Adhikary *et al.*, 2008). Therefore modifications of the composition of the structural units represent one of the main approaches to the modification of polymer behaviours.

In addition to the chemical nature and composition of the structural units that constitute the polymer backbone, molecular architecture also contributes to the ultimate properties of polymeric products. Thus rubber modification can be accomplished by employing one or more of the following techniques (Adhikary *et al.*, 2008):

- (i) Alloying and blending of two or more rubbers
- (ii) Control of molecular architecture
- (iii) Further chain reaction involving functional/reactive group introduced deliberately into the rubber main chain or side groups such as grafting.

2.6.2 Composites formation using fibres, fillers and selective additives

The above property modification techniques are associated with the control of the chemical composition, and structural nature of the rubber, which is effected largely during the distributive process. Rubber in its pure form is useless for engineering and other community designs. All commercially available rubber materials and products are a combination of one or more polymeric system with various additives designed, with

due consideration to cost factors, to produce an optimum property and / process profile for specific applications (Additives, 2004).

Modification of composites through the use of chemical additive and reinforcements through alloying and blending procedures and by composite are key processes in the development of rubber and rubber-like products. Here, there are three parameters that must be held to a working balance such as (Additives, 2004):

- (i) Price/cost of the additives and the final products.
- (ii) Processability and products production procedures and techniques.
- (iii) Final and expected vulcanisates properties/product performance criteria and brief.

2.6.3 Additives in compounding

A rubber compound is obtained by mixing a base polymer or crude mixture with a series of additives. The choice of the polymer and the additives closely linked to the types of properties to be achieved. The resulting product is a vulcanized compound. The quantity of additives used varies for 20- 130% as a percentage on the weight. The most common additives are (Additives, 2004):

2.6.3 (a) Fillers

There are different types of fillers and possibly different ways of classifying them. But generally, they are either reinforcing or non-reinforcing in performance. Carbon black is also commonly used as reinforcing filler. This is also the reason why most rubber products are black. Calcium carbonate is an example of non- black and non-reinforcing filler that is of wide usage in rubber products development. Three main properties of filler are (Additives, 2004):

- (i) Particle size: The diameter of Spheric particles is the fundamental property which largely affects the dispersibility when fillers mixed with resins or other vehicles. In general, the smaller the particle size; the more reinforcing the filler will be. Dispersion, however, becomes difficult due to an increase in coagulation force.
- (ii) Structure: Like particle size, the size of the structure also affects dispersibility and colour intensity of the filler. Generally, the increase of structure size improves dispersibility and possibly, excellent conductive property.
- (iii) Surface chemistry: Various functional groups exist on most filler surfaces. The affinity of the filler to the polymer changes depending on the type and amount of the functional groups. Carbon black, with a large amount of hydroxyl group given with oxidation treatment, has a greatly enhanced affinity to prints inks or varnishes, showing an excellent dispersibility.

2.6.3(b) Plasticisers

Besides fillers, plasticisers play the biggest quantity role in building a rubber compound. The reasons for the use of plasticisers are (Stella *et al.*, 2011): Improvement of flow of the rubber during processing, improved filler dispersion, influence on the physical properties of the vulcanisates at low temperatures, mineral oils and paraffins are widely used as plasticisers.

Requirements for an effective plasticiser include partial or complete miscibility with the host polymer and a low T_g . The T_g of the plasticised polymer depends upon the plasticiser concentration and the T_g of each component as estimated by a number of theoretical or empirical equation. In plasticisation, the actual reduction in polymer T_g

per unit weight of plasticiser is called the plasticiser efficiency. High efficiency indicates the glassy – to – rubbery transition to occur over a very broad temperature range (Stella *et al.*, 2011). The problem with high – efficiency plasticisers is that they can diffuse out of the polymer in time due to their low miscibility with the polymer. Plasticisers that are susceptible to migration are said to have low performance. Loss of plasticiser will lead to a gradual increase in brittleness as the T_g (and, therefore, the modulus) of the plasticised polymer slowly increases to that of the unplasticised (i.e. glassy) polymer.

When T_g reduction is obtained by compounding a polymer with a low T_g compound, The process is called external plasticisation. In some cases, plasticiser function can be obtained by copolymerising the polymer with the monomer of a low T_g polymer, such as poly(vinyl acetate). This process is called internal plasticisation.

2.6.3 (c) Vulcanisation chemicals

Vulcanisation is the conversation of rubber molecules into a network by formation of crosslink. Vulcanising agents are necessary for the crosslink formation. These vulcanising agents are mostly sulphur or peroxides and sometimes other special vulcanising agents or high energy radiation. Since vulcanisation is the process of converting the gum–elastic raw material into the rubber–elastic end product, the ultimate properties like hardness and elasticity depend on the course of the vulcanisation (Sobaike *et al.*, 2005 and Stella *et al.*, 2011).

The double bonds in natural rubber permit formation of sulphur bridges between different chains. These crosslink are responsible for removing the tackiness of untreated rubber. Vulcanised materials are less sticky and have superior mechanical properties. The term vulcanised fibre refers to cellulose that has been treated in a zinc chloride

solution to cross-link the cellulose fibres (Sombatsompop *et al.*, 2004; Sogbaike *et al.*, 2005; Stella *et al.*, 2011).

Uncured natural rubber is sticky, deforms easily when warm, and is brittle when cold. In this state, it is a poor material when a high level of elasticity is required. The reason for inelastic deformation of unvulcanised rubber can be found in its chemical structure- rubber is composed of long polymer chains. These chains can move independently relative to each other, which let the material change shape. Crosslinking introduced by vulcanisation prevent the polymer chain from moving independently. As a result, when stress is applied the vulcanised rubber deforms, but upon release of the stress it reverts to its original shape (Stella *et al.*, 2011).

By far the most common vulcanising methods depend on sulphur, sulphur, by itself, is a slow vulcanising agent and does not vulcanise synthetic polyolefin, even with natural rubber, large amount of sulphur, as well as high temperature and long heating periods are necessary and one obtains an unsatisfactory crosslinking efficiency with unsatisfactory strength and aging properties. Only with vulcanisation accelerators can the quantity corresponding to today's level of technology be achieved. The multiplicity of vulcanization effects demanded cannot be achieved with one universal substance, a large number of diverse additives, comprising the "cure package", are necessary. The combined cure package a typical rubber compound consists of sulphur together with an assortment of compounds that modify the kinetics of crosslinking and stabilise the final product. These additives include accelerators, activators like zinc oxide and stearic acid and antidegradants, the accelerators and activators are catalysts. An additional level of control is achieved by retarding agents that inhibit vulcanisation until some optimal time or temperature. antidegradants are used to prevent degradation of the vulcanised product by heat, oxygen, and ozone (Sombatsompop *et al.*, 2004).

2.6.3 (d) Acceleration agents

Acceleration agents increase the rate of the cross-linking reaction and lower the sulphur content necessary to achieve optimum vulcanisates properties. In order to obtain a well-cured product, a heating time of several hours, sometimes up to eight hours, was required and this was considered commercially unfavourable. This time, however, was considerably reduced when oxides of zinc, calcium, magnesium and lead were included in the mix. These compounds are known as vulcanisation accelerators as they speed up the rate of chemical reaction between the rubber and the sulphur and consequently maximum strength is reached in a shorter length of time or at a lower cure temperature or both (Stella *et al.*, 2011).

In addition, less sulphur is used in the vulcanisation. Inorganic accelerators are of little practical importance today in the face of a huge range of organic accelerators. Accelerators may be classified by their acidic or basic nature or by the speed with which they accelerate certain rubber-sulphur reaction. No single classification made is suitable for all cases because accelerators do not behave the same way in each rubber compound. However, classification based on speed of activity is preferred since it is of greater practical importance (Sogbaike *et al.*, 2005).

2.6.3 (e) Activators

Like zinc oxide and stearic acid, they activate the vulcanisation process and help the accelerators to achieve their full potential. It is thought that activators form intermediate complexes with the accelerators which activate the sulphur in the mixture. They are grouped into inorganic activators which are mainly metal oxides, organic activators which are mainly fatty acids such as stearic, oleic, lauric, palmitic and myristic acids, and alkali substances such as ammonia, amines and salts of amines with weak acids.

Among inorganic activators are zinc oxide which is the most common, litharge, red lead, white lead, magnesium oxides, alkali carbonates and hydroxides, and hydrated lime. The quantities normally used are 3-5 pphr of inorganic activators (Sogbaike *et al.*, 2005).

The vulcanising agents, accelerators and activators, constitute the curing system or curatives. A formulation consisting only of the elastomer and curatives is known as the pure-gum mix. Addition of carbon black or other fillers is termed loading and the compound loaded stock (Stella *et al.*, 2011).

2.6.3 (f) Antidegrading agents

These agents increase the resistance to attacks of ozone, UV light and oxygen. Antidegradants are used to protect rubber products from a variety of deteriorating influences during their service life. Deterioration leads to loss in physical properties such as loss of strength, hardening or softening, cracking, surface crazing and chalking. It is caused by chain scission, cross-linking or changes in the polymer structure. This is largely the result of oxidation by atmospheric oxygen or ozone, accelerated by heat, light, exposure to solvents, flexing and certain metals (Sombatsompop *et al.*, 2004).

The mechanism of oxidative degradation is fairly well understood and is typically a chain process. Typical anti-oxidants used to protect elastomers are sterically hindered phenols and amines such as phenyl-betanaphthylamine, PBNA (or PBN) and butylated hydroxytoluol, BHT, and phosphites. They are classified as staining or non-staining depending on whether or not they cause darkening of white or light coloured articles. Two important considerations in selecting antioxidants are toxicity and colour formation. In general, the amines are efficient but they stain materials and are toxic.

Phenolics and phosphites have low efficiency, minimum or no stain and some are non-toxic, for example, BHT, hence they are used in food applications (Stella *et al.*, 2011).

2.6.3 (g) Processing aids

These are class of chemicals which improve the process ability. The process aids or softeners must be completely compatible with the rubber and other compounding ingredients. Softeners act in a physical manner by getting between the long-chain molecules as lubricants would, spread them apart. They include fatty acids, vegetable oils, tar products, petroleum oil and waxes, pine products, factice and coumarone resins (Additives, 2004).

Processing aids such as factice controls die swell during processing, prevents shape distortion during vulcanisation and controls 'nerve'. Nerve is the elastic memory and/or orientation effects due to strains and stresses imparted during milling, calendaring, extrusion or moulding operations. This reduction in nerve leads to easier dispersion and incorporation of powders into rubbers. Larger amounts of factice serve as extending filler, especially where a product which will float in water, a floating compound, is required (Additives, 2004).

2.6.3 (h) Pigments

Organic and inorganic pigments are used to colour rubber compounds. The colour pigments are also considered inactive fillers (Additives, 2004).

2.6.4 Mechanism of mixing

The process of mixing refers to the alteration of the original distribution in space of a non-random collection of components and increases the probability of finding a particle of any one component at any particular point, so that an acceptable spatial probability

distribution is achieved. Thus mixing is an operation where two or more components of a mixture or other appropriate level to an acceptable degree, so that the random or entropy of a mixture is increased without affecting the physical state of the components.

The mixing of rubber involves the following stages of operations (Blow and Hepburn, 1971; Additives, 2004): Viscosity reduction, distributive mixing, incorporation and dispersive mixing.

Elastic rubber on being fed into the mixer has to be rapidly converted to a viscous state, which will accept the particulate additives. This stage is called viscosity reduction, which can be achieved by temperature rise, chain extension and mastication. The elastic stiffness of the rubber requires considerable mechanical energy to deform it. This is converted by heat causing a rapid rise in temperature and thus viscosity reduction. In natural rubber, viscosity is irreversibly changed by chain scission, but the chains are recoverable when the viscosity is changed by temperature. The viscosity reduction by chain scission (mastication) influences mixed compound behaviours and has to be controlled. Rubber after viscosity reduction can be made to incorporate and enclose the additive, which will depend upon free surface folding flows (Additives, 2004 and Stella *et al.*, 2011).

Incorporation and distributive mixing takes place simultaneously, which also reduces the size of the volume of additives. The rubber flows around filler particle agglomerates and penetrates between the particles in the agglomerate. This reduction increases the viscosity. The incompressibility of the mixture allows high forces to be applied to particle agglomerates causing them to fracture. This action is known as dispersive mixing and will continue. The forces being applied to the particle are agglomerates of filler and the products are sufficient to cause fracture (Stella *et al.*, 2011).

These forces are progressively reduced as the occluded rubber is released and the size of the agglomerates is reduced. With the increase in temperature due to mixing, the viscosity will be further reduced and the efficiency of dispersive mixing will decrease more rapidly. It is observed that increasing of rotor or screw speed does not improve dispersive mixing and increase of temperature deteriorates it. This may be due to non-Newtonian behaviours of rubber (Additives, 2004 and Matador, 2007).

Distributive mixing occurs concurrently with dispersive mixing which separates the fragments of agglomerates once they are fractured. Additives in the form of pellets, flakes or other forms are rapidly incorporated. In case chain scission (mastication) is not carried out, mixing time is governed by distributive mixing where large size particles are used and by dispersive mixing where reinforcing fillers or carbon black is used. The smaller the volume fraction of additive particles, the more mixing is needed to ensure uniform, distribution of additives (Matador, 2007).

2.6.5 Mastication process of rubber

Mastication is a process during which the elastic rubber achieves plastic properties. During mastication breaking of chemical bonds in its macromolecules take place by means of high shear forces. This process results in the decreasing of molecular weight and viscosity of rubber and consequently it becomes treatable. Mastication of NR is performed either at low temperature on mills or at higher temperature in closed mixers, often in the presence of Peptisers (they act as donors of electrons or hydrogen), that increases its efficiency. Besides mechanical degradation of rubbery macromolecules also their oxidation degradation occurs in this process and its rate is upgraded with mastication temperature increasing (Blow and Hepburn, 1971).

Mastication of the NR is most efficient at temperatures below 60-70⁰C and above 120-130⁰C, its efficiency is low in interval between these temperatures. Mastication of synthetic rubbers is much less efficient, and thus they are either produced with the molecular weight and viscosity suitable for their processing or they are modified in final production stages by means of suitable oils (e.g. SBR extended by oil). Advantage of such modification is in possibility to keep the high molecular weights, that normally afford better physical-mechanical and dynamic properties to vulcanisates and also processing of rubbers is good (Boonstra, 1975).

High masticated rubber is used in friction compounds like sponges, rubber solutions or cements. Medium plasticised rubber is used in calendaring compounds and lightly masticated rubber is used for stiff compounds. The breakdown of rubber is carried out either in a roll mill, an internal mixer or a screw plasticator. Generally a chemical plasticiser is added to the rubber when masticating in an internal mixer or plasticator. These plasticisers are found to work better at elevated temperatures (Blow and Hepburn, 1971; Boonstra, 1975).

2.6.6 Principle of compounding

The object of compounding rubber or elastomer is to modify it physically or chemically either by mixing additives or other elastomers. The melting or softening behaviour and packing and adhesion properties of rubber or elastomer and additives, and the melt flow behaviour are very important. Thus, compounding requires not only appropriate relative movements of the volume elements of the components, but also heat have to be supplied to the system (Boonstra, 1979).

Softening or melting behaviour will depend on the chemical structure, which will not only be determining the transition temperature of the rubber and additives, but also

properties like specific heat, thermal conductivity and diffusivity. Moreover, variation in particle size will generally permit the particles to peak more closely. Thus increased surface is available for heat transfer from one particle to another. The heat transfer will also be affected by the shape of the particles. It is experienced that the additives of low compatibility with rubber will tend to concentrate on the surface of the particles and to interfere with adhesion (Additives, 2004).

Keeping in view the above points, it is essential to select the most suitable combination of material in their correct proportions, based on treatment that the combination will be required to and undergo, to obtain the end products of desired properties. The most important additive, apart from lubricants antistatic agents and slip agents, is the filler material (Additives, 2004).

2.6.7 Rheological determination

The preparation of rubber compound is influenced by several factors that influence the results obtained such as (Jikan *et al.*, 2008):

- i. Variability in the quality of the ingredients: Polymer, vulcanising agent, cure activator, cure accelerator, fillers (reinforcing, diluents), softener/process aids/tackifiers, plasticiser, protective agent(s), miscellaneous ingredients (pigments, blowing agent, etc.).
- ii. Variability originated by the weighing system (automatic or manual) used for the ingredients.
- iii. Variability originated by the environmental conditions (temperature and humidity) which influence the dispersion and the activity level of the ingredients.

- iv. Variability originated by the mixing parameters (time and temperature).
- v. In addition, the characteristics of the compound change significantly when the product is stored.

All the influence factors described above has a considerable effect on the characteristics of the compound produced. In many cases the variations are small and do not have a significant effect on the results obtained after the transformation of the compound into finished products (Patternman, 1986; Jikan *et al.*, 2008).

In any case, compound producers, even with automatic weighing system, statistically produced between 1% and 5% of non-conforming compounds that require additional re-work activity to correct the defects.

It is very important that the non-conforming compounds are identified as quickly as possible in order to (Additives, 2004):

- (i) Remove the reason of the default and avoid the production of more non-conforming products.
- (ii) Prevent the non-conforming products from being transferred to the next production stage.

One of the biggest differences between rubber and other products is the fact that many of the defects in the compound; such as dispersion problems or mistakes in the dosage of accelerators can be invisible during the transformation process and be detected only when the final product is used. For this reason, the final cost for a non-detected defect can be very high (Additives, 2004).

Normally a test of the compound made with a Rheometer permits to identify most of the possible problems in a rubber compound. The test only takes a few minutes (generally

between 3 and 5 minutes) and is normally done on 100% of the batches (Additives, 2004).

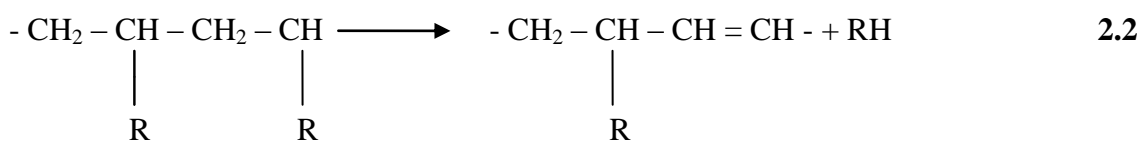
This instrument permits to measure the change of the properties of a rubber compound during the course of vulcanisation. Rheometer permit to apply a cyclic strain to a test piece and the associated force is measured. The test is carried out at a pre-determined constant temperature and the measure of stiffness is recorded continuously as a function of time. The two types of the Rheometer existing presently are (Additives, 2004): Moving die rheometer (MDR) and oscillating disk rheometer (ODR).

2.6.8 Rubber degradation processes

Rubbers deteriorate through a complex sequence of chemical reactions resulting from the separate or combined effects of heat, oxygen, and radiation. In addition, rubbers may be susceptible to attack and mechanical failure on exposure to water (hydrolysis) or a variety of chemical agents. Molecular weight is changed considerably in most of these reactions by chain scission and/or cross-linking. However, deterioration can also occur without significant change in the size of the rubber molecules (Thwe and Liao, 2002).

2.6.8 (a) Non-chain-scission reactions

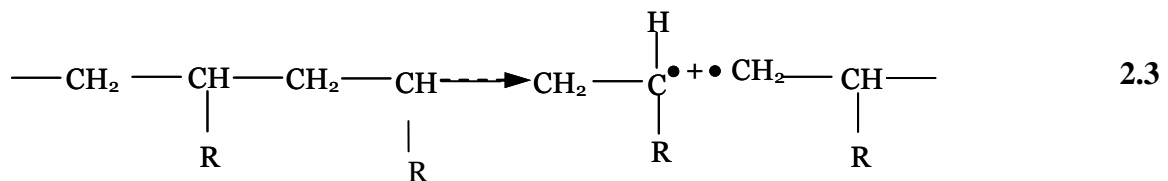
Non-chain-scission reactions resulting, for example, from the application of heat, involves elimination of a small molecule – usually a pendant group – leaving the backbone essentially unchanged as seen in Eqn. (2.2).



Rubbers are susceptible to thermal degradation as often as in other polymers experiencing a non-chain-scission reaction such as Poly (vinyl acetate). When heated at elevated temperature, PVA_C can liberate acetic acid, which is followed by Polyene formation (Thwe and Liao, 2002).

2.6.8 (b) Chain-scission reactions

The chemical bonds in a polymer backbone may be broken with the generation of free radicals by heat, ionising irradiation, mechanical stress, and chemical reactions as represented in Eqn. (2.3).



Chain can occur by one of three mechanisms. These include (Thwe and Liao, 2002):

- (i) Random degradation, where the chain is broken of random site.
- (ii) Depolymerisation, where monomer units are released at an active chain and
- (iii) Weak-link degradation, where the chain breaks of the lowest energy bonds.

In addition to thermal energy, degradation may be initiated by photochemical action, irradiation or mechanical action. Random hemolytic cleavage of a polymer chain will result in a complex mixture of low-molecular-weight degradation products. Polyethylene and Polypropylene degrade in this manner also (Thwe and Liao, 2002; Vignesh *et al.*, 2013).

2.6.8 (c) Oxidative degradation

In practice oxidative ageing may occur within the time scale of an experiment or more importantly, within the time scale of desired service of a rubber component. Such long-term ageing can lead to chain scission and breakdown of networks in the case of natural rubber vulcanisates and can be monitored and studied by the use of stress-relaxation techniques. Any such analysis assumes that slippage in the unaged network is negligible. If however chain scission occurs, then the stress required to maintain a constant extension will drop (Thwe and Liao, 2002).

In treatment of rubber elasticity in uniaxial tension, the Gaussian theory of rubber elasticity leads to the following relationship between tensile stress (\mathbb{T}) and extension ratio (x) (See Eqn. (2.4) (Tabsan *et al.*, 2010):

$$\mathbb{T} = G \left(x - \frac{1}{x^2} \right) \quad 2.4$$

Where, G is the shear modulus. The extension ratio is the extended length divided by the original length. If it is assumed that eqn. (2.4) holds and also that the shear modulus is inversely proportional to the molecular weight between cross-links, then it can be shown that (Tabsan *et al.*, 2010):

$$\mathbb{T} = \mathbb{T}_o \frac{(Mc)_o}{(Mc)} \quad 2.5$$

Where, (\mathbb{T}_o) and (\mathbb{T}) are stresses required to maintain a constant strain before and after ageing and $(Mc)_o$ and Mc are the molecular weight between cross-links before and after ageing. It can thus be seen that the decay in stress at constant extension during ageing provides a direct measure of the degradation of the elastic network. Two types of stress relaxation measurement may be thus distinguished (Sywatthana and Cattaleeya, 2010): continuous stress relaxation measurements, intermittent stress relaxation measurements.

In the continuous relaxation experiment, the extension is maintained throughout experiment. If in addition to the chain scission reactions, cross-linking occurs then although the original network will be under strain the “new network”, i.e. the contribution made to the overall network by the new cross-links will be under strain and will therefore not be part of the stress supporting network. It will therefore make no contribution to the overall network by the new cross-links; it will not be under strain and will therefore not be part of the stress supporting network. It will therefore make no contribution to the magnitude of the stress (Sywatthana and Cattaleeya, 2010).

If the sample is strained only in order to make a measurement but for most of the time is held at rest (intermittent stress relaxation), then most cross-links formation will occur when the sample is at rest, and this will contribute to the stress supporting networks. The difference obtained in continuous and intermittent experiments thus provides a measure of the extent of cross-link during oxidation (Tabsan *et al.*, 2010; Sywatthana and Cattaleeya, 2010)

2.6.8 (d) Ozone cracking

The most common characteristics of atmosphere ozone attack are the formation of cracks perpendicular to the direction of stress in a strained piece of rubber. However, where the sample is stressed simultaneously in two directions, as can happen in a tyre sidewall, small square crack patterns may occur which could be confused with photo-oxidative degradation (Additives, 2004).

The severity of ozone attack on a rubber compound does not simply depend on the type and level of anti-ozonant used. Obviously the choice of rubber will be very significant, but also important are the conditions under which the product will be used. Exposure of a diene rubber vulcanisates to atmospheric ozone will cause cracks to occur in a

direction perpendicular to the applied stress. It has been observed that a number of cracks increase as the extension increases. If many cracks are formed, they tend to interfere with each other and reduce stress concentrations, on the other hand, if there are few cracks catastrophic failure can occur; the problem is often greatest at low strains (Additives, 2004).

2.6.8 (e) Stages of ozone cracking

Ozone cracking has two stages namely; crack initiation stage, crack growth/propagation stage. There is a threshold stress below which cracking did not occur and this varies with the square root of the modulus of the elastomer. The rate of crack initiation in NR reaches a maximum at about 70% strain. It was also found that there was a critical stress at which crack growth reaches a maximum, equivalent to a strain of the order of 3 – 5%, and that this was inversely proportional to the cross-link density. Rates of crack growth also tend to rise with temperature and plasticiser content. It is therefore concluded that; polymer type, cross-link density, vulcanisate modulus and levels of stress and strain in service are all import to the successful use of a rubber in the presence of atmospheric ozone (Additives, 2004).

2.7 Physico-Mechanical Properties of Rubber

Every formulation and composites prepared thereof is always targeted at achieving certain end use designs and properties. Modification at appropriate levels keeps these properties at their optimum in a prescribed application. Some of these key properties are explained in the following sub-sections (Additives, 2004):

2.7.1 Hardness

Hardness is the measure of how resistant solid material is when a force is applied. There are three main types of hardness measurements; Scratch indentation and rebound. We

will only be talking about the indentation hardness for elastomers. Indentation hardness is the materials resistance to indentation by an indenter.

Rubber is made in different hardness for several reasons. Some sealing surfaces may not be totally smooth. The little voids, pits and scratches allow a pathway for fluid or air to escape through. Softer materials tend to flow better into these voids and imperfection on the sealing surface creating a better seal. On the other hand, harder rubbers will not do this as well but they do resist extrusion cause by high pressures. Also, coefficient of friction is also affected by the hardness of the rubber. Softer rubber has a lower coefficient of friction. Coefficient of friction plays a factor when the rubber seal is sealing a part that moves (Brydson, 1978; Additives, 2004).

2.7.2 Abrasion resistance index

Abrasion resistance is a performance factor of paramount importance for many rubber products, such as tyres, conveyor, belts, power transmission belts, hoses, footwear and floor covering. A test capable of measuring resistance to abrasion of rubber, including uniformity of wear behaviour under abrasive/frictional service conditions is therefore highly desirable (Hong *et al.*, 2007).

This test method may be used to estimate the relative abrasion resistance of different rubbers. Since conditions of abrasive wear in service are complex and vary widely, no direct correlation between this accelerated test and actual performance can be assumed. This test method is suitable for comparative testing, quality control, specification compliance testing, referee purposes, research and development work (Burfield *et al.*, 1984; Hong *et al.*, 2007).

2.7.3 Compression set strength and deflection

The purpose of the compression set test is to measure the ability of the rubber specimen to retain its elastic properties after compressive forces have been applied for a prolonged period of time at elevated temperatures. Compression set results can be useful to know when rubber seals, mounts or dampeners are subject to compressive forces in the application (Viksne *et al.*, 2010). This is particularly important when the seal is in a prolonged compressed state and even more so when simultaneously being exposed to elevated temperatures. When an O-ring is squeezed the rubber has elasticity. It wants to go back to its original shape. This elasticity is how the O-rings seals, especially under low or no pressure. When pressure is applied to the system the O-ring seal pushes against the groove wall opposite the direction of the pressure, forcing it to expand perpendicular to the direction it is being squeezed. This expansion provides additional sealing capability.

When an O-ring is squeezed and subjected to excessive heat it can lose some or all of its elasticity and take a permanent set. Then, when you pull the O-ring out it no longer has a nice round cross section but instead has flat spots where it was squeezed in the application. This permanent set will reduce the sealing ability of the O-ring. The compression set test is a great way to see how the compound will react to compressive forces while subjected to heat. Also, poor compression set along with poor tensile strength can be an indication of the state of cure of the specimen. If you do not cure the compound enough these properties will diminish (Liang *et al.*, 2010; Liang, 2011).

2.7.3 (a) Measuring compression set

The specimen, usually a molded rubber disk, is squeezed between two metal plates to about 75% of its original thickness and then placed in an oven at elevated temperatures

for a period of time. Specimens are allowed to cool and measurements percentage of original deflection calculated.

The original deflection is the amount you compressed the specimen in the fixture. If you have a 1 cm thick specimen and compress it to 0.750" thickness, the original deflection is 0.250". Now let's say the 1 cm thick sample measured 0.875" thick after the test. It took a 0.125" set. 0.125 is 50% of the original deflection of 0.250" or a compression set of 50%. The higher the percentage recorded, the poorer the results. Compression tests are covered under the ASTM D2000 specification method (Liang, 2011).

2.7.3 (b) Compression-deflection

The purpose of the compression-deflection test is to compare the stiffness of the rubber materials under a compressive force. This test can tell you how much a part will deflect under a given load or, alternatively, how much load it will take to deflect a part within a given distance. Rubber mounts and dampeners are some examples of parts that are subject to compressive forces and knowing the relationship between compressive forces and deflection can be important (Lin *et al.*, 2002).

2.7.3 (c) Measuring compression-deflection

Compression-deflection is measured on a compression testing machine or can be measured on any other type of machine that can apply a measurable force to a specimen at a given rate and be able to measure the deflection to one thousandths of an inch. The last is performed by compressing the specimen to a specified compressive force and measuring the deflection results or compressing to a specified deflection and measuring the compression force result (Lin *et al.*, 2002).

2.7.4 Tensile strength and tensile set

Ultimate tensile strength, or just tensile strength, is the maximum force a material can withstand without fracturing when stretched. It is the opposite of compressive strength. Tensile strength is an indication of how strong a compound is. A few rubbers that tensile strength is important would be bungee cords, rubber tie downs, drive belts. Some elastomeric compounds, like silicon, have a low tensile strength making them unsuitable for dynamic types of seal because they can fracture easily (Rana *et al.*, 2003; Pradhan *et al.*, 2004)

2.7.4 (a) Measuring tensile strength

Tensile strength is measured with a tensometer. A tensometer is special machine that is designed to apply a tensional or compressive force to a specimen, in our case a die cut dumb bell shape, and measure how much force it takes to deform and fracture the specimen. The force is typically displayed on a stress-strain curve that shows how much force was required to stretch the specimen to deformation and ultimately break (Rana *et al.*, 2003).

2.7.4 (b) Tensile set

Tensile set is the extension remaining after a specimen has been stretched and allowed to relax for a predefined period of time. Tensile set is expressed as the percentage of the original length. Tensile set results are not found on the stress-strain curve. It is a measurement that can be performed after the tensile strength test. Tensile set is different from the elasticity of the material. Elasticity is the mechanical property of a material to return to its original shape while tensile set is the amount on extension remaining after been stretched (Pulford, 1983; Ramaraj, 2006).

2.7.4 (c) Measuring tensile set

To determine tensile set after break, wait 10 minutes after the specimen breaks and then fit the two halves of the specimen back together so there is good contact along the full length of the break. Measure the distance between the bench marks, this will give indication of the tensile set. Another way to test without breaking is to stretch the specimen to a specified elongation and hold for 10 minutes. Release the specimen as quickly as possible, and let it sit for 10 minutes. Measure the distance between the bench marks, and evaluate tensile set (Pulford, 1983).

2.7.5 Elongation at break

Maximum elongation with respect to tensile testing is the measure of how much a specimen stretches before its breaks. Elongation is usually expressed as a percentage.

2.7.5 (a) Measuring elongation

Elongation is measured with a ruler or an extensometer. An extensometer is an electronic ruler that is attached to the tensometer and will measure the extension of the specimen while torsional force is being applied. Another way of measuring elongation is with a regular ruler. To measure the elongation with a ruler, make two bench marks 1 inch apart on the specimen. This is the initial gauge length (L_0) and then measure the distance between the marks just before the specimen breaks. This is the final gauge length (L_x). Calculate the elongation with the following equation (eqn. 2.6) (Roberts, 1988; Roger, 2002).

$$\text{Elongation}\% = 100(L_x - L_0) / L_0 \qquad \qquad \qquad 2.6$$

2.7.6 Young's modulus

Young modulus is also known as tensile modulus, elastic modulus and modulus of elasticity. It is the measure of the stiffness of the material. When performing a tensile

strength test, a plot is made of the stress versus strain or amount of force required to stretch (deform) the specimen given length. This plot is called a stress–strain curve. The peak of the curve is the tensile strength and the Young’s modulus is the slope of the stress–strain curve. If the curve is steep; the specimen resists deformation, making it tougher. But if the slope is gentle the material will deform easily. At any given point on the stress–strain curve the tangent modulus can be read. Knowing how easily a material deforms under strain can be important in some applications (Additives, 2004; Vilay *et al.*, 2008).

2.7.6 (a) Measuring young’s modulus

Young’s modulus is measured during a tensile strength test. A stress–strain curve is plotted when performing a tensile strength test. The slope of this curve is the Young’s modulus and any point on that curve is a tangent modulus (US Army, 2002; Additives, 2004).

2.7.6 (b) Yield point

Yield point is the force at which the specimen starts to deform permanently. It is difficult to point to the exact yield point on the curve because the transition is gradual, so a 2% offset (0.2% for metals) from the linear elastic region is used to indicate the offset yield strength. Although yield strength is meant to show the exact point where the specimen becomes permanently deformed, a 2% offset is an acceptable sacrifice because of how much easier it makes it to determine yield strength (Takashi *et al.*, 2007).

Just prior to the yield point is the linear elastic region. The slope of the line in this region is called Young’s modulus. This is the area which the specimen retains its elasticity. When the force is removed in this area the specimen will return to its original shape. After this area the specimen transits from elastic to plastic behaviour. This means

that after the yield point, permanent deformation occurs in the specimen and it will no longer return to its original shape (Rout *et al.*, 2001; Additives, 2004).

2.7.7 Tear strength/resistance

The tearing of rubber is a mechanical rupture process started where forces are concentrated in an area usually caused by a cut, defect or deformation (Rout *et al.*, 2001).

2.7.7 (a) Measuring tear resistance

Tear resistance is tested on a tensometer in the same manner as the tensile strength test except the specimen is one of 5 specific shapes: type A, B, C, T or CP. A graph is produced in the same manner as the stress-strain curve except the Tear strength graph is forced over jaw separation length. Tear strength is calculated by taking the maximum force divided by the median thickness of the specimen using eqn. (2.7) (Rana *et al.*, 2003).

$$TS = F/d$$

2.7

Type A – crescent shaped specimen with a nick or cut

Type B – tab end specimen with a nick or cut

Type C – right angle specimen with a nick or cut

Type T (trouser) – moulded block, 150 x 15 x 2 mm with a 40 mm cut.

Type CP (constrained path) – moulded specimen 125 x 28.5 x 5.33 mm. This is a special moulded shape with fabric reinforcement moulded in the mid-plane of the sample. The specimen has a narrow groove down the length in the centre.

2.7.8 Weathering/ozone resistance

Ozone (O₃), resistance is used to test the relative ability of the rubber compound to resist outdoor weathering or ozone chamber testing. Some applications like door and window trim would be subject to weathering so testing would give an estimation of how the rubber compound will react to weathering. Other sources of ozone exposure include air purifiers and ozone generators used to purify, deodorize, disinfect and kill bacteria in just about everything from air to food (Pulford, 1983).

2.7.8 (a) Measuring weathering/ozone resistance

ASTM method D1171 addresses how to test weathering and Ozone resistance. In D1171, rectangular cross section samples are wrapped around a wooden mandrel and left in the sun or placed in an ozone chamber. After a period of time either method “A” or method “B” is used to grade the samples. In method “A” no cracking is permitted fewer than 2 x magnifications and in method “B”, three samples are checked and graded depending on the severity of cracking and given a quality retention value (expressed as a percentage). ASTM method D1149 is used to test the effects of specific levels of Ozone concentration on specimens that are under dynamic or static surface strain conditions (Pulford, 1983; Rowel, 2005).

2.7.9 Flexural testing

This test is performed in accordance with ASTM method D790 to measure the flexural modulus. Many brittle materials are flexed to the breaking point in order to measure the flexural strength. The test is stopped when the specimen reaches 5% deflection or the specimen breaks before 5% deflection is reached. The flexural test measures the force required to bend a beam at a specific rate (Stokke *et al.*, 2001). Flexural force required to bend a beam at a specific rate. Flexural modulus is an indication of a material's

stiffness when bent on a three-point apparatus. The three point bending fixture support the specimen and the load is applied to the centre by the loading nose producing three point bending at a specified rate. The main parts of this test are specimen depth (thickness), the support span, the speed of the loading and the maximum deflection for the test (Stokke *et al.*, 2001).

Bending tests compliant with ASTM standards and deflection measurement during bending test can be conducted to high precision. Various test specimen thicknesses can be accommodated by replacing the punch and supports of the bending Jig, enabling compatibility with different types of standards (Stokke *et al.*, 2001) Singleton *et al.*, 2003).

2.8 Qualitative Parameters Study

The chemical analysis of polymers is not basically different from the analysis of low-molecular-weight organic compounds provided that appropriate modifications are made to ensure solubility or the availability of sites for reaction. Insoluble specimens should be ground to expose a large surface area. The usual methods for functional group and elemental analysis are generally applicable, as many other standard analytical techniques (Vilay *et al.*, 2008).

2.8.1 Fourier transforms infrared spectroscopy (FTIR)

In infrared spectroscopy, IR radiation is passed through a sample. Some of the infrared radiation is absorbed by the sample and some of it is passed through (transmitted). The sample resulting spectrum represents the molecular absorption and transmission, creating a molecular finger print of the sample. Like a finger print no two unique molecular structures produce that same infrared spectrum (Vilay *et al.*, 2008). This makes infrared spectroscopy useful for several types of analysis. Infrared can provide information on the following:

- (i) It can identify unknown materials
- (ii) It can determine the quality or consistency of a sample
- (iii) It can determine the amount of components in a mixture.

An infrared spectrum represents a fingerprint of a sample with absorption peaks which correspond to the frequencies of vibration between the bonds of the atoms making up the material. Because each different material is a unique combination of atoms, no two compounds produce the exact same infrared spectrum. Therefore, infrared spectroscopy can result in a positive identification (qualitative analysis) of every different kind of material. In addition, the sized of the peaks in the spectrum is a direct indication of the amount of material present. With modern soft-ware algorithms, infrared is an excellent tool for quantitative analysis (Wada *et al.*, 2001; Vilay *et al.*, 2008).

Fourier transform infrared spectroscopy is preferred over dispersive or filter methods of infrared spectral analysis for several reasons?

- (i) It is a non-destructive technique
- (ii) It provides a precise measurement method which requires no external calibration
- (iii) It can increase speed, collecting a scan every second
- (iv) It can increase sensitivity-one second scans can be co-added together to ratio out random noise
- (v) It has greater optical throughput
- (vi) It is mechanically simple with only one moving part.

These advantages, along with several others, make measurements made by FTIR extremely accurate and reproducible (Yalegin *et al.*, 2000). Thus, it is a very reliable technique for positive identification of virtually any sample. The sensitivity benefits enable identification of even the smallest of contaminants. This makes FTIR an invaluable tool for quality control or quality assurance applications whether it is batch-

to-batch comparison to quality standards or analysis of unknown contaminants. In addition, the sensitivity and accuracy of FTIR detectors, along with a wide variety of software algorithms, have dramatically increased the practical use of infrared for quantitative analysis. Quantitative methods can be easily developed and calibrated and can be incorporated into simple procedures for routine analysis (Yalegin *et al.*, 2000).

Thus, the Fourier Transform Infrared Technique has brought significant practical advantages to infrared spectroscopy. It has made possible the development of many new sampling techniques which were designed to tackle challenging problems which were impossible by older technology. It has made the use of infrared analysis virtually limited.

2.8.2 Scanning electron microscopy (SEM)

The scanning electron microscope (SEM) uses a focused beam of high-energy electrons to generate a variety of signals of the surface of solid specimens. The signal that derive from electron-sample interactions reveal information about the sample including external morphology (texture), chemical composition, and crystalline structure and orientation of materials making up the sample. In most applications, data are collected over a selected area of the surface of the sample and a 2-dimensional image is generated that displays spatial variation in these properties (Zhang *et al.*, 2000). Areas ranging from approximately 1 cm to 5 microns in width can be imaged in a scanning mode using conventional SEM techniques (magnification ranging from 20X to approximate 30,000X, spatial resolution of 50 to 100 nm). The SEM is also capable of performing analysis of selected point locations on the sample; this approach is especially useful in quantitatively or semi-quantitatively determining chemical compositions (using EDS), crystalline structure, and crystal orientations (using EBSD) (Wergin and Erbe, 1994; Zhang *et al.*, 2000).

Accelerated electrons in a SEM carry significant amounts of kinetic energy and this energy is dissipated as a variety of signals produced by electron-sample interactions when the incident electrons are decelerated in the solid sample. These signals include secondary electrons that produce SEM images), backscattered electron (BSE), diffracted backscattered electrons (EBSD) that are used to determine crystal structures and orientations of minerals, photons (characteristic X-rays that are used for elemental analysis and continuum X-rays), visible light (Cathode Luminescence – CL), and heat. Secondary electrons and backscattered electrons are most valuable for illustrating contrasts in composition in multi-phase samples (i.e. for rapid phase discrimination). X-ray generation is produced by inelastic collision of the incident electrons with electrons in discrete orbital (shells) of atoms in the sample. As the excited electrons return to lower energy states, they yield X-rays that are of a fixed wavelength (that is related to the difference in energy levels of electrons in different shells for a given element). Thus, characteristic X-rays are produced for each element in a mineral that is “excited” by the electron for beam. SEM analysis is considered to be “Non-Destructive”; that is, X-rays generated by electron interactions do not lead to volume loss of the sample, so it is possible to analyze the same materials repeatedly (Barnes *et al.*, 2002; Bakar *et al.*, 2008)

2.8.2 (a) Application

The SEM is routinely used to generate high-resolution images of shapes of objects (SEI) and to show spatial variations in chemical compositions such as:

- (i) Acquiring elemental maps or spot chemical analysis using EDS.
- (ii) Discrimination of phases based on mean atomic number (commonly related to relative density) using BSE, and

- (iii) Compositional maps based on difference in trace element “activators” (typically transition metal and rare earth elements) using CL.

The SEM is also widely used to identify phases based on qualitative chemical analysis and/or crystalline structure. Precise measurement of very small features and objects down to 50nm in size is also accomplished using the SEM. Backscattered electron images (BSE) can be used for rapid discrimination of phases in multi-phase samples. SEMs equipped with diffracted backscattered electron detectors (EBSD) can be used to examine micro-fabric and crystallographic orientation in many materials (Carrillo *et al.*, 2004; Fahma *et al.*, 2011).

2.8.2 (b) Sample preparation

Sample preparation can be minimal or elaborate for SEM analysis, depending on the nature of the samples and the data required. Minimal preparation includes acquisition of a sample that will fit into the SEM chamber and some accommodation to prevent charge build-up on electrically insulating samples. Most electrically insulating samples are coated with a thin layer of conducting material, commonly carbon, gold, or some other metal or alloy. The choice of materials for conductive coating depends on the data to be acquired; carbon is most desirable if elemental analysis is a priority, while metal coatings are most effective for high resolution electron imaging applications. Alternatively, an electrically insulating sample can be examined without a conductive coating in an instrument capable of “low vacuum” operation (Garde *et al.*, 1999; Ganiyu *et al.*, 2010).

2.8.3 X-ray diffraction study (XRD)

X-ray diffraction techniques are some of the most useful in the characterization of crystalline materials, such as metals, intermetallics, ceramics, minerals, polymer,

plastics or other inorganic or organic compounds. X-ray diffraction techniques can be used to identify the phases present in samples from raw starting materials to finished product and to provide information in the physical state of the sample, such as grain size, texture, and crystal perfection. Most X-ray diffraction techniques are rapid and non-destructive; some instruments are portable and can be transported to the sample. The sample may be as small as an airborne dust particle or as large as an airplane wing (Hull, 1996; Howell, 2008; Hidaka *et al.*, 2010). In general, X-ray analysis is restricted to crystalline materials, although some information may be obtained on amorphous solids and liquids. XRD samples are acceptable in many forms, depending on the availability of the material and the type of analysis to be performed. Single crystals from a few microns to a few inches in diameter or loose or consolidated aggregate of many small crystals can be used.

Although the overall sized of the sample may be large, the actual area of the sample examined in a given experiments rarely exceeds 1cm^3 . The type of information obtained from X-ray diffraction studies ranges from sample composition to details of the crystal structure or the state of orientation of the crystallites. Phase identification can be conducted on virtually all single crystal or powder samples. Also useful are measurements of the physical state of a sample that detect differences from the ideal crystal (presence of defects, strain etc) (Larson and Von-Dreele, 1994).

2.8.3 (a) X-ray powder diffraction

X-ray powder diffraction techniques are used to characterize samples in the form of loose powder or aggregates of finely divided material. These techniques cover various investigations, including qualitative and quantitative phase identification and analysis, determination of crystallinity, micro-identification, lattice-parameter determinations, high-temperature studies, this film analysis. The powder method is perhaps best known

for its use as a phase characterization tool, partly because it can routinely differentiate between phases having the same chemical composition but different crystal structures (Polymorphs). The ability of X-ray powder diffraction to perform such identification more simply, conveniently, and routinely than any other analytical method explains its importance in many industrial applications as well as wide availability and prevalence.

In general, an X-ray powder diffraction characterization of a substance consists of placing a powder sample of a crystalline material in a collimated monochromatic beam of X-radiation. The diffraction pattern is recorded on film or using detector techniques, and then analyzed to provide X-ray powder data (Newman, 2008; Nie, 2008; Nurdina, 2009).

In X-ray powder diffraction analysis, samples usually exist as finely divided powder (usually less than 44 μm in size) or can be reduced to powder form. The particles in a sample comprise one or more independently diffraction regions that coherently diffract the X-ray beam. These small crystalline regions are termed crystallites. Consolidated samples, such as ceramic bodies or as received metal samples, will likely have crystallites small enough to be useful for powder diffraction analysis. The size limitation is important in X-ray powder diffraction because most applications of powder diffraction rely on X-ray signals from a statistical sample of crystallites. A powder pattern from a single-phase material will have maxima at positions dictated by the size and shape of its unit cell and will increase in complexity as the symmetry of the material decreases. A pattern of a mixture of phases in which all the individual patterns are superimposed will produce a complex experimental pattern, especially when the number of phases present in the mixture exceeds approximately three or when the phases constituting the mixture are all of very low symmetry or have very large unit cell dimensions (Segal *et al.*, 1999; Sumari *et al.*, 2013).

2.8.4 Thermal gravimetric analysis

Thermal gravimetric analysis (TGA) measures the amount and rate of change in the weight of a material as a function of temperature or time in a controlled atmosphere. Measurements are used primarily to determine the composition of materials and to predict their thermal stability at temperatures up to 1200⁰C. The technique can characterize materials that exhibit weight loss/gain due to decomposition, oxidation, or dehydration. TGA can tell the following information (Wambua *et al.*, 2003; Wongsiriamnuay and Tippayanwong, 2010):

- (i) Thermal stability of materials
- (ii) Oxidative stability of materials
- (iii) Composition of multi-component systems
- (iv) Estimated lifetime of a product
- (v) Decomposition kinetics of materials
- (vi) The Effect of reaction or corrosive atmosphere on materials
- (vii) Moisture and volatiles content of materials

2.8.4 (a) Mechanisms of weight change in TGA

Weight Loss (Wambua *et al.*, 2003):

- (i) Decomposition: The breaking apart of chemical bonds
- (ii) Evaporation: The loss of volatiles with elevated temperature
- (iii) Reduction: Interaction of sample to a reducing atmosphere (hydrogen, ammonia, etc.)
- (iv) Desorption

Weight Gain (Wambua *et al.*, 2003):

- (i) Oxidation: Interaction of the sample with an oxidizing atmosphere
- (ii) Absorption

TGA: Purge Gas (Wambua *et al.*, 2003)

(i) Nitrogen most common

(ii) Helium often provides best baseline but will make furnace work hard at high temperature.

(iii) Air can sometimes improve resolution because of differences in the oxidative stability (versus thermal stability) of components.

(iv) Copper oxalate can be used to detect any oxygen contamination.

TGA curves are not “fingerprint” curves because most events that occur in a TGA are Kinetic in nature (meaning they are dependent on absolute temperature and time spent at the temperature), many experimental parameter that can affect the reaction rate will change the shape/transition temperatures of the curve. These things include (Yorkitis, 1984; Yao *et al.*, 2003; Yao *et al.*, 2008): Pan material type, shape and size, ramp rate, purge gas and, sample mass, volume/form and morphology.

2.8.4 (b) Resolution enhancement in TGA

Means of enhancing resolution in a standard TGA could be as follows: slower heating rate-longer runs, reduced sample size-detection of small weight losses compromised, change purge gas if need be-not applicable in all cases and pin-hole hermetic pans-not applicable in all cases (Vink *et al.*, 2003).

The rate at which a kinetic process proceeds depends not only on the temperature the specimen is at, but also the time it has spent at that temperature. Typically kinetic analysis is concerned with obtained parameters such as activation energy (E_a), reaction order (K), etc. and/or with generating predictive curves. Activation energy (E_a) can be defined as the minimum amount of energy needed to initiate a chemical process (Vink *et al.*, 2003; Zickler *et al.*, 2007).

2.8.5 X-ray fluorescence analysis (XRF)

X-ray fluorescence (XRF) spectrometer is an X-ray instrument used for routine, relatively non-destructive chemical analyses of rocks, minerals, sediments and fluids. It works on wavelength-dispersive spectroscopic principles that are similar to an electron microprobe (EPMA). However, an XRF cannot generally make analyses at the small spot sizes typical of EPMA work (2-5 microns), so it is typically used for bulk analyses of larger fractions of geological materials. The relative ease and low cost of sample preparation, and the stability and ease of use of X-ray spectrometers make this one of the most widely used methods for analysis of major and trace elements in rocks, minerals, and sediment as well as other materials such as polymeric materials (Shin-ya *et al.*, 1981; Gwon *et al.*, 2010).

2.8.5 (a) Underlying physics

When materials are exposed to short-wavelength X-ray or to gamma rays, ionization of their component atoms may take place. Ionisation consists of the ejection of one or more electrons from the atom, and may occur if the atom is exposed to radiation with an energy greater than its ionisation potential. X-rays and gamma rays can be energetic enough to expel tightly held electrons from the inner orbital of the atom. The removal of an electron in this way makes the electronic structure of the atom unstable, and electrons in higher orbitals “fall” into the lower orbital to fill the hole left behind. In falling, energy is released in the form of a photon, the energy of which is equal to the energy difference of the two orbitals involved. Thus, the material emits radiation, which has energy characteristic of the atoms present. The term fluoresces applied to phenomena in which the absorption of radiation of a specific energy results in the re-emission of radiation of a different energy (Edwards *et al.*, 1997; Eiras and Pessan, 2009).

2.8.5 (b) Characteristic radiation

Each element has electronic orbitals of characteristic energy. Following removal of an inner electron by an energetic photon provided by a primary radiation source, an electron from an outer shell drops into its place. There are a limited number of ways in which this can happen. The main transitions are given names: an L→K transition is traditionally called $K\alpha$, an M→K transition is called $K\beta$, and an M→L transition is called $L\alpha$, and so on. Each of these transitions yields a fluorescent photon with a characteristic energy equal to the difference in energy of the initial and final orbital. The fluorescent radiation can be analyzed either by sorting the energies of the photons (energy-dispersive analysis) or by separating the wavelengths of the radiation (wavelength-dispersive analysis). Once sorted, the intensity of each characteristics radiation is directly related to the amount of each element in the material (Edwards *et al.*, 1997).

2.8.5 (c) Crystals

The desirable characteristics of a diffraction crystal are (Edwards et al., 1997; Zickler, 2007):

- (i) High diffraction intensity
- (ii) High dispersion
- (iii) Narrow diffracted peak width
- (iv) High peak-to-background
- (v) Absence of interfering elements
- (vi) Low thermal coefficient of expansion
- (vii) Stability in air and on exposure to x-rays
- (viii) Ready availability
- (ix) Low cost

Crystals with simple structure tend to give the best diffraction performance. Crystals containing heavy atoms can diffract well, but also fluoresce themselves, causing interference. Crystals that are water-soluble, volatile or organic tend to give poor stability (Edwards *et al.*, 1997; Zickler, 2007).

2.8.5 (d) Applications

X-ray fluorescence is used in a wide range of applications, including (Flory, 1943; Gwon *et al.*, 2010):

- (i) Research in igneous, sedimentary, and metamorphic petrology
- (ii) Soil surveys
- (iii) Mining (e.g. measuring the grade of ore)
- (iv) Cement production
- (v) Ceramic and glass manufacturing
- (vi) Metallurgy (e.g., quality control)
- (vii) Environmental studies (e.g., analysis of particulate matter on air filters)
- (viii) Petroleum industry (e.g. sulphur content of crude oils and petroleum products)
- (ix) Field analysis in geological and environmental studies (using portable, hand-held XRF spectrometers).
- (x) Chemical and polymeric materials based analysis.

X-ray fluorescence is limited to analysis of (Gwon *et al.*, 2010):

- (i) Relatively Large Samples, Typically > 1 gram
- (ii) Materials that can be prepared in powder form and effectively homogenised
- (iii) Materials for which compositionally similar, well characterised standards are available

- (iv) Materials containing high abundances of elements for which absorption and fluorescence effects are reasonably well understood.

2.9 Predicting the Performance of Products/Processes using Mathematical Models

Performance of the optimized design from the coconut shell and fibre could be predicted to an extent where predicted results will be significant and possessing some degree of correlation with experimental results and performance. Such models are referred to as mathematical models.

A mathematical model is a description of a system using mathematical concepts and language. The process of developing a mathematical model is termed mathematical modeling. Mathematical models are used in the natural sciences (such as physics, biology, earth science, meteorology, engineering disciplines, technology, etc.). A model may help to explain a system and to study the effects of different components, and to make predictions about behaviour (Billings, 2013).

Mathematical models can take many forms, including dynamic systems, statistical models, differential equations, or game theoretical models. These and other types of models can overlap, with a given model involving a variety of abstract structures. In general, mathematical models may include logical models. In many cases, the quality of a scientific field depends on how well the mathematical models developed on the theoretical side agree with results of repeatable experiments. Lack of agreement between theoretical mathematical models and experimental measurements often leads to important advances as better theories are developed (Whishaw *et al.*, 2001; Algina and Olejnik, 2003; Cardinal *et al.*, 2006).

The traditional mathematical model contains four major elements. These are: Governing equations, constitutive equations, constraints and kinematic equations. Mathematical models are usually composed of relationships and variables. Relationships can be described by operators, such as algebraic operators, functions, differential operators, etc. Variables are abstractions of system parameters of interest that can be quantified. Several classifications criteria can be used for mathematical models according to their structure: Linear versus non-linear, static versus dynamic, explicit versus implicit, discrete versus continuous, deterministic versus probabilistic (Stochastic), deductive, inductive, or floating (Levy and Neill, 1990; Cortina and Nouri, 2000; Wright, 2006).

Any model which is not pure white-box contains some parameters that can be used to fit the model to the system it is intended to describe. If the modeling is done by a neural network, the optimization of parameters is called training. In more conventional modeling through explicitly given mathematical functions, parameters are determined by curve fitting. A crucial part of the modeling process is the evaluation of whether or not a given mathematical model describes a system accurately. Usually the easiest part of model evaluation is checking whether a model fits experimental measurements or other empirical data. In models with parameters, a common approach to test this fit is to split the data into two disjoint subsets: training data and verification data. The training data are used to estimate the model parameters. An accurate model will closely match the verification data even though these data were not used to set the model's parameters. This practice is referred to as cross-validation in statistics (Richard, 2004; Fay and Proschan, 2010).

2.9.1 Analysis of variance (ANOVA)

Analysis of variance (ANOVA) tests the hypothesis that the means of two or more populations are equal. ANOVAs assess the importance of one or more factors by comparing the response variable means at the different factor levels. The null hypothesis states that all population means (factor level means) are equal while the alternative hypothesis states that at least one is different. To perform an ANOVA, you must have a continuous response variable and at least one categorical factor with two or more levels (Fay and Proschan, 2010).

The name “analysis of variance” is based on the approach in which the procedure uses variances to determine whether the means are different. The procedure works by comparing the variance between group means versus the variance within groups as a way of determining whether the groups are all part of one larger population or separate populations with different characteristics. ANOVA type model and design properties are as follows (Wright, 2006; Fay and Proschan, 2010):

- (i) One- way: One fixed factor (levels set by investigator) which can have either an unequal (unbalanced) or equal (balanced) number of observations per treatment.
- (ii) Balanced: Model may contain any number of fixed and random factors (levels are randomly selected), and crossed and nested factors, but requires a balanced design.
- (iii) General linear: Expands on balanced ANOVAs by allowing unbalanced designs and model covariates (continuous variables).

When ANOVA is runned, an attempt is being made to determine if there is a statistically significant difference between groups that is not related to sampling error. If you find that there is a difference, you will then need to see between which of the groups the difference lays. This is to say, all groups might be different, or perhaps only

one of several groups is statistically different from others (Wright, 2006, Fay and Proschan, 2010).

2.9.2 T-test

A t-test is most commonly applied when the test statistic would follow a normal distribution if the value of a scaling term in the test statistic were known. When the scaling term is unknown and is replaced by an estimate based on the data, the test statistics (under certain conditions) follow a student's t-distribution.

At this point you could run several t-tests to test the means between the groups, but this would not control for error as again you would be testing for several hypothesis at the same time. There are several multiple comparison tests that can be conducted that will control the type one error rate such as (Cortina and Noun, 2000; Whishaw *et al.*, 2001; Richard, 2004):

- (a) If you are concerned about violations of the assumptions use Scheff's test.
- (b) If you are not concerned about violations to the assumptions and are testing compound and pair wise tests, use Dunn's test or the modified Bonferroni test.
- (c) If you are not concerned with violations of the assumptions and are just comparing the treatment to the control, use Dunnette's test.
- (d) If you are not concerned with violations of the assumptions and are comparing all possible pair wise use Tukey's test or modified Tukey's test.
- (e) If you are not concerned with violations of the assumptions and are testing more than half of the possible pair wise comparisons again use Tukey's test or modified Tukey's test.

- (f) If you are not concerned with violations to the assumptions and are testing less than half of the possible pair wise comparisons, use Dunn's test or the modified Bonferroni test.

All of these tests will ensure that the "type 1" error rate remains under control as was established by the researcher and will tell you exactly which groups are different from one another (Richard, 2004).

CHAPTER THREE

MATERIALS AND METHODS

3.1 Collection, Treatment of Materials and Reagents

The research work commenced with the sourcing of coconut shells and fibres which was in abundance in Auchi and its environs in Edo State, Nigeria. All compounding ingredients such as zinc oxide, stearic acid, plasticiser/processing oil, sulphur, mercaptobenzothiazole disulphide (MBTS), Tetramethylthiuram disulphide (TMTD), and trimethylquinoline (TMQ); were of commercial grades and they were used without further treatment. Natural rubber (Standard African Rubber, SAR) having the properties given in Table 3.1.

Table 3.1: Properties of Standard African Rubber (SAR)

Parameters	Content
Volatile Matter	0.40
Dirt Content Retained on 45 mm Sieve (%)	0.02
Nitrogen (%)	0.23
Ash Content (%)	0.32
Initial Plasticity (P^0)	36
Plasticity after Aging for 30 min at 140 ⁰ C (P30)	24
Plasticity Retention Index (PRI)	67
Money Viscosity, ML (1+4), 100 ⁰ C	70

Source: Professional Association of Natural Rubber in Africa, Standard African Rubber (SAR) Manual, 1998

The collected shells and fibres were washed in water to remove debris and sands before being oven dried at 95⁰C to remove moisture. A portion of the shells and fibres were crushed and ground to form a powder using a grinding machine. A second portion was measured for carbonisation at 300⁰C, 400⁰C, 500⁰C, 600⁰C and 700⁰C for a period of 3hrs each. This second portion was also further crushed and ground using a grinding machine. All powders; both raw and carbonised were taken through a series of sieve

with mesh sizes ranging from 450 μm -100 μm in order to fully achieve an eventual particle size of 100 μm .

3.2 Characterisation of the Raw and Carbonised Fillers

Raw shell and fibre as well as carbonised shell and fibre were characterised in terms of loss on ignition, pH, bulk density, iodine adsorption number, moisture content, oil absorption and ash content. All reagents were used without any modification or treatment. The loss on ignition was determined gravimetrically according to ASTM 1509 standard test method (ASTM 1509, 1985). The pH of slurry was determined using SCAN-P39 method. Bulk density was determined using ASTM D 6111-13a (1983). Iodine adsorption number method ASTM D1510 (1984) was used to measure the surface area. Moisture content and oil absorption were measured according to standard procedures described by ASTM D1510 (1983) and B5 3483, Part 7 (1984) respectively. Ash content was determined according to ASTM D5630 (1983) standard test method.

3.2.1 Determination of loss on ignition

25g of the filler samples were heated at a constant temperature of 800°C for 24hrs, the mass loss of the specimens were recorded as a percent of the original mass. These values were identified as the loss- on - drying (LOD) values. The LOD values were functions of both temperature and time. Therefore these values were identified and reported in accordance to ASTM 1509 (1985). This test method is used to estimate the amount of volatile materials present in the filler samples. These results were useful for design purposes, service evaluation, regulatory statues, manufacturing control, quality control, specification acceptance, development and research.

3.2.2 Measurement of pH

Using SCAN-P39 on the slurry of the various samples; a semi-micro combination pH electrode and standard pH of all the slurry prepared as a standard solutions. A bio-radiation laser scanning confocal microscope was employed for confocal imaging. This system is equipped with a Krypton/Argon mixed gas ion laser (excitation lines at 488, 568 and 647 nm) and is mounted on a Nikon Optiphot-2 microscope. All images were collected at a magnification of 40X. The SC pH profiles were measured directly in the second set of experiments with a flat surface combination pH electrode.

3.2.3 Determination of bulk density

Using standard test method, ASTM D6111-13a, 1983; 100g of powder was passed through a sieve with apertures greater than 1.0 mm to gently break up agglomerates that may have formed during storage. Into a dry graduated cylinder of 250 ml; 100g of the test sample was weighed with 0.1 % accuracy and gently introduced without compacting, and the unsettled apparent volume to the nearest graduated unit was measured. The bulk density in (g/ml) was calculated using the formula m/v_0 , where m stands for mass of sample and v_0 represent apparent volume of sample.

3.2.4 Determination of iodine adsorption number

This test method is based upon a three-point adsorption isotherm according to ASTM D1510 (1984). A standard iodine solution was treated with three different weights of activated carbon under specified conditions. The carbon treated solutions were filtered to separate the carbon from the treated iodine solution (filtrate). Iodine remaining in the filtrate was measured by titration. The amount of iodine removed per gram of carbon was determined for each carbon dosage and the resulting data used to study adsorption isotherm. The amount of iodine adsorbed (in milligram) per gram of carbon at a residual

iodine concentration of 0.02 *N* is reported as the iodine number. The iodine number is a relative indicator of porosity in an activated carbon, and this may be used as an approximation of surface area for reaction rates.

3.2.5 Determination of moisture content

Using standard direct test method; ASTM D 1510 (1983). Direct methods are considered to provide true measurements of moisture content, and are used to calibrate more practical and faster indirect methods. 100g of the sample was placed in a crucible with a perforated cover fitted with a graduated thermometer reading up to 250°C. Initial weights were taken and final weights were again assessed after 3hrs. Percentage moisture loss was then obtained.

3.2.6 Determination of oil absorption

BS 3483, part 7 (1984) standard was used. Spontaneous uptake of oil was determined on 100 mg of samples. Using a device made of one-ml pipette, graduated in 1/100 ml connected to Tygon tubing of 30 cm long and then to a plastic bacteriological field monitor. The field monitor had a diameter of 4 cm. The oil absorption was measured by the pipette adjusted to a horizontal position. The pipette and connecting tube were fitted with oil through the open field monitor until the meniscus passed the zero mark on the pipette. The glass filter was then placed in the field monitor and allowed to imbibe oil.

3.2.7 Determination of ash content

Ash content was determined using ASTM D5630 (1983) standard test method. 10g of samples were weighed and placed in a high temperature muffle furnace at 650°C. Water and other volatile materials are vaporised and organic substances are burned in the presence of the oxygen in air to CO₂, H₂O and N₂. Most minerals are converted to

oxides, sulphates, phosphates, chlorides or silicates. The ash content was expressed as percentage ash.

3.2.8 Determination of particle dimensions and lumen

Cumulative Scanning Electron Microscopic (SEM) properties in length, width, diameter, conductivity and lumen were weighted by volume and by count using SEM X-pro Shimadzu equipment with full back scattered electron (BSD), were particle properties such as circle equivalent diameter, major and minor axes, circumference, convex hull, area, volume by area, pixel count, aspect ratio, circularity, convexity and grayscale were determined. All of these affected the transparency and conductivity of the micro structural surfaces.

3.3 Formulation Design, Mastication and Mixing

Table 3.2 outlines the formulation used for the preparation of the natural rubber composites. Mastication was done in order to reduce the viscosity and to break down the molecular weight of the natural rubber in preparation for the incorporation of the selected and weighed-out additives. The formation of band and bank on the mill was monitored. The laboratory two-roll mill (180 x 360mm size capacity) in accordance with ASTM D3182 (1984) standard method of compounding rubber was used. The Nip gap, mill roll speed ratio (1:1.25), sequence of addition and time of dispersive and distributive mixing of the additives were kept uniform for the entire composite samples. The roll temperature was maintained at 70°C. Sheeted rubber compounds were allowed for maturation at 32°C for 24h.

All the additives were held constant. The investigation was centred on the variation in temperature of the carbonisation process which was the main modification method for

the coconut palm wastes. Control fillers were those of the raw fillers for the purpose of monitoring.

3.4 Determination of Cure Characteristics

Rheological evaluations were done to determine the cure characteristics, rubber compound monitoring and control. The Monsanto oscillating disk rheometer (ODR 2000 Model) was used to measure the cure temperature at 145°C, using a pressure of 150kg/Cm² for an average of about 15 minutes for each of the formulations. This was carried out in accordance to ASTM D 1632-07 (1985), standard method of press curing of rubber compound.

Table 3.2: Compound Design/Formulation in PPHR (g)

Additives (PPHR)	Raw CSP	Raw CFP	CSP 300	CSP 400	CSP 500	CSP 600	CSP 700	CFP 300	CFP 400	CFP 500	CFP 600	CFP 700
Natural Rubber (NR)	100	100	100	100	100	100	100	100	100	100	100	100
Filler	50	50	50	50	50	50	50	50	50	50	50	50
Plasticizer	5	5	5	5	5	5	5	5	5	5	5	5
Zinc Oxide	5	5	5	5	5	5	5	5	5	5	5	5
Stearic Acid	2	2	2	2	2	2	2	2	2	2	2	2
MBTS	1	1	1	1	1	1	1	1	1	1	1	1
TMTD	1	1	1	1	1	1	1	1	1	1	1	1
TMQ	1.5	1.5	1.5	1.5	1.5	1.5	1.5	1.5	1.5	1.5	1.5	1.5
Sulphur	2	2	2	2	2	2	2	2	2	2	2	2

Key:

CSP: Coconut shell powder

CFP: Coconut fibre powder

MBTS: Mercaptobenzylthiazole Sulphenamide

TMTD: Tetramethylthiuram Disulphide

TMQ: Trimethyl Quinoline

3.5 Physico-Mechanical Testing/Measurements

The mechanical properties of the various samples prepared were determined through hardness, abrasion resistance index, compressive strength, tensile strength, elongation at break and flexural tests analyses.

3.5.1 Hardness test

The test was carried out in line with international standard test measurement, ASTM D 2240 (2003); (Ashori and Raverty, 2007) using the shore A scale for the determination of hardness numbers. Test specimens were cut from each of the samples being investigated as shown in the formulation design. The prepared specimen were secured on the Durometer-type A machine platform while the 1.40 mm indenter with a force of 8.06N was applied gradually onto the specimen for a duration of 15 seconds. The load was then removed and the indented diameter read from the screen. The obtained diameter was loaded into the measuring system of the tester so as to display the hardness number on the screen. Three readings were taken from which the average value was obtained for each sample.

3.5.2 Abrasion resistance index test

The test was carried out in line with international standard test of measurement, ASTM D 596-04 (2015); using the rotary drum abrader. The test was carried out at 32°C the densities of the samples were determined using a hydrostatic method (ASTM D5963-04 (2015)). Test method A was used. Method A is run with a non-rotating test piece, using standard rubber number 1 as reference. Prior to each test, debris left on the abrasive sheet from a previous abrasion test was removed by vigorous brushing. First, three test runs were made with the standard rubber, followed by ten runs for the tested samples. Then another three runs with the standard rubber. The test pieces were weighed to the

nearest 1mg and firmly fixed into the holder so that it protrudes 2.0 ± 0.2 mm from the opening holder. The vacuum was then turned on and the survival arm moved into starting position to start the automatic test run. After completing an abrasion path of 40m, the test piece were automatically disengage from the abrasive sheet and reweighed to the nearest 1mg.

3.5.2 (a) Calculation of abrasion resistance index (ARI_A).

To calculate the abrasion resistance index, eqn. (3.1) was used. The ratio off the volume loss of standard rubber number 1 to that of the test rubber was expressed in percentage

$$ARI_A = \frac{\Delta m_1 \cdot dt}{\Delta m_t \cdot d_1} \times 100 \quad 3.1$$

where:

ARI_A =Abrasion resistance index in percent (non-rotating test piece).

Δm_1 = Mass loss of the standard rubber number 1 test piece in mg.

d_1 = Density of standard rubber number 1 in mg/m^3 ,

Δm_t =Mass loss of the test rubber piece in mg, and

dt = Density of the test rubber in mg/m^3 .

Results of abrasion resistance index are shown in Table 4.3.

3.5.3 Compressive strength measurements

Compressive tests were carried out in accordance with the international standard, ASTM D575-91 (2012) method of testing compressive strength of rubber compound. The test samples were cut to 45 mm diameters with anvil height of 8.65 mm. Maximum compressive stress; compressive strain at maximum compressive stress; energy at maximum compressive stress and compressive load at maximum compressive stress versus compressive strain.

3.5.4 Tensile strength/modulus/elongation at break measurement

The tensile test was carried out in accordance with international standard, ASTM D 3039/D (2015) standard test method for tensile properties of composite materials. The test samples from various composites under study were cut into rectangular shapes with an average dimension of 10x50 mm. The thickness 3.2 mm, width dimension of 10 mm and length of 50 mm was used. The samples were mounted on Hounsfield tensometer with a maximum capacity of 20 KN. The various samples were loaded to fracture. After fracture, the elongation and tensile strength were recorded.

3.5.5 Flexural strength/modulus measurement

Flexural test were performed using three point bending method according to ASTM D790-03 procedure. The composite samples were tested at a cross head speed of 2 mm/min, at a temperature of 22°C and humidity of 50%. In each case three samples were taken and average values were recorded. The flexure stress in a three point bending test was found out by using eqn. (3.2).

$$\sigma_{\max} = \frac{3P_{\max} L}{bh^2} \quad 3.2$$

where:

P_{\max} is the maximum load of failure (N), L is the span (mm) b and h represents the width and thickness of specimen (mm) respectively. The flexure modulus was calculated from the slope of the initial portion of the load-deflection curve which was found out by using the equation shown below:

$$E = \frac{mL^3}{4bh^3} \quad 3.3$$

where, m is the initial slope of the load deflection curve for each stacking sequence, three specimens were tested and average result was obtained and plotted.

3.5.5 (a) Test sample

The test sample was in the form of a bar 76.2 mm x 25.4 mm x 6 mm. It was sawed from the composite samples so as to have smoothed edges free from cracks. The cut edges smoothen by finishing with zero number emery cloth. Sawing and sand preparing operation was done slowly enough, so that the material is not heated appreciably. Graphical plots of flexural results are shown in Figures 4.7- 4.9, and tabular results are indicated in Table 4.6. Fixture type was 3-point; support span of 65 mm, thickness of 3.2 mm and width of 25 mm were used.

3.6 Qualitative and Quantitative Analysis

The qualitative and quantitative characteristics of the various modified and raw filler were analyzed by Fourier Transform Infrared Spectroscopy (Shimadzu FTIR Model 7000); Scanning Electron Microscopy (Pro-X-2000 SEM); X-Ray Diffractometer measurements (Shimadzu XRD 6000 Model) and Thermal Gravimetric Analysis (Shimadzu TGA 7000 Model).

3.6.1 Fourier transforms infrared spectroscopy (FTIR)

The infrared spectra of the raw and carbonised coconut shell filler as well as the coconut fibre filler were recorded on a Shimadzu FTIR-81001 spectrophotometer in accordance with ASTM D297-15(2013) standard method for sample preparation prior to testing on FTIR. A portion of 2 mg of dry samples were added to 300 mg of spectral grade potassium bromide (KBr). The mixture was ground and pressed to form a transparent disc. The transmittance technique was used, and the samples were scanned 16 times at a resolution of 8 cm⁻¹ for each spectrum. Sixteen background scans were also recorded and a range of 4000-650 (cm⁻¹) wave number was used.

3.6.2 Scanning electron microscopy (SEM)

Scanning Electron Microscopy was conducted to evaluate the cell morphologies of the composites with filled carbonised coconut shell and fibre fillers modified at the various temperatures of (300, 400, 500, 600 and 700)^oC in order to ascertain the level of surface modification achieved. Microscopic magnification was done at 1000X with a resolution of 80 μm.

The composites filled with carbonised and raw fillers were treated with liquid nitrogen and coated in gold for this examination. Images were taken on the SEM operated in the secondary electron mode at a 10 kv mapping, accelerating voltage with full back scattered electron (BSD). Particle properties were weighted by volume and by count and average values were noted.

All samples were appropriately sized to fit in the specimen chamber and were mounted rigidly on a specimen holder (stub); and some accommodation to prevent charge build-up on the electrically insulating samples. The samples were coated with gold for high resolution electron imaging. Table 4.8 shows particle properties weighted by volume, while Table 4.9 shows particle properties weighted by count.

3.6.3 X-ray diffraction analysis

The Shimadzu XRD-600 model was used. This is a state of the art, multipurpose X-ray diffraction system that is optimized for powder diffraction studies of crystalline materials. The samples were dried in an oven at 60^oC for 30 minutes to remove the moisture content if any. The particle size of 100 μm (0.15 micron) was verified according to the recommended standards.

3.6.3 (a) Setting of the XRD-equipment

The machine was run (scan range) between 0° to 60° 2 Theta Bragg angle. The running rate (scan speed) was between 2 to 10 degrees per minute. The voltage used was 40V at a current of 30A. The auto-silts (divergence, scatter and receiving) used for the various aperture control are of sizes 1.0, 1.0 and 0.3 (degree) (Lojewska *et al.*, 2006)

3.6.3 (b) Bulk analysis

The powdered sample prepared is regarded as bulk sample. The sample was smeared evenly on the sample holder of aluminum material, with the aid of smooth slide. The setting was between angles of 2° to 60° degree theta as the bulk sample scanning range. The running rate (scanning speed) was set at 6 degree per minutes. The holder is carefully placed on the loading point of the moveable GONIOMETER arm that contains a clamp capable of gripping the sample firmly. The window will indicate readiness after being properly closed. By commanding the software, the analysis commenced automatically. The pronounced peaks or diffractograms displayed, expressed the minerals composition and crystallinity at the various angle of the degree theta.

3.6.3 (c) Generation of raw data

By accepting or rejecting entry of the marched peaks, the obtained peaks were successfully related and identified as *accepted peaks*, which bears the minerals names, chemical symbols, and the chemical name of the already known ones that correlate with the newly run data, basic process and search-march raw data.

3.6.4 X-ray fluorescence

The Thermoscientific Advant'x 1200 model was used. The samples were dried in an Oven at 60°C for 30 minutes to remove the moisture contents if any. The particle size of

100 μm (0.15 micron) was verified according to the recommended standards; and samples are ready for XRF machine (Lopattananon *et al.*, 2006).

3.6.4 (a) Pelletisation of samples

The powdered sample is mixed with binder lithium tetra-borate (BORAX). The mixture of the borax and the sample to analyse is in the ratio 4:1g. This implies that 1g of sample was weighed using Metler balance and mixed with 4g of the borax. This is mixed evenly and properly using Herzog vibrating cup miller at the speed of 8 rpm. The mixture is therefore loaded onto a cup of size 22 mm by 40 mm made of aluminum material. The pelletising machine is operated by allowing the stroke movement up and down only.

The pressing force was set at 240N and the movement stroke was at 6 rpm. The cup containing the mixed sample is placed on the stroke and allowed to go down to the limitation point. On the returning of the stroke with the plug already pegged at the loading point the pressing force pressed the cup against the fixed point, and a pellet is formed. The pellet sample is now ready for XRF analysis.

3.6.4 (b) Setting of the XRF equipment

The required parameters were set according to prescribed standard. Such parameters are pressure values set at 16 Pascal, environmental chamber for the opening and the lifting of the CASSETTE (a holder that houses the pellet sample). The voltage recommended level is 45V and current recommended level is 40A. The equipment was allowed to run for at least 4 to 5 hours to enable the standards and other mechanical parts responsible for analysis to stabilise and initialised.

3.6.4 (c) Loading and running of sample

The sample was loaded on the cassette by placing the surface side facing downward, with the help of spring attached to the cassette, the cassette is locked manually by turning it clockwise, to keep the pellet safe from falling off or scattered on the Goniometer when analysis was going on. The loading point and the cassette point are in position directly facing the Goniometer Position for easy analysis. The analysis starts immediately once the cassette has being lifted down with command L1 which resulted in the closure of the opening valve.

3.6.4 (d) Generation of raw data

After about twenty minutes, the analysis had finished and the data generated were collated automatically, followed by the manual results drag-dropping technique onto the save file where the results were produced in either ionic, carbonic, elemental, oxides or non-ionic forms. The results are produced once the concentrations of the parameters involved are equal or greater than the already calibrated and installed standards.

3.6.5 Thermal gravimetric analysis

Using ASTM E1641, the samples were heated from room temperature to above 850°C at a rate of 5°C/min nitrogen. Balance sensitivity of 0.1 microgram was achieved. The TGA curves were printed as machine plotted.

3.6.6 Sorption measurements

Vulcanised compositions were obtained as small sheets of about 1.5grams, and approximately 2x2x0.3 cm according to ASTM D3010 (1983) standard method of sorption/testing of swelling properties. The exact weight of time to a maximum of 72 hours until average values with ± 0.0001 g precision was obtained. The specimens were then immersed in benzene, toluene, xylene and hexane in 125 ml wide mouth bottle, at

32°C. At the end of the immersion period, the swollen specimens were blotted between filter paper, transferred to tarred weighing vessels and carefully weighed. The weight of the imbibed solvents were obtained as the difference between the weights of the swollen and dried samples (drying was done first at room temperature and then overnight at 70°C, in a vacuum oven). The weight of the rubber network was determined by subtracting the weight of initial sample from the final sample. The swelling values were then expressed in percentages. See table of results in Table 4.7.

3.7 Production of Vibration Dampener for Motor Cycle Hub and Industrial Oil Seals for Bambury Mixers

The ultimate purpose of every good research work is to contribute to knowledge and put discovered results into practical use. The best results obtained at modification temperatures of 500°C and 600°C for the coconut palm shell and fibre were used in the production of vibration dampeners and industrial oil seals and further evaluation of the products were done to confirm in-built service properties.

Generally, fillers can be termed as reinforcing, semi-reinforcing and non-reinforcing; and they are also preferred in that order when formulating for engineering wares and services. The nature and the modification process of the filler are great determining factors in the development of a good product.

3.7.1 Mould design for the vibration dampener

The mould was designed with mild steel, which consist of a single cavity. It has an impression that is a similitude of the intended product. The steel body enabled it to withstand the high clamping pressures exerted on the mould during the processing operation in the compression moulding press.

3.7.2 Compound mixing process for vibration dampener

This process involved the incorporation and distribution of uniform dispersion of the already weighted rubber additives. Appropriate formulation designs were made and the selected additives measured and weighed. Homogenisation and mixing of the recipe was carried out on a laboratory two-roll mill size (180x360) mm in accordance with ASTM-D3182. Roll speed ratio was at 1:1.25; while incorporation sequence and mixing time of additives were kept relatively uniform. A mill temperature of 70°C was maintained and sheeted composites were allowed for 24 hours maturation at 32°C before press curing.

3.7.3 Moulding process of the vibration dampener

Four (4) formulations were used for the moulding process:

- (i) The formulation of raw coconut shell filler
- (ii) The formulation of raw coconut fibre filler
- (iii) The formulation of carbonised coconut shell at best carbonisation temperature of 500°C
- (iv) The formulation of raw coconut fibre at the best carbonisation temperature of 600°C.

These formulation designs were repeated in Table 3.2

The moulding parameters selected from the cure characteristic study using ODR 2000 model rheometer were: a temperature of 150°C, pressure of 150kg and a mould cycle time of 15 minutes to achieve optimum property yield. The matured composites were then effectively compression moulded and products ejected for further evaluative test of dynamic flex fatigue and rebound resilience test, which are the primary properties required for a useful service life expected from a well-developed vibration dampener.

3.7.4 Product evaluative measurement (vibration dampener)

There are many different kinds of automobile vibration dampeners, depending on engine block types. This particular one evaluated is useful in most motor cycles. All previously evaluated tests of hardness, abrasion resistance, compressive strength, and tensile strength, and modulus, elongation at break, flexural strength and chemical sorption on the composites are further complemented with the dynamic flex fatigue and rebound resilience tests on the product (Fukahori and Yamazaki, 1994).

3.8 Production Process Conditions of Oil Seal

Significant environmental factors were considered and these factors are: reliable chemical resistance, strength and durability to low temperature and heat, ability to withstand weather aging and ozone, outstanding water resistance, superior elasticity, low compression set maintaining elastomeric properties and cost of raw materials for units of production. The base polymer must provide alkali, acid, oil and water resistance. Maximum temperature limits are contingent upon other conditions of operation.

3.8.1 Mould design for the oil seal

Mild steel was used for the design of the mould, which consists of simply one cavity well finished and polished from the mechanical workshop in Auchi Polytechnic, Auchi, Nigeria. Bolsters and inserts were critically machined-in and fitted for precise product clearances. The strength of the material for the steel mould was made to be relatively tough, hard and durable to withstand clamping forces and pressures of the compression moulding machine.

3.8.2 Formulation design for the oil seal

Again in this particular case, four (4) formulations were used for the moulding process and the choice of the formulations was from the outcome of the previous evaluative studies and measurements.

Table 3.3 Formulation for the Oil Seal Production (PPhr)- Parts Per Weight (g)

Additives (PPhr)	CSP (Raw)	CFP (Raw)	CSP @ 500°C	CFP @ 600°C
NR	100	100	100	100
Filler	50	50	50	50
Plasticizer	5	5	5	5
Zinc Oxide	5	5	5	5
Stearic Acid	5	5	5	5
MBTS	1	1	1	1
TMTD	1	1	1	1
TMQ	1.5	1.5	1.5	1.5
Sulphur	2	2	2	2

3.8.3 Compounding for the oil seal

Vulcanised polymers cannot be used without compounding. Various additives like curative system, protective system, reinforcing agents, cheapeners and other process aids were mixed with the rubber to make a coherent homogenous mass of all the additives in the formulation, which processed satisfactorily and gave a product capable of giving the desired performance on vulcanisation. The two-roll mill was used for the mixing; curing and product formation achieved using the compression press machine (Avion Crydon Press Machinery, 8500 Model)

3.8.4 Evaluative measurement of the oil seal

Furtherance to the results achieved from the previously evaluated analysis (hardness, abrasion resistance index, compressive strength, tensile strength, modulus, and

elongation at break, flexural strength and sorption tests); the following confirmatory evaluations on the manufactured products were carried out:

- (a) Alkali, acid, oil and water resistance measurements
- (b) Resistance to weathering and ozone

3.8.5 Chemical resistance evaluation of the oil seal

Using a prescribed standard test method, ASTM-D2240 (2003); where 15 g of test pieces were cut and placed in the variously selected chemicals-using 500 ml conical flask containing 250 ml of alkali (15% conc. NaOH), acid (10% conc.H₂SO₄), oil (hydraulic), and water. The experiments were allowed to stay for 36h at a room temperature of 35°C. The samples were then removed, dried and weighted again to evaluate sorption levels.

3.8.6 Weathering/ozone resistance measurement of the oil seal

According to ASTM-D1171, rectangular cross section samples were cut and wrapped around a wooden mandrel and then placed in an Ozone chamber with 45% concentration for 24h and crack measurement studies were carried out using DeMattia flex fatigue machine.

3.9 Predicting the Performance of the Optimised Coconut Fibre and Shell Filled Composites

An appropriate computer/statistical model using analysis of variance (Promex Origin Software), estimated marginal means, post hoc test of multiple comparison, homogeneous subset and regression analysis were performed on the mechanical and sorption properties of the optimised coconut fibre and shell from the formulation design used in the production of the motor cycle vibration dampeners and industrial oil seals

for bambury mixers. These were done in order to evaluate the levels of significance of results obtained through experiment and theoretical evaluations.

CHAPTER FOUR

RESULTS

4.1 Characterisation

Table 4.1: Characterisation of Raw Coconut Shell and Fibre; Carbonised Coconut Shell and Fibre

Parameter	CSP	CFP	CSP 300	CSP 400	CSP 500	CSP 600	CSP 700	CFP 300	CFP 400	CFP 500	CFP 600	CFP 700
pH of Slurry at 32 ^o c	3.92	3.30	5.31	5.85	6.90	7.94	8.18	5.00	5.62	7.02	7.52	8.00
Moisture Constant (wt %)	10.02	10.13	9.45	7.10	8.92	7.82	7.10	9.82	9.42	8.54	8.41	8.02
Ash Content (%)	1.98	2.58	2.25	2.82	3.46	5.75	7.20	3.20	4.35	5.12	7.14	9.10
Loss on Ignition (800 ^o c) (%)	8.40	19.5	21.40	32.63	49.82	76.80	87.94	28.50	36.20	58.40	79.00	82.40
Iodine Adsorption Number (mg/g)	31.40	56.10	62.00	64.50	71.40	72.42	73.50	58.00	64.50	68.90	71.00	72.00
Bulk Density (g/mg)	0.83	0.57	0.74	0.71	0.65	0.59	0.51	0.51	0.48	0.42	0.34	0.30
Oil Absorption (kg)	6.48	6.25	4.14	4.00	3.16	2.89	2.50	4.00	3.84	3.10	2.61	2.51
Conductivity (Ω /mm)	–	0.83	–	–	–	–	–	2.14	2.48	2.85	3.20	3.35
Length (mm)	–	0.38	–	–	–	–	–	0.30	0.28	0.22	0.15	0.09
Width (mm)	–	0.02	–	–	–	–	–	0.009	0.006	0.004	0.003	0.001
Diameter (mm)	–	0.05	–	–	–	–	–	0.02	0.02	0.01	0.006	0.005
Lumen (mm)	–	0.01	–	–	–	–	–	–	–	–	–	–

4.2 Hardness Properties

Table 4.2: Results of Hardness Test (\AA)

Sample Type	Shore “A” Hardness (\AA)
CSP Raw	73
CSP 300	75
CSP 400	78
CSP 500	86
CSP 600	80
CSP 700	76
CFP Raw	64
CFP 300	68
CFP 400	75
CFP 500	79
CFP 600	80
CFP 700	76

All test evaluations were done using sample configuration of 35° truncated cone (frustum), 1.40 mm diameter, and extension of 2.54 mm and a spring force of 8.06 N. Also the results were an average of three (3) measurements performed per sample.

4.3 Abrasion Resistance Index

Table 4.3 Results of Abrasion Resistance Indices (ARI_A)

Test Rubber Compound	Mean Value of ARI _A (%)
CSP Raw	22.51
CSP 300	28.42
CSP 400	32.10
CSP 500	36.10
CSP 600	44.84
CSP 700	37.42
CFP Raw	20.40
CFP 300	25.32
CFP 400	29.95
CFP 500	32.40
CFP 600	36.55
CFP 700	34.15

The method for abrasion resistance index measured was test method A (ARI_A), a cut method was used for the test piece preparation at a test temperature of 32°C. Results reported were a mean value of three (3) running-in test for each sample.

4.4 Compression Set Results

Table 4.4: Results of Compression set.

Sample Piece	Compression (%)
CSP Raw	28.90
CSP 300	26.40
CSP 400	24.80
CSP 500	22.30
CSP 600	23.00
CSP 700	23.20
CFP Raw	26.92
CFP 300	24.65
CFP 400	20.96
CFP 500	19.85
CFP 600	19.46
CFP 700	22.85

4.5 Compressive Stress-Strain Relationship

All data points are indicated in appendix I as these are universal testing machine (UTM) values. All triangular (\blacktriangledown) marks on each plot indicate the point of breakage from machine grips of samples.

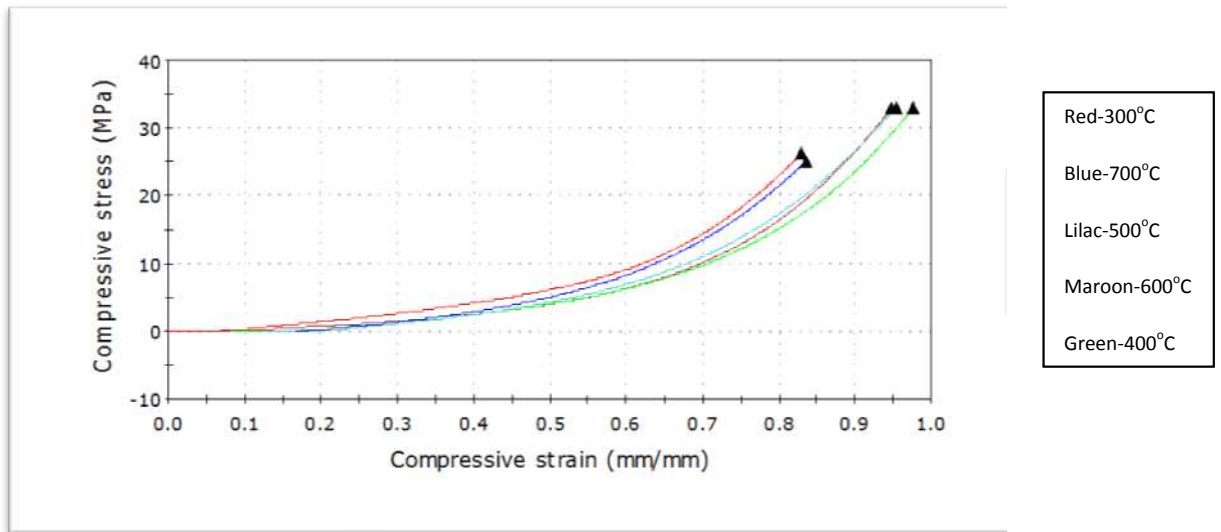


Figure 4.1: Compressive Stress versus Compressive Strain Curves for (1) 300°C, (2) 700°C, (3) 500°C, (4) 600°C and (5) 400°C Carbonisation Treatment for Coconut Shell

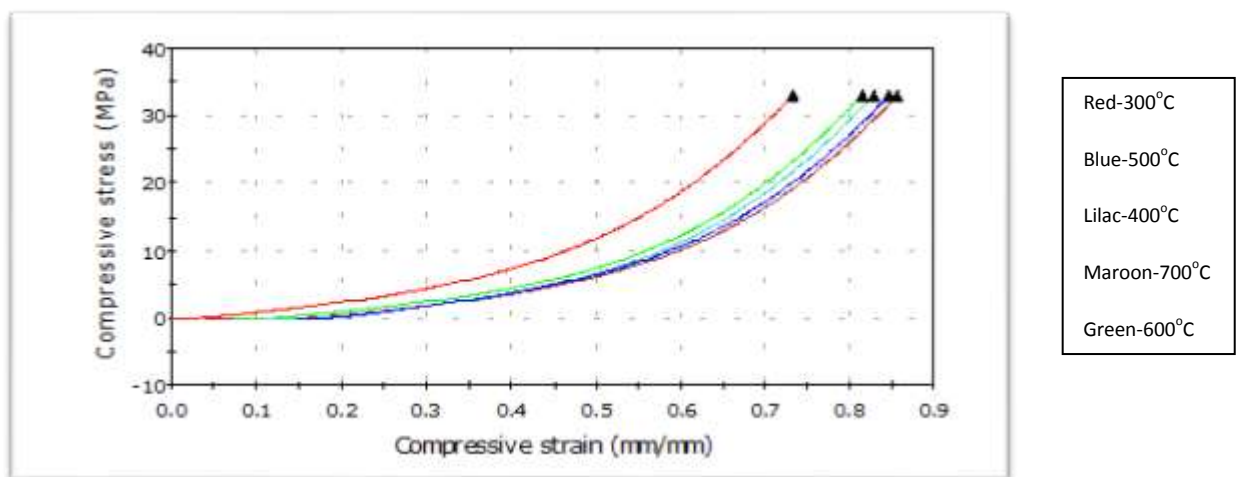


Figure 4.2: Compressive Stress versus Compressive Strain Curves for (1) 300°C, (2) 600°C, (3) 400°C, (4) 500°C and (5) 700°C Carbonisation Treatment for Coconut Fibre

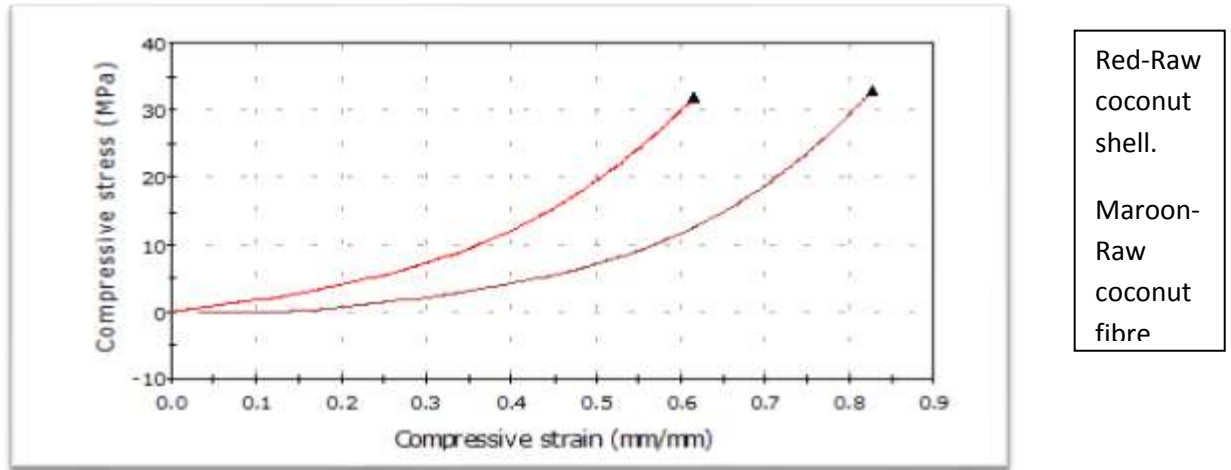


Figure 4.3: Compressive Stress versus Compressive Strain Curves for (1) Raw Coconut Shell and (2) Raw Coconut Fibre

4.6 Results of Tensile Strength/Modulus/EAB

Table 4.5: Results of Tensile, Modulus and EAB

Samples	Tensile Strength (MPa)	Modulus (%)	Elongation (%)
CSP Raw	3.91	1.92	494.50
CSP 300	4.21	3.10	484.60
CSP 400	4.30	4.35	420.00
CSP 500	5.20	5.40	398.20
CSP 600	4.90	5.38	395.00
CSP 700	4.80	5.12	398.20
CFP Raw	5.96	2.85	520.50
CFP 300	7.25	3.20	515.80
CFP 400	7.97	3.84	498.20
CFP 500	8.45	4.22	488.50
CFP 600	8.68	4.25	455.70
CFP 700	7.85	4.00	468.85

4.7 Tensile Stress-Strain Relationship

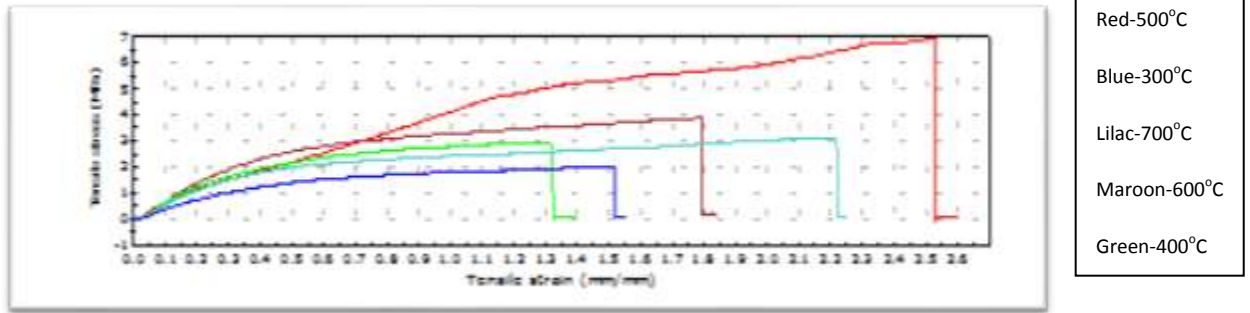


Figure 4.4: Tensile Stress versus Tensile Strain Curves for (1) 500°C, (2) 600°C, (3) 700°C, (4) 400°C and (5) 300°C Carbonisation Treatment for Coconut Shell

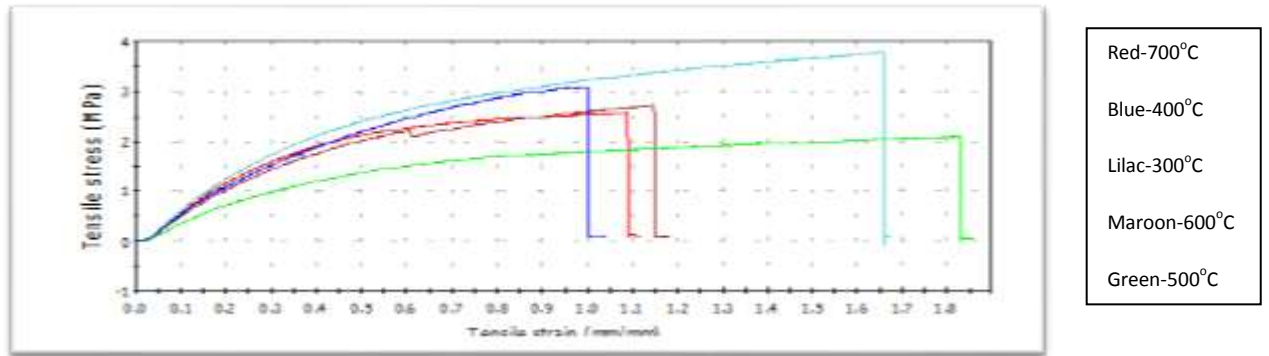


Figure 4.5: Tensile Stress versus Tensile Strain Curves for (1) 300°C, (2) 400°C, (3) 700°C, (4) 600°C and (5) 500°C Carbonisation Treatment for Coconut Fibre

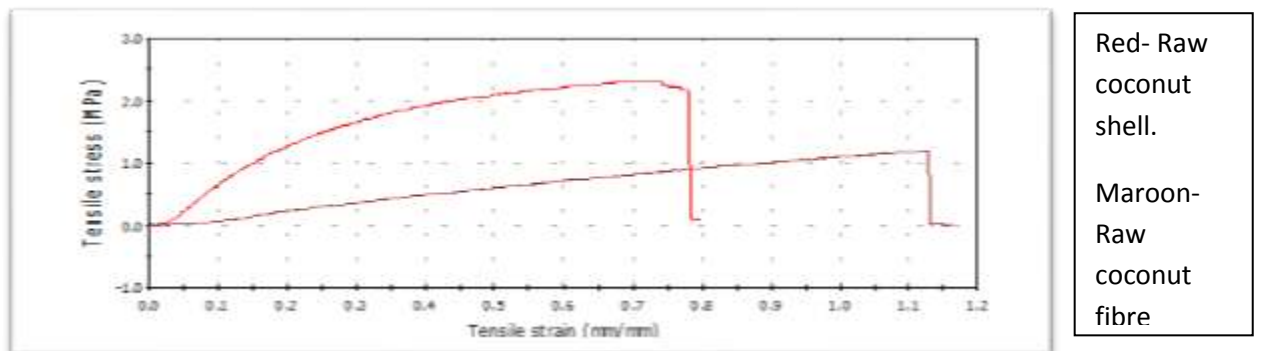


Figure 4.6: Tensile Stress versus Tensile Strain Curves for (1) Raw Coconut Shell and (2) Raw Coconut Fibre.

4.8 Results of Flexural Strength

Table 4.6: Results of Flexural Strength

Test Samples	Mean Flexural Strength (Mpa)
CSP Raw	0.15
CSP 300	0.39
CSP 400	0.28
CSP 500	0.46
CSP 600	0.38
CSP 700	0.21
CFP Raw	0.44
CFP 300	1.40
CFP 400	1.42
CFP 500	1.65
CFP 600	1.99
CFP 700	1.48

4.9 Flexure Stress-Strain Relationship

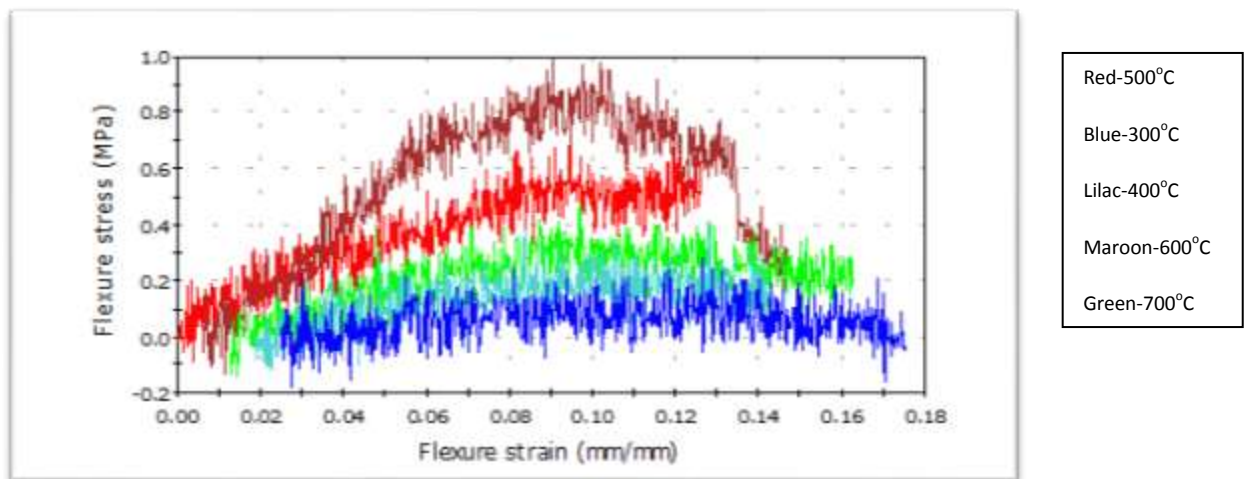


Figure 4.7: Flexure Stress versus Flexure Strain Curves for (1) 600°C, (2) 500°C, (3) 700°C, (4) 400°C and (5) 300°C Carbonisation Treatment for Coconut Shell

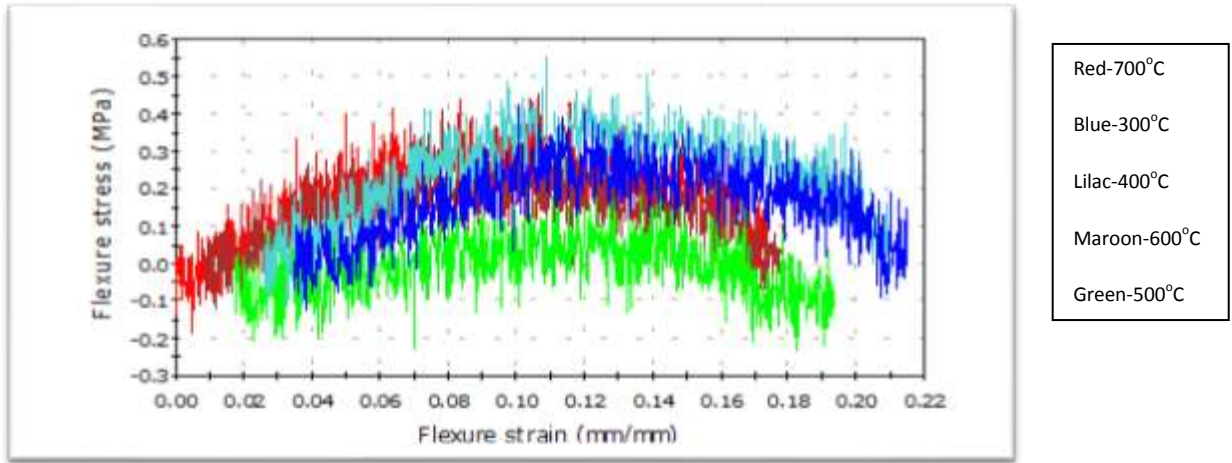


Figure 4.8: Flexure Stress versus Flexure Strain Curves for (1) 700°C, (2) 400°C, (3) 300°C, (4) 600°C and (5) 500°C Carbonisation Treatment for Coconut Fibre

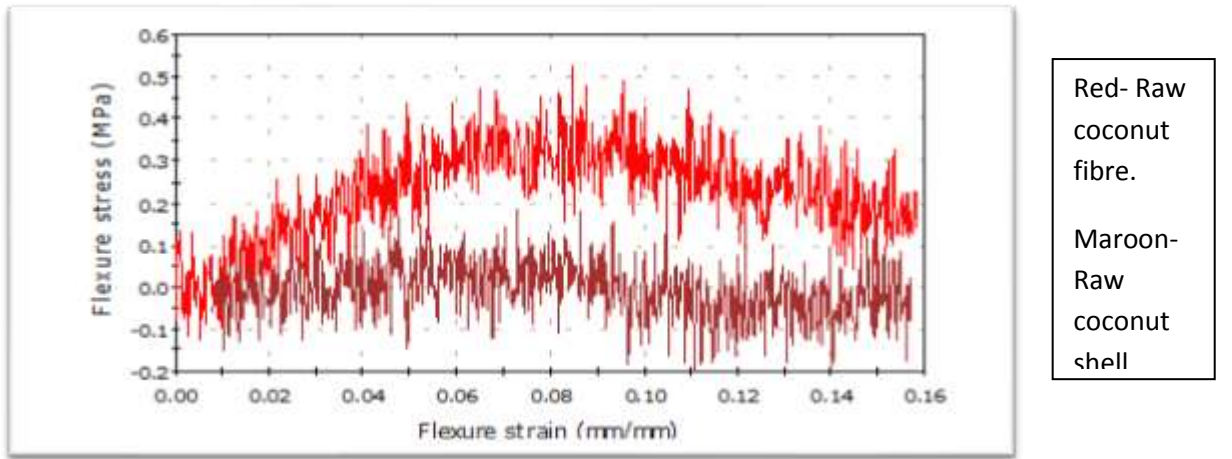


Figure 4.9: Flexure Stress versus Flexure Strain Curves for (1) Raw Coconut Fibre and (2) Raw Coconut Shell.

4.10 3-D Plots Presentation of Mechanical Analysis

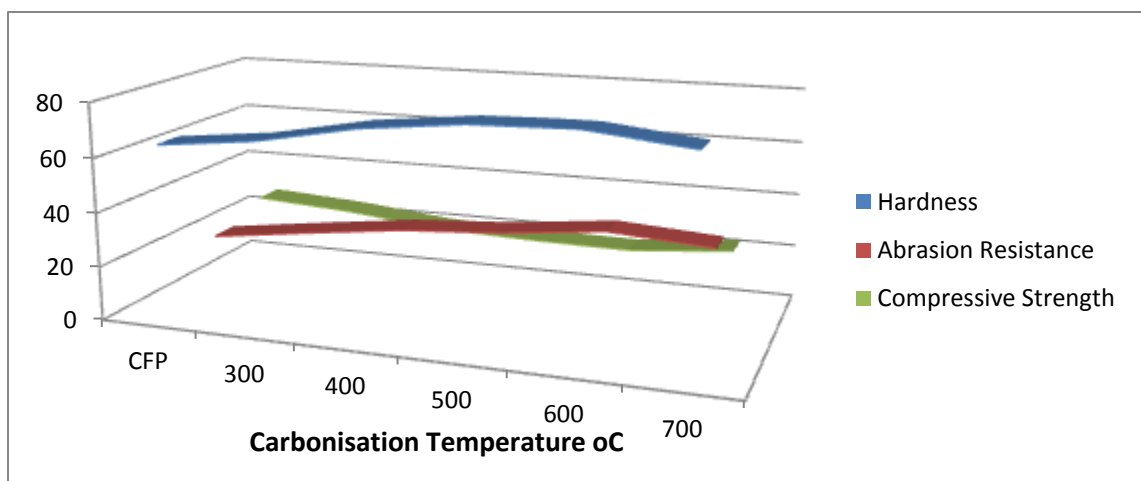


Figure 4.10: 3-D Plots of Hardness, Abrasion, Compressive Strength versus Carbonisation Temperature for Fibre Filled Composites

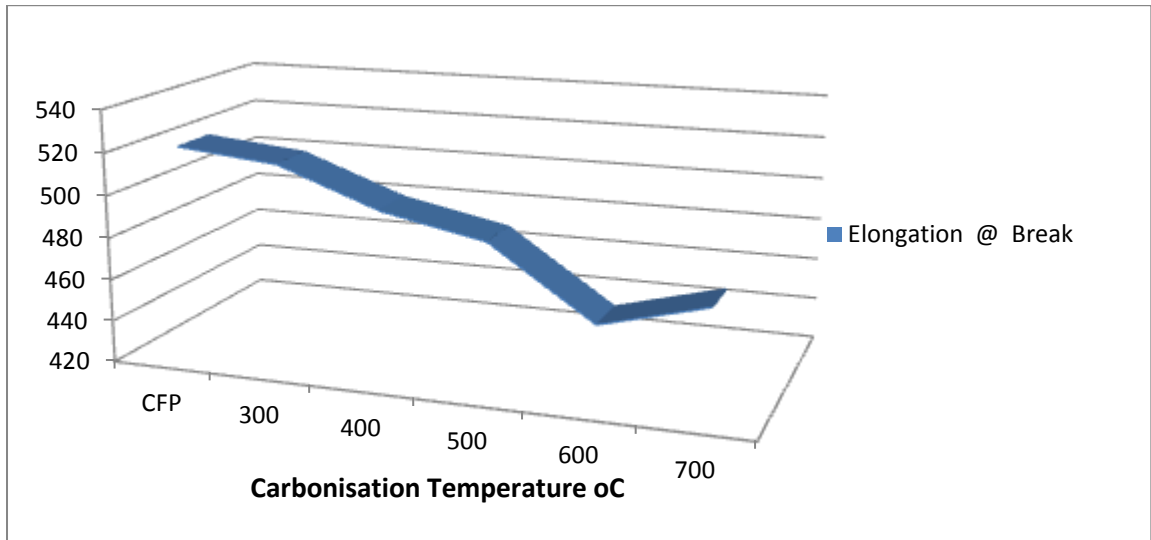


Figure 4.11: 3-D Plot of Elongation @ Break versus Carbonisation Temperature for Fibre Filled Composites

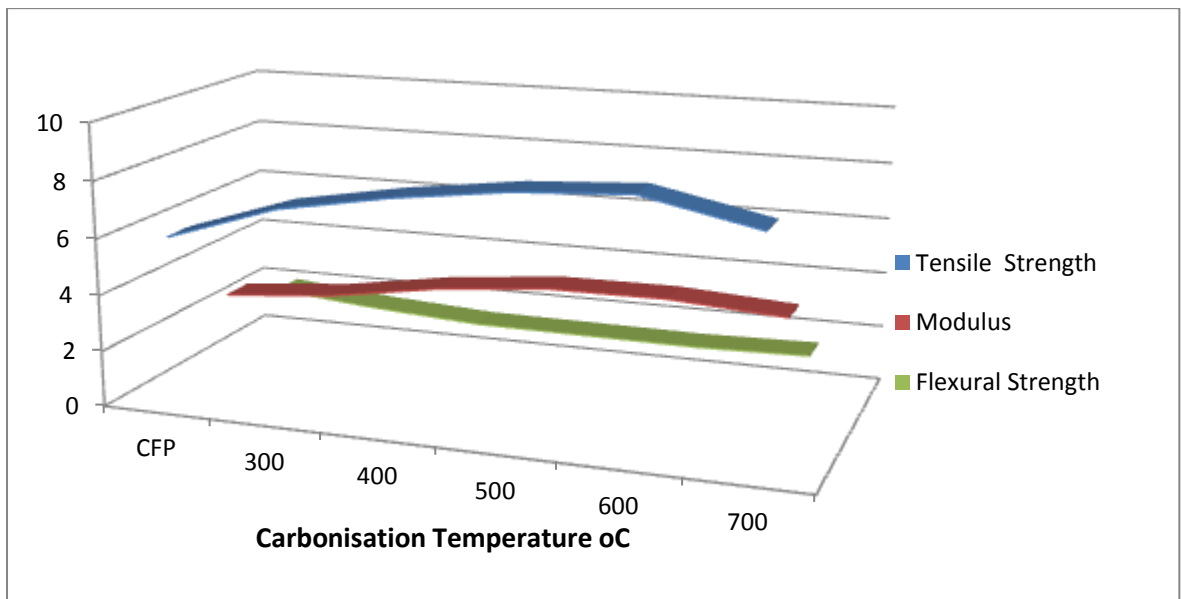


Figure 4.12: 3-D Plots of Tensile Strength, Modulus, Flexural Strength versus Carbonisation Temperature for Fibre Filled Composites

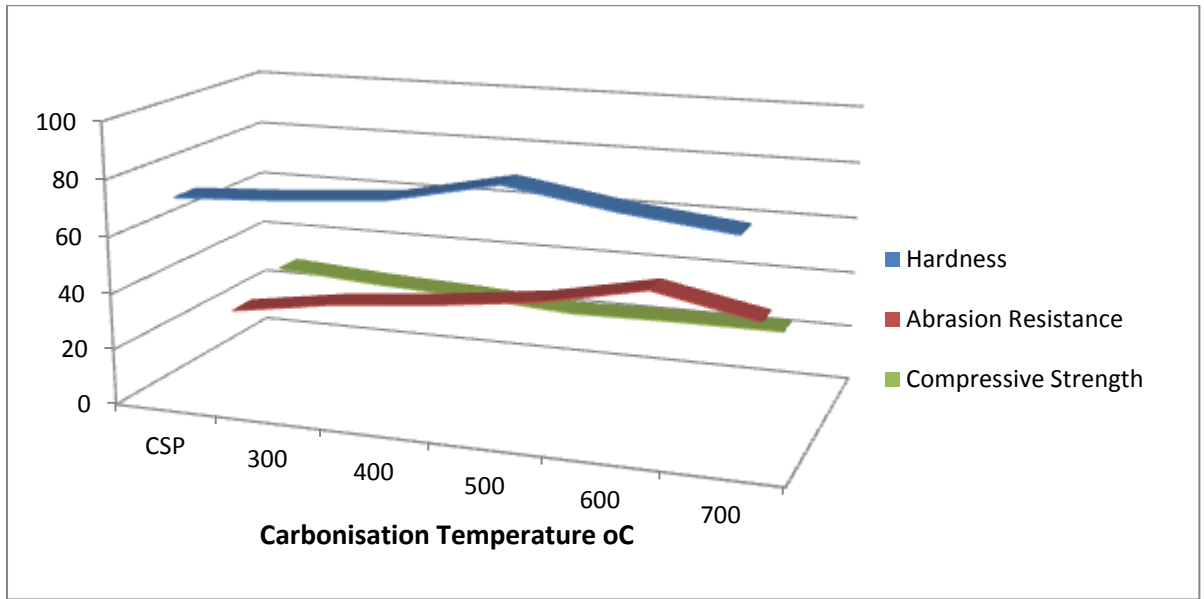


Figure 4.13: 3-D Plots of Hardness, Abrasion Resistance, Compressive Strength versus Carbonisation Temperature for Shell Filled Composites

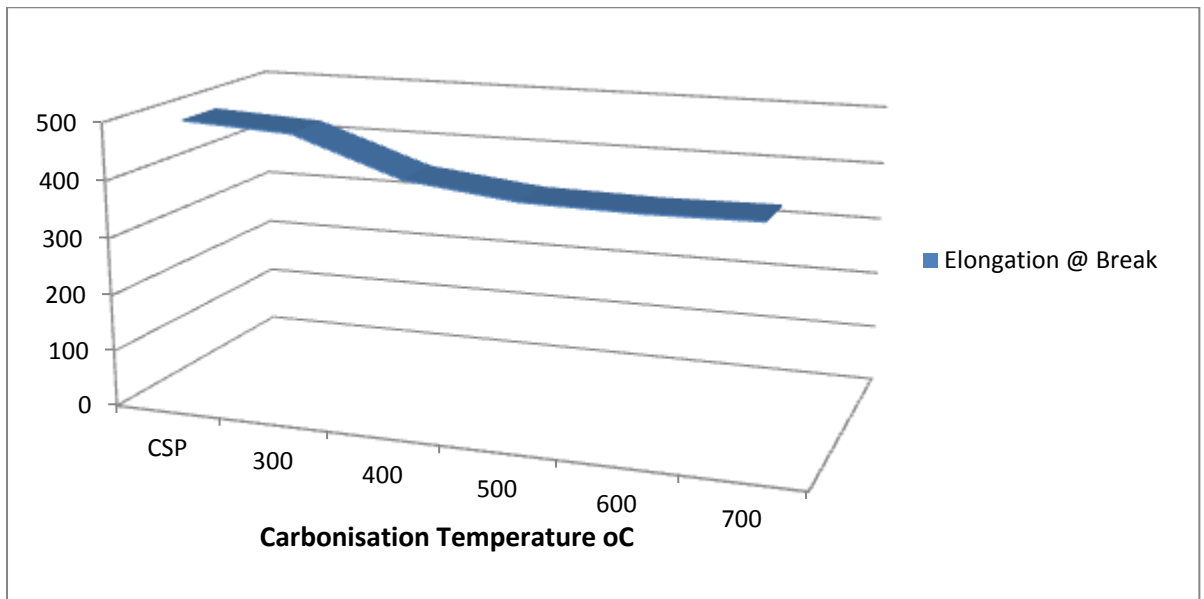


Figure 4.14: 3-D Plot of Elongation @ Break versus Carbonisation Temperature for Shell Filled Composites

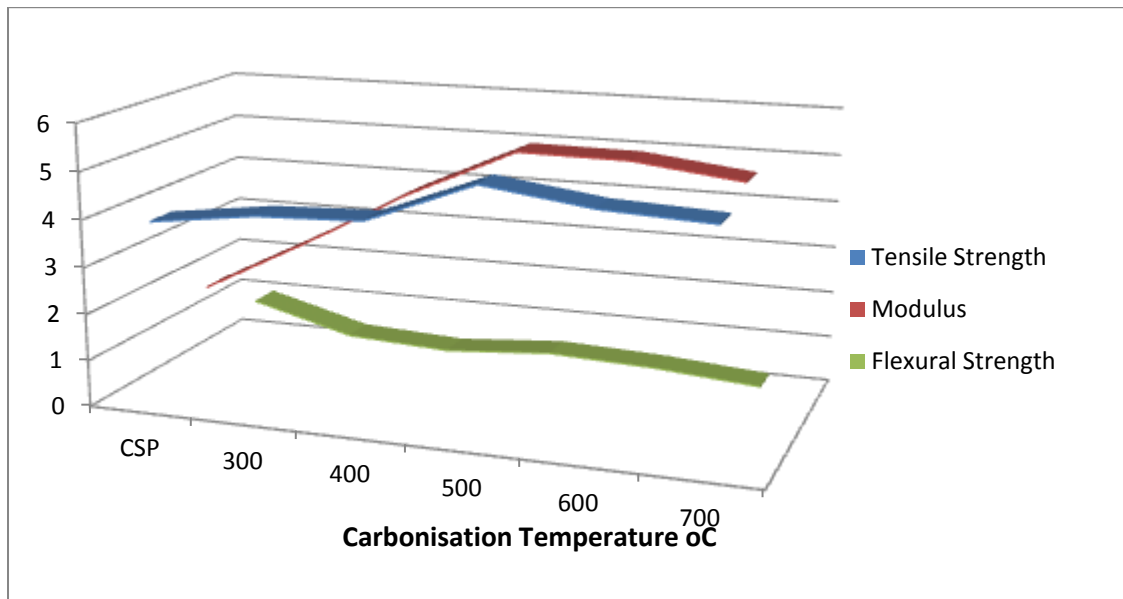


Figure 4.15: 3-D Plots of Tensile Strength, Modulus, Flexural Strength versus Carbonisation Temperature for Shell Filled Composites

4.11 Sorption Tests Results and Plots

Table 4.7 Sorption Capacity (%)

Samples	Hexane	Xylene	Toluene	Benzene
CSP Raw	425	400	402	248
CSP 300	394	385	394	240
CSP 400	342	372	368	230
CSP 500	274	281	300	228
CSP 600	236	240	256	222
CSP 700	221	218	248	200
CFP Raw	525	520	495	312
CFP 300	500	492	445	258
CFP 400	484	490	415	218
CFP 500	425	472	358	201
CFP 600	412	422	325	198
CFP 700	415	425	368	200

4.12 Infra-Red Spectroscopic Analysis

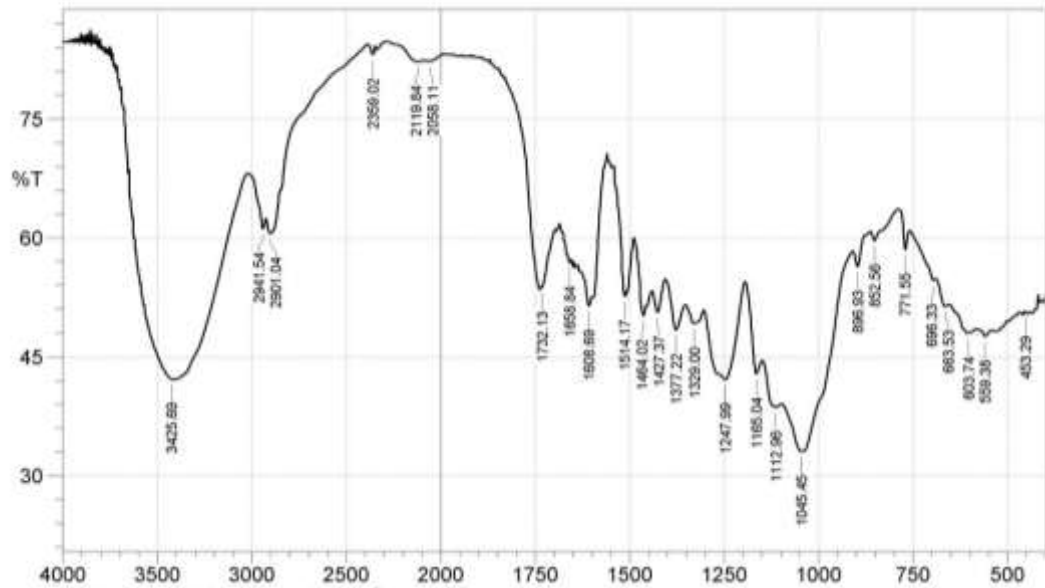


Figure 4.16: FTIR Spectrum for Raw Coconut Shell

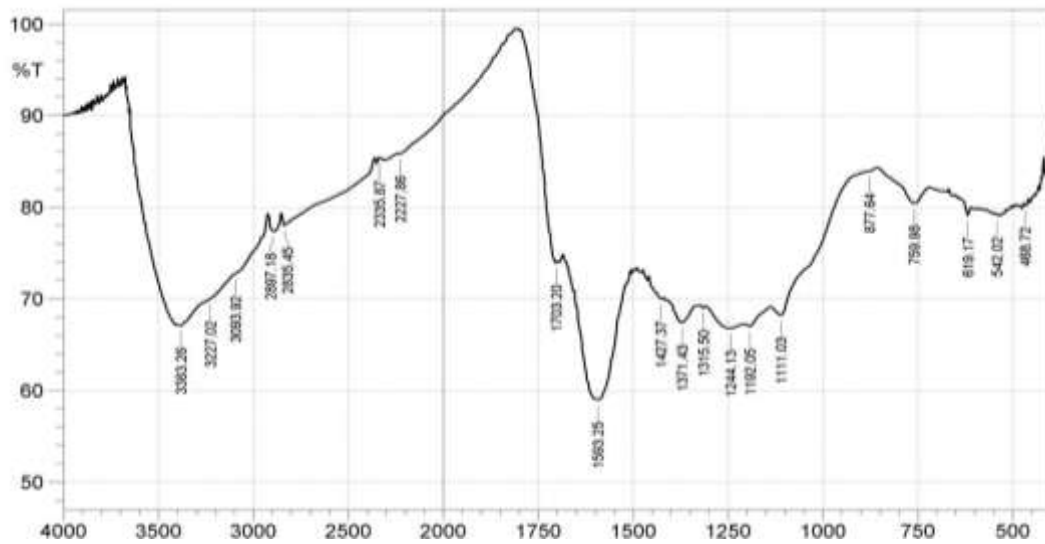


Figure 4.17: FTIR Spectrum for Coconut Shell at 300°C

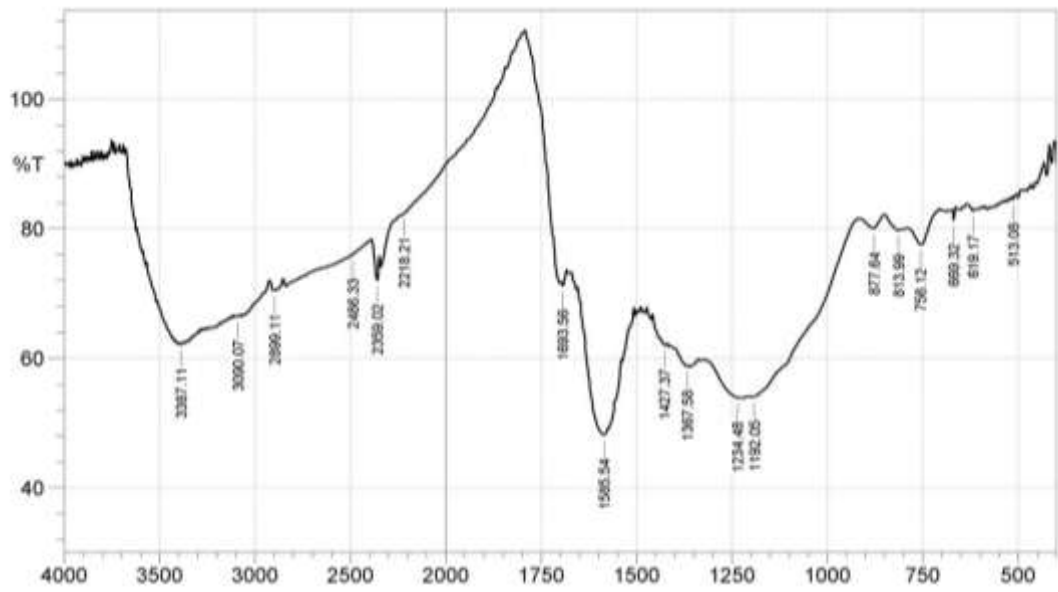


Figure 4.18: FTIR Spectrum for Coconut Shell at 400°C

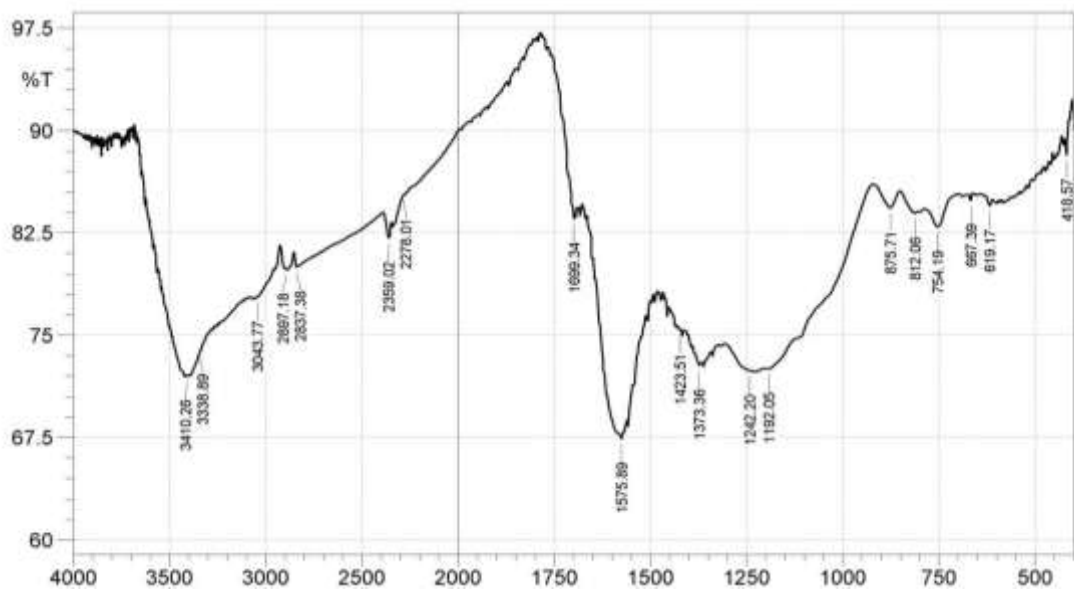


Figure 4.19: FTIR Spectrum for Coconut Shell at 500°C

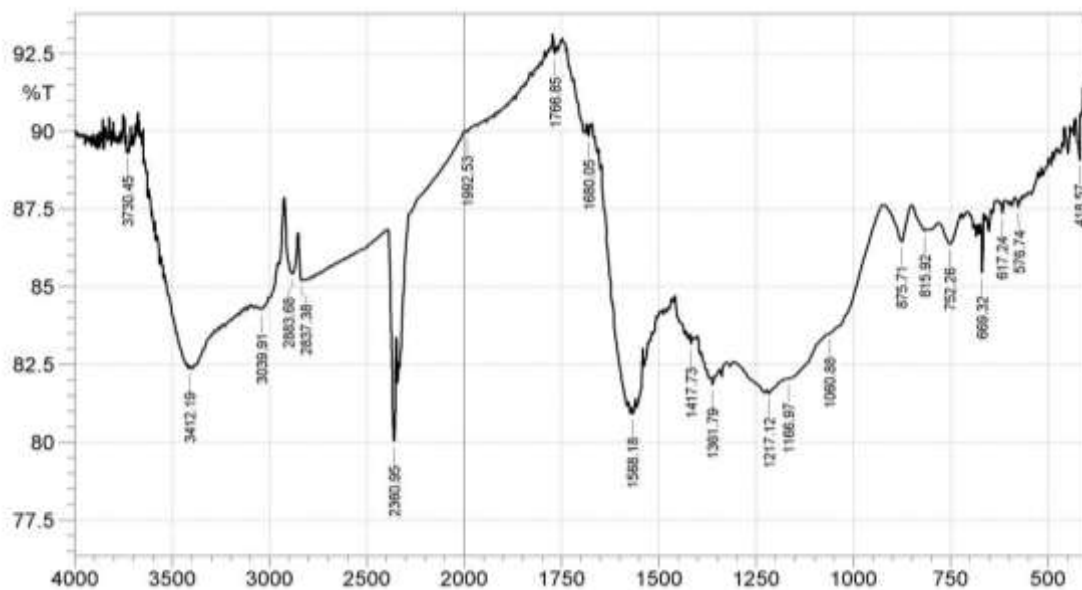


Figure 4.20: FTIR Spectrum for Coconut Shell at 600°C

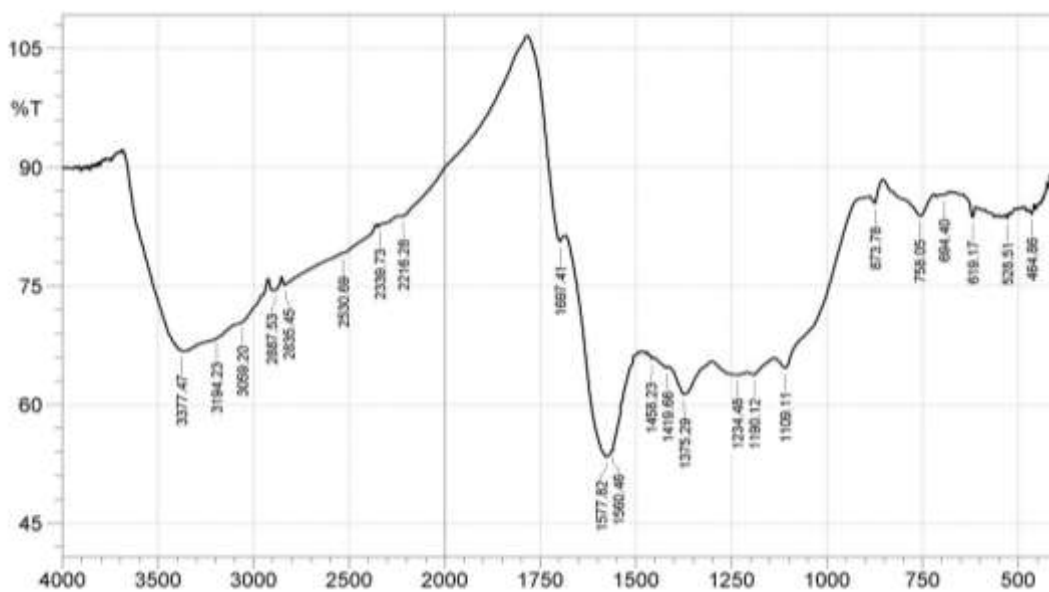


Figure 4.21: FTIR Spectrum for Coconut Shell at 700°C

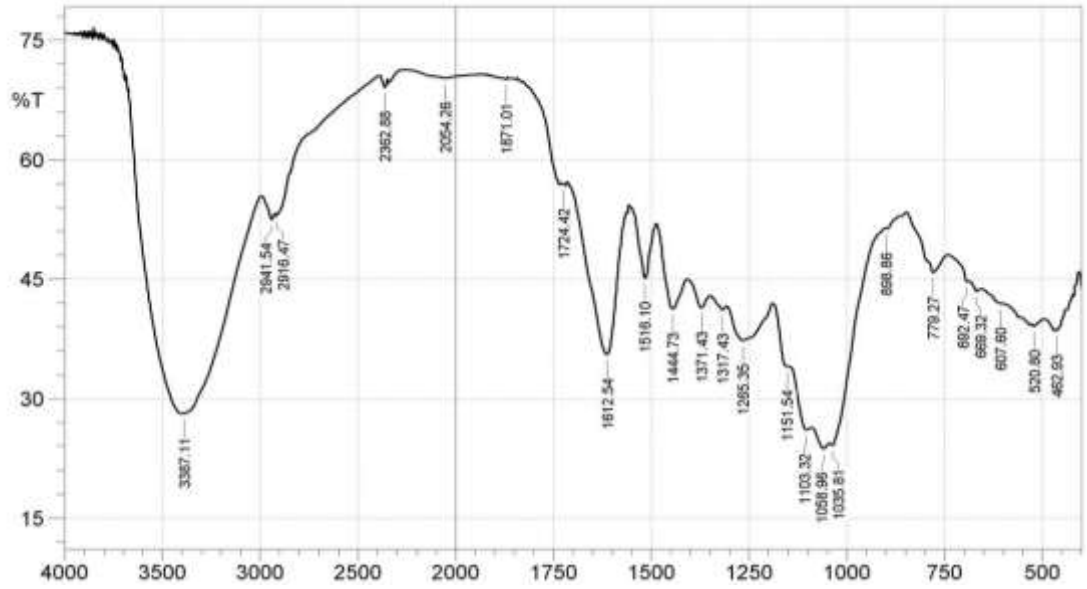


Figure 4.22: FTIR Spectrum for Raw Coconut Fibre

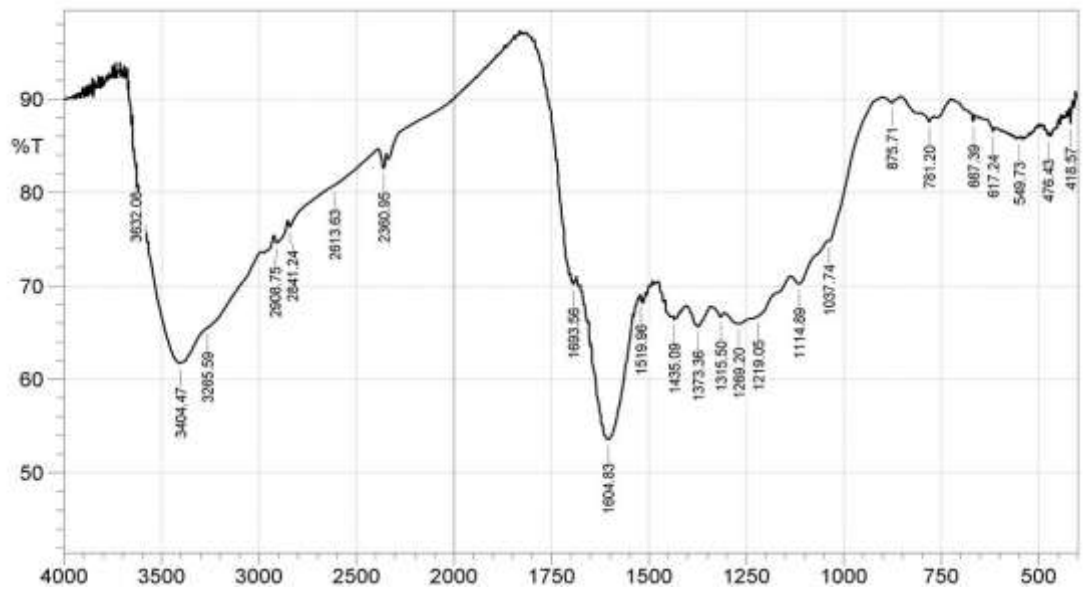


Figure 4.23: FTIR Spectrum for Coconut Fibre at 300°C

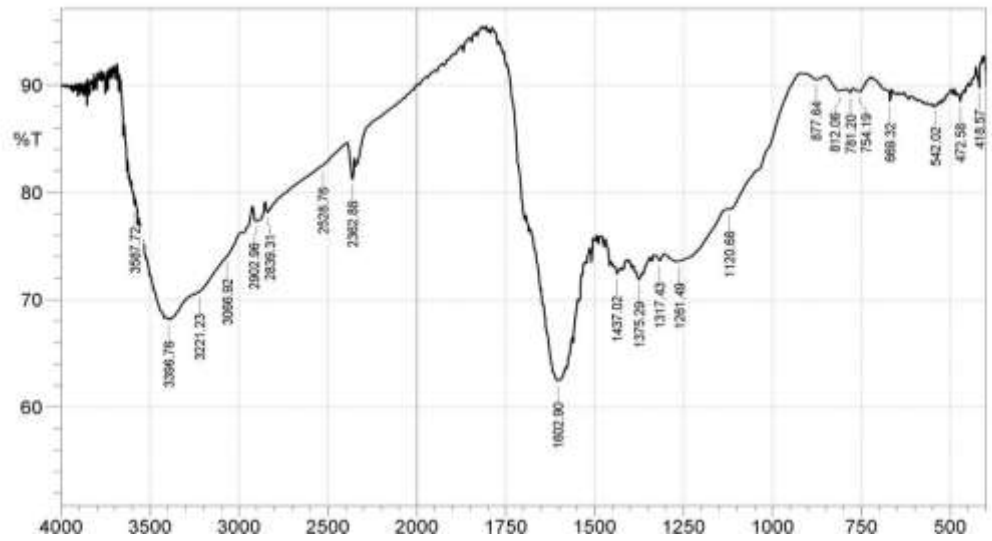


Figure 4.24: FTIR Spectrum for Coconut Fibre at 400°C

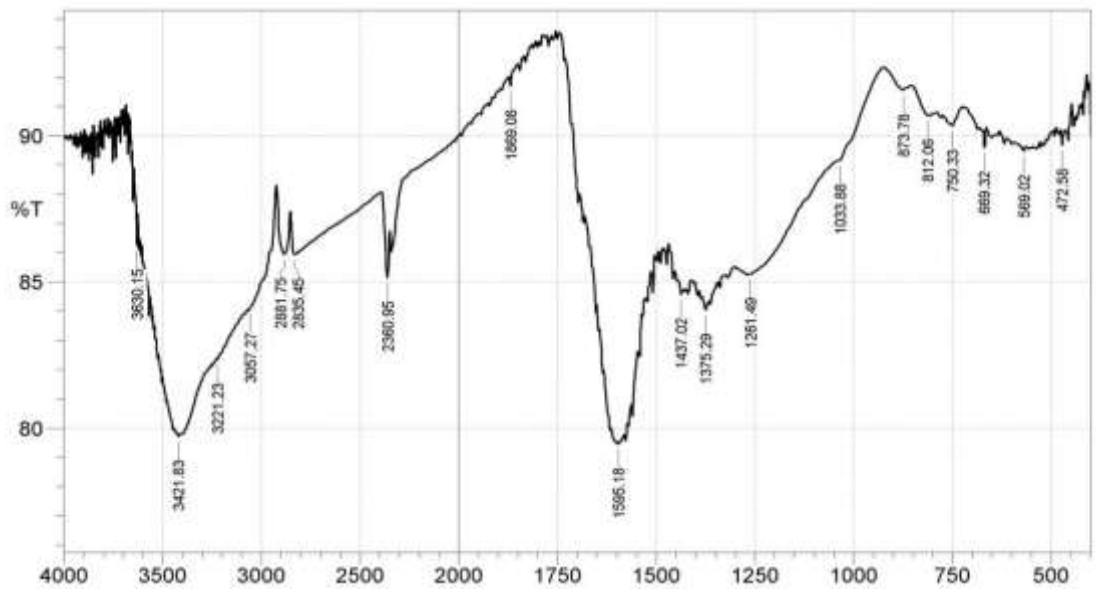


Figure 4.25: FTIR Spectrum for Coconut Fibre at 500°C

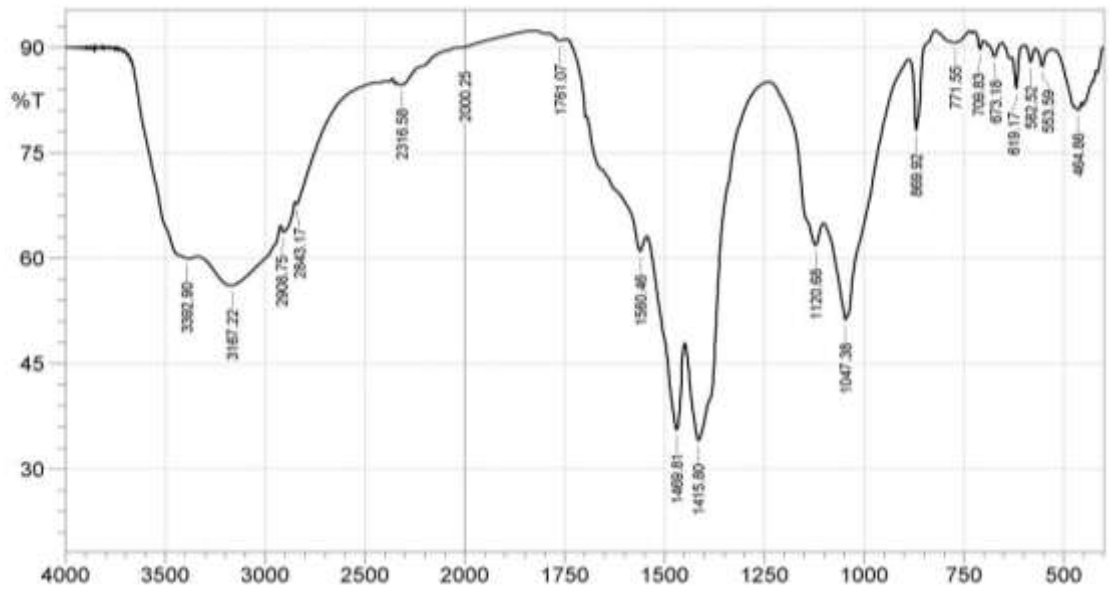


Figure 4.26: FTIR Spectrum for Coconut Fibre at 600°C

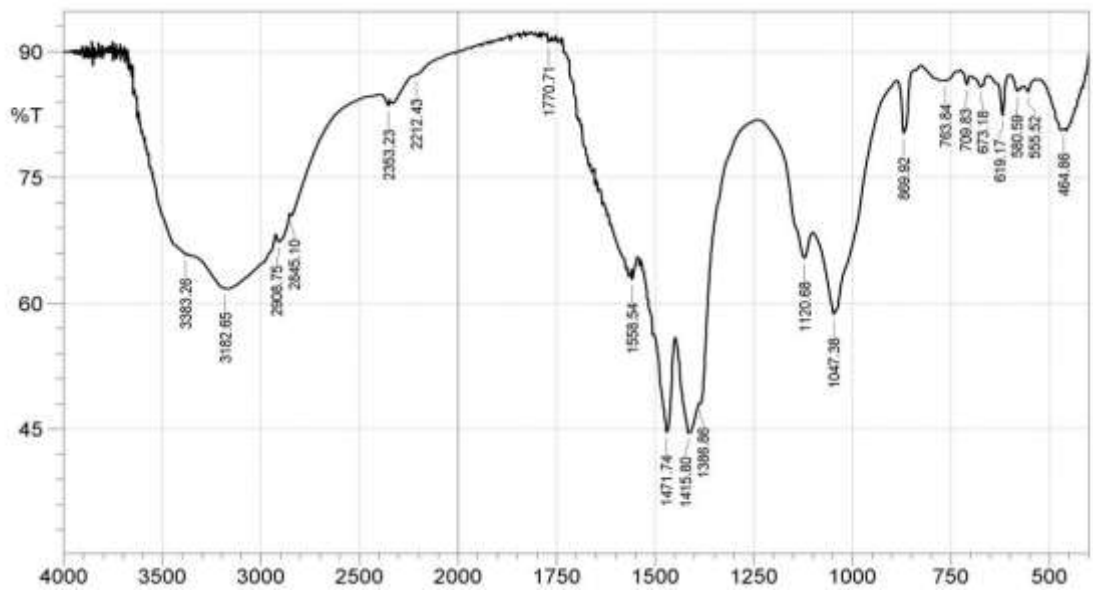


Figure 4.27: FTIR Spectrum for Coconut Fibre at 700°C

4.13 Scanning Electron Microscopy Results and Plates

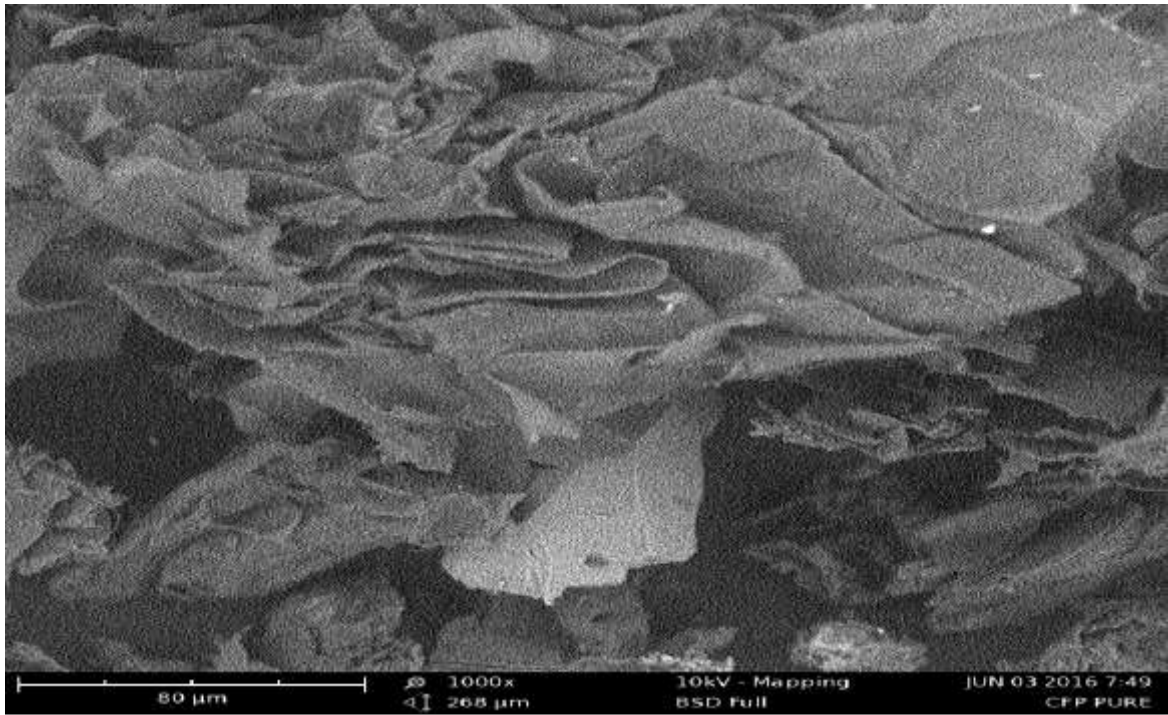


Plate 4.1: SEM Monograph of Composite with Raw Coconut Fibre



Plate 4.2: SEM Monograph of Composite with Coconut Fibre at 300°C

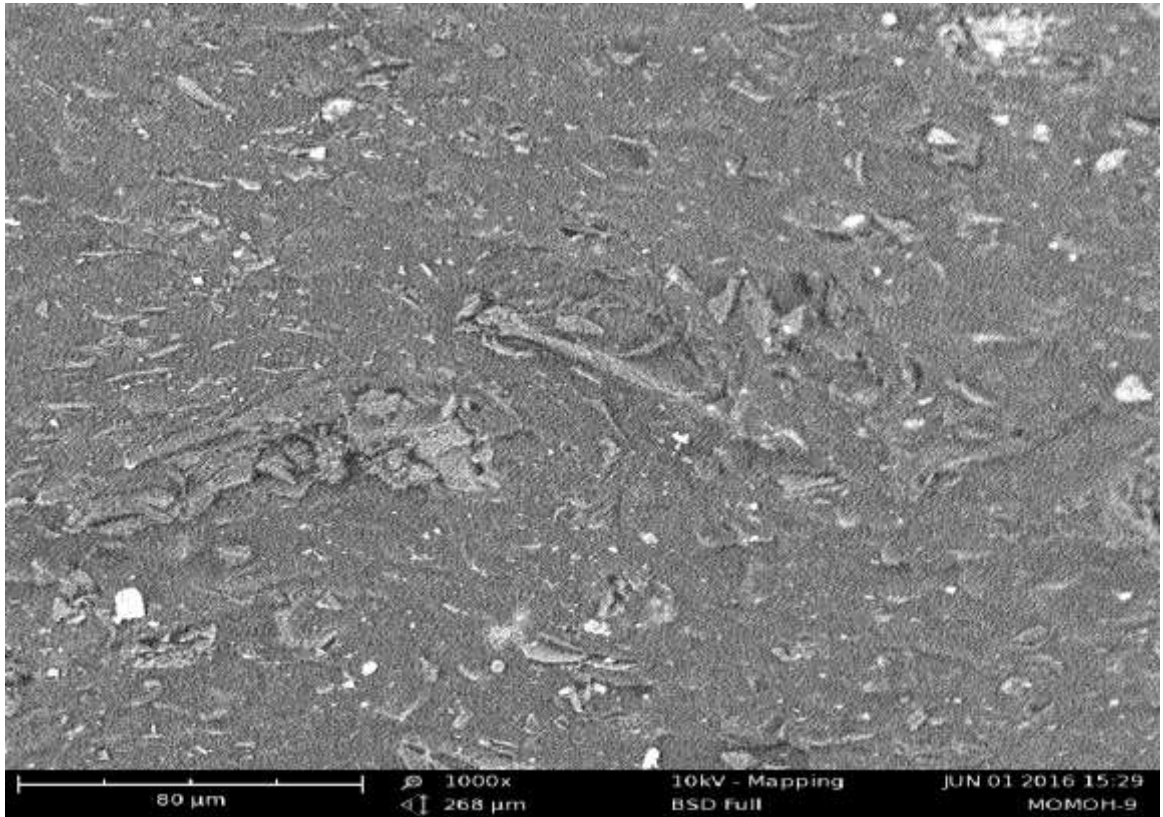


Plate 4.3: SEM Monograph of Composite with Coconut Fibre at 400°C

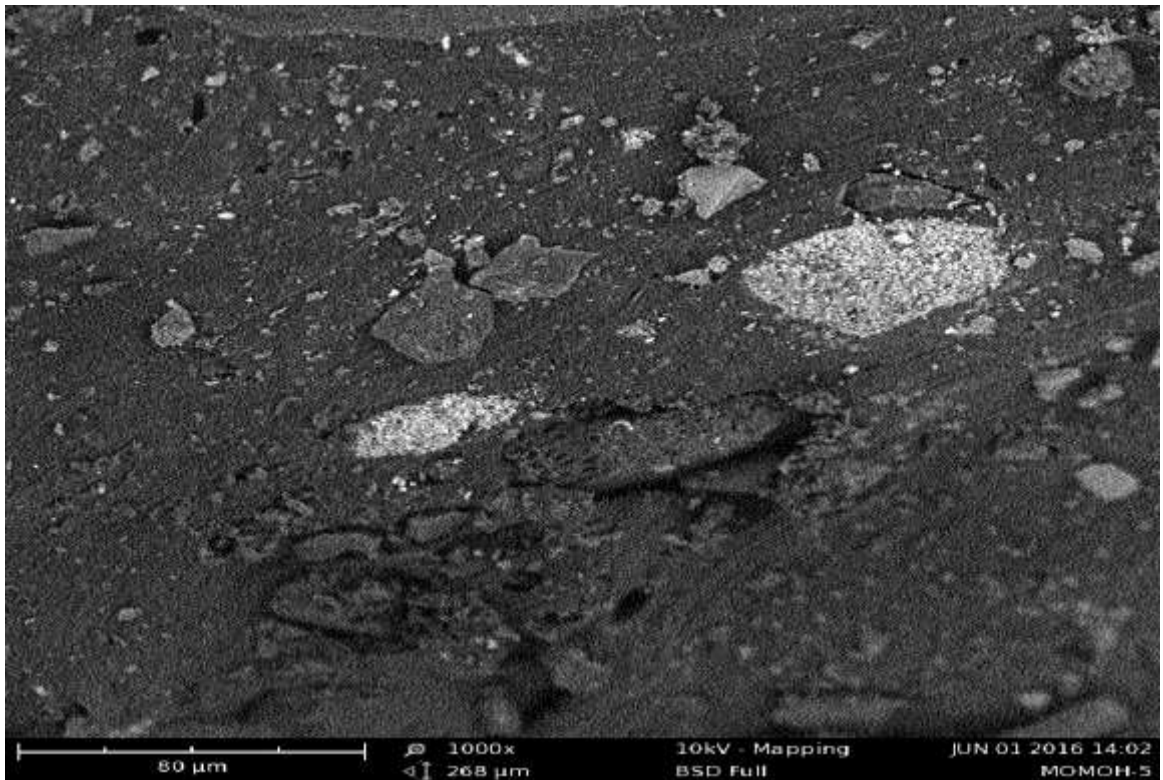


Plate 4.4: SEM Monograph of Composite with Coconut Fibre at 500°C

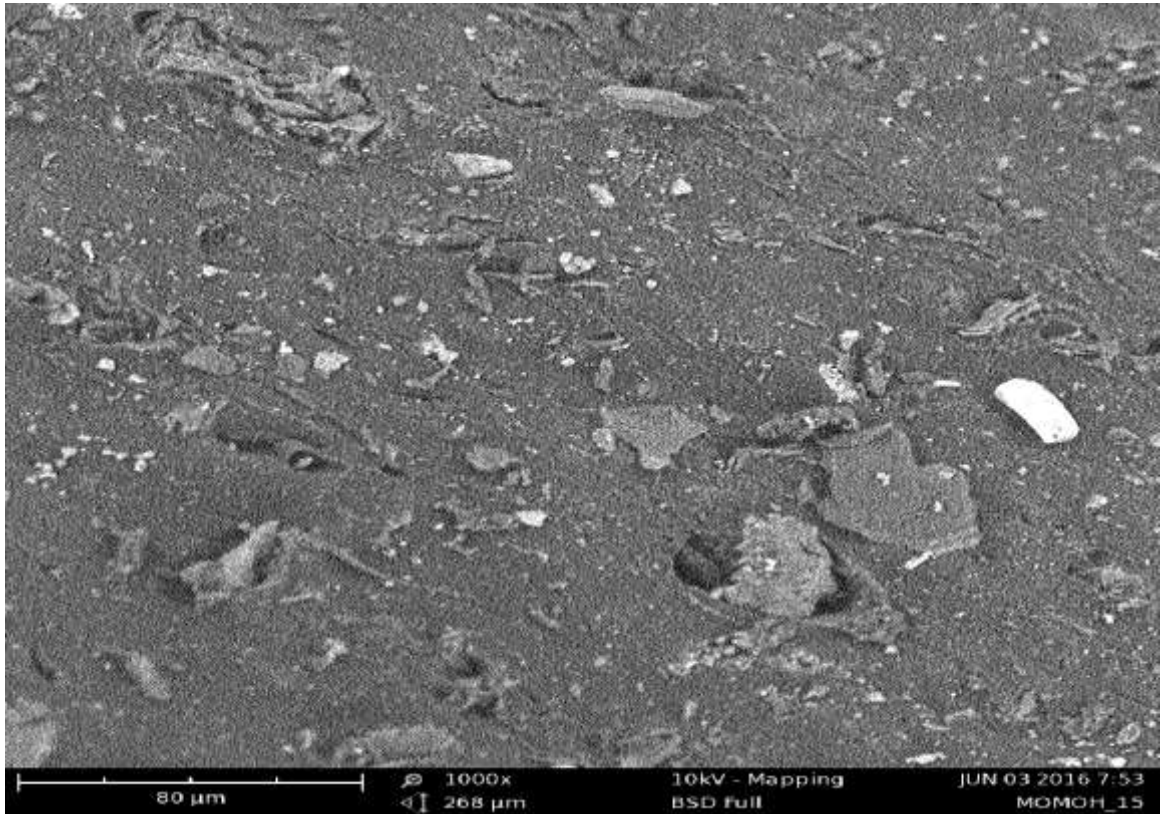


Plate 4.5: SEM Monograph of Composite with Coconut Fibre at 600°C

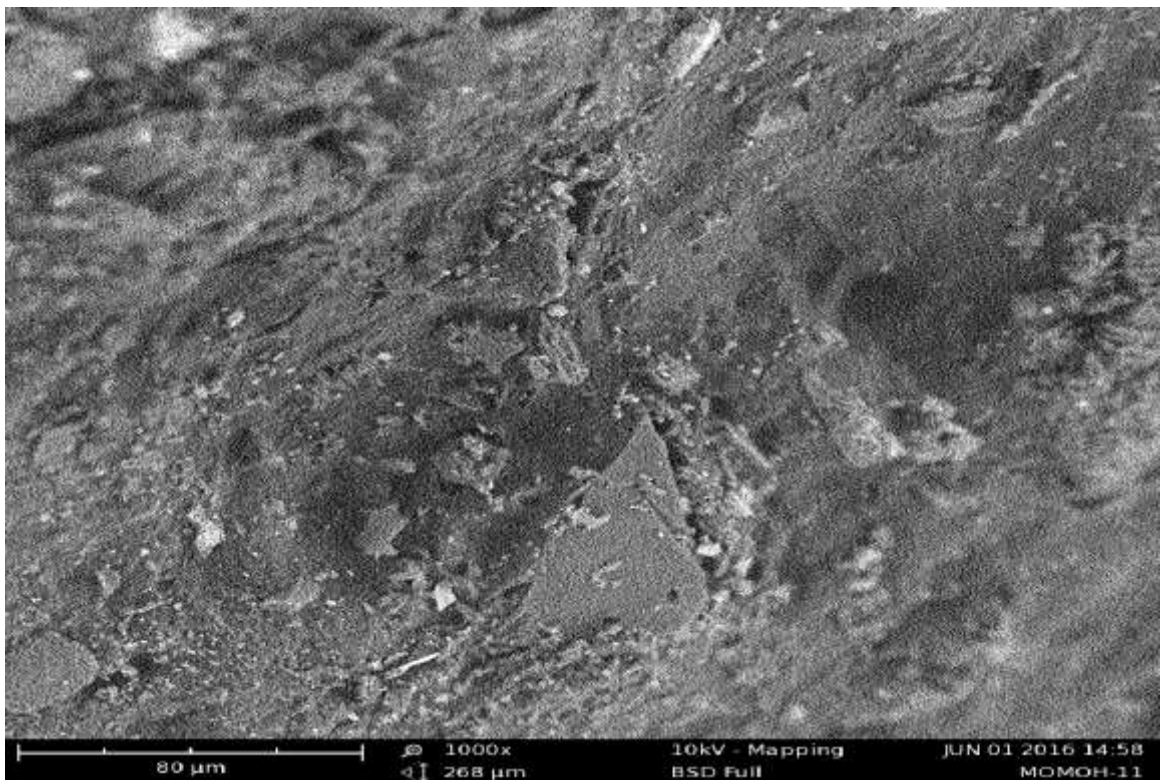


Plate 4.6: SEM Monograph of Composite with Coconut Fibre at 700°C



Plate 4.7: SEM Monograph of Composite with Raw Coconut Shell

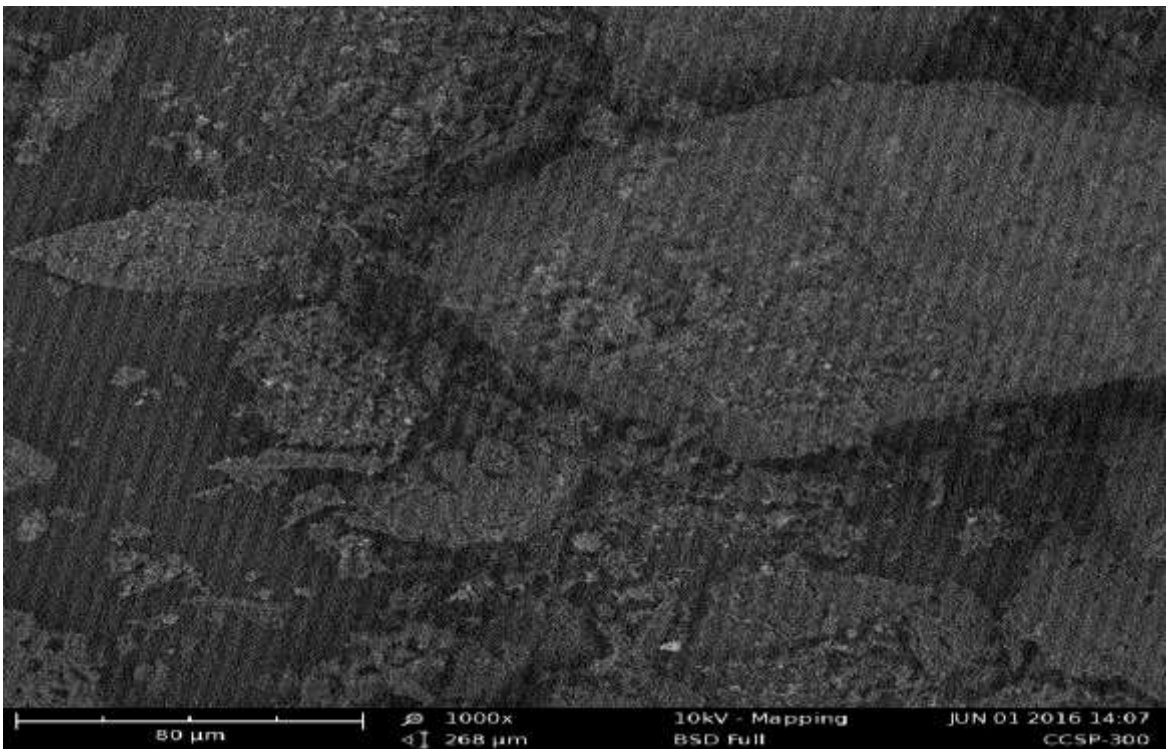


Plate 4.8: SEM Monograph of Composite with Coconut Shell at 300°C

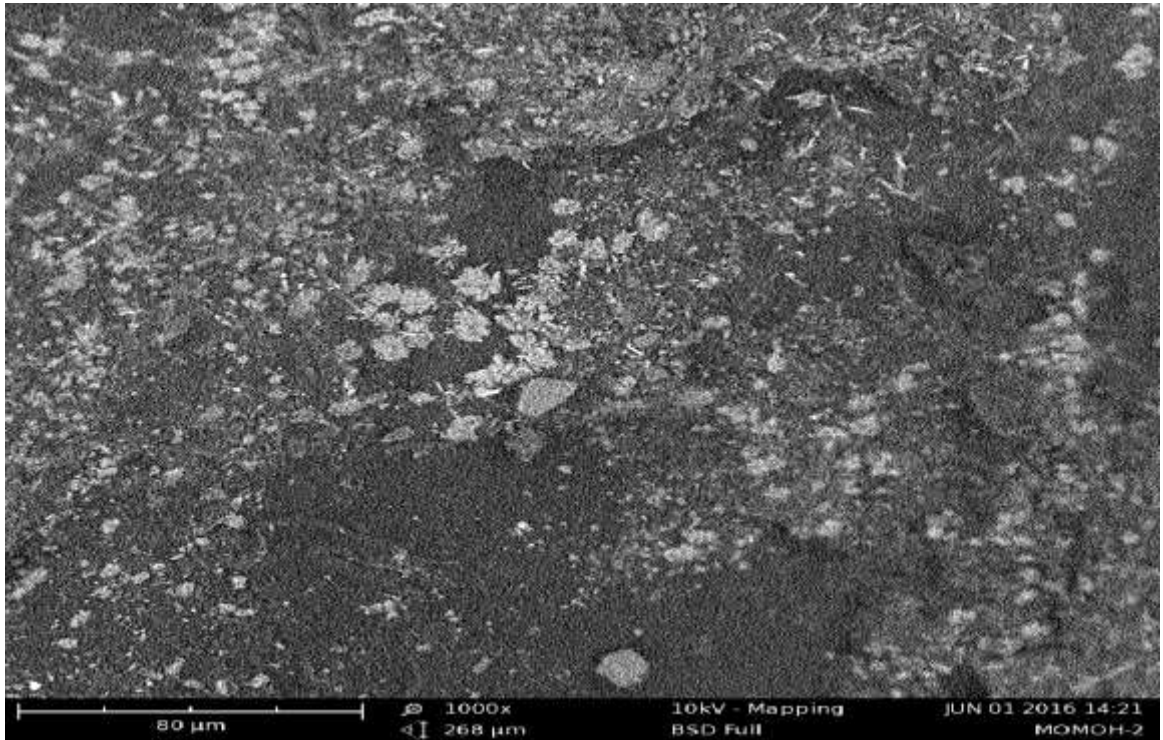


Plate 4.9: SEM Monograph of Composite with Coconut Shell at 400°C

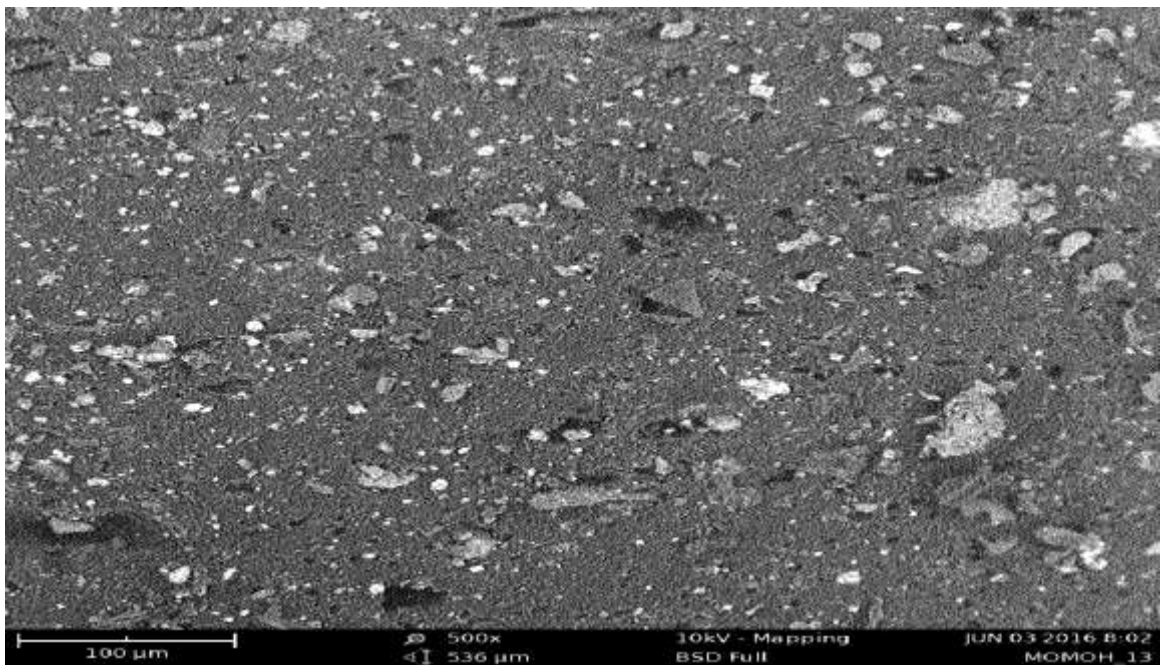


Plate 4.10: SEM Monograph of Composite with Coconut Shell at 500°C

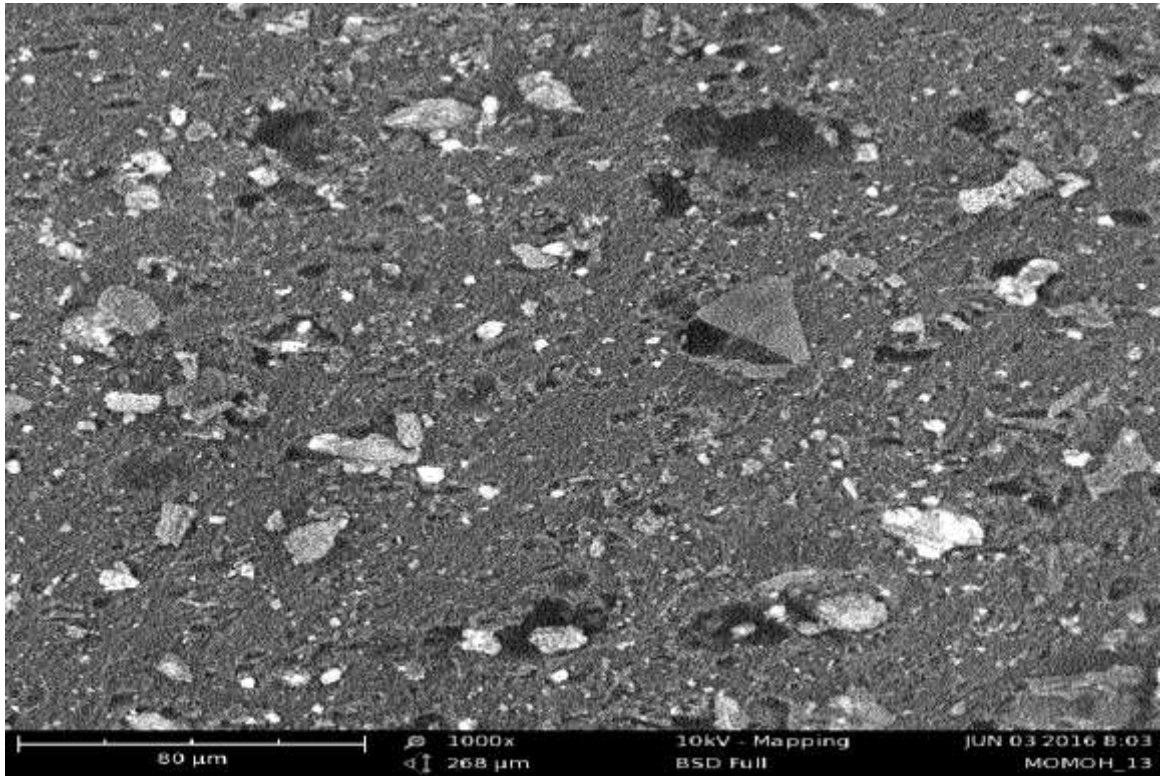


Plate 4.11: SEM Monograph of Composite with Coconut Shell at 600°C

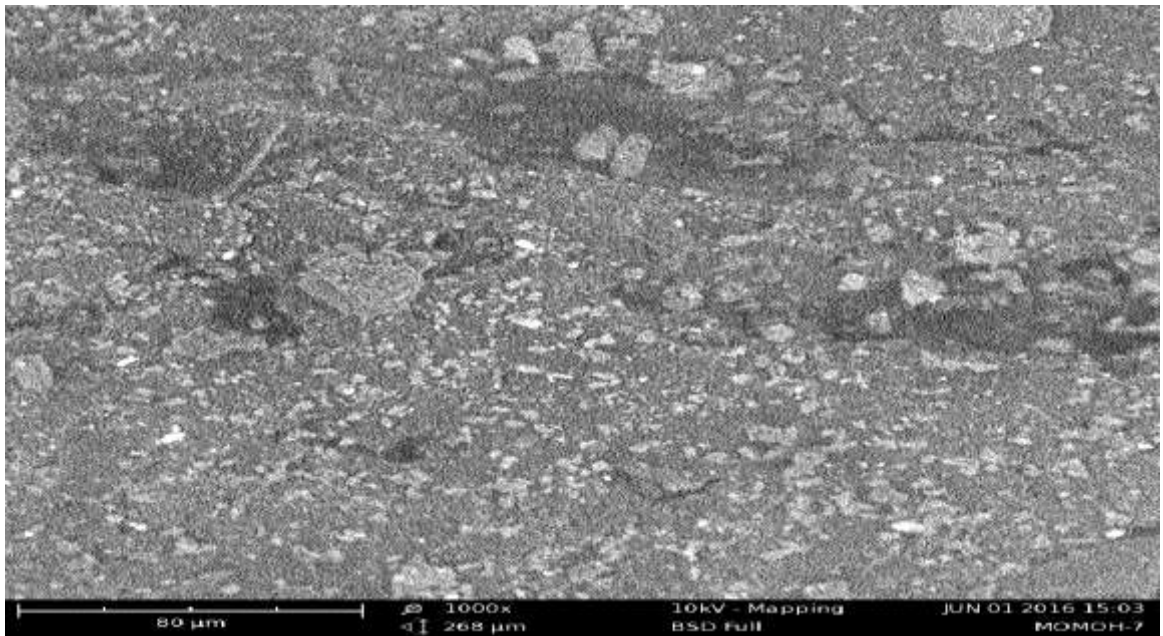


Plate 4.12: SEM Monograph of Composite with Coconut Shell at 700°C

Table 4.8 Particle Properties of SEM Weighted by Volume

Property	Median	Average
Circle equivalent diameter(mm)	36.5	40.3
Major axis (mm)	47.8	53.1
Minor axis (mm)	29.6	30.9
Circumference (mm)	173	206
Convex hull (mm)	141	161
Circumscribed diameter (mm)	58.3	64.3
Area (mm ²)	1.05E+03	1.44E+03
Volume (mm ³)	2.54E+04	4.85E+04
Pixels	1868	2567
Aspect ratio	0.595	0.596
Circularity	0.437	0.45
Convexity	0.818	0.824
Elongation (mm)	0.405	0.404
Grayscale	89.5	90.7

Table 4.9 Particle Properties of SEM Weighted by Count

Property	Median	Average
Circle equivalent diameter(mm)	27.2	30
Major axis (mm)	37	40
Minor axis (mm)	20.9	23
Circumference (mm)	121	137
Convex hull (mm)	106	117
Circumscribed diameter (mm)	43.1	47.2
Area (mm ²)	58.2	767
Volume (mm ³)	1.06E+04	1.84E+04
Pixels	1.040	1370
Aspect ratio	0.599	0.592
Circularity	0.513	0.519
Convexity	0.894	0.877
Elongation (mm)	0.401	0.408
Grayscale	90.5	91.7

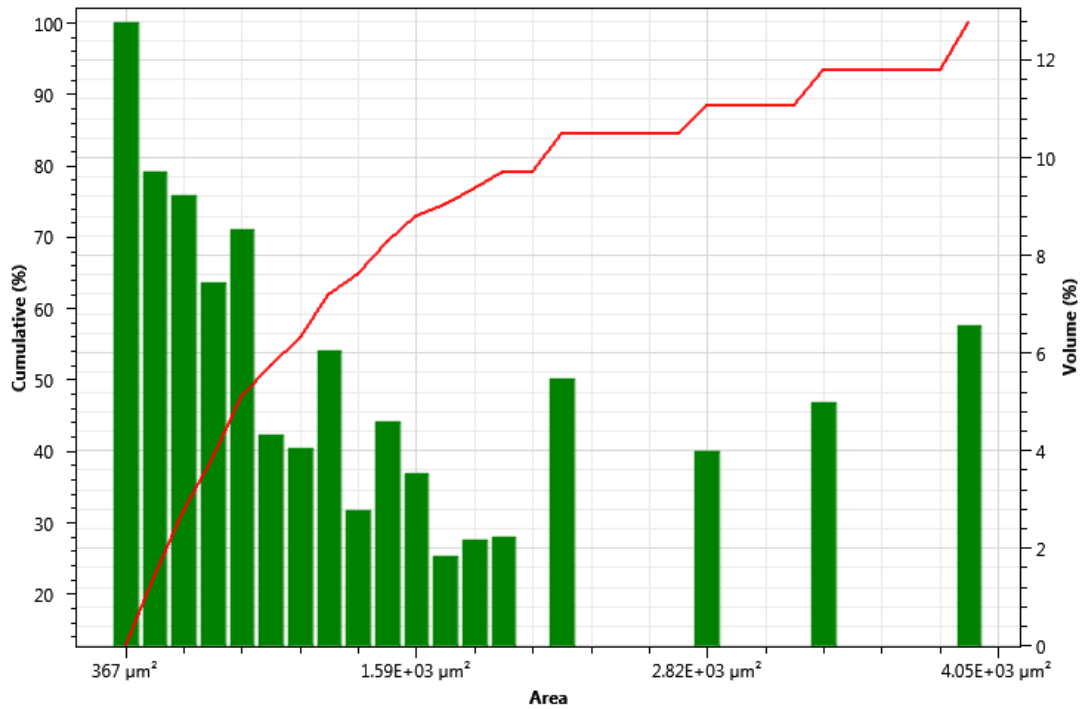


Figure 4.28: Graphs for Cumulative SEM Properties Weighted by Volume and by Count

4.14 X-Ray Diffractograms Results and Evaluation of the Degree Crystallisation

Table 4.10 Crystalline Parameters for Coconut Shell

Parameter for Xrd	CSP	300	400	500	600	700
Crystallinity (%)	60.2	71.2	82.9	87.7	86.2	85.6
ACD (A°)	≈3.7	≈3.7	≈3.7	≈3.7	≈3.7	≈3.7
Intensity Counts	44	52	72	87	85	84
FWHM	0.20150	0.16520	0.16000	0.15970	0.15180	0.11820
2θ Maximum Peak	21.0759	22.0729	23.0465	24.9875	23.9441	23.0659

*ACD- Average Crystalline Dimensions in A°

*FWHM- Full Width at Half Maximum

Table 4.11 Crystalline Parameters for Coconut Fibre

Parameter for Xrd	CFP	300	400	500	600	700
Crystallinity (%)	68.4	73.8	79	86.9	92.4	89.5
ACD (A°)	≈3.7	≈3.7	≈3.7	≈3.7	≈3.7	≈3.7
Intensity Counts	49	58	78	82	89	83
FWHM	0.30250	0.30110	0.28610	0.24250	0.20010	0.19850
2θ Maximum Peak	21.9560	22.6590	23.8960	25.6650	25.9890	24.1020

*ACD- Average Crystalline Dimensions in A°

*FWHM- Full Width at Half Maximum

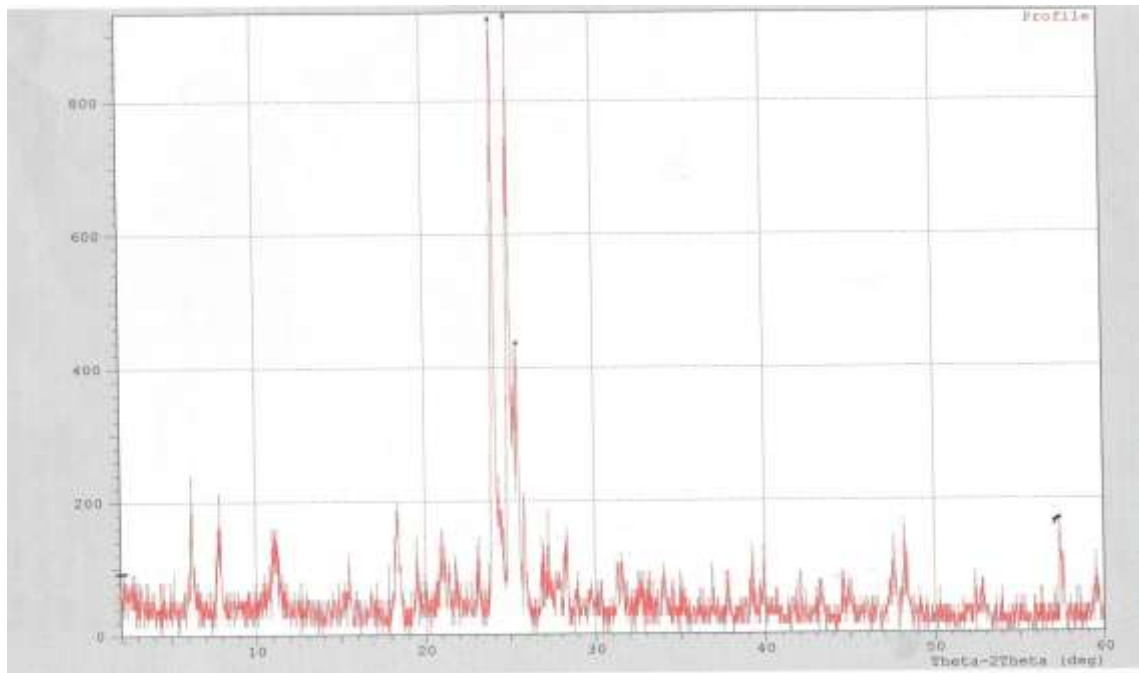


Figure 4.29: X-Ray Diffractogram of Raw Coconut Shell Filler.

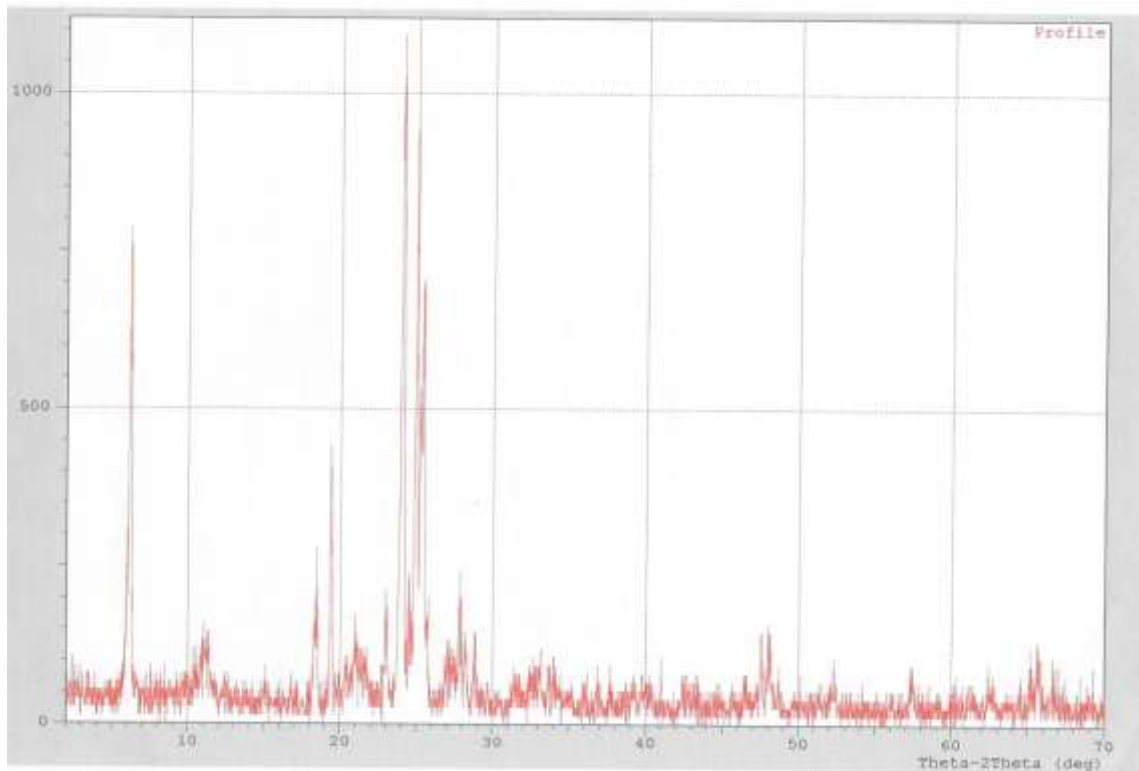


Figure 4.30: X-Ray Diffractogram of Coconut Shell Filler at 300°C

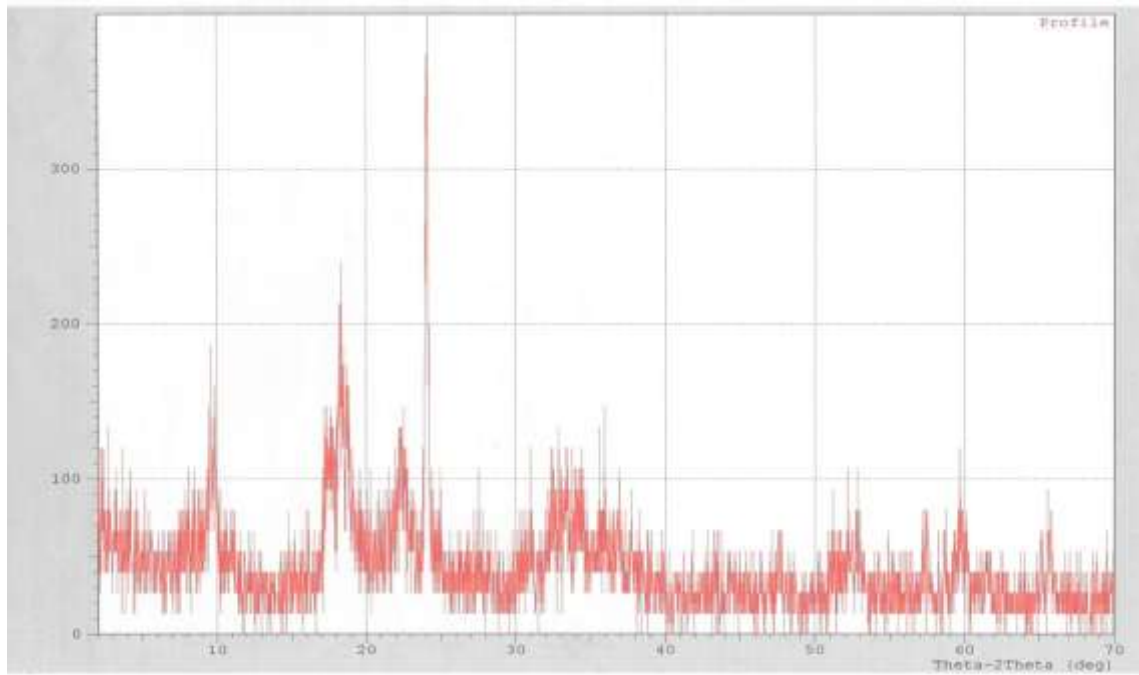


Figure 4.31: X-Ray Diffractogram of Coconut Shell Filler at 400°C

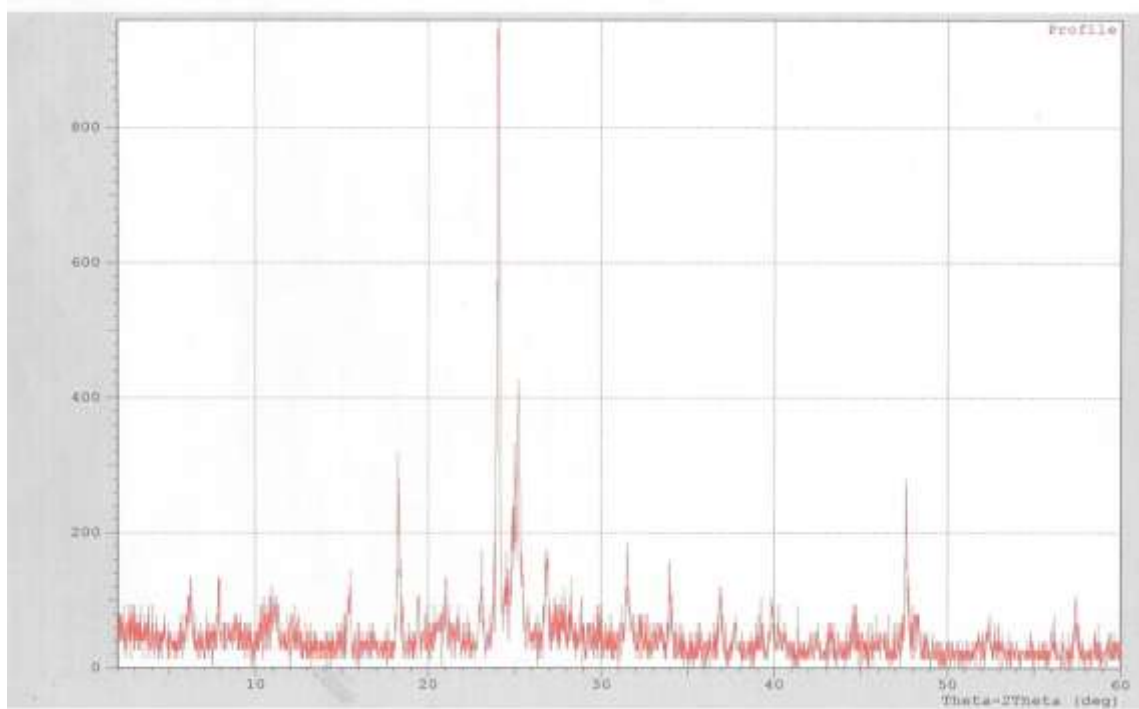


Figure 4.32: X-Ray Diffractogram of Coconut Shell Filler at 500°C

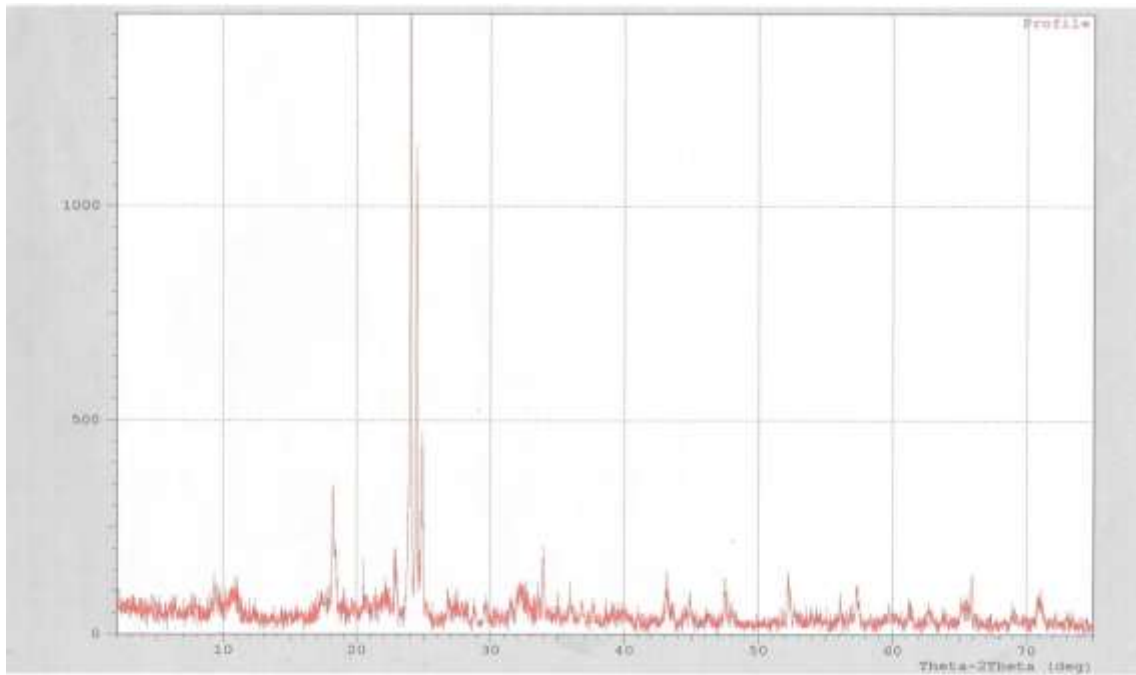


Figure 4.33: X-Ray Diffractogram of Coconut Shell Filler at 600°C

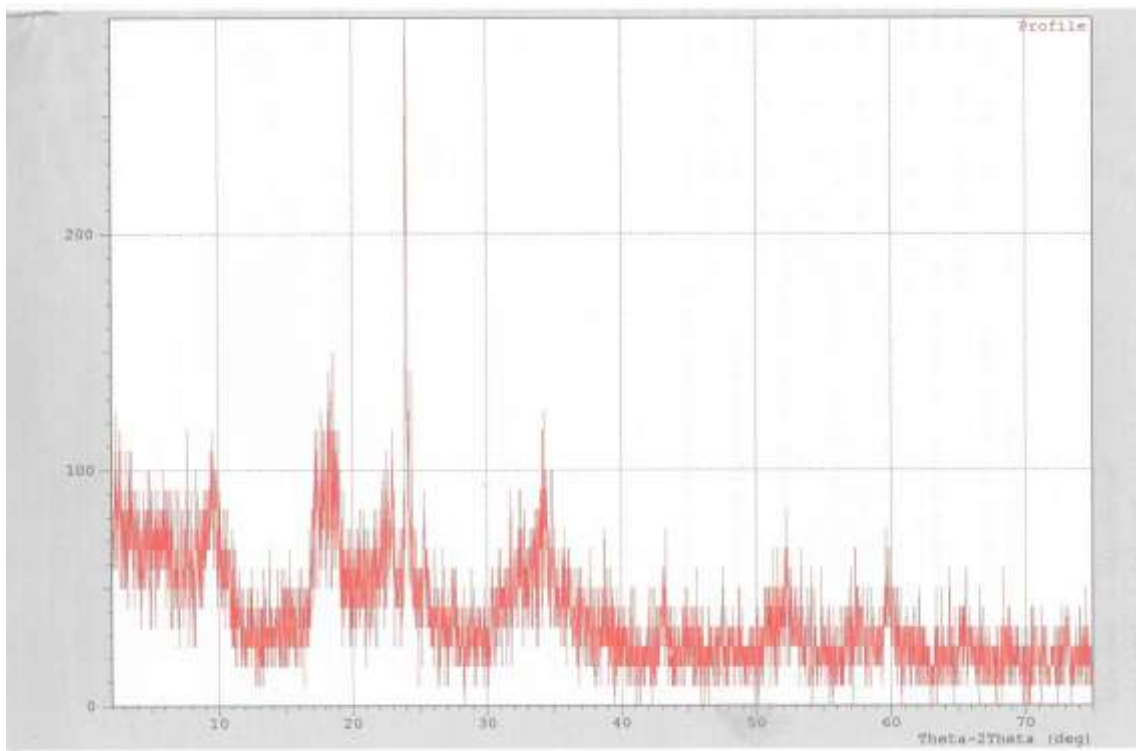


Figure 4.34: X-Ray Diffractogram of Coconut Shell Filler at 700°C

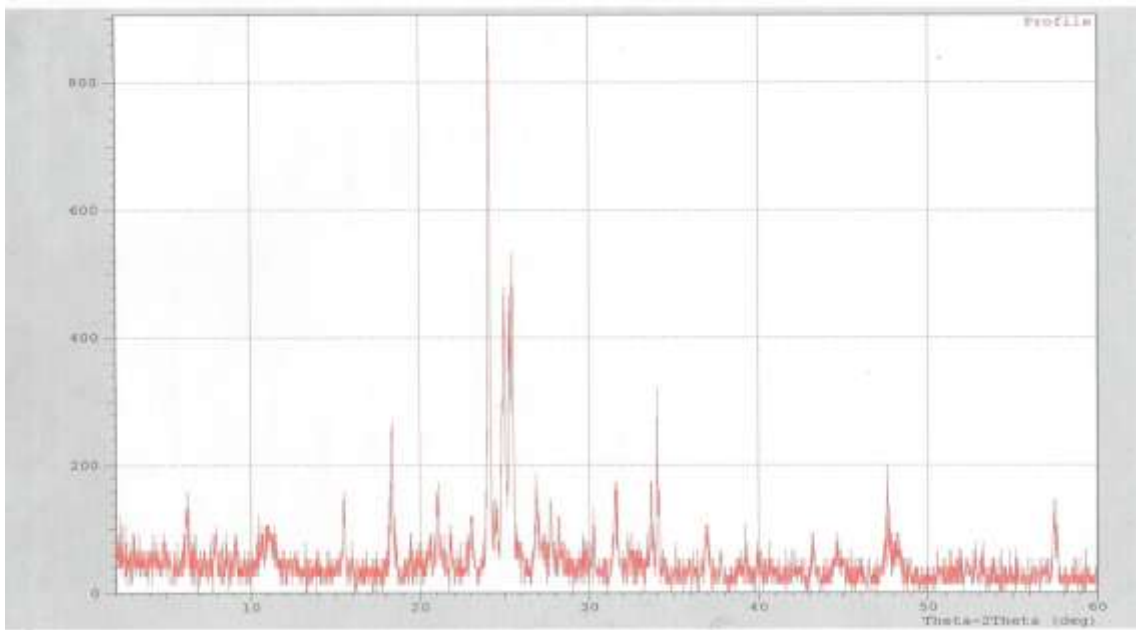


Figure 4.35: X-Ray Diffractogram of Raw Coconut Fibre Filler.

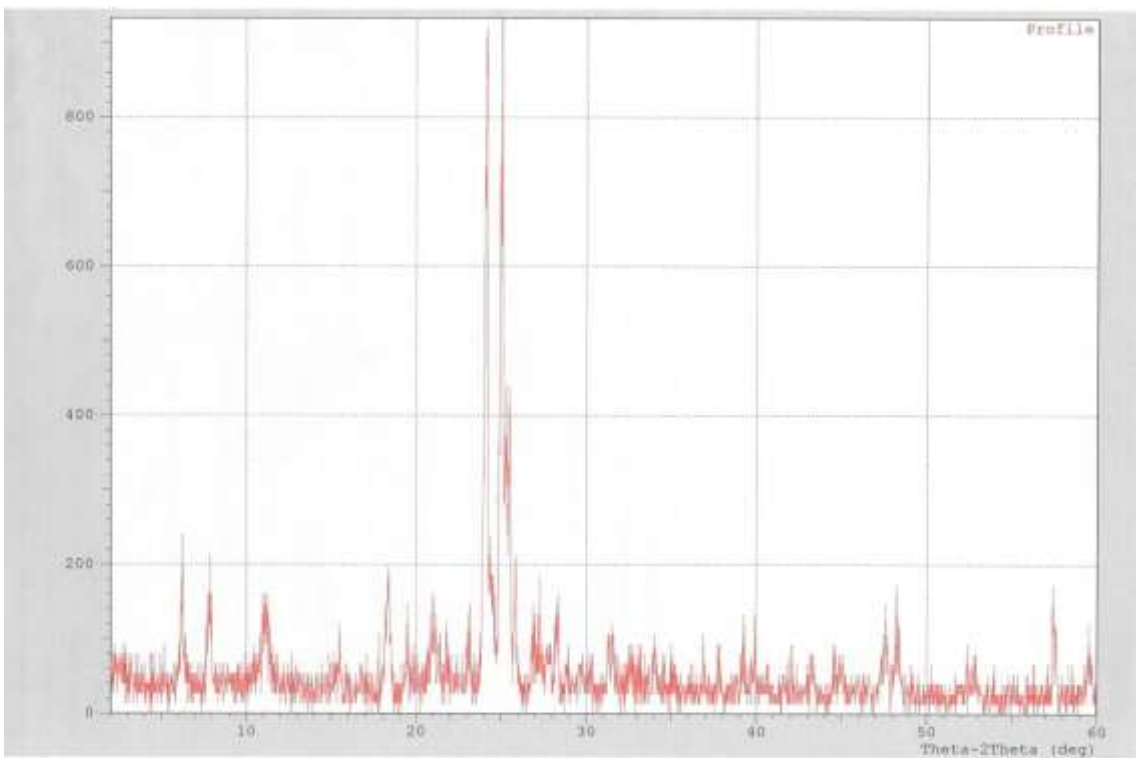


Figure 4.36: X-Ray Diffractogram of Coconut Fibre Filler at 300°C

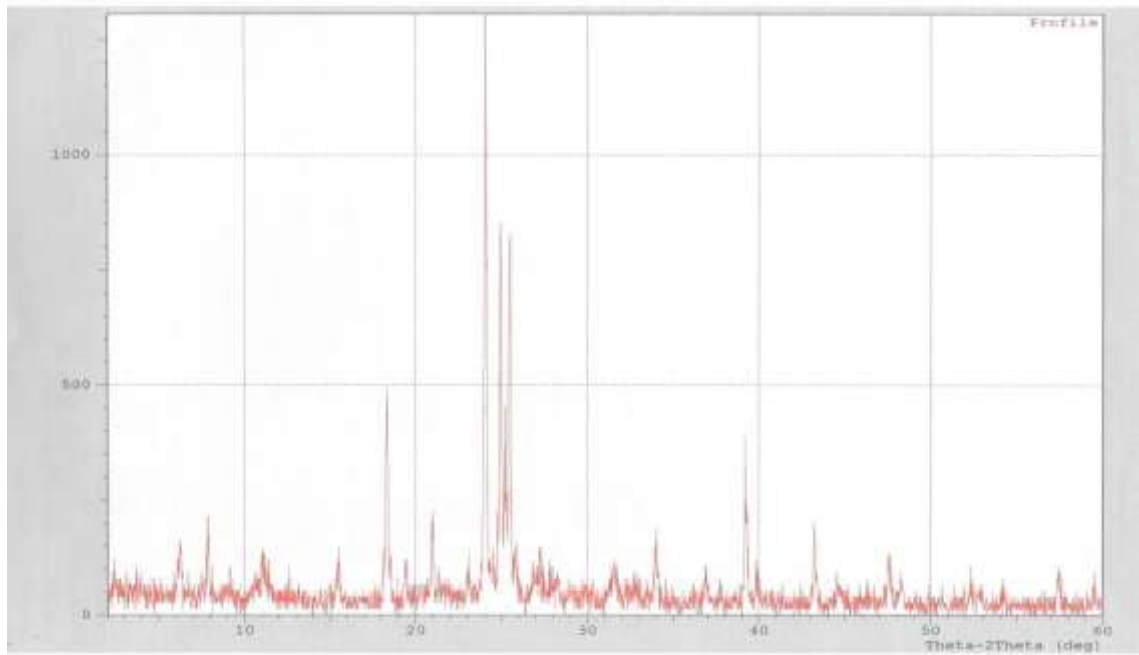


Figure 4.37: X-Ray Diffractogram of Coconut Fibre Filler at 400°C

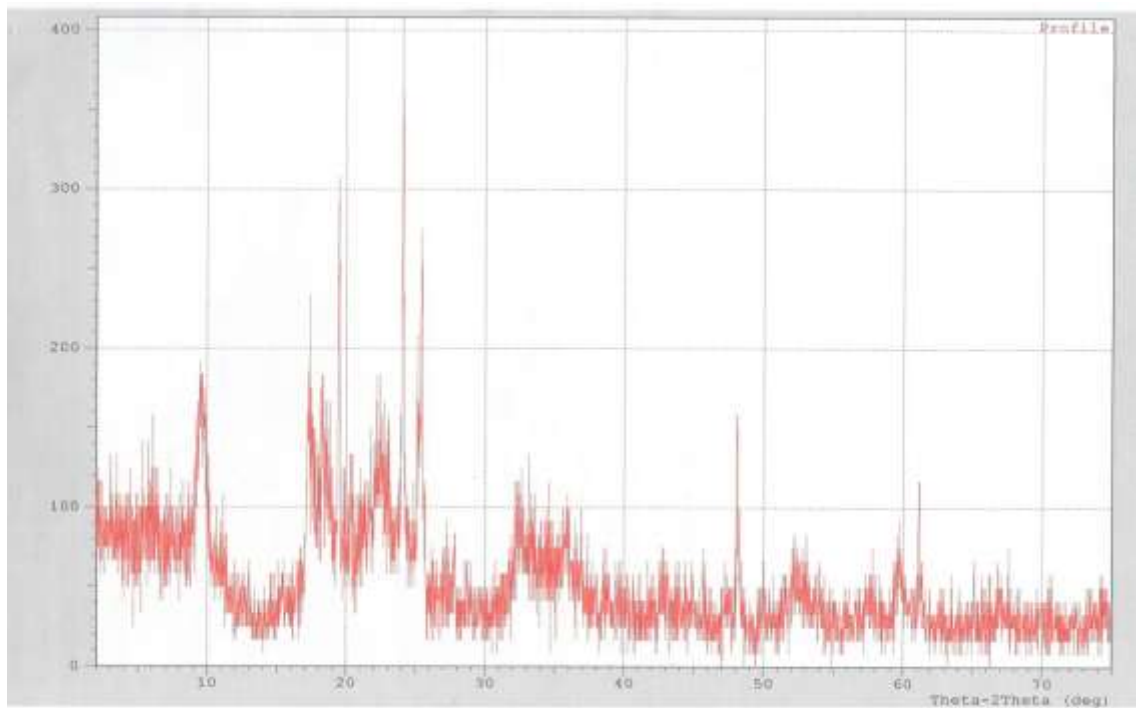


Figure 4.38: X-Ray Diffractogram of Coconut Fibre Filler at 500°C

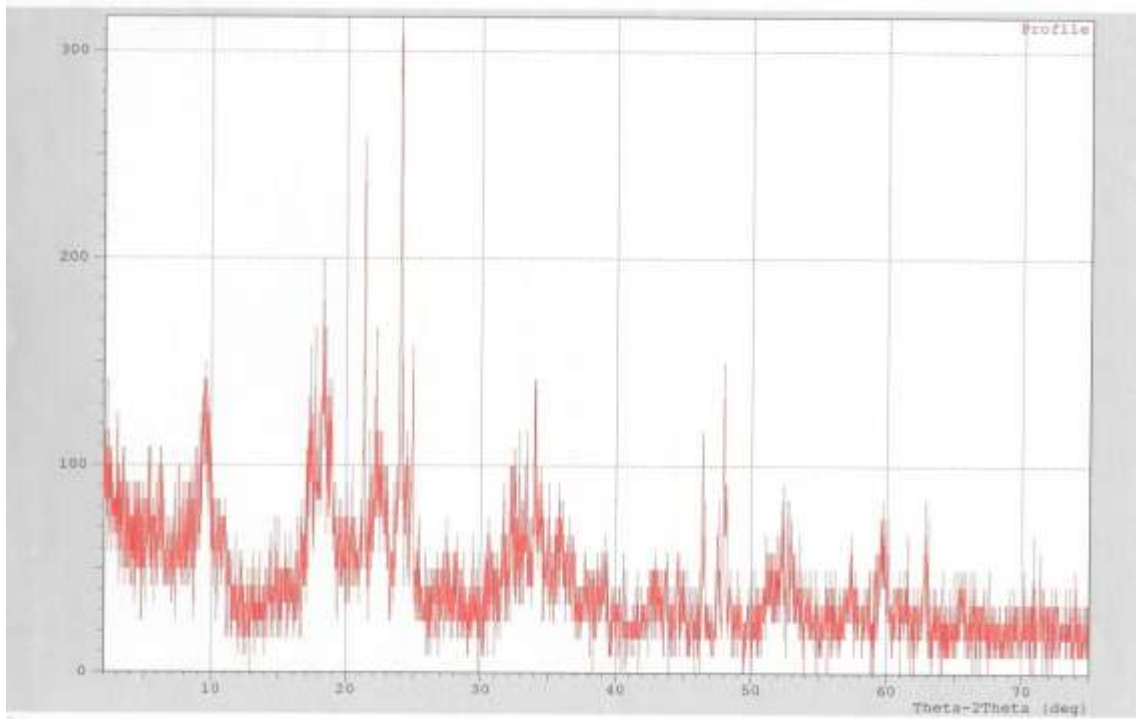


Figure 4.39: X-Ray Diffractogram of Coconut Fibre Filler at 600°C

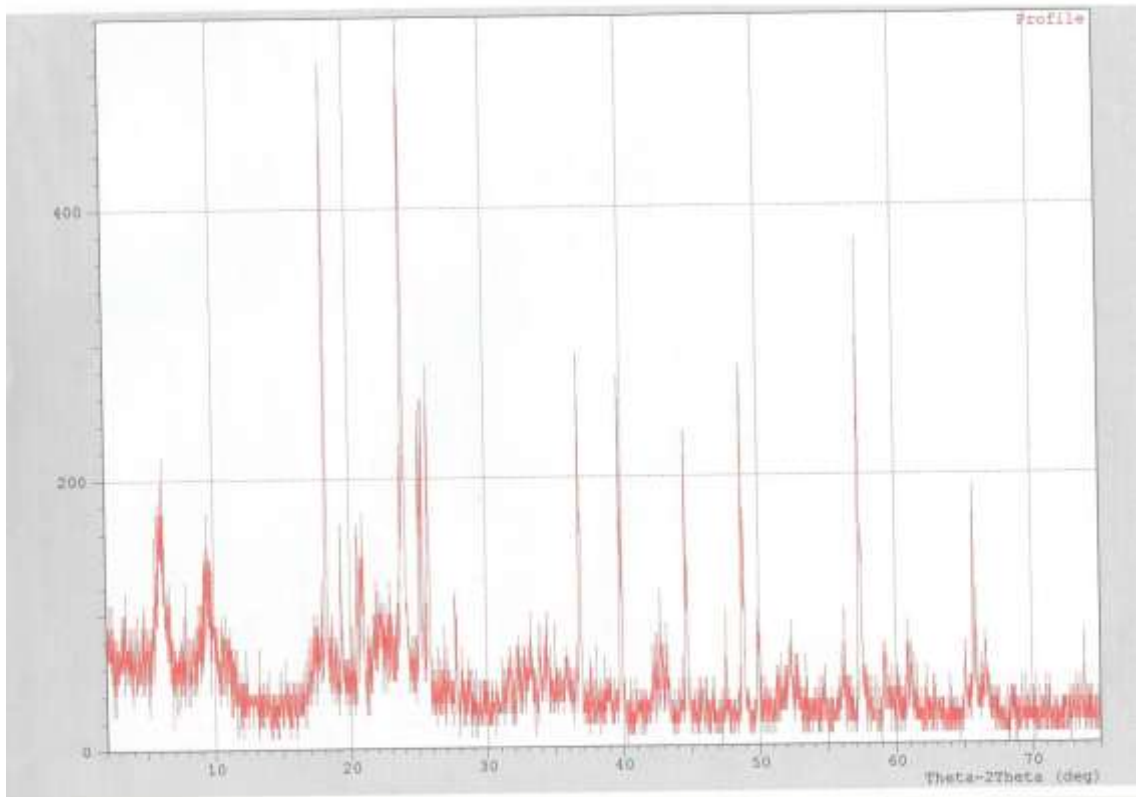


Figure 4.40: X-Ray Diffractogram of Coconut Fibre Filler at 700°C

4.15 X-Ray Fluorescence Analysis of Elemental Oxides

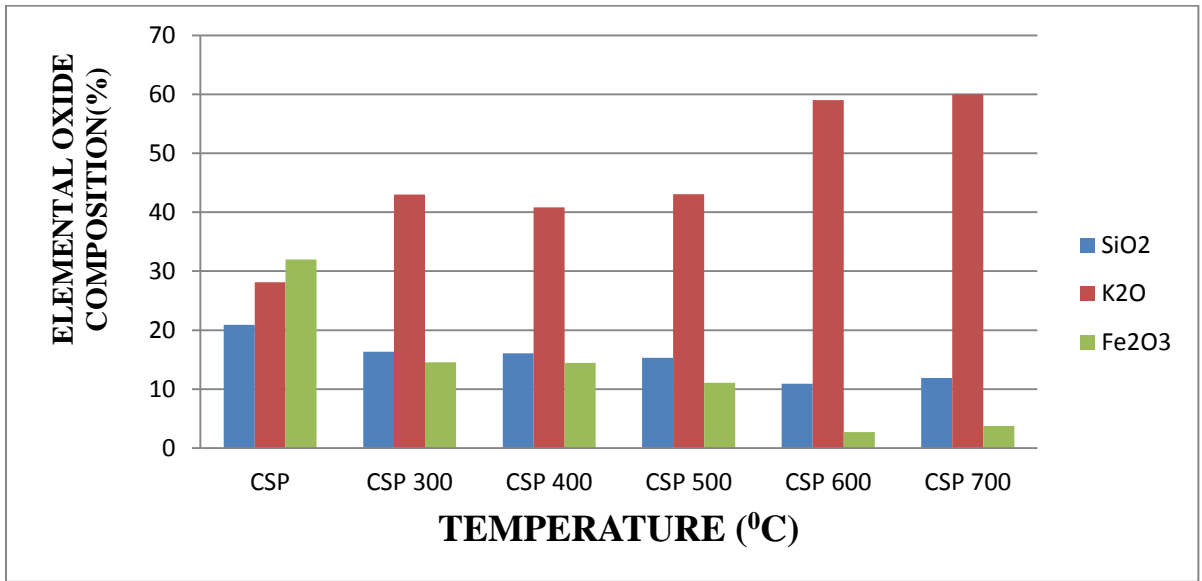


Figure 4.41: Compositional Chart of Major Elemental Oxides of Coconut Shell as a Function of Carbonisation Temperature.

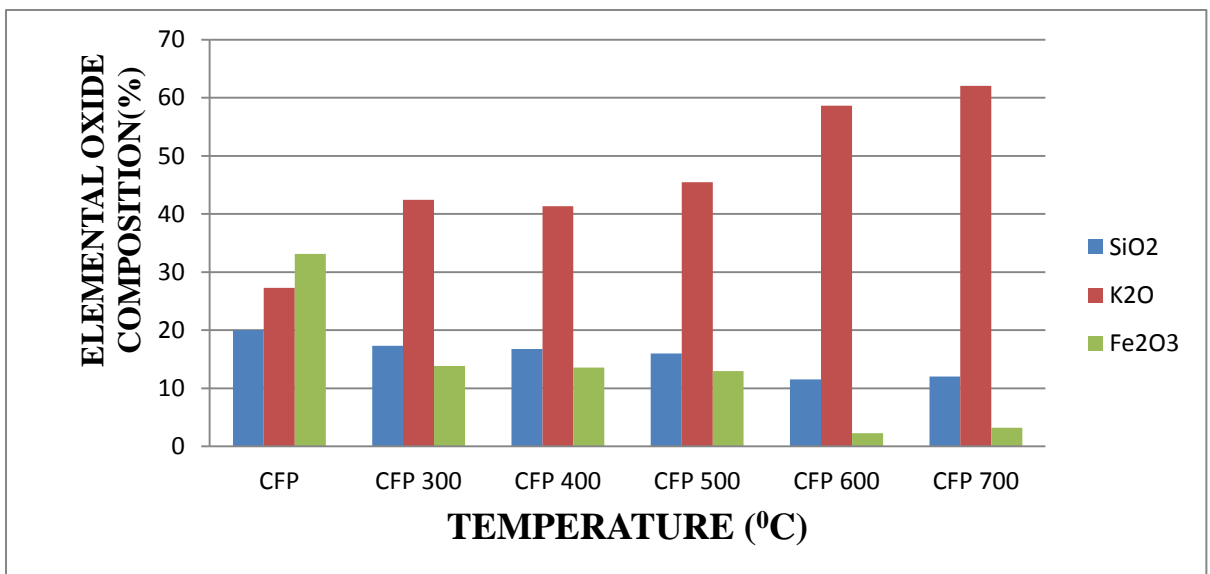


Figure 4.42: Compositional Chart of Major Elemental Oxides of Coconut Fibre as a Function of Carbonisation Temperature.

4.16 Thermal Gravimetric Results and Evaluation

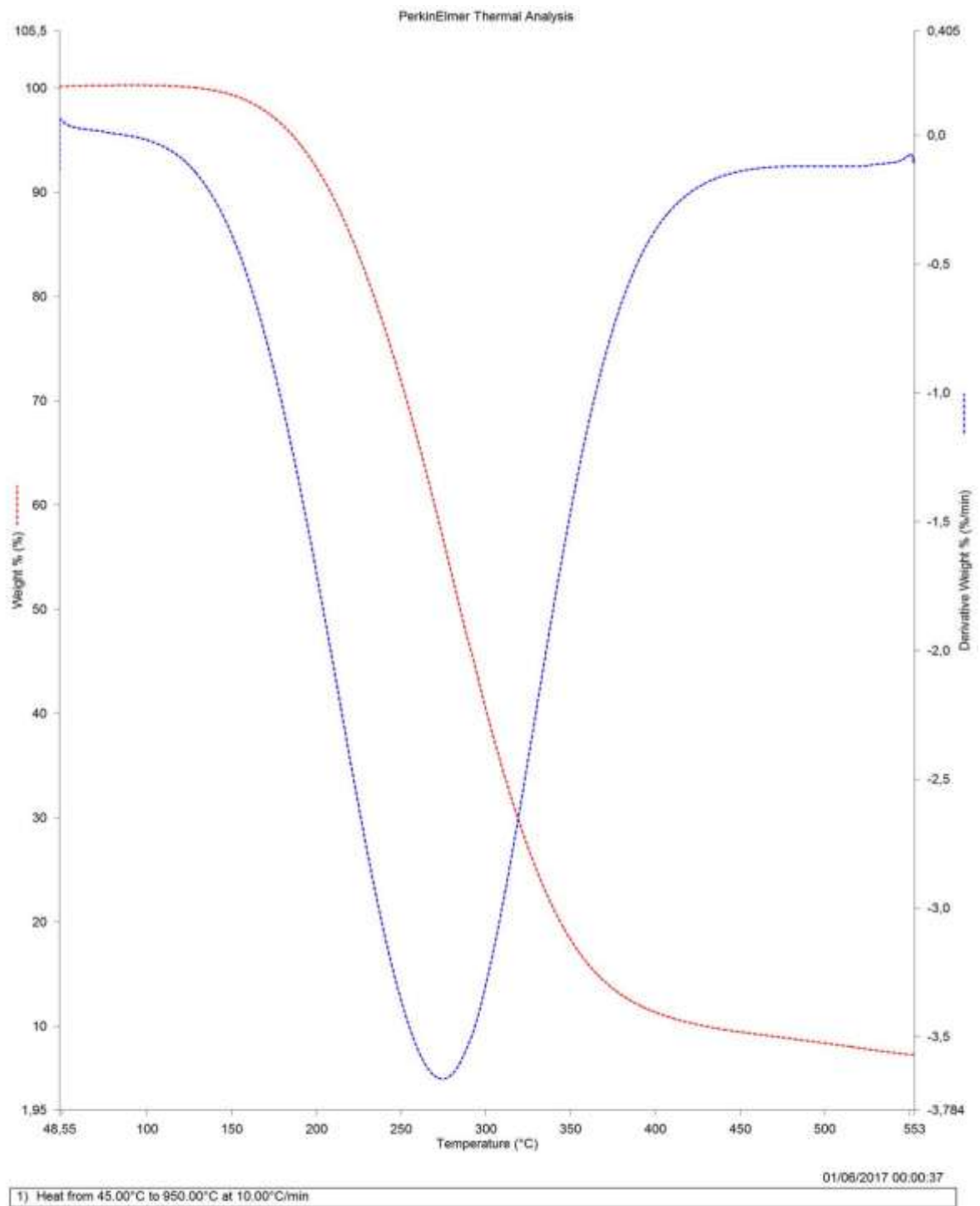


Figure 4.43: TGA Plot Showing Percentage Weight Loss (Lignocelluloses of Coconut Shell)

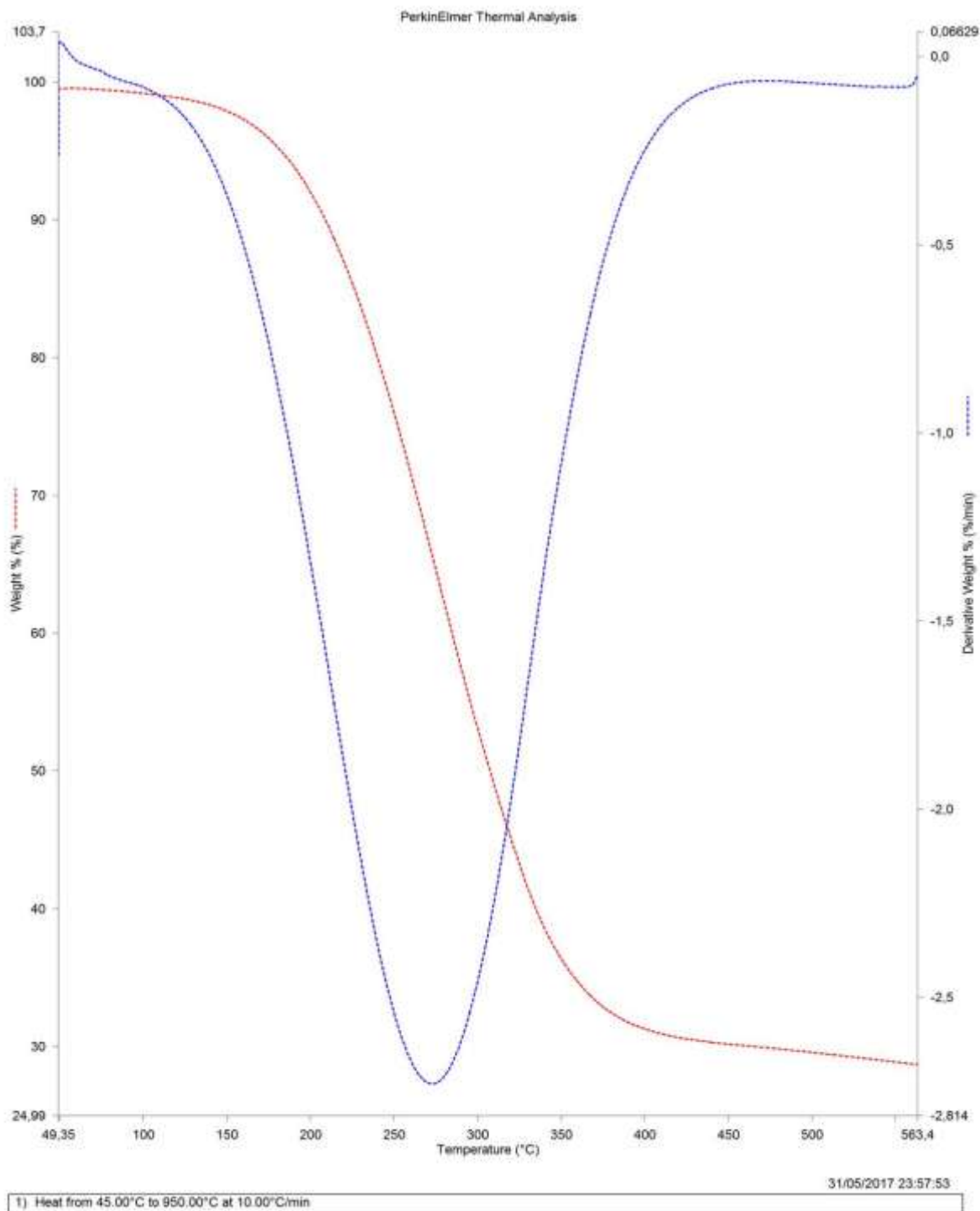


Figure 4.44: TGA Plot Showing Percentage Weight Loss (Lignocelluloses of Coconut Fibre)

4.17 Motor Cycle Vibration Dampener Evaluation Study

4.17.1 Dynamic fatigue evaluative test for the vibration dampener

Table 4.12 Crack Initiation Time of the Motor Cycle Dampener.

Samples	Crack Initiation Time (Minutes)
Raw Shell	44
Raw Fibre	62
Carbonised Shell @ 500°C	130
Carbonised Fibre @ 600°C	221

4.17.2 Resilience evaluation by vertical rebound of the vibration dampener

Table 4.13 Resilience/Rebound Percentage Evaluation of the Motor Cycle Dampener.

Samples	Resilience/Rebound (%)
Raw Shell	60
Raw Fibre	70
Carbonised Shell @ 500°C	55
Carbonised Fibre @ 600°C	60

4.17.3 Comparative evaluation of the produced vibration dampener with commercial grade

Table 4.14 Comparative Study of the Produced Vibration Dampener and “Dampener A” (Commercial Type).

Parameters	Vibration Dampener From Shell @500°C	Vibration Dampener From Fibre@600°C	Dampener “A” Commercial Type
Hardness (Shore “A”)	86	80	89
Abrasion Resistance	36.90	36.55	48.63
Compressive Strength (%)	22.30	19.46	10.20
Tensile Strength (MPa)	5.20	8.68	6.96
Elongation @ Break (%)	398.20	455.70	298.20
Modulus (%)	5.40	4.25	6.80
Flexural Strength (MPa)	0.46	1.38	2.92
Dynamic Crack			
Initiation Time (Mins)	130	221	240
Resilience/Rebound (%)	55	60	35

4.18.1 Chemical evaluative measurement for the oil seal

Table 4.15 Chemical Evaluative Measurement Results for the Oil Seal

Chemicals	Raw CSP			Raw CFP			CSP at 500°C			CFP at 600°C		
	Initial Wt(g)	Final Wt(g)	Percent Swell	Initial Wt(g)	Final Wt(g)	Percent Swell	Initial Wt(g)	Final Wt(g)	Percent Swell	Initial Wt(g)	Final Wt(g)	Percent Swell
NaOH	15	22.3	48.7	15	20.4	36.0	15	18.3	22.0	15	17.5	16.7
H ₂ SO ₄	15	26.5	76.7	15	23.3	55.3	15	22.2	48.0	15	20.2	34.7
Hydraulic Oil	15	19.4	29.3	15	17.5	16.7	15	16.3	8.67	15	15.8	5.3
Water	15	16.5	10	15	16.1	7.3	15	15.5	3.3	15	15.2	1.3

4.18.2 Flex fatigue evaluation on the oil seal

Table 4.16 Crack Initiation Time after Weathering/Ozone Exposure of the Oil Seal

Oil Seal Samples	Initial Crack Time Prior to Ozone Exposure (Minutes)	Final Crack Time After Ozone Exposure (Minutes)
Raw CSP	44	32
Raw CFP	62	48
CSP@500°C	130	98
CFP@600°C	221	130

4.19 Statistical Modeling on Performance Prediction

The results of multiple range tests and least significance difference carried out on the modified products using analysis of variance (ANOVA) to mathematically evaluate the relevance of carbonisation treatment in the eventual reinforcement properties of compounded composites are showed at appendices xxvii and xxviii.

4.20 Pictorial Presentation Stages of Experimental Sampling



Plate 4.13: Sample of Collected Coconut Shell Waste



Plate 4.14: Sample of Collected Coconut Fibre Waste



Plate 4.15: Sample of Grounded Coconut Fibre Waste and Sieved to 100 μm



Plate 4.16: Sample of Grounded Coconut Shell Waste and Sieved to 100 μm



Plate 4.17: Samples of Carbonised Coconut Shell and Fibre Treated at Various Temperatures of 300°C, 400°C, 500°C, 600°C, 700°C and Sieved to 100µm

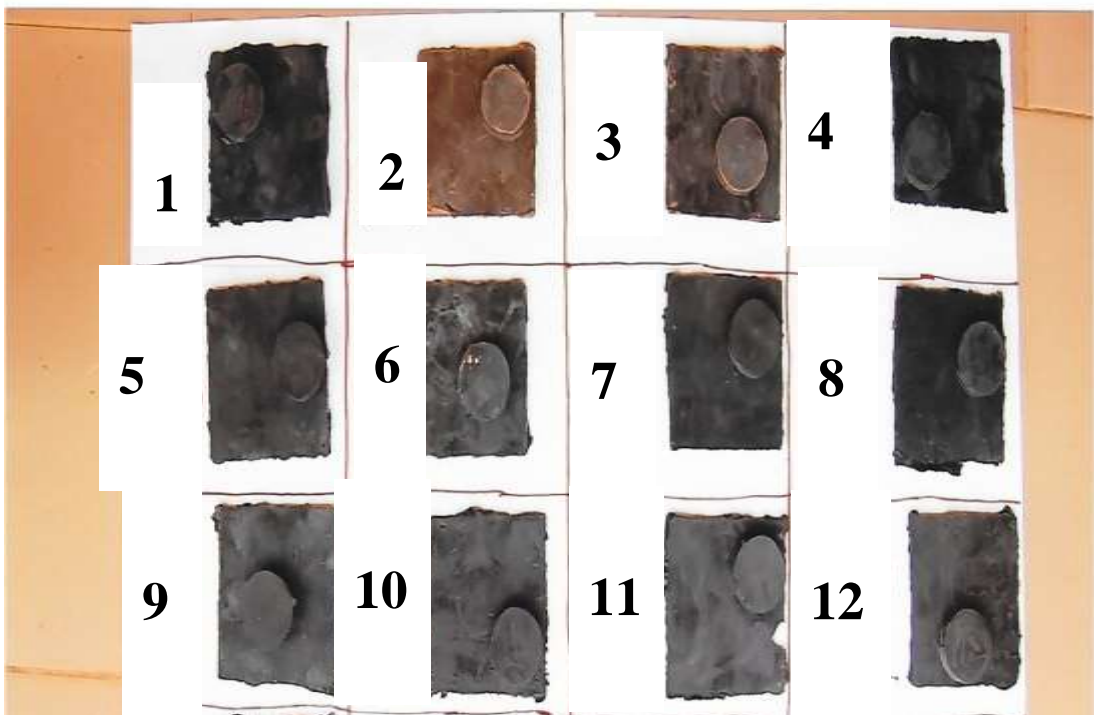


Plate 4.18: Sheeted Samples and Test Pieces of Composites Compound from Raw and Treated Coconut Shell and Fibre.



Plate 4.19: Samples of Raw and Treated Shell and Fibre Prepared for the Various Quantitative/Qualitative Analyses and Evaluative Studies.



Plate 4.20: Vibration Dampeners for Motor Cycle Hubs from Optimised Formulation of Raw Coconut Shell, Raw Coconut Fibre, Carbonised Shell at 500°C and Carbonised Fibre at 600°C

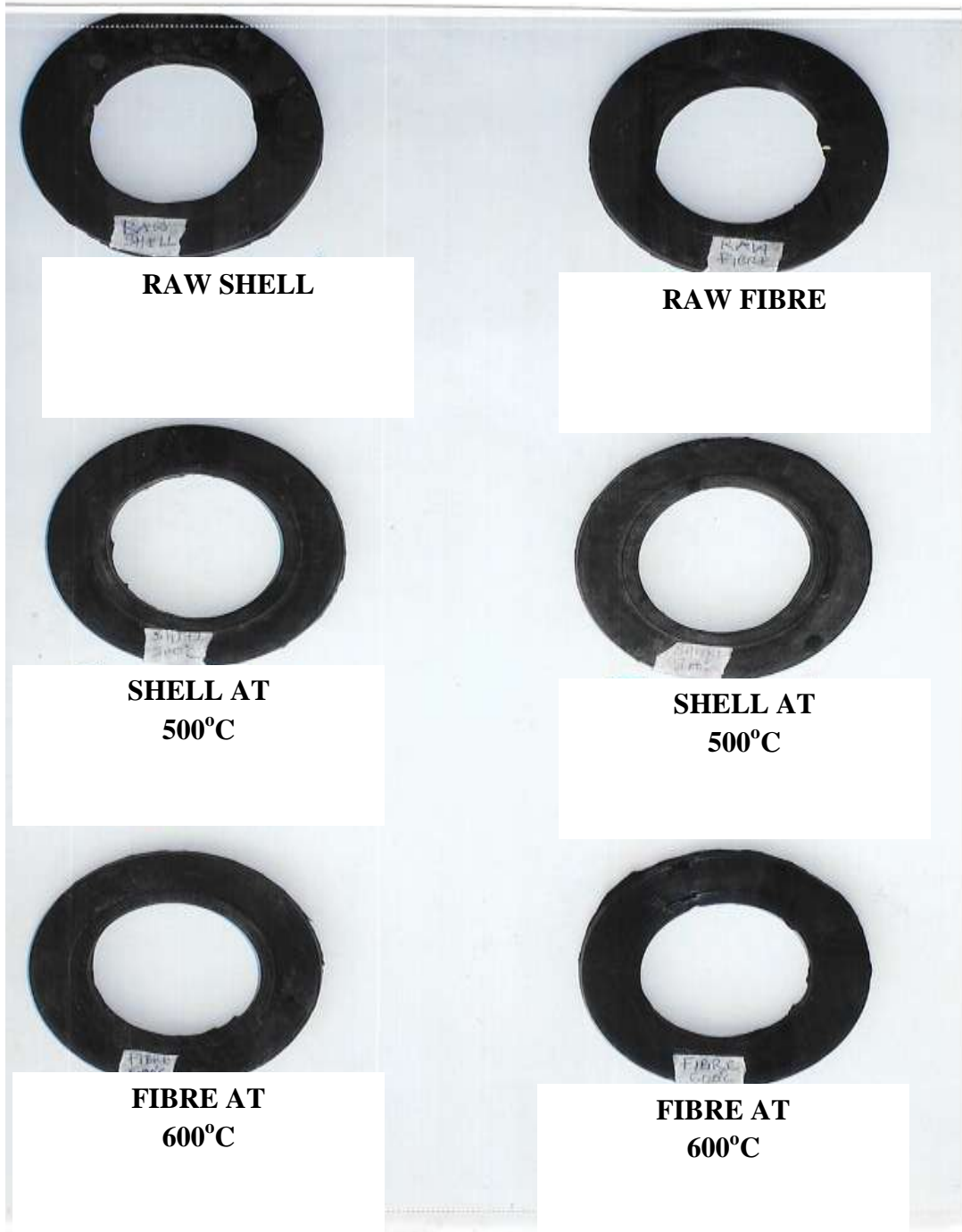


Plate 4.21: Oil Seals for Bambury Mixers (Two Roll Mills) from Optimised Formulation of Raw Coconut Shell, Raw Coconut Fibre, Carbonized Coconut Shell at 500°C and Carbonised Coconut Fibre at 600°C



Plate 4.22: Designed and Constructed Mould consisting of the Male and Female Parts used for the Compression Moulding Process of Vibration Dampeners of Motor Cycle Hub



Plate 4.23: Designed and Constructed Mould consisting of the Male and Female Parts used for the Compression Moulding Process of Industrial Oil Seals useful in Bambury Mixers (Two Roll Mills)

CHAPTER FIVE

DISCUSSION

5.1 Characterisation

The specific filler properties of the raw and treated shell and fibre were clearly identified during the characterisation process and the results are presented in Table 4.1. The results show that the pH value increased from slightly acidic level to alkaline level as the carbonisation temperature increases, because as the residual materials are lost with increasing temperature, alkalinity increases due to a corresponding loss of H₃O and the formation of metal oxides (Cazaurang *et al.*, 1991; Ayo *et al.*, 2011; Momoh *et al.*, 2017a).

There was a decrease of moisture content with increase in carbonisation temperature, thereby drastically eliminating bound moisture. Decrease of moisture with temperature leads to firmer adherence of filler to the rubber matrix with the elimination of shrinkages (Sapuan *et al.*, 2003; Chanap, 2012).

Ash content and loss on ignition increased with increase in carbonisation temperature. Carbonisation was done for 3hrs each and the higher temperature beyond 600°C burns off all residual materials into ash level and therefore leading to degradation in particles reinforcing properties (Chang and An, 2002; Husseinayah and Mostapha, 2011). The weight loss on ignition was as a result of loss in the lignocelluloses content during combustion. The concentration level of the carbon content due to carbonisation increased with bulk material loss of lignocelluloses. This is a measure of the effectiveness of the filler at interacting with the rubber matrix which is a necessary factor in filler reinforcements. The higher the value, the greater the reinforcement effect of the filler (Choi *et al.*, 2006; Egwaikhide *et al.*, 2007 a, b).

The iodine adsorption number is a measure of the surface reactivity of the filler. The higher the iodine adsorption number, the larger the surface area available for reaction and this subsequently increased reinforcement ability (Ayo *et al.*, 2011). The bulk density decreased with increase in carbonisation temperature. The densities are influenced by the particle size and structure of the shell. The decrease in bulk density created a better filler-matrix interaction. The interpenetrating network between filler and rubber gets stronger with increase in carbonisation temperature leading to a reinforced composite matrix (Chotirat *et al.*, 2007).

Particle dimensions especially for the fibre indicates that length, width and diameter decrease with increase in carbonisation temperature. Smaller particles have the ability to wet rubber surface more and therefore more reinforcement. Particles mobility also increased with increase in the temperature of carbonisation, possibly because of more kinetics created by energy difference (Dick, 2001; De Rosa *et al.*, 2010)

5.2 Hardness Properties

The mechanical properties of the filler-rubber composites depended largely on the stress-strain behaviours of the shell and fibre, the nature of their matrix phases, their phase volume fractions, the filler concentration, the distribution and orientation of the filler relative to one another (Gent and Liu, 1991; Ekebafe *et al.*, 2009).

The shore “A” hardness of the composites increased with increase in the temperature of carbonisation up to an optimum of 500°C for the shell, and 600°C for the fibre. This observed trend in hardness was influenced greatly by decrease in particle sizes. Beyond 500°C and 600°C respectively, the particle sizes have become too minute for a sustainable formation of network structure. Bond structure becomes weak and therefore less reinforcing (Hortola, 2005; Han-Seung *et al.*, 2006).

5.3 Abrasion Resistance

Abrasion resistance has remarkable influence. Resistances to wearing by composites increased with carbonisation temperature up to 500°C for shell and 600°C for fibre. The bonding between filler particles and the rubber matrix was gets stronger as treatment via carbonisation increased. The noticeable decrease in particle sizes created a denser network and therefore increased the resistance of composites to wear.

5.4 Compressive Strength

The compressive strength results showed that raw filler filled composites had the largest compression and therefore least compression strength. Compression decreases with increase in carbonisation temperature. This is because the smaller particle sizes which results from carbonisation subsequently lead to particles compartment in the filled matrix. The degree of filler dispersion increased as treatment proceeds to the optimum carbonisation temperatures of 500°C and 600°C for shell and fibre respectively; where desired reinforcements were ideal. The compressive strength of the filler surface is primarily a function of surface energy of the filler (Nemour, 1986; Ishak, 1995). The stress-strain curves showed a depression path as carbonisation temperature increases given an indication of lower compression percentage (Ayo *et al*, 2011). The raw coconut shell powder filled composites also showed more compression and therefore has less compressive strength than the raw coconut fibre filled composites.

5.5 Compressive Stress-Strain Relationship

The compressive stress- strain curves of rubber reinforced coconut shell and fibre are shown in Figures 4.1-4.3. The compressive strains of both shell and fibre filled composites increased with increase in stress. It was also evident from these plots that as carbonisation temperatures increased, the compressive strain of the composites increased. The maximum increase in compression strain is at 500°C for the shell filled and 600°C for the fibre filled. This increase in

compressive strains of the shell and fibre filled composites with increase in carbonisation temperature was an indication of the increase in the ductility of the composites and hence an improvement in reinforcement interaction level between filler and rubber matrix (Ishak, 1995). The compressive stress-strain response in the raw fibre filled composites was more than in the raw shell filled composites.

5.6 Tensile Strength/Modulus/EAB

Tensile strength and modulus of the composites increased with increase in the carbonisation temperature. This observation is expected and it is attributed to better filler dispersion and filler-matrix interactions. Generally, the smaller the particle sizes of filler, the greater the tensile strength of the composites. Carbon content increases with carbonisation temperature and fillers with higher carbon content provide greater reinforcement than those with lower carbon content because carbon to carbon bonding itself is a source of very good reinforcement in filler application (Jeffrey and Read, 1991; Ismail *et al.*, 1997; Hortola, 2015). Tensile strength and modulus are affected by filler particle size, filler surface area and filler geometry. The filler geometry may be responsible for the poor strength properties shown by raw and lower-temperature carbonised shell and fibre. Also irregularly shaped fillers could cause decrease in the strength of composites. This observation is attributable to the inability of effective filler – rubber interaction within the matrix. The increase in modulus is an indication of increase in stiffness of the composites with increase in carbonisation temperatures which leads to the creation of stiffer carbon content bonds.

Reduction in particle size provides a greater surface area and reinforcement (John and Thomas, 2008; John and Samuel, 2010). The carbonised filler has a very high surface activity, which provided greater reinforcement in comparison with the raw fillers. Thus,

the rubber matrix-filler interaction is an important factor controlling the tensile, modulus and hardness of the composites. Modulus and hardness of filled composites can be enhanced by improving the surface and surface reactivity of fillers, dispersion and rubber-matrix interaction.

It can be seen that the tensile strength of the carbonised fillers were superior to those of the raw fillers. Since the raw fillers have a larger particle interspaces compared to the carbonised fillers (Joseph *et al.*, 2003 a, b; Jun *et al.*, 2011; Momoh *et al.*, 2017a). The inferior modulus of the raw fillers to the carbonised fillers may be accounted for by two main factors. It is known that the raw fillers have a larger particle interspaces and hence a smaller surface area than the carbonised with increase carbon content. Secondly, the raw fillers show a greater tendency towards bolder filler agglomeration in converse to smaller filler agglomeration in the carbonised.

The elongation at break decreases with increase in carbonisation temperature. The decrease in elongation at break has to do with adherence of the filler to the rubber phase leading to the stiffening of the rubber chain. The stiffening of the chain leads to high resistance to stretch when strain is applied (Lake, 1983; Kim *et al.*, 2010). The carbonised filler impart greater stiffness to the rubber matrix than the raw fillers. It is known that filler, which impart a higher stiffness on the matrix, can increase the modulus of the composites but generally it is reciprocal to elongation at break. Also, this decrease in elongation at break as carbonisation increase arises due to the decreased deformability of rigid interface between filler and rubber matrix. When filler content increase because of smaller particle size, more weak interfacial regions between filler and the matrix are formed. Thus, the crack travel more easily through the weaker interfacial regions, hence decrease the elongation at break. Graphical plots indicated the shearing action in the composite samples before generating the mathematical values in

the tables. The machine plotted graphs showed the dimensional relationship between tensile stresses and tensile strains in tensile analysis of the shell and fibre composites.

5.7 Tensile Stress-Strain Relationship

The tensile stress-strain relationship of the composites filled with coconut shell and fibre filled composites as indicated in Figures 4.4 - 4.6 showed a level of extension and eventually break beyond its yield point at different levels of strain as the treatment temperature increased. Maximum point of breakage for the coconut shell filled composite occurred at 500°C and that of the fibre occurred at 600°C. Ductility of the composites increased with strain until at the yield point and the material became brittle. The ductility and brittleness of the composites materials was a direct response to tensile stress-strain deflections. Carbonisation increased the extent of ductility and therefore a positive influence on the filler-matrix reinforcement (Kim *et al.*, 2010; Jun *et al.*, 2011; Momoh *et al.*, 2017c).

5.8 Flexure Strength

Flexural strength is also affected by filler particle size, filler surface area and filler geometry. The filler geometry has been proven to be responsible for the poor strength properties shown by raw and lower temperature carbonised fibre. The raw shell and carbonised shell showed anomalous behaviour to flexural analysis, probably due to discontinuity in the filler-matrix interactions. Raw fibre showed better flexural behaviour than raw shell (Mohanty *et al.*, 2000). Thus, the rubber matrix-filler interaction is important factors controlling the flexural strength (Lake, 1983; Mohanty *et al.*, 2000; Momoh *et al.*, 2017b, c). The graphical plots indicated the type and nature of shearing action demonstrated on the composite samples before the generation of the

tabulated values. The dimensional relationship between flexure stresses and strains as analysis proceeds where indicated in the flexographs below.

5.9 Flexure Stress-Strain Relationship

The flexure stress-strain relationship as showed in Figures 4.7 - 4.9 gave a lucid indication of the level of bending and deflection energy the composites filled with coconut shell and fibre are capable of withstanding. It is possible to observe that longitudinal elements of the beam near the bottom are stretched and those near the top are compressed, thus indicating the simultaneous existence of both tensile and compressive stresses on transverse planes. The stress distributions of beams were necessary for determining the levels of performance of the composites (Mohanty *et al.*, 2000). Increase in carbonisation/treatment temperatures to an optimum temperature of 500°C for the shell filled composite and 600°C for the fibre filled composite gave better bending beams and an indication of positive contribution to filler-matrix interactions and resulting in eventual product reinforcements. The ultimate engineering stress that may be sustained without fracture is known as maximum tensile stress. The change in length of specimen divided by its original length is known as maximum tensile strain. The increase in treatment temperature results in the increase in tensile stress, strain and fracture or bending properties (Sapuan *et al.*, 2003; Momoh *et al.*, 2016a, b).

5.10 Mechanical Analysis Using 3-D Plots

These were three-dimensional plots to visualize a function of the various mechanical variables in a vector-valued function, or 3-D data set. The plots display the path of the mechanical properties as a function of carbonisation time and temperature in a clearly depicted manner. Changes in physical properties hardness, abrasion resistance, and compressive strength, elongation at break, tensile strength, modulus and flexural

strength with increase in carbonisation temperature for shell and fibre were clearly depicted as represented. Dimensional changes in width (Z-direction), length (X-direction) and thickness (Y-direction) were noticeable.

5.11 Sorption Evaluation

Several factors can influence the equilibrium sorption of composites in organic solvents. Such factors are level of cross-link, filler dispersion, nature of solvent and fillers, solubility parameter values. Higher sorption values were obtained for hexane, than xylene, toluene and benzene both for the shell and fibre because hexane has a lower molecular weight and may be expected to diffuse faster and be accommodated in the rubber matrix with fewer hindrances than with others with cyclic ring structure which could cause some steric hindrances. The decrease in sorption with increase in temperature of carbonisation could be as a result of the smaller aggregate particles resisting the penetration of the solvent. The reinforced matrix therefore became less porous in structure. The filler-matrix cross-links became firmer and therefore resistance to chemical sorption. As the filler particle reduces with increase in carbonisation level, more and more obstacles are created to the diffusing molecule and thus reduce the amount of penetrated solvent (Zadoreeki and Foldin, 1986; Yu and Wu, 2010; Momoh *et al.*, 2016b). The percentage swelling decreased with carbonisation temperature, because of the increased activities of the particulate fillers which increases the cross-link density.

5.12 Infrared Spectroscopic Evaluation

The raw coconut shell and fibre fillers showed high value of lignocelluloses (composed mainly of cellulose, hemicellulose and lignin) as well as high moisture content which creates poor surface adhesion to hydrophobic polymers. The lignocelluloses are made up of free and hydrogen bounded alcohols, phenols and carboxylic acids of absorption

frequency bands ranging from 3400-2400 (carboxylic acids); 3500-3200 (hydrogen bounded); and 3650-3600 (free). There were also heavy presence of C=C–H asymmetric stretch aromatic (benzene) rings of absorption range of 3100-3000 as well as high hydroxyl (-OH) groups as shown in the raw spectrums.

The spectra of carbonised coconut shell and fibre showed the gradual removal of the major lignocelulosic functional group as temperature of carbonisation increase to an optimum of 500°C for the shell of 600°C for the fibre. Carbonisation made the absorption band range of alkenes (1680-1600; C=C) Alkynes (2250-2100; C≡C) and Aromatic (1600-1475) to become more prominent. The presence of the prominent functional groups increased the reinforcement of the filler-matrix network possibly, due to the strengthening of the C–C bonds between main chain of the rubber and the linking chains of the carbonised fillers (Newman, 1999; Orfao and Figueiredo, 2001; Lojewska *et al.*, 2005; Lojewska *et al.*, 2006; Momoh *et al.*, 2016b).

The Alkynes band region (C≡C; 2250-2100) in the carbonised fillers was prominent and the bond strength was sharp and the intensity was strong. The =C–H and C=C stretch were dominant and the bond strengths were sharp with strong intensity in the carbonised filler. The –OH components that indicated hydrophobic constituents were being pronouncedly depleted as the carbonisation temperature increased. This process accounted for a remarkable increase in composite reinforcement.

5.13 Scanning Electron Microscopy

It could be seen that as carbonisation temperature increases, the surface of the fibre and shell gets finer and cleaner than the raw fillers. The SEM micrographs revealed that the interfacial bonding between the carbonised filler and the rubber matrix as temperature increases was significant; suggesting that better dispersion of the filler into the matrix

was achieved upon carbonisation of the coconut shell and fibre (Muhr and Roberts, 1992; Rowel *et al.*, 1997; Mc Mullan, 2006). Also, the localised bunch of shell and fibres as well as patches in the raw fillers indicated the poor dispersion of filler within the rubber matrix. Figure 4.28 shows graphs in cumulative percentage of the particle properties weighted by volume and by count plotted from SEM results. The increase in carbonisation temperature leads to increase in surface area and increase in volume by area thereby contributing to interfacial bonding strength in the carbonised filler than for the raw filler (Sheng *et al.*, 1996; Sarki *et al.*, 2011; Sanjay and Yogesha, 2016; Momoh *et al.*, 2016a,b).

Darker stacked arrangements of aggregated particles are visible. Obvious optical clarity with the presence of tiny-like shining particles could be observed as carbonisation temperature increased to the optimum of 500°C for the shell and 600°C for the fibre. The tiny glassy-like particles suggested regular arrangement, properly aligned morphologies and structures which could have resulted from modification. The more glassy and structured the particles are the better the interfacial interactions between filler and the rubber compound (Eiras and Pessan, 2009). The agglomerated area created stress concentration zones which might act as a hardness initiator and therefore leading to reinforcement in mechanical properties. Large agglomerates of particles will contribute to weaker matrix, while tiny/fine agglomerates will contribute to stronger matrix (Sae-Ovi *et al.*, 2002; Sae-Ovi *et al.*, 2004).

5.14 X-Ray Diffractograms Evaluation

As mathematically indicated in Tables 4.10 and 4.11, using a combination of the Bragg's Law in eqn. (5.1) and Scherer equation (Eqn.(5.2)), the D-spacing, crystalline indices and crystallite sizes (Newman, 1999, 2008 and Popescu *et al.*, 2011) percentage crystallisation were obtained from the diffractograms in Figures 4.29 – 4.40

$$\mathbf{C.I} = \frac{I_{002} - I_{am}}{I_{002}} \times \mathbf{100} \quad \mathbf{5.1}$$

Where: I_{002} and the I_{am} are the intensities of the crystalline and amorphous regions. The average crystallite size (L) (Eqn. (5.2)) was calculated using the Scherer equation (Popescu *et al.*, 2011; Shuaibu and Mamza, 2016).

$$\mathbf{L} = \frac{K * \lambda}{\beta * \cos \theta} \quad \mathbf{5.2}$$

Where: K is a constant of value 0.9, λ is the X-ray wavelength (0.1542 nm), β is the half-height width of the diffraction band and θ is the Bragg angle corresponding to the (200) plane.

From Tables 4.10 and 4.11; as carbonisation temperatures increase, the amorphous regions (the non peak regions) tend to diminish, while the more stable crystalline region becomes more intensified, thereby leading to increase in percentage crystallinity (Popescu *et al.*, 2011; Momoh *et al.*, 2017b). The average crystalline dimensions (ACD) are averagely the same possibly because the particle sizes of the fillers were all at 100 μm . Intensity counts increased with carbonisation temperature leading to more crystalline region up to the 500°C and 600°C for shell and fibre respectively. Full width at half maximum (FWHM) decreased with carbonisation temperature thereby reducing the D-spacing between particles and improvement on crystallinity. The smaller the D-spacing, the smaller the particle sizes and the better the reinforcement level in the polymer composites. The Bragg's angle (2θ) peaked within narrow range of values for the temperatures used; possibly around the characteristics peak value for the coconut shell and fibre (Ismail *et al.*, 2012). Increase in the percentage of crystallinity will

increase the mechanical, chemical, optical and thermal properties of the composites (Eiras and Pessan, 2009; Joseph *et al.*, 2003 a).

5.15 Elemental Oxides Evaluation

Figures 4.41 and 4.42 showed the results of the major elemental oxides of SiO₂, K₂O and Fe₂O₃ present in the coconut shell and fibre respectively. Many more other oxides exist but in trace and minute fraction. See full table of elemental oxides at the appendices. X-ray fluorescence spectroscopy opens the possibility of getting additional information on the carbonised coconut shell and fibre in an attempt to further investigate the composite networks (Larson and Dreele, 1994).

The raw fillers from the coconut shell and fibre have a higher percentage of Fe₂O₃, followed by K₂O. The fillers consist of 80% elemental oxides of Fe₂O₃, SiO₂ and K₂O; while the carbonised coconut shell and fibre consists of 70% Fe₂O₃, Fe₂O₃ and K₂O put together. Increased in carbonisation temperature diminished iron and silicon oxides but increased potassium oxide. The FTIR cannot show these because they are shaded. The XRF procedure under depleted the shading power and revealed their presence in the fillers (Momoh *et al.*, 2017a, c.).

The concentration of potassium oxide which is highly electrovalent on the carbon surface (from carbonisation) is changed by contact with oxygen at a higher temperature resulting in a marked enhancement in catalytic activities and therefore contributing to the reinforcement of the composites (Shin-ya *et al.*, 1981). The ionisation energy of potassium oxide increased with increase in carbonisation temperature and leading to greater and stronger interpenetrating network between the carbonised coconut shell/fibre and the composites matrix. This kind of interpenetrating network enhances

the mechanical, thermal and chemical properties of natural rubber composites (Ismail *et al.*, 2002).

5.16 Thermal Gravimetric Evaluation

Figures 4.43 and 4.44, clearly, showed the results of the thermal gravimetric analysis performed on the raw and carbonised coconut shell and fibre respectively. The figures give the percentage of weight loss as a function of carbonisation temperature, and the derivative values for thermal degradation, residue and percent weight loss at 800°C. Water loss was observed around 100°C, and further thermal degradation takes place as two-step process. In the first step, the degradation of hemicellulose present in the coconut shell and fibre takes place at around (300-400) °C. At about (400-500) °C, the main, degradation of cellulose occurred and a prominent peak appears beyond a slight shoulder of the temperature corresponding to the commencement of maximum decomposition rate around 75% weight loss of lignocelluloses. According to Kim *et al.*, 2006, the depolymerisation of chain stiffened hemicelluloses occur between 180 and 350°C; the random cleavage of the glycoside linkage of cellulose between 275 and 350°C and degradation of lignin between 250 and 500°C.

The burning-off of the lignocelluloses which has random amorphous structure (Han-Seung *et al.*, 2006; Shebani *et al.*, 2009), gradually gave way to an improved crystalline region which improves the thermal stability of the coconut shell and fibre. The lignin components which decomposed at about 500°C has a high thermal stability and difficult to decompose initially (Larson and Van Dreele, 1994; Shen and Gu, 2009). As the carbonisation temperature increased, a considerable fraction of the lignocelluloses gets burnt-off; the residue diminished and the percentage losses of lignocelluloses increased. Percentage loss improved the crystalline region and consequently the reinforcements in the mechanical properties of the composites (Vink *et al.*, 2003; Momoh *et al.*, 2017c).

5.17 Dynamic Fatigue of Vibration Dampener

The standard method used was ASTM D430-06 (2012). The test was to simulate the continually repeated distortions received in service by the vibration dampener. Dynamic flex fatigue is perhaps the most complex potential mode of failure for rubber materials, and consequently one of the most challenging to address in the design and development of rubber components. In its simplest form flex fatigue is the cracking of a rubber component due to cyclical stresses and strains. It typically starts off as micro-cracking virtually at the molecular level, and with successive cycling, it propagates into macro-cracking that ultimately result in product failure.

Results shown indicated that, the products from formulated composites showed a greater resistance to crack initiation with the modified fibre exceeding that of the modified shell. The raw fibre also performed better than the raw shell filler filled composites. The number of revolutions recorded before the initiation of cracks increased from raw shell, raw fibre, carbonised shell at 500°C to carbonised fibre at 600°C respectively. The effects of the distortions are to weaken the rubber until rupture occurs. These distortions may be produced by extension, compressive, and bending forces or combinations thereof.

5.18 Resilience by Vertical Rebound Evaluation for Vibration Dampener

The standard method used was ASTM D2632-15. Resilience is a function of both dynamic modulus and internal friction of a rubber. It is sensitive to temperature changes and to depth of penetration of the plunger. Resilience or rebound is a compound ability to regain its original size and shape after temporary deformation without distortion or loss of alignment.

From the results obtained, one would observe the fact that resilience is largely an inherent property of the rubber. The rebound percentage values for the raw fillers were slightly higher than for the carbonised fillers. The elastic and the elongation at break properties have higher values than that of the raw filler filled composites. The difference is that modification via carbonisation created an ordered and oriented deformation and recovery than the raw filler filled composites. Resilience and rebound are within control range for the modified at 500°C and 600°C than for the raw filled formulations.

The resilience of a rubber compound is a measure of how elastic it is when exposed to various stresses. This measurement will assist with choosing the right material and appropriate modifications for vibration dampeners. Resilience gives the ratio of energy released in the deformation recovery to the energy that caused the deformation. The result obtained was an indication of energy loss by hysteresis. The percent rebound measured in the test was inversely proportional to hysteretic loss.

5.19 Comparative Evaluation Study of Vibration Dampener

To ascertain standardisation and competitiveness in the quality of the modified products at the best carbonisation temperatures of 500°C and 600°C for shell and fibre respectively; a comparative mechanical analysis was carried out on the modified vibration dampener and one of the highest qualities of automobile vibration dampeners available in the market. For the avoidance of Litigation the commercial vibration dampener shall be referred to as “Dampener A”.

From the comparative studies, it was observed that results obtained from modified coconut shell and fibre at 500°C and 600°C respectively possessed high competitive values to a high standard “Dampener A” which was formulated and manufactured from N330 natural rubber filled carbon black filler – a renowned standard reinforcing filler. With results obtained, modified coconut shell and fibre at 500°C and 600°C

carbonisation temperature is highly recommended for automobile parts, using a vibration dampener for a practical example.

5.20 Chemical Evaluation of Oil Seal

The results in Table 4.15 showed that the acid (H_2SO_4) had a greater effect on the oil seals with highest percentage at 76.7% for the raw coconut shell and 34.7% for the carbonised coconut fibre at 600°C. The alkali (NaOH) had a great effect on the oil seals with the highest percentage value at 48.7% for the raw coconut shell and 16.7% for the carbonised coconut fibre at 600°C. The hydraulic oil scored a medium performance effect on the oil seals with the highest percentage value standing at 29.3% for the raw coconut shell and 5.3% for the carbonised coconut fibre at 600°C. Water had the least performance effect on the oil seals; depicting the highest percentage value occurrence at 10% for the raw coconut shell and almost negligible value of 1.3% for the carbonised coconut fibre at 600°C.

The general trend showed more resistance to alkali, acid, oil and water from the carbonised coconut fibre treated at 600°C, followed by carbonised coconut shell treated at 500°C, then raw coconut fibre and finally, the least resistance was raw coconut shell filled composites. This trend showed the impact of modification on the coconut shell and fibre. Carbonised coconut fibre is therefore highly recommended for the production of industrial oil seals fitting for a bambury mixer.

5.21 Flex Fatigue Evaluation of Oil Seal

Weathering and ozone exposure on the oil seal samples have a great effect on performance rating as the time of crack initiation reduces for all the samples evaluated. The presence of ozone reduces resistance to crack initiation for both raw samples and treated samples alike (Ski, 1970). This observation suggest that filler modification did

not increase the resistance of the samples to weathering and ozone attack; since all samples were equally protected with same amount of trimethyl quinoline (TMQ), as indicated in the formulation design on Table 3.3.

5.22 Performance Prediction using Modeling via ANOVA

The purpose of this section is to demonstrate the commercial potential of the shell and fibre composites which have been developed throughout this thesis. The optimised shell and fibre composites will be simulated in a large scale test setup. An unguided formulation can be an unwanted design in the long run. Therefore a prerequisite of early commercialising of a product is to carry out full-scale correlations between formulation and expected design in terms of performance rating.

However, this is costly and time consuming technique. Manufacturing and testing a several design criteria can be impracticable especially for academic institutions. For this reason, computer and statistical modeling can be very helpful to demonstrate materials performance when placed in a real life scenario where product failure can be a threat either to the product or the user of the product. The objective of this section is to give a brief overview into the field of product modelling and use a specific software package to predict material performance.

Statistical analysis was done on the *mechanical properties* and chemical *sorption* of the designed and produced motor cycle vibration dampeners and industrial oil seals for bambury mixers (two roll mill). These were the primary evaluative tests required to ascertain prescribed product performance. The mechanical properties of the optimized and modified coconut palm waste composites are significantly affected by temperature of carbonisation. The specifications used in the design criteria of the modeled products of motor cycle vibration dampeners and industrial oil seals for bambury mixers are

particularly important in load bearing and product reliability especially where consistency, precision and performance integrity are necessarily required parameters by which the prediction of product failures could be hinged upon. The basic mechanical properties that influence good product design and integrity needed for engineering designs include, but not limited to: hardness, abrasion resistance, compression set, tensile strength, elongation at break, modulus and flexural properties. In designs of engineering wares, the construction products directive (CPD) should be relatively predictable in order to guide against unnecessary efforts often expended in designs that may lead to failures.

Products models are of course purely computer and statistically based analysis done in order to give a theoretical overview of real experimental representation. The modeled products for the productions made from the optimized formulation were accomplished through the use of experimental and mathematical techniques. The stochastic and deterministic models using Duncan's multiple range test (DMRT), as well as least significance differences (LSD) were used to aid statistical analysis.

The stochastic model (probabilistic model) was used with the sequence of events and steps with probability of occurring. The mechanical properties, coupled with probabilities of modification through carbonisation were used to predict the progress of modification trends to significant or not significant levels.

The deterministic model predicts modification in mechanical properties based on the solution of mathematical equations that described the physical and chemical behaviour of the designed products.

The analysis of variance for the coconut fibre and shell composites were between subject factors of the mechanical properties (hardness, abrasion resistance, compression set, tensile strength, elongation at break, modulus and flexural strength) and the samples

temperature (300, 400, 500, 600 and 700) °C used for property modification. Eqn.5.3 was an applicable model. *See appendix xxvii and xxviii:*

$$S^2 = \frac{1}{n-1} \sum (y_i - \bar{y})^2 \quad 5.3$$

Where $n-1$ = the degrees of freedom, (DF) and the summation is called the sum of squares (SS), the result is called the mean square (MS) and the squared terms are deviation from the sample mean.

The descriptive statistics gave the mean values and standard deviational values of the dependable variable yield representing the mechanical properties. The tests of between subject effects after taken note of type I error (false positive) rate on the sum of squares. The sources of between subjects effects are: corrected model, intercept, properties, samples (temperatures of carbonisation) and allowable experimental errors of not more than ± 0.5 . The properties of coconut fibre and shell are statistically significant and related to experimentally determined results at 5% as the probability value of F-calculated is $0.00 < 0.05$. The tests of between subjects effects showed that the samples (temperature of carbonisation) for the fibre and shell are not statistically significant as F-calculated is 0.903 and $0.699 > 0.05$ respectively as indicated in appendices xxvii and xxviii.

The estimated marginal means for the properties (mechanical properties) and the samples (carbonisation temperatures) for the fibre and shell filled composites showed the lower bound and upper bound levels at 95% confidence interval of the mean ratings after considering standard errors at 4.427 and 9.793 respectively. What this mean is that the mechanical properties occurred at 95% confidence interval of the least and maximum properties statistically expected from experimental outcome. And for the

sample temperatures, the mean values also have 95% confidence interval pass; experimental values should therefore be accepted.

The Post Hoc tests of multiple comparisons within the properties and samples interrelationships with standard errors of 6.26133 for the fibre and 13.84927 using their mean differences showed a great deal of significances as outlined in the following:

- (i) Abrasion resistance has a least significance difference effects on all other mechanical properties except on compression set.
- (ii) Compression set has a least significance difference effects on all other mechanical properties except abrasion resistance.
- (iii) Tensile strength has a least significance difference effects on all other mechanical properties except on modulus and flexural strength.
- (iv) Elongation at break (EAB) has a least significance difference effects on all other mechanical properties without exceptions.

The 95% confidence interval pass of lower bound and upper bound were satisfied by the interactive relationship between the various mechanical properties at the least significance difference (LSD) level of analysis.

The homogeneous subsets analysis on the fibre and shell filled composites using the Duncan's harmonic mean sample size of seven (7) for the fibre and shell at 0.05 significance level with a mean square error term of 117.613 and 671.347 for the fibre and shell respectively. Flexural strength, modulus and tensile strength were closely related and are represented in subset 1. They exercise positive harmonic effects on one another. Compression set and abrasion resistance were in subset 2 and they exercise negative harmonic effects on each other in a synergistic manner. Hardness and elongation at break stood alone in harmonic behaviour in subsets 3 and 4. There was homogeneity amongst properties of the same subset whether positively or negatively.

The implication here was that the properties in subset 1 were more closely affected in a related manner by modification temperatures than those in subset 2, 3 and 4.

The subset reports on the properties and samples showed ranges of predictive results fitting experimentally determined results, with high performance of fibre summarily showing at 600°C and shell at 500°C.

The modeling analysis on chemical sorption was centred on regression analysis. The descriptive statistics have mean and standard deviation values for carbonisation temperatures and the chemical solvents used (hexane, xylene, toluene and benzene).

Pearson correlation coefficient (PCC) conducted showed linear correlations between the variables (solvents and carbonisation temperatures) with values between +1 and -1, where +1 is total positive linear correlation, 0 is no linear correlation, and -1 is total negative linear correlation.

The interactional relationships between solvents and the composites filled with coconut fibre and shell powder were negatively linear because as the carbonisation temperature increases, the dimensional changes in sample composites reduce. The interactions were more for hexane and xylene than for toluene and benzene. All data are shown in appendices xxvii and xxviii. The analysis of variance study in the modeling gave comprehensive theoretical information on the carbonisation and modification system employed in the filler-matrix interactions as related to predictions of reinforcement ability of the coconut shell and fibre on the modeled products of motor cycle vibration dampener and industrial oil seal for bambury mixers. Emphasis was centred on the mechanical and chemical sorption properties since they were the basic properties required for the assessment of product quality needed in the modelled products.

The analysis of variance study between the subject factors of properties and samples leading to product reinforcements was evaluated using the *hypotheses*:

(A) **H₀**: *There is no significant difference in the Physico-mechanical properties of composites filled with coconut fibre and shell treated at the various carbonisation temperatures.*

(B) **H₀**: *There is no significant difference in the chemical sorption behaviours of composites filled with treated coconut fibre and shell at the varying carbonisation temperatures.*

Final decisions are indicated at the conclusion section of thesis report.

CHAPTER SIX

SUMMARY, CONCLUSION AND RECOMMENDATIONS

6.1 Summary

Coconut shell and fibre were collected, washed to remove debris and sand; and then oven dried at 95⁰C for 2h to remove moisture. The shell and fibre were physically treated through carbonisation at varying temperatures of 300, 400, 500, 600 and 700⁰C. The raw and carbonised shell/fibre was crushed, ground and serially sieved using graded sieves until a 100 particle sizes were obtained. Both raw and carbonised samples were the characterised using the following parameters and standard method: Ash content, loss on ignition, pH of slurry, bulk density, iodine adsorption value, moisture content, oil absorption. Others especially for the fibre are: conductivity, lumen, width, length, diameter, area and volume.

Furthermore, a suitable formulation was designed and twelve (12) formulations were compounded. The formulations include: Raw shell and shell carbonised at (300, 400, 500, 600 and 700)⁰C. Also raw fibre and fibre carbonised at (300, 400, 500, 600 and 700)⁰C.

Additives used for compounding were: Natural rubber of TSR 10 grade, zinc oxide, stearic acid, mercaptobenzothiazole disulphide (MBTS), tetramethylthiuram disulphide (TMTD), trimethyl quinoline (TMQ), sulphur, fillers and mineral oil as processing aid.

Homogenisation, dispersive and distributive mixing were done using a laboratory two-roll mill at 70⁰C with a mill roll speed of 1:1.25 ratio. Compounded sheets were allowed for maturation at 32⁰C for 24h.

Rheological tests using ODR 2000 model was carried out before press curing. From the ODR curves/charts, a temperature of 150⁰C, pressure of 150kg/Cm and a cycle time of 15 minutes were used for the curing process. Physico-mechanical evaluations were made according to standard test methods in order to evaluate the level of reinforcement attained during composites built-up. Evaluations carried out include: hardness (Shore A)

abrasion resistance index, compressive strength, tensile strength, elongation at break, modulus and flexural strength. The purpose was to evaluate the level of reinforcement in the composites. Sorption analysis/swollen tests were carried out using four (4) major solvents for 72 hours at 32°C. The solvents used were: benzene, toluene, xylene and hexane. The prescribed standard method used is ASTM D3010. This was done to investigate the level of chemical resistance of cross-linked network.

Other qualitative evaluative analysis carried out include: Fourier Transform Infrared Spectroscopy (FTIR) for functional group determination; Scanning Electron Microscopy (SEM) for micro-structural and morphological determination; X-ray Diffraction Analysis (XRD) for Determination of Percentage Crystallinity; X-ray Fluorescence (XRF) of elemental oxide determination; Thermal gravimetric Analysis (TGA) for the evaluation of thermal stability and degradation as a result of temperature effect.

Productions of vibration dampeners for motor cycle hubs and industrial oil seals for bambury mixers were carried out using the best formulation achieved from the simulated analysis evaluated. The formulations with 500°C carbonisation temperature for coconut shell and 600°C carbonisation temperature for coconut fibre were used. Four (4) formulations were drawn and were used. Further evaluative field analyses on the moulded products were dynamic flex fatigue, rebound resilience, crack initiation analysis, weathering/ozon resistance. Analysis of variance study using DMRT and LSD evaluated with appropriate hypotheses for test of significance were carried out.

6.2 Conclusion

The Properties of composites filled with carbonised fillers were superior to the uncarbonised fillers. In comparison to a standard product filled with carbon, reinforcements were relatively high and product performance in oil seal and vibration dampener were of high performance without suspicious health challenges as the hazardous nitrosamines content of carbon black are absent in the agro-fillers which are also renewable. Carbonisation temperature ranges from (300-700)^oC, with the optimum properties achieved at 500^oC for coconut shell and 600^oC for coconut fibre. pH increased from acidity to alkalinity as the carbonisation temperatures increase. Metal content activity increased leading to the alkalinity as residual materials were being lost. Increase in carbonisation decreased moisture content of the filler and therefore eliminates product shrinkage defects. The surface area of filler increased progressively during modification. Increase in surface area activities resulted in higher modulus at higher strain, abrasion resistance and lower hysteresis.

Bulk density decreased with filler modification. The density was influenced by the particle size and structure of the shell and fibre. The lower the particle size; the lower the density and therefore, the better the interaction between the rubber matrix and the modified fillers. The physico-mechanical properties indicated that the modified fillers exhibited higher hardness, abrasion resistance, tensile strength and modulus as interaction between fillers and matrix increase.

Values of elongation at break decreased with modification. The decrease in elongation at break has to do with adherence of the filler to the polymer phase leading to the stiffening of the polymer chain. Compressive strength results showed a progressive decrease with modification process. The compressive strength was affected by the affinity of the rubber for the filler surface.

Fourier transform infra-red spectrum (FTIR) determined the functional groups present and showed how they were optimised/removed during carbonisation. The spectra results indicated the destruction of cellulose, hemicellulose and lignin components of the shell and fibre to ensure compatibility between the filler and the hydrophobic rubber matrix. The scanning electron microscopy (SEM) provided micro-structural evidence of characteristic cellular morphologies of composites as the modification process proceeds. X-ray diffraction (XRD) investigated the level of amorphousness and crystallinity of the modified filler. Modification diminished amorphousness and strengthened crystallinity; thereby giving the filler a penetrating ability into the rubber matrix. X-ray fluorescence (XRF) exposed the entire elemental oxides present in the shell and fibre and showed how they were optimised. Carbonisation increases the K_2O and increased the bond strength between filler and matrix through the existing electrovalent bond in potassium oxide.

Thermal gravimetric analysis (TGA) examined the thermal stability of the bulk components of the coconut shell and fibre. Carbonisation brought about modification by burning off lignocelluloses which hinders filler matrix interpenetrating network interactions. Carbonisation improved the surface morphology of the filler and upon the natural rubber matrix. Optimum properties were observed at 500°C treatment for the coconut shell and 600°C treatment for fibre and further evaluative analysis of dynamic flex fatigue, rebound resilience relationship, vulcanisate chemical resistance in organic solvents, weathering and ozone resistance tests confirmed improvement made by modification through carbonisation.

Physical modification actually took place through carbonisation. Increase in carbonisation temperatures attracted corresponding increase in the physico-mechanical, chemical, crystalline, thermal, morphological and elemental properties of the

composites. Modification through carbonisation gave a clear indication of reduction of potential surface hindrances of the developed fillers, thereby creating a high interactive surface between filler and rubber matrix of the composites as well as an increase in the carbon content of the fillers.

The experimentally evaluated results of mechanical and chemical sorption properties that gave the optimised formulation for the fibre and shell composites used in the modelled products (vibration dampeners and industrial oil seals) performed very well with high significant levels on a theoretical predictive evaluation as mathematically modelled by means of statistical analysis of variance (ANOVA). The predictive results obtained using the new Duncan's multiple range test (DMRT) presented a high significance differences between subject factors of mechanical properties and samples (modification temperatures) at 95% probability and deterministic levels. There was a high correlation between experimental values and theoretically predictive values. The formulation and design of other engineering items from the optimised composites is highly encouraged.

Decisions: Since $F_{cal} > F_{tab}$ in both hypothesis (A) and hypothesis (B) and in all their variances, we therefore accept ***H1: The physico-mechanical properties changes and chemical sorption properties leading to product reinforcements as carbonisation treatment at the evaluated varying temperatures were therefore significant. This significance positively supported the experimental results achieved using physico-mechanical properties as parameters for products reinforcements.***

Fibre and shell composites from coconut palm waste can be a material of choice not just for automobile parts and oil seals; but also for aerospace construction, building, bridge bearings and electrical appliances for conductivities. Removing them from the environment as wastes will guarantee a safer environment and open an entrepreneurial opportunity for the conversion of waste to wealth. A good knowledge of structural

designs, joining mechanisms, composites development and manufacturing techniques would enhance better applications in other areas of engineering.

6.3 Recommendations for Further Studies

Future work is needed to further the understanding of a wide range of modification; possibly chemical modification of the coconut palm wastes. Based on the results shown in this thesis, future work will need to be focused on the following aspects:

- (i) Chemical infusion and modifications. Carbonisation was a physical modification process. Other chemical modification means such as alkylation, benzylation, mercerisation and dehydroxylation could be encouraged to evaluate chemical grafting on the composites matrix; and possible reinforcements.
- (ii) Long-term weathering or accelerated weathering treatment on the produced models is needed to simulate the circumstances in real applications.
- (iii) Further range of mechanical tests such as creep, load bearing strength and intense mechanical deflections would be required before possible commercialisation can take place using the derived and optimised formulations.

Multiple mould cells that will be amenable to multi-moulding techniques capable of giving rise to at least five (5) moulded pieces at a moulding cycle instead of the one-off intermittent moulding technique used to produce the industrial oil seals and motor cycle dampener would be required. A polished mould surface would be a necessity at achieving precision engineering items using the optimised formulations.

REFERENCES

- Additives (2004): In Ullmann's Encyclopedia of Industrial Chemistry. Wiley – VCH, Weinheim. Dio: 10.1002/14356007. 923-365.
- Ademark, P.; Varga, A.; Medve, J.; Harjunpaa, V.; Drakenberg, T.; Tjerneld, F. and Stalbrand, H. (1998). Softwood Hemicellulose – Degrading Enzymes from *Aspergillus Niger*: Purification and Properties of a Beta-Mannanase. *Journal of Biotechnology* 63: 199 – 120.
- Adhikary, K.B.; Pang, S. and Mark, P.S. (2008). Dimensional Stability and Mechanical Behaviour of Wood Plastic Composites Based on Recycled and Virgin High-Density Polyethylene (HDPE). *Composites, Part B*: 39 (5): 807-815.
- Agunsoye, J.; Olumuyiwa, T.S. and Isaac, S.O.S. (2012). Study of Mechanical Behaviour of Coconut Shell Reinforced Polymer Matrix Composites. *Journal of Minerals and Materials Characterization and Engineering*, 4(2): 774 – 779.
- Ahmasebi, P.; Javadpour, F. and Sahimi, M. (2015). Three Dimensional Stochastic Characterizations of Shale SEM Images. *Transport in Porous Media*, 110 (3): 521-531.
- Ahmedna, M.; Johnson, M; Clarke, S. J.; Marshel, W. E. and Rao, R. N. (1997). Potential of Agricultural By-Products Based Activated Carbon for Use in Raw Sugar Decolonization. *Journal of Science and Food Agriculture* 75: 117 – 124.
- Ahmedna, M.; Marshal, W. E. and Rao, R. M. (2000). Granular Activated Carbons from Agricultural By-Products: Preparation, Properties and Application in Cane Sugar Refining. *Bulletin of Louisiana State University Agricultural Centre, Bio-Resource Technology*, 71: 113 – 123.
- Akay, M. (1993). Aspect of Dynamic Mechanical Analysis, in Polymeric Composites. *Composite Science and Technology*, 47: 419-423.
- Akinlabi, A. K.; Olayinka, O. M.; Dare, E. O. and Oyenekan, O. M. (2011). Mechanical Properties of Rubber Blends Filled with Carbonized *Pteriocarpussantalinoides* Seed Oil. *Nigerian Journal of Polymer Science and Technology*, 7 (1): 1-13.

- Algina, J. And Olejnik, S. (2003). Conducting Power Analysis for ANOVA and ANCOVA in between-Subjects Designs. *Evaluation and the Health Professions*, 26 (3): 288-314.
- Alok, S.; Savita, S. and Aditya, A. (2013). Study of Mechanical Properties and Absorption Behaviour of Coconut Shell Powder – Epoxy Composites. *International Journal of Materials Science and Applications*, 2(5): 157 – 161.
- American Society for Testing and Materials, ASTM (1983). Standard Method of Testing Ash Content, D5630; ASTM: West Conshohocken, PA.
- American Society for Testing and Materials, ASTM (1983). Standard Method for Bulk Density Measurement, D6111-13a; ASTM: West Conshohocken, PA.
- American Society for Testing and Materials, ASTM (1983). Standard Method for Chemical Sorption Measurement, D3010; ASTM: West Conshohocken, PA.
- American Society for Testing and Materials, ASTM (1984). Standard Method of Testing Iodine Adsorption Number, D1510; ASTM: West Conshohocken, PA.
- American Society for Testing and Materials, ASTM (1984). Standard Method for Compounding Rubber, D3182; ASTM: West Conshohocken, PA.
- American Society for Testing and Materials, ASTM (1985). Standard Method of Testing Loss on Ignition, D1509; ASTM: West Conshohocken, PA.
- American Society for Testing and Materials, ASTM (1987). Standard Method of Measurement of Cure Characteristics, D2084; ASTM: West Conshohocken, PA.
- American Society for Testing and Materials, ASTM (1989). Standard Method of Press Curing of Rubber Compound, D1632-07; ASTM: West Conshohocken, PA.
- American Society for Testing and Materials, ASTM (1989). Standard Method of Weathering/Ozone Measurement, D1171; ASTM: West Conshohocken, PA.
- American Society for Testing and Materials, ASTM (1998). Standard Method for Determination of pH, SCAN-P39; Ion Laser Technology, Salt Lake City, UT.
- American Society for Testing and Materials, ASTM (2003). Standard Method of Sorption/Testing of Swelling Properties, D2240; ASTM: West Conshohocken, PA.

- American Society for Testing and Materials, ASTM (2003). Standard Method of Testing Hardness – Shore A, D2240; ASTM: West Conshohocken, PA.
- American Society for Testing and Materials, ASTM (2003). Standard Method for Thermal Gravimetric Analysis Measurement, E1641; ASTM: West Conshohocken, PA.
- American Society for Testing and Materials, ASTM (2012). Standard Method of Testing Compressive Strength of Rubber Compound, D575-91; ASTM: West Conshohocken, PA.
- American Society for Testing and Materials, ASTM (2012). Standard Method for Testing Dynamic Fatigue of Materials, D430-06; ASTM: West Conshohocken, PA.
- American Society for Testing and Materials, ASTM (2015). Standard Method of Testing Tensile Strength, Modulus, Elongation at Break and Flexural Test, D3039/D; ASTM: West Conshohocken, PA.
- American Society for Testing and Materials, ASTM (2015). Standard Method of Testing Abrasion Resistance Index of Rubber, D5963-04; ASTM: West Conshohocken, PA.
- American Society for Testing and Materials, ASTM (2015). Standard Method of Testing Flexural Strength, D790-03; ASTM: West Conshohocken, PA.
- American Society for Testing and Materials, ASTM (2015). Standard Method for Testing Resilience Properties of Materials, D2632-15; ASTM: West Conshohocken, PA.
- American Society for Testing and Materials, BS (1984). Standard Method for Testing Oil Absorption, 3483 Part 7; BS: West Conshohocken, PA.
- Andrzej K. and Abdullah A. (2010). Barley Husk and Coconut Shell Reinforced Polypropylene Composites: The Effect of Fibre Physical, Chemical and Surface Properties. *Composites Science and Technology*, 70 (5): 840 – 846.

- Ansarifar, A.; Lim, H. P. and Nijahwan, R. (2004). Assessment of the Effect of a Bifunctional Organosilane on the Bound Rubber and Properties of Some Natural Rubber Compounds. *International Journal of Adhesion and Adhesives*, 24: 9-22.
- Ansarifar, A.; Shiah, S. F. and Bennett, M. (2005). Optimizing the Chemical Bonding between Silanized Silica Nano-Filler and Natural Rubber and Assessing its Effect on the Properties of the Rubber. *International Journal of Adhesion and Adhesives*, 26(66): 454 – 463.
- Ansarifar, M. A. and Nijahwan R. (2000). Effects of Silane on Properties of Silica Filled Natural Rubber Compounds. *Journal of Rubber Research*, 3: 169 – 184.
- Araújo, J. R.; Waldman, W. R. and De Paoli, M. A. (2008). Thermal Properties of High Density Polyethylene Composite with Natural Fibre: Coupling Agent Effect. *Polymer Degradation Stabilization*, 93: 1770 – 1775.
- Arayapranee, W. and Rempel, G. L. (2009). Synthesis and Mechanical Properties of Di-imide-Hydrogenated Natural Rubber Vulcanisates. *Journal of Applied Polymer Science*, 114: 4066-4075.
- Arayapranee, W. and Rempel, G.L. (2008). A Comparison of the Properties of Rice Husk Ash, Silica, and Calcium Carbonate Filled-75:25 NR/EPDM Blends. *Journal of Applied Polymer Science*, 110: 1165-1174.
- Arayapranee, W; Na-Ranoug, N. and Rempel, G. L. (2005). Application of Rice Husk Ash as Fillers in the Natural Rubber Industry. *Journal of Applied Polymer Science*, 98: 34-41.
- Aribike, D. S.; Latinwo, G. K. and Susu, A. A. (2007). Effects of Kaolin Filler Material on the Mechanical Properties of Flexible Polyurethane Foam. *Journal of Science, Technology and Environment*, 7(182): 25-30.
- Arroyo, M.; Lopez – Manchado, M. A. and Herrera, B. (2003). Organo-Montmorillonite as Substitute for Carbon Black in Natural Rubber Compounds. *Polymer*, 44(8): 2447 – 2453.
- Ashori, A. and Raverty, A. (2007). Printability of Sized Kena (*Hibiscus cannabinus*) Papers. *Plastic Technology and Engineering* 46 (7):683-687.

- Awatefe, K. J.; Akaranta, O. and James, A. (2014). Compounding and Rheometric Studies of Natural Rubber Vulcanisates Filled with Kaoline and Palm Kernel Shell Powder. *Journal of Chemical Society of Nigeria*, 39 (1): 97-102.
- Awatefe, K. J.; Akaranta, O.; James, A. (2016). Comparism of Percent Equilibrium Swelling Properties of Palm Kernel Shell Powder (PKSP), Versus Conventional Fillers in Natural Rubber Vulcanisates. *Nigerian Polymer Journal of Polymer Science and Technology*, 32 (2): 28-32.
- Ayeni, A.O.; Banerjee, S.; Omoleye, J.A.; Hymore, F.K.; Giri, B.S.; Deskmukh, S.C.; Pandey, R.A. and Mudliar, S.N. (2013a). Optimization of Pretreatment Conditions Using Full Factorial Design and Enzymatic Convertibility of Shea Tree Sawdust. *Biomass and Bioenergy*, 48: 130-138.
- Ayeni, A.O.; Hymore, F.K.; Mudliar, S.N.; Deskmukh, S.C.; Satpute, D.B.; Omoleye, J.A. and Pandey, R.A. (2013b). Hydrogen Peroxide and Lime Based Oxidative Pretreatment of Wood Waste to Enhance Enzymatic Hydrolysis for a Biorefinery: Process Parameters Optimizing Using Response Surface Methodology. *Fuel*, 106: 187 – 194.
- Ayeni, A.O.; Omoleye, J.A.; Mudliar, S.; Hymore, F.K. and Pandey, R.A. (2014). Utilization of Lignocellulosic Waste for Ethanol Production: Enzymatic Digestibility and Fermentation of Pretreated Shea Tree Saw dust. *Korean Journal of Chemical Engineering*, 31(7): 1180 – 1186.
- Ayo, M. D.; Madufor, I. C.; Ekebafé, L. O. and Chukwu, M. N. (2011). Effect of Filler Carbonization Temperature on the Mechanical Properties of Natural Rubber Composites, *Researcher* 3(11): 7-10.
- Bakar, M. B. A.; Leong, Y. W.; Ariffin, A. and Ishak, Z. A. M. (2008). Effect of Chemical Treatments on the Mechanical, Flow, and Morphological Properties of Talc and Kaolin-Filled Polypropylene Hybrid Composites. *Journal of Applied Polymer Science*, 110, 2770 – 9.
- Barnes, P.R.F.; Mulvaney, R.; Wolf, E.W. and Robinson, K.A. (2002). A Technique for the Examination of Polar Ice Using the Scanning Electron Microscope. *Journal of Microscopy*, 205(2): 118-124.
- Belmárs, H.; Barrera, A. and Monjaras, M. (1983). New Composite Materials from Natural Hard Fibres Part 2. Fatigue Studies and a Novel Fatigue

Degradation Model. *Industrial Engineering Chemical Product Research and Developments*, 22:643-652.

- Bhaskar, J. and Singh, V. K. (2013). Physical and Mechanical Properties of Coconut Shell Particles Reinforced Epoxy Composite. *Journal of Material Environmental Science*, 4(2): 227 – 232.
- Billings, S.A. (2013). Non Linear System Identification: NARMAX Methods in the Time, Frequency, and Spatio- Alexandre, M. And Dubois, P. (2000), Polymer Layered Silicate Nanocomposites; Preparation, Properties, and uses of a New Class of Materials. *Materials Science and Engineering: Reports*, 28 (1-2): 63. *Temporal Domains*, Wiley.
- Bledzki, A.L.K. and Gassan, J. (1999). Composite Reinforced with Cellulose Fibre. *Progress in Polymer Science*, 24 (1): 221-274.
- Blow, C. M. and Hepburn, C. (1971). Rubber Technology and Manufacture. *Butterworth and Company Limited (3rd Edition) London, UK*, PP 126-145.
- Boonstra, B.B. (1975), Rubber Properties. *In Rubber Technology and Manufacture*. (Blow C.M. and Hepburn C., Editors), *Newnes – Butterworths, London, UK*, PP 222-254.
- Boonstra, B.B. (1979). Reactions in Rubbery Materials. *Polymer*, 20: 691.
- Boyle, J. F.; Manas – Zloczower, I. and Feke, D. L. (2004). Hydrodynamic Analysis of the Mechanisms of Agglomerate Dispersion. *Powder Technology*, 153:127–133.
- Brahma, K.M.; Pavithran, C. and Pillai, R. M. (2005). Coconut Fibre Reinforced Polyethylene Composites: Effect of Natural Waxy Surface Layer of the Fibre on Fibre/Matrix Interfacial Bonding and Strength of Composites. *Composites Science and Technology*, 65 (2-4): 563-569.
- Brydson, J.A. (1978). Rubber Chemistry. *Applied Science Publishers Ltd., London, UK*, PP 26-34.
- Burfield, R. O.; Kooi-Ling, L. and Kia-Sang, L. J. (1984). Mechanism of Polymeric Reactions. *Journal of Polymer Science*, 29: 1661-1673.
- Cao, Q.; Zhu, S.; Pan, N.; Zhu, Y. and Tu, H. (2009). Characterization of Archaeological Cotton (G. herbaceum) Fibres from Yiugpan. *Technical Briefs in Historic Archaeology*, 4: 18-28.

- Cardinal, R.N. and Aitken, M.R.F. (2006). ANOVA for the Behavioural Sciences Researcher. *Mahwah, NJ: Lawrence Erlbaum Associates*. PP 23-34
- Carrillo, F.; Colom, X.; Suriol, J.J. and Saurina, J. (2004). Structural FTIR Analysis and Thermal Characterization of Lyocel and Viscose–Type Fibres. *European Polymer Journal*, 40: 2229-34.
- Cazaurang, M.; Herrera, P.; Gouzalez, I. and Aguilar, V. M. (1991). Physical and Mechanical Properties of Henequen Fibres. *Journal of Applied Polymer Science*, 43: 749 – 756.
- Chanap, R. (2012). Study of Mechanical and Flexural Properties of Coconut Shell Ash Reinforced Epoxy Composite. *Bachelor's Thesis, National Institute of Technology, Rourkela*, 21: 245-265.
- Chand, N.; Dan, T. K.; Verma, S. and Rohatgi, P. K. (1987). Rice Husk Filled Polyester Resin Composites. *Journal of Materials Science Letters*, 6(6), 733 – 735.
- Chang, J. H. and An, Y. U. (2002). Nano-Composites of Polyurethane with Various Organoclays: Thermomechanical Properties, Morphology, and Gas Permeability. *Journal of Polymer Science: Part B: Polymer Physics*, 40: 670 – 677.
- Chen, H. Y. (1966). Morphological Properties of Organoclays as Filler Materials *Journal Polymer Science*, B₄: 891.
- Chen, H.L. and Porter, R.S. (1994). Composite of Polyethylene and Kenaf, a Natural Cellulose Fibre. *Journal of Applied Polymer Science*, 54: 1781-1790.
- Choi, N. W.; Mori, I. and Ohama, Y. (2006). Development of Rice Husk–Plastic Composites for Building Materials. *Waste Management*, 26(2), 189 – 194.
- Chotirat, L.; Chaochanchaikul, K. and Sombatsompop, N. (2007). On Adhesion Mechanism and Interfacial Strength in Acrylonitrile Butadiene Styrene/Wood Sawdust Composites. *International Journal of Adhesion and Adhesives*, 27: 669-678.
- Ciolacu, D.; Ciolacu, F. and Popa, V.I. (2011). Amorphous Cellulose-Structure and Characterization, *Cellulose Chemistry and Technology*, 45(1-2): 13-21.
- Colthup, N. B.; Daly, L. H. and Wiberley, S. E. (1990). Introduction to Infrared and Raman Spectroscopy (3rd Edition), *Academic Press Inc*, UK, PP 212-221.

- Cortina, J.M. and Nouri, H. (2000). Effect Size for ANOVA Designs, Thousand Oaks, CA: Sage Publications. *Effect Size for ANOVA Designs (Quantitative Applications in the Social Sciences)*, PP 20-26.
- Da Dosta, H. M.; Visconte, L. L. Y.; Nunes, R. C. R. and Furtado, C. R. G. (2002). Mechanical and Dynamic Mechanical Properties of Rice Husk Ash-Filled Natural Rubber Compounds, *Journal of Applied Polymer Science*, 83: 2331-2346.
- Dailatos, G. D. (2009). Theory of the Gaseous Detector Device in the ESEM, *Advances in Electronics and Electron Physics*, 78:1-102.
- Daniel, D.; Punyanich, I.; Quang, N. T.; Fredderic, G. and Charoen, N. (2009). Graft Copolymers of Natural Rubber and Poly (Dimethyl(acryloxymethyl) Phosphate)(NR-g-PDMAMP) or Poly (Dimethyl(methacryloyloxy ethyl) Phosphate) (NR-g-PDMMED) from Photo-Polymerization in Latex Medium, *European Polymer Journal*, 45: 820 – 8260.
- De Rosa, I.M.; Kenny, J.M.; Maniruzzaman, M. D.; Monti, M.; Puglia,D.; Santulli, C. and Sarasini, C. (2010). Morphological, Thermal and Mechanical Characterization of Okra (*Abelmoschus esculentus*) Fibres as Potential Reinforcement in Polymer Composites. *Composites Science and Technology*, 70: 116-122.
- Dhakal, H. N.; Zhang, Z. Y. and Richardson, M. O. W. (2007). Effect of Water Absorption on the Mechanical Properties of Hemp Fibre Reinforced Unsaturated Polyester Composites. *Composites Science and Technology*, 67: 1674–1683.
- Dick, J. S. (2001). Vulcanisates Physical Properties, Performance Characteristics and Testing; In: *Rubber Technology Compounding and Testing for Performance*, Hanser, Ohio, USA, PP 66-67.
- Edwards, H.G.M.; Farwell, D.W. and Webster, D. F.T. (1997). Raman Microscopy of Untreated Natural Plant Fibres. *Spectrochimica Acta part A*, 53: 2383-2392.
- Egwaikhide, P. A.; Akporhonor, E. E. and Okieimen, F. E. (2007a). An Investigation on the Potential of Palm Kernel Husk as Fillers in Rubber Reinforcement. *Middle East Journal of Scientific Research*, 2(1): 28 – 32.

- Egwaikhide, P. A.; Akporhonor, E. E. and Okieimen, F. E. (2007b). Effect of Coconut Fibre Filler on the Cure Characteristics, Physico-Mechanical and Swelling Properties of Natural Rubber Vulcanisates. *International Journal of Physical Sciences*, 2(2): 039 – 046.
- Eiras, D. and Pessan, L.A. (2009). Crystallization Behaviour of Elastomer/Filler Composites. Effect of Elastomer Polarity. *Polymer*, 41: 9283 – 9290; 355 – 356.
- Ekebafé, L. O.; Ayo, M. D.; Okuofu, P. O. and Erhuanga, G. O. (2009). Effects of Primary Amine Modified Clay (Organoclay) on the Mechanical Properties of Natural Rubber Vulcanisates. *Journal of Applied Science and Technology*, 4(1), PP 112-122.
- El-Tayeb, N. S. M. and Nasir, R. Md. (2007). Effect of Soft Carbon Black on Tribology of Deproteinized and Polyisoprene Rubbers. *Wear*, 262: 350-361.
- Fahma, F.; Iwamoto, S.; Hori, N.; Iwata, T. and Takemura, A. (2011). Effect of Pre-Acid-Hydrolysis Treatment on Morphology and Properties of Cellulose Nano Whiskers from Coconut Husk. *Springer Science Business Media B.V.*; 18(2): 443-450.
- Fay, M.P. and Proschan, M.A. (2010). Wilcoxon-Mann-Whitney or T-Test? On Assumptions for Hypothesis Tests and Multiple Interpretations of Decision Rules. *Statistics Surveys*, 4: 1-39.
- Flory, P.J. (1953). In Principles of Polymer Chemistry. *Cornell University Press, Ithaca, New York*, PP 11-16.
- Flory, P.J. and Rehner, J. Jr. (1943). Development in Molecular Layers of Polymeric Films, *Journal of Chemistry and Physics*, 11: 521.
- Fukahori, Y. and Yamazaki, H. (1994). Mechanism of Rubber Abrasion-Part 1; Abrasion Pattern Formation in Natural Rubber Vulcanisates. *Wear*, 171: 195-202.
- Ganiyu, K.L.; David, S.A.; Alfred, A.S. and Semiu, A.K. (2010). Effects of Different Filler Treatments on the Morphology and Mechanical Properties of Flexible Polyurethane Foam Composites. *Nature and Science Journal*, 8(6): 23 – 31.

- Garde, K.; McGill, W. J. and Woolard, C. D. (1999). Surface Modification of Fly Ash Characterization and Evaluation as Reinforcing Filler in Polyisoprene. *Plastics, Rubber and Composites*, 28: 1 – 10.
- Gent, A. N. (1989). A Hypothetical Mechanism for Rubber Abrasion. *Rubber Chemistry and Technology*, 62: 750-756.
- Gent, A.N. and Pulford, C.T.R. (1983). Mechanism of Rubber Abrasion. *Journal of Applied Polymer Science*, 28: 946-960.
- Gent, N. and Lui, G. L. (1999). Swelling and Electrical Properties of Rubber Vulcanisates Loaded with Paraffin Wax. *Journal of Polymer Science and Polymer Physics* 29: 1313-1319.
- George, J.; Sreekala, M. S. and Thomas, S. A. (2001). Review on Interface Modification and Characterization of Natural Fibre Reinforced Plastic Composites. *Polymer Engineering and Science*, 41(9): 1471-1485.
- George, W. (2000). Handbook of Filler (2nd Edition). *Chemical Technology Publishing, USA*, PP 24-35.
- Ghosh, P. (2007). Polymer Science and Technology: Plastics, Rubbers, Blends and Composites, Second Edition. *Tata Mc Graw-Hill Publishing Company Limited; New Delhi*, PP 493-501.
- Gilman, J.W.; Bourbigot, S.; Bellayer, S.; Stretz, H. and Paul, D.R. (2005). In Fire Retardancy of Polymers New Application of Mineral Fillers: (Le Bras, M.; Wilkie, C.A. Bourbigot, S.; Duquene, S. Jama, C. Editors). *The Royal Society of Chemistry: Cambridge, UK*, PP 177-186.
- Golub, M. A.; Fuqua, S. A. and Bhacca, N. S. (1962). Polymer Modification Networks and Characterization, *Journal of American Chemical Society*, 84: 491.
- Guo, Z. and Fang, Z. (2009). Dynamic Rheological Analysis as a Sensitive Method for Analyzing Structural Change during Thermo-Oxidation of Polyolefin Elastomers. *Chinese Journal of Polymer Science*, 27 (2): 183 – 188.
- Gwon, J. G.; Lee, S. Y.; Doh, G. H. and Kim, J. H. (2010). Characterization of Chemically Modified Wood Fibres using FTIR Spectroscopy for Bio Composites. *Journal of Applied Polymer Science*, 116(6): 3212 – 9.
- Habibi, Y.; Zawawy, W. K.; Ibrahim, M. M. and Dufresne, A. (2008). Processing and Characterization of Reinforced Polyethylene Composites Made with

Lignocellulosis Fibres from Egyptian Agro-Industrial Residues. *Composites Science and Technology*, 68 (7 - 8): 1877 – 1885.

- Hafsat, R. S.; Abubakar, M.B.; Thirmizir, M. Z. A.; Adefila, S. S.; Yakubu, M.K.; Ishiaku, U.S.; Kolawole, E. G. and Ishak, Z. A. M. (2016). Effect of Epoxy Concentration and Fibre Loading on Melt Flow Index, Dynamic Modulus and Crystallinity of Engineering Thermoplastic ABS/Epoxy-Coated Kenaf Fibre Composites. *Nigerian Journal of Polymer Science and Technology*, 11: 12-20.
- Han, S.O.; Mechdi, K.I.; Na-Sin, A.B.; Young, H.J.; Jonathan, G. and Kyriaki, K. (2012). Understanding the Reinforcing Mechanizations in Kenaf Fibre/PLA and Kenaf Fibre/PP Composites; A comparative study. *International Journal of Polymer Science*, 1-8.
- Han-Seung, Y.; Hyun-Joong, K.; Hee-Jun, P.; Bum-Jae, L. and Taek-Sung, H. (2006). Water Absorption Behaviour and Mechanical Properties of Lignocellulosic Filler-Polyolefin Bio-Composites. *Elsevier, Composite Structures*, 72: 429 – 437.
- Helge, B.B.; Axel, Z.; Kirsten, P. and Dieter, J. (2000). “Physiological and Chemical Investigations into Microbial Degradation of Synthetic Poly (Cis-1, 4 Isoprene)”. *Applied and Environmental Microbiology*, PP 66-72.
- Herrera-Franco, P. A.; Valadez, G. and Cervantes, U. C. (1997). Development and Characterization of a HDPE-Sand-Natural Fibre Composites. *Composites Part B: Engineering*, 28B (3): 331 – 343.
- Herrera-Franco, P. J. and Valedez-Gonzalez, A. (2004). Mechanical Properties of Continuous Natural Fibre-Reinforced Polymer Composites. *Composites Part A*, 35: 339 – 45.
- Hidaka, K.; Kim, U.J. and Wada, M. (2010). Synchrotron X-ray Fibre Diffraction Study on the Thermal Expansion Behaviour of Cellulose Crystals in Tension Wood of Japanese Poplar in the Low-Temperature Region. *Holzforschung*, 64: 167-171.
- Hon, D. N. S. and Shiraishi, N. (2001). Wood and Cellulosic Chemistry. *Marcel Dekker, Incorporated New York*.

- Honday, L. (1966). Composite Material. *Elsevier, New Nostrand, New York*, 313.
- Hong, C.K, Kim, H, Ryu, C, Mah, C, Huh, Y. and Kaang, S. (2007). Effect of Particle Size and Structure of Carbon Blacks on the Abrasion of Filled Elastomer Compounds. *Journal of Materials Science*, 42: 8391-8399.
- Hortola, P. (2005). SEM Examination of Human Erythrocytes in Uncoated Bloodstains on Stone; Use of Conventional as Environmental-like SEM in a Soft Biological Tissue (and Hard Inorganic Material). *Journal of Microscopy*, 281 (2): 94-103.
- Hortola, P. (2015). Evaluating the Use of Synthetic Replicas for SEM Identification of Blood Stains (with Emphasis on Archaeological and Ethnographic Artifacts). *Microscopy and Microanalysis*, 6: 1504.
- Hosler, D.; Burkett, S.L. and Tarkanian, M.J. (1999). Prehistoric Polymers; Rubber Processing in Ancient Mesoamerica. *Science*, 284(5422): 1986-1991.
- Howell, C. L. (2008). Understanding Wood Biodegradation through the Characterization of Crystalline Cellulose Nano-Structures. *Doctoral Thesis University of Maine*.
- Hull, P.K. and Clyne, T.W. (1996). An Introduction to composite materials. *Cambridge University Press, UK*, PP 67.
- Husseinsyah, S. and Mostapha, M. (2011). The Effect of Filler Content on Properties of Coconut Shell Filled Polyester Composites. *Malaysian Polymer Journal*, 6 (1): 87 – 97.
- Igwe, I. O. and Ejim, A. A. (2011). Studies on Mechanical and End-use Properties of Natural Rubber Filled with Snail Shell Powder. *Material Sciences and Application*, 2: 802 – 810.
- Ishak, Z. A. M. and Bakar, A. A. (1995). Investigation on the Potential of Rice Husk Ash as Fillers for Epoxidized Natural Rubber (ENR). *European Polymer Journal*, 31(3): 259 – 269.
- Ismail, H., Edyhan, M. and Wirjosentono, B. (2002). Bamboo Fibre Filled Natural Rubber Composites: The Effects of Filler Loading and Bending Agent. *Polymer Testing*, 21(2): 139 – 144.

- Ismail, H., Rozman, H. D.; Jaffri, R. M. and Ishak, Z. A. (1997). Oil Palm Wood Flour Reinforced Epoxidized Natural Rubber Composites; Effects of Filler Content and Size. *European Polymer Journal*, 33(10 - 11): 1627 – 1632.
- Iyasele, J. U. and Okieimen, F. E. (2004). Cure Characteristics and Rheological Properties of Melon Seed Shell-Filled Natural Rubber. *Proceedings of 27th International Conference of Chemical Society of Nigeria, Benin City*, 272-277.
- Jacob, O.A.; Ayogu, H. and Olawale, M.S. (2014). Evaluation of Mechanical Properties of Coconut Shell Fibre as Reinforcement Material in Epoxy Matrix. *International Journal of Engineering Research and Technology*, 3 (2): 2337-3348.
- Jae, G.G.; Sun, Y.E.; Sang, J.C.; Geum, H.D. and Jung, H.K. (2010). Effects of Chemical Treatments of Hybrid Fillers on the Physical and Thermal Properties of Wood Plastic Composites. *Elsevier Limited, Composites:Part A*, 5 (1): 1491 –1497.
- Jain, S.; Kmar, R.; Jindal, U. C. (2012). Mechanical Behaviours of Bamboo and Bamboo Composites, *Journal of Materials Science*, 27: 4598 – 4604.
- James, E.M.; Burak E. (2005). Sulphur Vulcanization of Natural Rubber for Benzothiazole Accelerated Formulations: From Reaction Mechanisms to a Rational Kinetic Model. *Science and Technology of Rubber*, PP 768.
- Jeffree, C. E. and Read, N.D. (1991). Ambient-and Low Temperature Scanning Electron Microscopy. In *Hall, J.L.; Hawes, C.R. Electron Microscopy of Plants Cells. London, Academic Press*, 313-413.
- Jikan, S. S.; Samsudin, M. S. F.; Ariff, Z. M.; Ishak, Z. A. M. and Ariffin, A.; (2008). Relationship of Rheological Study with Morphological Characteristics of Multi-component (Talc and Calcium Carbonate) Filled Polypropylene Hybrid Composites. *Journal of Reinforced Plastics Composites*, 4 (2): 233-242.
- John M. J. and Thomas S. (2008). Bio-Fibres and Bio-Composites. *Carbohydrate Polymer*, 71: 343 – 64.

- John, O. O. and Samuel, I. A. (2010). Potential of Carbonized Bagasse Filler in Rubber Product. *Journal of Emerging Trends in Engineering and Applied Science*, 1(2): 157 – 160.
- Joseph, S.; Sreekala, M. S.; Oommen, Z.; Koshy, P. and Thomas, S. A. (2002). Comparison of Mechanical Properties of Phenol Formaldehyde Composites Reinforced with Banana Fibres and Glass Fibres. *Composite Science and Technology*, 62: 1857-1867.
- Joseph, P. V.; Josepha, K.; Thomas, S.; Pillai, C. K. S.; Prasad, V. S. and Groeminckx, G. (2003a). The Thermal and Crystallization Studies of Short Sisal Fibre Reinforced Polypropylene Composites. *Composites Part A*, 34: 253 – 66.
- Joseph, P. V.; Matthew, G.; Joseph, K.; Groeninckx, G. and Thomas, S. A. (2003b). Dynamic Mechanical Properties of Short Sisal Fibre Reinforced Polypropylene Composites. *Composites A₃₄*, 35: 275 – 290.
- Jun, Y. J.; Tae, K. J.; Hwa J. O. and Jae, R. Y. (2011). Thermal Stability and Flammability of Coconut Fibre Reinforced Poly (Lactic Acid) Composites. *Composites Part B: Engineering*, 43 (5): 2434-2438.
- Jurkowska, B.; Jurkowski, G.; Nadolny, K.; Krasnov, P.; Studnier, Y. N.; Pesetskii, S.S.; Koral, V N.; Pinchuck, L.S. and Olkhow, Y. A. (2006). Influence of Fluorine Containing Lubricant on Properties of NR/BR Rubber. *European Polymer Journal*, 42: 1676-1687.
- Kabir, M. A.; Islam, M. R. and Huque, M. M. (2006). Studies on the Effect of Hydroxybenzene Diazonium Salts on Physico-Mechanical Properties of Jute Fibre. *Journal of Polymer and Plastics Technology Engineering*, 45: 591 – 596.
- Kamdem, D.P.; Jiang, H.; Cui, W.; Freed, J. and Matuana, L.M. (2004). Properties of Wood Composites Made of Recycled HDPE and Wood Flour from CCA-Treated Wood Removed from Service. *Compose part A*, 35 (30): 347-354.
- Karmakar, A.; Chauhau, S. S.; Modak, J. M. and Chanda, M. (2007). Mechanical Properties of Wood–Fibre Reinforced Polypropylene Composites, *Composites A₃₈*: 227 – 233.

- Kim, H. S.; Kim, S.; Kim, H. J. and Yang, H. S. (2006). Thermal Properties of Bio Flour Filled Polyolefin Composites with Different Compatibilizing Agent Type and Content, *Thermochemistry, Acta*, 451: 181 – 188.
- Kim, H. S.; Lee, B. H.; Choi, S. W.; Kim, S. and Kim, H. J. (2007). The Effect of Types of Maleic Anhydride–Grafted Polypropylene on the Interfacial Adhesion Properties of Bio-Flour-Filled Polypropylene Composites. *Composite Part A: Applied Science and Manufacturing*, 38(6): 1473 – 1482.
- Kim, U.J.; Eom, S.H. and Wada, M. (2010). Thermal Decomposition of Native Cellulose: Influence on Crystallite Size. *Polymer Degradation and Stability*, 95: 778-781.
- Lake, G. J. (1983). Aspects of Fatigue and Fracture of Rubber. *Progress of Rubber Technology*, 45: 89-143.
- Larbig, H.; Scherxer, H.; Dahlke, B. and Poltrock, R. (1998). Natural Fibre Reinforced Based on Renewable Resources for Automotive Interior Applications. *Journal of Cellular Plastics*, 12 (2): 361-379.
- Larson, A. C. and Von-Dreele, R. B. (1994). General Structure Analysis System (GSAS). *Los Alamos National Laboratory Report LAUR 86 – 748*.
- Lee, S. Y.; Chun, S. J.; Doh, G. H.; Kang, I. A.; Lee, S. and Paik, K. H. (2009). Influence of Chemical Modification and Filler Loading on Fundamental Properties of Bamboo Fibres Reinforced Polypropylene Composites. *Journal of Composites Materials*, 43(15): 1639 – 57.
- Levy, M.S. and Neill, J.W. (1990). Testing for Lack of Fit in Linear Multiresponse Models Based on Exact or Near Replicates. *Communications in Statistics Theory and Methods*, 19 (6): 1987-2002.
- Liang, H.; Fukahori, Y.; Thomas, A.H. and Busfield, J.C. (2010). The Steady State Abrasion of Rubber; Why are the Weakest Rubber Compounds so Good in Abrasion? *Rubber Wear Journal*, 268: 756-762.
- Liang, J. Z. (2011). Dynamic Mechanical Properties and Characterization of Inorganic Particulate-Filled Polymer Composites. *Journal of Thermoplastic Composite Materials*, 24: 207-220.

- Lin, C. J., Hergenrother, W. L. and Hilton A. S. (2002). Mooney Viscosity Stability and Polymer Filler Interactions in Silica Filled Rubbers. *Rubber Chemistry and Technology*, 75: 216 – 245.
- Lin, J. C.; Chang, L. C.; Nien, M. N. and Ho, H. L. (2006). Mechanical Behaviour of Various Nano-Particle Filled Composites at Low-Velocity Impact. *Composite Structures*, 27: 30 – 36.
- Lojewska, J.; Miskowiec, P.; Lojewski, T. and Proniewicz, L.M. (2005). Cellulose Oxidative and Hydrolytic Degradation: In situ FTIR Approach. *Polymer Degradation and Stability*, 88: 512-520.
- Lojewska, J.; Lubanska, A.; Miskowiec, P.; Lojewski, T. and Proniewicz, L.M. (2006). FTIR in Situ Transmission Studies on the Kinetic of Paper Degradation via Hydrolytic and Oxidative Reaction Paths. *Applied Physics A*, 84: 597-603.
- Lopattananon, N.; Panawarangkul, K.; Sahakaro, K. and Ellis, B. (2006). Performance of Pineapple Leaf Fibre-Natural Rubber Composites: The Effect of Fibre Surface Treatments. *Journal of Applied Polymer Science*, 102: 1974 – 1984.
- Lou, C. W.; Lin, C. W.; Lei, C. H.; Su, K. H.; Hsu, C. H.; Liu, Z. H. and Lin, J. H. (2007). PET/PP Blend with Bamboo Charcoal to Produce Functional Composites. *Journal of Materials Process Technology*, 3 (1): 428 – 433.
- Lovely, M.; Joseph, K. U. and Joseph, R. (2006). Swelling Behaviour of Isora/Natural Rubber Composites in Oils used in Automobiles. *Bulletin Materials Science*, 29(1): 91-99.
- Madhukiran, J.; Srinivasa, R. and Madhusudan, S. (2013). Fabrication and Testing of Natural Fibre Reinforced Hybrid Composites Banana/Pineapple. *International Journal of Modern Engineering Research*, 3 (4): 2239-2243.
- Mandal, S.; Alam, S. (2012). Dynamic Mechanical Analysis and Morphological Studies of Glass/Bamboo Fibre Reinforced Unsaturated Polyester Resin-Based Hybrid Composites. *Journal of Applied Science*, 125: E382-E387.
- Mark, H.F. (1964). Encyclopedia of Polymer Sciences and Technology. *Interscience New York*, PP 12-42.

- Matador, P. (2007). Rubber Chemistry, Vert Publication, Matador Rubber, UK, PP 1
10.
- Maulida, A.; Nasir, M. and Khalil, H. P. S. A. (2000). Hybrid Composites Based on
Natural Fibre. *Proceedings of Symposium on Polymeric Materials, Penang,
China*, 5 (4): PP 216 – 219.
- Mc Mullan, D. (2006). Scanning Electron Microscopy. *Scanning*, 17 (3): 175-185.
- Md. Rezaur, R.; Md. Nazrul, I.; Md. Monimul, H.; Sinin, H. and Abu, S.A. (2010).
Effect of Chemical Treatment on Rice Husk Reinforced Polyethylene (PE)
Composites. *Bio-resources*, 5(2): 854 – 869.
- Megiatto, J. D.; Silva, C. G.; Rosa, D. S. and Frollini, E. (2008). Sisal Chemically
Modified with Lignins: Correlation Between Fibres and Phenolic Composites
Properties. *Polymer Degradation and Stability*, 93: 1109 – 1121.
- Michael, P. and Wolcott, K. (1999). Development of Composite Flakes,
33rd International Particleboard Composite Material Symposium, England, 34(4):
112-145.
- Mishra, S. and Shimpi, N. G. (2005). Mechanical Properties of Flame-Retardant
Properties of Styrene-Butadiene Rubber Filled with CaCO₃ as Filler and Linseed
Oil as an Extender. *Journal of Applied Polymer Science*, 98(6): 2563 – 2571.
- Móczó, J. and Pukánszky, B. (2008). Polymer Micro and Nano-Composites: Structure,
Interactions, Properties, *Journal of Industrial Engineering and Chemistry*, 14:
535 – 63.
- Mod, R.R.; Ory, R.L.; Morris, N.M. and Normand, F.L. (1981). Chemical Properties
and Interactions of Rice Hemicelluloses with Trace Minerals in Vitro. *Journal of
Agriculture and Food Chemistry*, 29: 449 – 454.
- Mohanty, A. K.; Khan, M. A. and Hinrichsen, G. (2000). Surface Modification of Jute
and its Influence on Performance of Biodegradable Jute–Fabric/Biopol
Composites. *Composites Science and Technology*, 60(7): 1115 – 1124.

- Mohanty, A.K.; Misra, M. and Drzal, L.T. (2002). Sustainable Bio-composites from Renewable Resources; Opportunities and Challenges in the Green Material World. *Journal of Polymer and Environment*, 10 (1): 19-26.
- Momoh, F.P.; Mamza, P.A.P.; Gimba, C.E. and Nkeonye, P. (2016a). Effects of Carbonization on Coconut Shell as Filler in Natural Rubber Compounding, *Nigerian Journal of Polymer Science and Technology*, 11: 115-123
- Momoh, F.P.; Mamza, P.A.P.; Gimba, C.E. and Nkeonye, P. (2016b). Morphological Trends of Modified Coconut Fibre in Natural Rubber Reinforcement, *Journal of Emerging Trends in Engineering and Applied Sciences (JETEAS), Scholarlink International Research Institute Journals*, 7(4): 167-172.
- Momoh, F.P.; Mamza, P.A.P.; Gimba, C.E. and Nkeonye, P. (2017a). Effect of Carbonization Time on the Morphology and Mechanical Properties of Natural Rubber Composites, *International Organization of Scientific Research Journal of Polymer and Textile Engineering (IOSR-JPTE)*, 4 (2,): 06-13.
- Momoh, F.P.; Mamza, P.A.P.; Gimba, C.E. and Nkeonye, P. (2017b). Morphology and Crystallinity of Modified Coconut Shell Powder in Natural Rubber Development, *International Journal of Innovative Research and Advanced Studies (IJIRAS)*, 4; 257-262.
- Momoh, F.P.; Mamza, P.A.P.; Gimba, C.E. and Nkeonye, P. (2017c). Thermal and Elemental Evaluation of Modified Coconut Shell Fibre in Natural Rubber Reinforcement, *International Journal of Engineering Research and Technology (IJERT)*, 6 (4): 663-669.
- Morreale, M.; Scaffaro, R.; Maio, A. and La Mantia, F.P. (2008). Effect of Adding Wood Flour to the Physical Properties of a Biodegradable Polymer. *Composites part A*, 39 (3): 503-513.
- Morton, M. (1987). Rubber Technology, 3rd Edition. *Vani Nostrain, New York, USA*, PP 74-82.
- Mueller, D. H. and Krobjilowski, A. (2003). New Discovery in the Properties of Composite Reinforced with Natural Fibres. *Journal of Industrial Textiles*, 33 (2): 11-30.
- Muhr, A. H. and Roberts, A.D. (1992). Rubber Abrasion and Wear. *Wear*, 158: 21-28.

- Myhre, M. and Mackillop, D. A. (2002). "Rubber Recycling". *Rubber Chemistry and Technology*, 75 (3): 474-479.
- Nasir, M. and Choo, C. H. (1989). Chemical Modification of Natural Rubber Latex with Per-Acetic Acid. *European Polymer Journal*, 25: 355-362.
- Nemour, E. I. (1986). *Polymer Product Department*. The Language of Rubber. Washington, DC, PP 45-56.
- Newman, R. H. (1999). Estimation of the Internal Dimensions of Cellulose Crystallites Using ^{13}C NMR Signal Strength. *Solid State Nuclear Magnetic Resonance* 15: 21 – 29.
- Newman, R. H. (2008). Simulation of X-ray Diffractograms Relevant to the Purported Polymorphs Cellulose iv_i and iv_{ii}. *Cellulose*, 15: 769 – 778.
- Nie, Z. and Kumachera, E. (2008). Patterning surfaces with Functional Polymers, *Nature Materials*, 7(4): 277-290.
- Nurdina, A. K.; Mariatti, M. and Samayamutthirian, P. (2009). Effect of Single-Mineral Filler and Hybrid-Mineral Filler Additives on the Properties of Polypropylene Composites. *Vinyl Additives Technology*, 15: 20 – 8.
- Okieimen, F. E. and Imanah, J. E. (2003a). Characterization of Agricultural Waste Products as Fillers in Natural Rubber Formulation. *Nigerian Journal of Polymer Science and Technology* 3(1): 201 – 207.
- Okieimen, F. E.; Akinlabi, A.K.; Aigbodion, A. I.; Bakare, I.O. and Oladoja, N. A. (2003b). Effect of Epoxidised Natural Rubber. *Nigerian Journal of Polymer Science and Technology*, 3 (1): 233-239.
- Onyeagora, G. N. (2012a). Influence of Carbonized Dika (*Irivalgia gabone*) Nutshell Powder on the Vulcanisates Properties of Natural Rubber/Acrylonitriles Buta-Rubber Blend. *Academic Research International*, 2(3): 218 – 229.
- Onyeagoro, G. N. (2012b). Cure Characteristics and Physico-Mechanical Properties of Carbonized Bamboo Fibre Filled Natural Rubber Vulcanisates. *International Journal of Modern Engineering Research*, 2 (6): 4683 – 4690.

- Orfao, J.J.M and Figueiredo, J.L. (2001). A Simplified Method for Determination of Lignocellulosic Materials Pyrolysis Kinetics from Isothermal Thermogravimetric Experiments. *Thermochemistry, Acta*, 380: 67-78.
- Osabohien, E.; Egboh, S.H.O. and Okoh, B. E. (2006). The Cure Characteristics and Physico-Mechanical Properties of Natural Rubber Filled with Pineapple Leaf Fibre. *Bioscience and Biotechnology Resources, Asia*, 3 (1a): 111-116.
- Osabohien, E. and Egboh, S.H.O. (2007). Cure Characteristics and Physico Mechanical Properties of Natural Rubber Filled with the Seed Shells of Cherry (*Chrysophyllum albidum*). *Journal of Applied Science and Environmental Management*, 11(2): 43 – 48.
- Osman, H.; Ismail, H. and Mostapha, M. (2010). Effect of Maleic Anhydride Polypropylene on Tensile, Water Absorption and Morphological Properties of Recycled Newspaper Filled Polypropylene/Natural Rubber Composites. *Journal of Composite Materials*, 44(12): 1477 – 1491.
- Pandey, K. N.; Setua, D. K. and Mathur, G. N. (2003). Material Behaviour Fracture Topography of Rubber Surfaces; a SEM Study. *Polymer Testing*, 22: 353-359.
- Park, B. D.; Wi, S. G.; Lee, K. H.; Singh, A. P.; Yoon, T. H. and Kim, Y. S. (2003). Characterization of Anatomical Features and Silica Distribution in Rice Husk using Microscope and Micro-Analytical Techniques. *Bio-Mass Bio-Energy*, 25: 319 – 327.
- Park, J. M.; Kim, P. G.; Jang, J. H.; Wang, Z.; Hwang, B. S.; Devries, K. L. (2008). Interfacial Evaluation and Durability of Modified Jute Fibres/Polypropylene (pp) Composites using Micromechanical Test and Acoustic Emission. *Composites Part B*, 39: 1042 – 61.
- Patternman, M. Q. (1986). Chemo-Rheology of Model Filled Rubber Compound during Curing. *Rubber World*, 194:38-43.

- Pino, G. H.; Souza de Mesquita, L. M.; Torem, M. L. and Seavedra Pinto, G. A. (2006). Biosorption of Cadmium by Green Coconut Shell Powder. *Journal of Minerals Engineering*, 19: 380 – 387.
- Poh, B. T.; Ismail, H. and Tan, K. S. (2002). Modification and Micro-structural Development in Rubber, *Polymer Testing*, 21: 801-809.
- Poletto, M.; Dettenborn, J.; Pistor, V.; Zeni, M. and Zattera, A. J. (2010). Materials Produced from Plant Biomass, Part 1: Evaluation of Thermal Stability and Pyrolysis of Wood. *Material Resources*, 13: 375 – 379.
- Poletto, M.; Pistor, V.; Zeni, M. and Zattera, A. J. (2011). Crystalline Properties and Decomposition Kinetic of Cellulose Fibres in Wood Pulp Obtained by Two Pulping Process. *Polymer Degradation and Stability*, 96: 169-685.
- Popescu, M. C.; Popescu, C. M.; Lisa G. and Sakata, Y. (2011). Evaluation of Morphological and Chemical Aspects of Different Wood Species by Spectroscopy and Thermal Methods. *Journal of Molecular Structures*, 988: 65 74
- Pothan, L. A.; Thomas, S. and Groeninckx, G. (2006). The Role of Fibre/Matrix Interactions on the Dynamic Mechanical Properties of Chemically Modified Banana Fibre/Polyester Composites. *Composites Part A: Applied Science and Manufacturing*, 37: 1260 – 1269.
- Pradhan, K. S.; Dwarakadasa, S. E. and Reucroft, J. P. (2004). Processing and Characterization of Coconut Shell Powder Filled UHMWPE. *Materials Science and Engineering, Polymer Testing Journal*, 367 (1 – 2): 57 – 62.
- Prakash, T. (2009). Procedures and Characterization of Natural Fibre Reinforced Polymer Composites. *Bachelor's Thesis, National Institute of Technology, Rourkela*, PP 235-243.
- Premlal, H. G. B.; Ismail, H. and Baharin, A. (2002). A Comparison of the Mechanical Properties of Rice Husk Powder Filled Polypropylene Composites with Talc Filled Polypropylene Composites. *Polymer Testing*, 21(7): 833 – 839.
- Professional Association of Natural Rubber in Africa, Standard African Rubber (SAR) Manual*. (1998). 2, Specification and Test Methods, Malaysia, PP 678-694.

- Pulford, C.T.R. (1983). Antioxidant Effects during Blade Abrasion of Natural Rubber. *Journal of Applied Polymer Science*, 28: 709-713.
- Ramaraj, B. (2006). Mechanical and Thermal Properties of ABS and Leather Waste Composite, *Journal of Applied Polymer Science*, 101: 3062-3066.
- Rana, A. K.; Mandal, A. and Bandyopadhyay, S. (2003). Short Jute Fibre Reinforced Polypropylene Composites: Effects of Compatibilizer, Impact Modifier and Fibre Loading. *Composites Science and Technology*, 63: 801 – 806.
- Richard, M. (2004). The Story of Mathematics (Paperback Editor) *Princeton, NJ; Princeton University Press*, PP 158-163.
- Rivin, D. (1963). Polymer–Filler Interaction in Rubber Reinforcement. *Rubber Chemistry and Technology*, 36: 719-729.
- Roberts, A. D. (1988). Rubber Adhesion at High Rolling Speeds. *Journal of Natural Rubber Research*, 3: 239-247.
- Roger, B. (2002). Handbook of Polymer Testing; Short-Term Tests. *Rapra Technology Limited, UK*, PP 34-40.
- Rout, J.; Mishra, M.; Tripathy, S. S.; Nayak, S. K. and Mohanty, A. K. (2001). The Influence of Fibre on the Performance of Coir-Polyester Composites. *Composites Science and Technology*, 61: 1303 – 1310.
- Rowel, R. M.; Sanadi, A. R.; Caulfield, D. F. and Jacobson, R. E. (1997). Utilization of Natural Fibres In Composites: Problems and Opportunity in Lignocellulosic Plastic Composite Editors, 6 (3): 56-67.
- Rowel, R. (2005). Handbook of Wood Chemistry and Wood Composts. *CRC Press, Boca Raton, USA*, PP 30-37.
- Sae-Ovi, P.; Rakdee, C. and Thanmathorn, P. (2002). Use of Rice Husk Ash as Filler in Natural Rubber Vulcanisates; In Comparisons with Other Commercial Fillers. *Journal of Applied Polymer Science*, 83: 2485-2493.
- Sae-ovi, P.; Sirisinha, C.; Thepsuwan, U. and Hatthapanit, K. (2004). Comparison of Reinforcing Efficiency between Si-69 and Si-264 in a Conventional Vulcanization System. *Polymer Testing*, 23: 871 – 879.
- Sanjay, M.R. and Yogesha, B. (2016). Studies on Mechanical Properties of Jute/E-Glass Fibre Reinforced Epoxy Hybrid Composites. *Journal of Minerals and Materials Characterization and Engineering*, 4: 15-25.

- Sapuan, S. M.; Harimi, M. and Maleque, M. A. (2003). Mechanical Properties of Epoxy/Coconut Shell Filler Particle Composites. *The Arabian Journal for Science and Engineering*, 28(2b): 171 – 181.
- Sarki, J.; Hassan, S. B.; Aigbodiona, V. S. and Oghenevweta, J. E. (2011). Potential of Using Coconut Shell Particle Fillers in Eco-Composite Materials. *Journal of Alloys and Compounds*, 509 (5): 2381-2385.
- Satyanarayana, K. G.; Pillai, C. K. S. and Sukumaran, K. (1982). Structure Property Studies of Fibres from Various Parts of the Coconut Tree. *Journal of Materials Science*, 17: 2453 – 2462.
- Segal, L.; Creely, L.; Martin, A.E.; Comrade, C. M. (1999). An Empirical Method for Estimating the Degree of Crystallinity of Native Cellulose using X-ray Diffractometer. *Textile Resources Journal*, 29: 786-794.
- Shebani, A. N.; Van-Reenen, A. J. and Meincken, M. (2009). The Effect of Wood Extraction on the Thermal Stability of Different Wood–LLDPE Composites. *Thermochemistry. Acta*, 481: 52 – 56.
- Shen, D.K. and Gu, S. (2009). The Mechanism for Thermal Decomposition of Cellulose and Its Main Products. *Bioresources and Technology*, 100: 6496-6504.
- Sheng, E.; Sutherland, I.; Bradley, R. H. and Freakley, D. K. (1996). Effects of a Multifunctional Additive on Bound Rubber in Carbon Black and Silica Filled Natural Rubbers. *European Polymer Journal*, 32: 25 – 41.
- Shin-ya, Y.; Ken-ichi, T. and Minoru, S. (1981). Accumulation of Potassium Oxide on Carbon and Enhancement of Catalytic Activity for Isomerisation by O₂. *Journal of Chemical Society and Chemistry Community*, 7 (3): 1051 – 1062.
- Shuaibu, M.A. and Mamza, P.A.P. (2016). Characterization of Polypropylene Filled Composites Using Scanning Electron Microscopy and X-ray Diffraction. *International Journal of Innovative Research and Development*, 5 (3): 130 – 135.
- Singleton, A. C. N.; Baillie, C. A.; Beaumont, P. W. R. and Pejis, T. (2003). On the Mechanical Properties, Deformation and Fracture of a Natural Fibre/Recycled Polymer Composite. *Composites B₃₄*: 519 – 526.

- Ski, K. B. (1970). Engineering Materials, Properties and Selection. *Reston Publishing Company*, UK, 5: 32- 40.
- Sogbaike, O. E.; Okieimen, F. E. and Edojarioba, P. (2005). Effect of Substitution of (N330) Carbon Black with Carbonized Plantain Peels on the Cure Characteristics, Physico-Mechanical and Swelling Properties of Natural Rubber Vulcanisates. *Chemical Technical Journal*; PP 24-29.
- Sombatsompop, N. Thongsang, S. Markpin, T. and Wimolmala, E. (2004). Fly Ash Particles and Precipitated Silica as Fillers in Rubbers: Part 1: Untreated Fillers in NR and SBR Compounds. *Journal of Applied Polymer Science*, 93: 2119-2130.
- Stella, U.; Lawrence, O. E. and Ayo, M. D. (2011). Effect of Carbonization Temperature of Filler on the Tensile Properties of Natural Rubber Compounds Filled with Cassava (*Manihot esculenta*) Peel Carbon. *The Pacific Journal of Science and Technology*, 12(1): 339 – 343.
- Stokke, D.D.; Kuo, M.; Curry, D.G. and Gisesman, H.H. (2001). Grassland Flour/Polyethylene Composites. In: *Proceedings of 6th International Wood Fibre Plastic Composites Conference, Madison, WI, USA*, 43-53.
- Sullivan, A.C.O. (1997). Cellulose: The Structure Slowly Unravels. *Cellulose* 4(3): 73-207.
- Sumari, S.; Achmad, R. and Sumarno, S. (2013). Effects of Ultrasound on the Morphology, Particle Size, Crystallinity, and Crystallite Size of Cellulose. *Scientific Study and Research*, 14(4): 229 – 239.
- Sywatthana, P. and Cattaleeya, P. (2010) .Compatibility Improvement of Rice Husk and Bagasse Ashes with Natural Rubber by Molten State Maleation. *European Journal of Scientific Research*, 43(3): 411 – 416.
- Tabzan, N. Wirasate, S. and Suchiva, K. (2010). Abrasion Behaviour of Layered Silicate Reinforced Natural Rubber. *Wear*, 269: 394-404.
- Takashi, K.; Mitsuhiro, I. and Tomohiro, I. (2007). Epoxy Resin Composition for Fibre Reinforced Composite Materials. *Connolly Bove Lodge and LLP, Washington DC. USA*, PP 78-89.

- Thwe, M. M. and Liao, K. (2002). Effects of Environmental Aging on the Mechanical Properties of Bamboo-Glass Fibre Reinforced Polymer Matrix Hybrid Composites. *Composites A*₃₃, 6 (1): 43 – 52.
- US Army Research Laboratory Weapons and Materials Research Directorate. (2002). Polymer Matrix Composites Guidelines for Characterization of Structural Materials, PP 78-89.
- Vignesh, K.; Natarajan, U. and Pachiyappan, P. (2013). Effect of Coir Fibre Length on the Mechanical Properties of Coconut Shell Powder/Polyester Resin Composites. *Proceedings of the National Conference on Emerging Trends in Mechanical Engineering*, PP 143-151.
- Viksne, A.; Berzina, R.; Andersone, I. and Belkova, L. (2010). Study of Plastic Compounds Containing Polypropylene and Wood Derived Fillers from Waste of Different Origin. *Journal of Applied Polymer Science*, 117: 368–77.
- Vilay, V.; Mariatti, M.; Mat-Taib, R. and Todo, M. (2008). Effect of Fibre Surface Treatment and Fibre Loading on the Properties of Bagasse Fibre-Reinforced Unsaturated Polyester Composites. *Composites Science and Technology*, 68: 631-638.
- Vink, E. T. H.; Rabago, K. R.; Glassner, D. A. and Gruber, P. R. (2003). Application of Life Cycle Assessment to Nature Works Polylactide (PLA) Production. *Polymer Degradation and Stability*, 80: 403–419.
- Wada, M.; Okano, T. and Sugiyama, J. (2001). Allomorphs of Native Crystalline Cellulose Evaluated by Two Equatorial D-spacings. *Journal of Wood Science*, 47: 124-128.
- Wambua, P.; Ivens, U. and Verpoest, I. (2003). Natural Fibres: Can They Replace Glass in Fibre Reinforced Plastic? *Composites Science and Technology*. 64: 1259-1264.
- Wergin, W.P. and Erbe, E.F. (1994). Snow Crystals Capturing Snowflakes for Observation with the Low-Temperature Scanning Electron Microscope, *Scanning Materials Journal*, 16: IV, 88.
- Whishaw, I.Q.; Hines, D.J. and Wallace, D.G. (2001). Dead Reckoning (Path Integration) Requires the Hippo Campal Formation: Evidence from

- Spontaneous Exploration and Spatial Learning Tasks in Light (Allothetic) and Dark (Idiothetic) Tests. *Behavioural Brain Research*. 127 (1-2): 49-69.
- Wongsiriamnuay, T. and Tippayanwong, N. (2010). Non-Isothermal Pyrolysis Characteristics of Giant Sensitive Plants using Thermogravimetric Analysis. *Bioresources and Technology*, 101: 5638-5644.
- Wright, D.B. (2006). Comparing Groups in a Before-After Design: When T-Test and ANCOVA Produce Different Results. *British Journal of Educational Psychology*, 76: 663-675.
- Yalegin, N. and Selving, V. (2000). Studies of the surface Area and Porosity of Activated carbons Prepared from Rice Husk. *Carbon*, 38: 1943-1945.
- Yang, H.; Yan, R.; Chen, H.; Zheng, C.; Lee, D.H. and Liang, D.T. (2006). In-depth Investigation of Biomass Pyrolysis Based on Three Major Components; Hemicelluloses, Cellulose and Lignin. *Energy Fuels*, 20: 288-393.
- Yao, F.; Wu, Q.; Lei, Y.; Guo, W. and Xu, Y. (2008). Thermal Decomposition Kinetics of Natural Fibres; Activation Energy with Dynamic Thermogravimetric Analysis. *Polymer Degradation and Stability*, 93: 90-98.
- Yao, W.; Chen, B. and Wu, K. (2003). Smart Behaviour of Carbon Fibres Reinforced Cement-Based Composite. *Journal of Material Science and Technology* 19(3): 239-242.
- Yorkitis, E.M. (1984). In Rubber-Modified Thermoset Resins (*ed. Riew, K. and Gillhan, J.K.*). Advances in Chemistry Series No. 208. Washington. D.C.; *American Chemical Society*, PP 130-137.
- Yu, Y. and Wu, H. (2010). Significant Differences in the Hydrolysis Behaviour of Amorphous and Crystalline Portions within Microcrystalline Cellulose in Hot-Compressed Water. *Industrial and Engineering Chemistry Research*, 49 (8): 3902-3909.
- Zadoreeki, P. and Foldin, P. (1986). Surface Modification of Cellulose Fibres. In: Durability of Cellulose-Polyester Composites under Environmental Aging. *Journal Applied Polymer Science*, 31: 1966-1970
- Zhang, H.; Wang, Y.; Zhang, L. and Yang, J. (2004). Preparation and Processing of Novel Polymer Materials. *Journal of Applied Polymer Science*, 97(3): 844 – 849.

- Zhang, L.; Wang, Y.; Way, V.; Sin, Y. and Yu, D. (2000). Morphology and Mechanical Properties of Clay/Styrene Butadiene Rubber Nano-Composites. *Journal of Applied Polymer Science*, 78(11): 1873 – 1878.
- Zhao, M. and Xiang, Y. (2004). Natural Rubber Vulcanisates Reinforced by Modified Coal Shale-Based Fillers. *Journal of Applied Polymer Science*, 93(3): 1397-1400.
- Zickler, G. A.; Wagermaier, W.; Funari, S. S.; Burghammer, M. and Paris, O. (2007). In Sit X-ray Diffraction Investigation of Thermal Decomposition of Wood Cellulose. *Journal of Analytical and Applied Pyrolysis*, 80: 134 – 140.

APPENDICES

Appendix I

Data Points for Tensile, Compressive and Flexural Stress-Strain Relationship for Fibre and Shell

Tension Test on Polymer

	Load at Maximum Tensile stress (N)	Tensile strain at Maximum Tensile stress (mm/mm)	Tensile extension at Maximum Tensile stress (mm)	Energy at Maximum Tensile stress (J)	Tensile stress at Break (Standard) (MPa)
1	222.88461	2.52667	126.33336	17.38488	0.06244
2	125.25063	1.79467	89.73330	8.16808	0.21015
3	94.18571	1.27600	63.80005	4.32624	0.09201
4	100.39365	2.21200	110.59999	8.07772	0.07532
5	64.19197	1.47467	73.73337	3.38399	0.05439
Mean	121.38131	1.85680	92.84001	8.26818	0.09886
Standard Deviation	60.76305	0.51529	25.76459	5.53522	0.06381
	Load at Maximum Tensile stress (N)	Tensile strain at Maximum Tensile stress (mm/mm)	Tensile extension at Maximum Tensile stress (mm)	Energy at Maximum Tensile stress (J)	Tensile stress at Break (Standard) (MPa)
6	82.52212	1.08800	54.39999	3.25535	0.10780
7	86.93578	1.14400	57.20005	3.37573	0.08146
8	67.12368	1.82533	91.26661	4.49039	0.04763
9	120.97817	1.65867	82.93336	7.09608	0.08090
10	98.84624	0.97467	48.73337	3.03182	0.07974
Mean	91.28120	1.33813	66.90668	4.24987	0.07951

	Load at Maximum Tensile stress (N)	Tensile strain at Maximum Tensile stress (mm/mm)	Tensile extension at Maximum Tensile stress (mm)	Energy at Maximum Tensile stress (J)	Tensile stress at Break (Standard) (MPa)
Standard Deviation	20.11424	0.37831	18.91538	1.68787	0.02134
	Load at Maximum Tensile stress (N)	Tensile strain at Maximum Tensile stress (mm/mm)	Tensile extension at Maximum Tensile stress (mm)	Energy at Maximum Tensile stress (J)	Tensile stress at Break (Standard) (MPa)
11	74.07360	0.74133	37.06662	1.89820	0.09797
12	37.82719	1.12533	56.26668	1.13812	0.00753
Mean	55.95039	0.93333	46.66665	1.51816	0.05275
Standard Deviation	25.63008	0.27153	13.57649	0.53746	0.06396

Compression Test on Polymer

	Compressive extension at Maximum Compressive stress (mm)	Compressive stress at Break (Standard) (MPa)	Compressive load at Break (Standard) (N)	Compressive strain at Break (Standard) (mm/mm)
1	7.18075	26.30733	41839.99300	0.83014
2	7.84500	33.01349	52505.68986	0.90694
3	7.73188	33.01164	52502.75135	0.89386
4	7.16825	33.01376	52506.11901	0.82870
5	5.78763	25.06248	39860.14724	0.66909
Mean	7.14270	30.08174	47842.94009	0.82575

	Compressive extension at Maximum Compressive stress (mm)	Compressive stress at Break (Standard) (MPa)	Compressive load at Break (Standard) (N)	Compressive strain at Break (Standard) (mm/mm)
Standard Deviation	0.81833	4.03780	6421.85078	0.09461
	Compressive extension at Maximum Compressive stress (mm)	Compressive stress at Break (Standard) (MPa)	Compressive load at Break (Standard) (N)	Compressive strain at Break (Standard) (mm/mm)
6	6.33837	33.01167	52502.79903	0.73276
7	7.09244	33.01031	52500.63539	0.81993
8	6.41187	33.01010	52500.30160	0.74126
9	6.21725	33.01019	52500.44465	0.71876
10	6.06075	33.01112	52501.91092	0.70066
Mean	6.42414	33.01068	52501.21832	0.74267
Standard Deviation	0.39654	0.00069	1.09054	0.04584
	Compressive extension at Maximum Compressive stress (mm)	Compressive stress at Break (Standard) (MPa)	Compressive load at Break (Standard) (N)	Compressive strain at Break (Standard) (mm/mm)
11	5.32331	32.02997	50941.46729	0.61541
12	6.89681	33.00993	52500.02742	0.79732
Mean	6.11006	32.51995	51720.74735	0.70637

	Compressive extension at Maximum Compressive stress (mm)	Compressive stress at Break (Standard) (MPa)	Compressive load at Break (Standard) (N)	Compressive strain at Break (Standard) (mm/mm)
Standard Deviation	1.11263	0.69294	1102.06844	0.12863

Flexural Test on Polymer

	Energy at Break (Standard) (J)	Flexure stress at Yield (Zero Slope) (MPa)	Flexure load at Yield (Zero Slope) (N)	Energy at Yield (Zero Slope) (J)
1	0.02644	0.31253	0.82059	0.00109
2	0.04423	0.83234	2.18542	0.01260
3	0.01820	0.20073	0.52705	0.00034
4	0.00960	0.23998	0.63011	0.00006
5	0.00475	0.22135	0.58118	-0.00005
Mean	0.02064	0.36139	0.94887	0.00281
Standard Deviation	0.01558	0.26662	0.70004	0.00549
	Energy at Break (Standard) (J)	Flexure stress at Yield (Zero Slope) (MPa)	Flexure load at Yield (Zero Slope) (N)	Energy at Yield (Zero Slope) (J)
6	0.01848	0.08659	0.22736	-0.00018
7	0.01377	0.26768	0.70283	0.00058
8	-0.00107	0.15101	0.39650	-0.00138
9	0.02586	0.55645	1.46105	0.00979
10	0.01768	0.42697	1.12107	0.00412

	Energy at Break (Standard) (J)	Flexure stress at Yield (Zero Slope) (MPa)	Flexure load at Yield (Zero Slope) (N)	Energy at Yield (Zero Slope) (J)
Mean	0.01494	0.29774	0.78176	0.00259
Standard Deviation	0.00996	0.19407	0.50955	0.00452
	Energy at Break (Standard) (J)	Flexure stress at Yield (Zero Slope) (MPa)	Flexure load at Yield (Zero Slope) (N)	Energy at Yield (Zero Slope) (J)
11	0.02051	0.26455	0.69461	0.00086
12	-0.00066	0.16902	0.44379	-0.00011
Mean	0.00993	0.21678	0.56920	0.00037
Standard Deviation	0.01497	0.06755	0.17736	0.00069

Appendix II

Data for FTIR Values of Raw Coconut Shell

	Peak	Intensity	Corr. Intensity	Base (H)	Base (L)	Area	Corr. Area
1	453.29	50.611	0.091	457.14	451.36	1.709	0.002
2	559.38	47.618	0.709	570.95	543.94	8.609	0.08
3	603.74	46.014	1.263	651.06	586.38	20.178	0.406
4	663.53	51.342	1.104	690.54	653.89	10.253	0.19
5	696.33	54.676	0.524	758.05	692.47	15.655	0.045
6	771.55	58.599	3.477	786.98	759.98	5.815	0.244
7	852.56	59.68	1.493	862.21	786.91	15.447	0.352
8	896.93	56.408	2.546	908.5	864.14	10.206	0.254
9	1045.45	33.077	11.33	1097.53	910.43	71.189	11.345
10	1112.96	38.606	1.956	1147.68	1099.46	19.147	0.763
11	1165.04	42.833	5.141	1193.98	1149.61	14.635	0.919
12	1247.99	42.143	10.587	1303.92	1195.91	36.497	6.421
13	1329	49.219	1.979	1350.22	1305.85	13.388	0.478
14	1377.22	48.396	4.663	1406.15	1352.14	15.818	0.968
15	1427.37	50.641	3.146	1438.94	1408.08	8.694	0.437
16	1464.02	50.192	2.858	1489.1	1458.23	8.227	0.315
17	1514.17	52.682	3.41	1541.18	1508.38	7.463	0.285
18	1608.69	51.392	2.244	1618.33	1599.04	5.417	0.197
19	1658.84	56.908	0.974	1685.84	1654.98	7.055	0.102
20	1732.13	53.726	0.523	1734.06	1697.41	8.78	0.047
21	2058.11	82.309	0.026	2090.04	2040.76	1.627	0.003
22	2119.84	82.24	0.075	2281.67	2115.96	12.873	0.049
23	2359.02	83.155	1.152	2384.1	2347.45	2.826	0.117
24	2901.04	60.553	3.094	2926.11	2850.88	15.616	1.15
25	2941.54	61.169	2.196	3020.63	2926.11	17.691	0.143
26	3425.69	42.204	0.107	3448.64	3421.83	10.062	0.032

Appendix III

Data for FTIR Values of Carbonized Coconut Shell at 300°C

	Peak	Intensity	Corr. Intensity	Base (H)	Base (L)	Area	Corr. Area
1	466.72	80.24	0.157	472.58	466.79	0.551	0.003
2	542.02	79.13	0.191	547.8	536.23	1.171	0.007
3	619.17	79.097	1.217	642.32	609.53	3.145	0.062
4	759.98	80.415	2.379	856.42	721.4	11.51	0.746
5	877.64	83.872	0.039	879.57	856.42	1.741	0
6	1111.03	68.222	2.383	1136.11	887.28	29.5	0.869
7	1192.05	66.988	0.662	1207.48	1138.04	11.634	0.091
8	1244.13	66.771	0.028	1246.06	1209.41	6.374	0.006
9	1315.5	69.011	0.221	1325.14	1307.78	2.781	0.009
10	1371.43	67.391	2.113	1411.94	1338.64	12.074	0.506
11	1427.37	69.97	0.2	1458.23	1425.44	4.909	0.077
12	1593.25	58.991	12.761	1654.98	1508.38	28.288	7.301
13	1703.2	73.924	0.721	1793.86	1701.27	5.813	-0.358
14	2227.86	85.81	0.344	2239.43	1869.08	17.984	2.744
15	2335.87	85.289	0.08	2341.66	2330.09	0.797	0.002
16	2835.45	78.046	1.509	2852.81	2364.81	44.953	3.671
17	2897.18	77.411	0.133	2924.18	2895.25	3.111	0.045
18	3093.92	72.746	0.087	3095.85	2958.9	17.581	0.255
19	3227.02	69.994	0.041	3228.95	3097.78	19.242	0.045
20	3383.26	67.046	0.163	3390.97	3365.9	4.336	0.017

Appendix IV

Data for FTIR Values of Carbonized Coconut Shell at 400°C

	Peak	Intensity	Corr. Intensity	Base (H)	Base (L)	Area	Corr. Area
1	513.08	84.579	0.514	516.94	505.37	0.822	0.015
2	619.17	82.715	0.523	636.53	613.38	1.837	0.014
3	669.32	81.345	1.739	673.18	663.53	0.606	0.031
4	756.12	77.585	0.15	790.84	754.19	3.769	-0.013
5	813.99	79.707	0.616	850.64	806.27	4.15	0.101
6	877.64	80.039	1.894	918.15	850.64	6.182	0.321
7	1192.05	54.073	0.211	1193.98	920.08	51.252	2.667
8	1234.48	53.879	0.14	1319.35	1232.55	21.526	0.187
9	1367.58	58.74	0.29	1375.29	1363.72	2.962	0.017
10	1427.37	62.019	0.354	1437.02	1423.51	2.767	0.021
11	1585.54	48.191	3.678	1654.98	1575.89	20.427	2.369
12	1693.56	71.194	1.15	1697.41	1683.91	1.922	0.055
13	2218.21	82.356	0.08	2220.14	1942.38	16.723	1.241
14	2359.02	72.067	4.292	2387.95	2349.38	4.893	0.515
15	2486.33	76.022	0.115	2490.18	2389.88	11.285	0.016
16	2899.11	70.483	0.068	2901.04	2897.18	0.585	0.001
17	3090.07	66.457	0.155	3099.71	3090.42	3.413	0.009
18	3387.11	62.22	0.071	3389.04	3385.16	0.794	0.001

Appendix V

Data for FTIR Values of Carbonized Coconut Shell at 500°C

	Peak	Intensity	Corr. Intensity	Base (H)	Base (L)	Area	Corr. Area
1	418.57	88.234	1.683	422.42	412.76	0.472	0.033
2	619.17	84.504	0.593	628.81	609.53	1.379	0.027
3	667.39	84.901	0.465	673.18	661.61	0.606	0.011
4	754.19	82.957	1.713	785.05	700.18	6.361	0.291
5	812.06	83.939	0.37	852.56	804.34	3.507	0.059
6	875.71	84.347	1.393	922	852.56	4.847	0.236
7	1192.05	72.534	0.102	1193.98	922	29.519	1.699
8	1242.2	72.381	0.132	1305.85	1238.34	9.141	0.089
9	1373.36	72.774	0.486	1384.94	1365.65	2.623	0.024
10	1423.51	75.351	0.134	1427.37	1421.58	0.707	0.001
11	1575.89	67.412	0.422	1579.75	1572.04	1.31	0.009
12	1699.34	83.557	2.272	1735.99	1691.63	2.62	0.269
13	2278.01	85.304	0.039	2279.94	2177.71	6.71	0.023
14	2359.02	82.15	1.331	2387.95	2347.45	3.29	0.146
15	2837.38	79.998	0.96	2852.81	2783.37	6.623	0.194
16	2897.18	79.827	0.237	2926.11	2893.32	3.096	0.046
17	3043.77	77.774	0.074	3045.7	2958.9	9.038	0.078
18	3338.89	73.891	0.07	3340.82	3281.02	7.552	-0.032
19	3410.26	72.003	0.043	3416.05	3406.4	1.374	0.001

Appendix VI

Data for FTIR Values of Carbonized Coconut Shell at 600°C

	Peak	Intensity	Corr. Intensity	Base (H)	Base (L)	Area	Corr. Area
1	418.57	89.053	1.043	422.42	414.71	0.361	0.012
2	576.74	87.566	0.261	584.45	572.88	0.658	0.006
3	617.24	87.378	0.365	621.1	609.53	0.665	0.007
4	669.32	85.463	1.72	673.18	665.46	0.491	0.031
5	752.26	86.379	0.816	779.27	723.33	3.451	0.123
6	815.92	86.797	0.158	850.64	810.13	2.426	0.022
7	875.71	86.451	1.167	918.15	850.64	4.048	0.173
8	1060.88	83.474	0.058	1062.81	925.86	9.516	0.241
9	1166.97	82.034	0.07	1170.83	1096.67	8.609	0.061
10	1217.12	81.564	0.159	1222.91	1170.83	4.536	0.01
11	1361.79	81.854	0.25	1369.5	1357.93	0.996	0.005
12	1417.73	83.169	0.274	1419.66	1413.87	0.46	0.005
13	1568.18	80.915	0.258	1570.11	1560.46	0.88	0.011
14	1680.05	89.641	0.381	1683.91	1676.2	0.353	0.008
15	1766.85	92.494	0.392	1772.64	1763	0.317	0.01
16	1982.53	89.96	0.078	1994.46	1977.1	0.789	0.002
17	2360.95	80.005	4.312	2391.81	2349.38	3.405	0.43
18	2837.38	85.196	0.565	2854.74	2827.74	1.816	0.043
19	2883.68	85.408	1.787	2924.18	2854.74	4.552	0.452
20	3039.91	84.27	0.044	3047.63	3036.06	0.859	0.001
21	3412.19	82.368	0.085	3417.98	3404.47	1.135	0.003
22	3730.45	89.333	0.091	3732.38	3728.53	0.188	0.001

Appendix VII

Data for FTIR Values of Carbonized Coconut Shell at 700°C

	Peak	Intensity	Corr. Intensity	Base (H)	Base (L)	Area	Corr. Area
1	464.86	84.055	0.482	466.79	459.07	0.566	0.014
2	528.51	83.551	0.594	536.23	524.66	0.888	0.017
3	619.17	83.679	1.698	644.25	611.45	2.27	0.088
4	694.4	86.466	0.117	698.25	688.61	0.606	0.003
5	758.05	83.812	1.782	777.34	717.54	4.225	0.263
6	873.78	85.432	1.747	887.26	854.49	2.031	0.107
7	1109.11	64.626	3.788	1138.04	906.57	31.127	3.041
8	1190.12	63.758	0.762	1207.48	1139.97	12.775	0.14
9	1234.48	63.742	0.012	1236.41	1232.55	0.754	0
10	1375.29	61.23	3.795	1415.8	1303.92	22.157	1.314
11	1419.66	64.593	0.265	1456.3	1417.73	7.138	0.024
12	1458.23	65.74	0.353	1471.74	1456.3	2.766	0.015
13	1560.46	54.107	0.489	1562.39	1506.46	12.204	0.015
14	1577.82	53.358	1.157	1683.91	1573.97	20.428	0.576
15	1697.41	80.587	3.274	1784.21	1687.77	3.029	0.04
16	2216.28	83.842	0.117	2218.21	1786.14	16.387	5.957
17	2339.73	82.693	0.109	2343.59	2326.23	1.425	0.006
18	2530.69	79.114	0.055	2532.62	2418.62	11.028	0.041
19	2835.45	75.108	0.849	2852.81	2806.52	5.674	0.131
20	2887.53	74.426	0.198	2891.39	2852.81	4.827	0.069
21	3059.2	70.4	0.086	3061.13	2956.97	14.894	0.124
22	3194.23	68.29	0.035	3196.15	3186.51	1.594	0.001
23	3377.47	66.764	0.063	3383.28	3373.61	1.69	0.002

Appendix VIII

Data for FTIR Values of Raw Coconut Fibre

	Peak	intensity	Corr. intensity	Base (H)	Base (L)	Area	Corr. Area
1	462.93	38.523	0.543	466.79	439.78	10.871	0.1
2	520.8	39.106	0.39	526.58	497.85	11.674	0.058
3	607.6	41.945	0.15	655.82	603.74	19.171	0.014
4	689.32	43.466	0.743	686.68	655.82	11.02	0.089
5	692.47	44.659	0.32	740.69	688.61	17.212	0.021
6	779.27	45.843	4.084	846.78	742.62	32.574	1.758
7	886.86	51.325	0.188	902.72	846.71	15.151	0.024
8	1035.81	24.133	1.792	1043.52	904.64	58.275	0.53
9	1058.96	23.726	1.271	1089.82	1045.45	26.955	0.497
10	1103.32	26.083	1.869	1147.68	1091.75	29.97	0.746
11	1151.64	34.057	0.409	1188.19	1149.61	16.528	0.234
12	1265.35	37.293	4.428	1305.85	1190.12	47.36	3.489
13	1317.43	41.172	0.759	1346.36	1307.78	14.615	0.169
14	1371.43	41.418	2.312	1408.08	1348.29	21.959	0.694
15	1444.73	41.309	6.815	1487.17	1410.01	27.086	2.674
16	1516.1	45.156	7.739	1556.61	1489.1	20.553	1.985
17	1612.54	35.536	19.066	1714.77	1564.32	51.839	13.058
18	1724.42	56.859	0.112	1732.13	1722.49	2.358	0.006
19	1871.01	70.056	0.291	1888.37	1867.16	3.26	0.019
20	2054.26	70.241	0.019	2063.9	2052.33	1.774	0.001
21	2362.88	69.095	1.173	2387.95	2349.38	6.041	0.145
22	2916.47	52.989	0.531	2924.18	2387.96	103.328	-10.619
23	2941.54	52.482	1.27	2991.69	2926.11	17.658	0.254
24	3387.11	26.137	0.298	3390.97	2993.62	161.901	3.849

Appendix IX

Data for FTIR Values of Carbonized Coconut Fibre at 300°C

	Peak	intensity	Corr. intensity	Base (H)	Base (L)	Area	Corr. Area
1	418.57	87.4	1.835	420.5	412.78	0.404	0.03
2	476.43	86.072	0.492	480.29	472.58	0.492	0.009
3	549.73	85.829	0.116	553.59	547.8	0.382	0.002
4	617.24	86.568	0.492	636.53	613.36	1.369	0.012
5	667.39	87.66	0.715	680.89	663.53	0.938	0.019
6	781.2	87.533	0.74	798.56	767.69	1.71	0.041
7	875.71	89.534	0.65	895	852.56	1.957	0.054
8	1037.74	74.778	0.486	1041.6	918.15	10.044	0.089
9	1114.89	70.195	1.661	1136.11	1041.6	13.347	0.381
10	1219.05	86.748	0.102	1220.98	1138.04	13.478	0.032
11	1269.2	85.914	2.044	1305.85	1138.04	28.554	1.566
12	1315.5	66.666	0.638	1340.57	1305.85	5.99	0.056
13	1373.36	65.61	0.288	1375.29	1340.57	6.114	0.029
14	1435.09	66.399	0.277	1438.94	1431.23	1.363	0.005
15	1519.96	68.389	0.475	1521.89	1518.03	0.631	0.006
16	1604.83	53.565	12.972	1654.98	1541.18	26.687	6.589
17	1693.56	70.155	0.635	1697.41	1685.84	1.78	0.028
18	2360.95	82.57	1.764	2387.95	2347.45	3.159	0.179
19	2613.63	80.733	0.033	2615.56	2389.88	18.743	0.108
20	2841.24	76.307	0.889	2852.81	2661.85	20.099	0.083
21	2808.75	74.577	1.174	2924.18	2852.81	8.796	0.372
22	3265.59	65.465	0.062	3267.52	2989.76	44.495	0.53
23	3404.47	61.691	0.362	3468.13	3398.69	14.177	0.278
24	3632.06	82.628	0.614	3643.65	3630.15	1.062	0.027

Appendix X

Data for FTIR Values of Carbonized Coconut Fibre at 400°C

	Peak	Intensity	Corr. Intensity	Base (H)	Base (L)	Area	Corr. Area
1	418.57	89.754	1.332	420.5	414.71	0.238	0.011
2	472.58	88.462	0.819	478.36	462.93	0.781	0.023
3	542.02	88.159	0.011	543.94	540.09	0.211	0
4	669.32	88.52	0.989	673.16	663.53	0.481	0.017
5	754.19	89.37	0.688	771.55	723.33	2.232	0.073
6	781.2	89.289	0.363	790.84	771.55	0.929	0.014
7	812.06	89.461	0.226	850.64	806.27	2.021	0.031
8	877.64	90.49	0.474	908.5	850.64	2.438	0.06
9	1120.68	78.435	0.267	1124.54	920.08	15.296	0.592
10	1261.49	73.607	0.085	1263.42	1126.47	16.637	0.365
11	1317.43	73.651	0.556	1332.86	1301.99	4.038	0.04
12	1375.29	71.834	0.766	1384.94	1365.65	2.725	0.042
13	1437.02	72.407	0.437	1444.73	1433.16	1.597	0.009
14	1602.9	62.464	0.265	1614.47	1599.04	3.132	0.024
15	2362.88	81.241	2.438	2389.88	2349.38	3.339	0.255
16	2528.76	82.503	0.061	2532.62	2389.88	11.119	-0.005
17	2839.31	78.144	1.098	2852.81	2659.93	19.051	0.416
18	2902.96	77.316	1.48	2924.18	2854.74	7.597	0.441
19	3066.92	73.985	0.129	3070.78	2991.69	9.837	0.033
20	3221.23	70.735	0.062	3223.16	3070.78	21.422	0.045
21	3396.76	68.185	0.155	3412.19	3389.04	3.837	0.014
22	3567.72	78.815	0.788	3593.5	3565.79	0.774	0.014

Appendix XI

Data for FTIR Values of Carbonized Coconut Fibre at 500°C

	Peak	Intensity	Corr. Intensity	Base (H)	Base (L)	Area	Corr. Area
1	472.58	89.686	0.511	476.43	466.79	0.442	0.01
2	569.02	89.475	0.149	574.81	563.23	0.554	0.004
3	669.32	89.603	0.612	673.16	663.53	0.443	0.012
4	750.33	90.345	0.477	775.41	729.12	1.992	0.054
5	812.06	90.7	0.068	852.56	810.13	1.705	0.009
6	873.78	91.566	0.148	922	868	1.984	0.024
7	1033.88	89.158	0.059	1035.81	927.79	4.553	-0.013
8	1261.49	85.267	0.053	1263.42	1043.52	13.181	0.092
9	1375.29	84.054	0.378	1384.94	1365.65	1.434	0.017
10	1437.02	84.578	0.249	1444.73	1433.16	0.828	0.004
11	1595.18	79.459	0.129	1599.04	1579.75	1.912	0.007
12	1869.08	91.705	0.383	1872.94	1851.72	0.753	0.007
13	2360.95	85.162	1.956	2389.88	2349.38	2.564	0.195
14	2835.45	85.937	0.471	2852.81	2827.74	1.6	0.044
15	2881.75	85.952	1.819	2924.18	2852.81	4.478	0.464
16	3057.27	84.088	0.045	3059.2	2956.97	7.279	0.109
17	3221.23	82.364	0.064	3225.09	3111.28	9.184	0.021
18	3421.83	79.725	0.069	3429.65	3417.98	1.135	0.002
19	3630.15	86.256	1.392	3645.58	3626.29	1.108	0.048

Appendix XII

Data for FTIR Values of Carbonized Coconut Fibre at 600°C

	Peak	Intensity	Corr. Intensity	Base (H)	Base (L)	Area	Corr. Area
1	464.86	81.134	0.767	474.5	455.22	1.718	0.045
2	553.59	87.301	2.451	570.95	536.23	1.781	0.15
3	582.52	87.928	2.15	596.02	570.95	1.247	0.112
4	619.17	84.177	5.171	630.74	605.67	1.464	0.244
5	673.18	88.693	1.863	688.61	655.82	1.542	0.131
6	709.83	89.759	1.689	725.26	702.11	0.932	0.057
7	771.55	90.695	0.089	773.48	736.83	1.445	0.037
8	869.92	78.286	11.157	887.28	823.63	3.778	0.974
9	1047.38	51.272	19.641	1101.39	889.21	34.741	9.44
10	1120.68	61.876	5.71	1238.34	1103.32	17.901	1.505
11	1415.8	34.088	19.662	1448.59	1240.27	46.448	10.444
12	1469.81	35.626	15.397	1543.1	1450.52	30.088	5.885
13	1560.46	61.007	3.87	1693.56	1545.03	23.893	1.794
14	1761.07	90.969	0.135	1790	1759.14	1.194	0.009
15	2000.25	90	0.042	2002.18	1925.02	3.276	-0.014
16	2316.58	84.633	0.327	2326.23	2094.76	13.645	-0.221
17	2843.17	67.681	0.679	2850.88	2476.68	38.807	0.083
18	2908.75	63.74	1.567	2922.25	2852.81	13.012	0.639
19	3167.22	56.112	0.084	3169.15	2924.18	56.204	2.334
20	3392.9	59.981	0.051	3414.12	3390.97	5.118	0.006

Appendix XIII

Data for FTIR Values of Carbonized Coconut Fibre at 700°C

	Peak	Intensity	Corr. Intensity	Base (H)	Base (L)	Area	Corr. Area
1	464.86	80.735	0.061	466.79	461	0.536	0
2	555.52	85.21	0.684	559.38	536.23	1.511	0.023
3	580.59	85.325	0.499	601.81	576.74	1.599	0.008
4	619.17	82.402	4.29	632.67	601.81	2.123	0.218
5	673.18	85.799	1.238	690.54	655.82	2.192	0.099
6	709.83	86.077	1.318	725.26	700.18	1.511	0.054
7	763.84	86.969	0.17	767.89	734.9	1.984	0.028
8	869.92	80.296	6.749	887.28	840.99	3.322	0.568
9	1047.38	58.712	14.165	1099.46	887.28	30.853	7.046
10	1120.68	65.41	4.935	1236.41	1101.39	17.45	1.085
11	1386.86	47.997	0.55	1388.79	1240.27	20.844	0.056
12	1415.8	44.538	7.096	1448.59	1388.79	19.118	2.007
13	1471.74	44.679	11.264	1500.67	1450.52	15.191	2.549
14	1558.54	62.849	1.345	1560.46	1545.03	2.971	0.059
15	1770.71	91.175	0.501	1774.57	1768.78	0.221	0.006
16	2212.43	87.252	0.037	2214.35	2171.92	2.446	0.017
17	2353.23	83.595	0.799	2399.53	2347.45	3.631	0.054
18	2845.1	70.455	0.593	2852.81	2522.98	34.086	-3.128
19	2908.75	67.342	1.417	2924.18	2852.81	11.811	0.517
20	3182.65	61.767	0.066	3331.18	3180.72	29.536	0.016
21	3383.26	65.838	0.134	3389.04	3377.47	2.095	0.005

Appendix XIV

Generated XRD Data for Raw Coconut Shell

Data : PURE-CFP							
# Strongest 3 peaks							
no.	peak no.	2Theta (deg)	d (Å)	I/I1	FWHM (deg)	Intensity (Counts)	Integrated Int (Counts)
1	37	24.0774	3.69320	100	0.20150	82	929
2	40	24.9834	3.56129	85	0.23970	70	922
3	42	25.4600	3.49569	37	0.17140	30	373
# Peak Data List							
peak no.	2Theta (deg)	d (Å)	I/I1	FWHM (deg)	Intensity (Counts)	Integrated Int (Counts)	
1	2.2500	39.23358	2	0.18000	2	33	
2	4.5800	19.27803	2	0.04000	2	8	
3	5.1900	17.01350	2	0.18000	2	22	
4	6.2400	14.15281	17	0.20000	14	153	
5	6.4200	13.75640	5	0.08000	4	24	
6	7.8333	11.27732	12	0.26670	10	138	
7	9.5550	9.24880	4	0.03000	3	11	
8	9.8800	8.94528	2	0.04000	2	10	
9	10.4650	8.44651	2	0.09000	2	12	
10	10.8000	8.18525	2	0.12000	2	18	
11	11.1000	7.96469	11	0.28000	9	125	
12	11.3000	7.82417	5	0.00000	4	0	
13	12.4500	7.10392	2	0.10000	2	13	
14	13.0500	6.77862	2	0.22000	2	46	
15	13.7900	6.41648	2	0.06000	2	10	
16	14.2900	6.19308	2	0.10000	2	17	
17	14.8500	5.96077	4	0.06000	3	17	
18	15.1300	5.85108	4	0.06000	3	24	
19	15.5000	5.71223	9	0.16000	7	75	
20	15.8700	5.57988	5	0.10000	4	36	
21	16.7700	5.28239	2	0.10000	2	15	
22	17.4000	5.09253	2	0.04000	2	7	
23	18.3300	4.83619	17	0.26000	14	191	
24	18.5200	4.78700	4	0.00000	3	0	
25	19.4666	4.55631	9	0.13330	7	67	
26	19.7400	4.49382	4	0.04000	3	10	
27	19.9200	4.45362	5	0.08000	4	31	
28	20.3450	4.36153	2	0.09000	2	14	
29	20.7000	4.28753	2	0.12000	2	16	
30	20.9900	4.22894	11	0.22000	9	111	
31	21.3500	4.15844	6	0.10000	5	35	
32	21.7950	4.07453	7	0.15000	6	47	
33	22.0600	4.02618	2	0.04000	2	8	
34	22.4600	3.95537	2	0.04000	2	12	
35	23.0700	3.85215	9	0.18000	7	87	
36	23.4100	3.79696	2	0.06000	2	7	
37	24.0774	3.69320	100	0.20150	82	929	
38	24.3600	3.65099	11	0.00000	9	0	
39	24.5200	3.62753	6	0.10000	5	74	
40	24.9834	3.56129	85	0.23970	70	922	
41	25.2600	3.52291	33	0.00000	27	0	
42	25.4600	3.49569	37	0.17140	30	373	
43	25.8250	3.44711	17	0.11000	14	90	
44	26.8900	3.31295	9	0.18000	7	86	
45	27.2200	3.27353	6	0.12000	5	48	
46	27.7000	3.21788	4	0.08000	3	23	
47	27.8800	3.19752	6	0.08000	5	26	
48	28.2650	3.15483	12	0.23000	10	113	
49	28.6350	3.11490	2	0.03000	2	3	
50	28.8650	3.09060	5	0.17000	4	43	

Appendix XV

Generated XRD Data for Carbonised Coconut Shell at 300°C

Data : CCFP							
# Strongest 3 peaks							
no.	peak no.	2Theta (deg)	d (Å)	I/I1	FWHM (deg)	Intensity (Counts)	Integrated Int (Counts)
1	46	23.9965	3.70547	100	0.21170	100	1213
2	48	24.9211	3.57005	96	0.11220	96	703
3	9	6.1890	14.26932	70	0.19530	70	681
# Peak Data List							
peak no.	2Theta (deg)	d (Å)	I/I1	FWHM (deg)	Intensity (Counts)	Integrated Int (Counts)	
1	2.3816	37.06594	4	0.14330	4	35	
2	2.6550	33.24963	4	0.13000	4	33	
3	2.8833	30.61742	5	0.07330	5	25	
4	3.1350	28.15977	4	0.09000	4	23	
5	3.5000	25.22389	6	0.08000	6	37	
6	3.9200	22.52222	4	0.06660	4	16	
7	4.7800	18.47186	3	0.04000	3	12	
8	5.9800	14.76755	19	0.12000	19	151	
9	6.1890	14.26932	70	0.19530	70	681	
10	6.6850	13.21166	3	0.03000	3	16	
11	7.0400	12.54623	3	0.04000	3	15	
12	7.2616	12.16385	5	0.05670	5	22	
13	7.5675	11.67282	6	0.04500	6	27	
14	7.7750	11.36175	4	0.05000	4	18	
15	7.9300	11.14002	4	0.10000	4	37	
16	8.3150	10.62506	3	0.05000	3	20	
17	8.8200	10.01781	3	0.04000	3	15	
18	9.2750	9.52737	3	0.03000	3	12	
19	9.6100	9.19599	5	0.10000	5	37	
20	9.9150	8.91378	5	0.13000	5	45	
21	10.1300	8.72507	3	0.08000	3	21	
22	10.5150	8.40645	4	0.15000	4	47	
23	10.9000	8.11038	5	0.14000	5	37	
24	11.0700	7.98621	8	0.18000	8	78	
25	11.3520	7.78844	9	0.09600	9	60	
26	12.6600	6.98655	3	0.04000	3	13	
27	13.7600	6.43040	3	0.04000	3	22	
28	15.0200	5.89368	5	0.04000	5	31	
29	15.2033	5.82304	5	0.04670	5	24	
30	16.3000	5.43363	3	0.02000	3	4	
31	16.7816	5.27877	6	0.06330	6	34	
32	17.2000	5.15129	3	0.02000	3	16	
33	18.3006	4.84390	16	0.14530	16	116	
34	18.4428	4.80687	18	0.11430	18	119	
35	19.0050	4.66592	3	0.03000	3	10	
36	19.3533	4.58273	42	0.10670	42	275	
37	19.6800	4.50738	3	0.04000	3	9	
38	19.9050	4.45694	4	0.05000	4	12	
39	20.2800	4.37536	3	0.04000	3	13	
40	20.4200	4.34568	4	0.12000	4	34	
41	20.7150	4.28445	3	0.05000	3	12	
42	20.9600	4.23492	8	0.12000	8	76	
43	21.3100	4.16615	5	0.10000	5	34	
44	21.5500	4.12029	5	0.06000	5	39	
45	22.9723	3.86831	17	0.08740	17	130	
46	23.9965	3.70547	100	0.21170	100	1213	
47	24.4640	3.63571	18	0.07200	18	99	
48	24.9211	3.57005	96	0.11220	96	703	
49	25.1800	3.53393	52	0.10580	52	301	
50	25.3629	3.50885	65	0.18760	65	631	

Appendix XVI

Generated XRD Data for Carbonised Coconut Shell at 400°C

Data : CCFP-400							
# Strongest 3 peaks							
no.	peak no.	2Theta (deg)	d (Å)	I/I1	FWHM (deg)	Intensity (Counts)	Integrated Int (Counts)
1	60	24.0241	3.70128	100	0.22170	32	394
2	42	18.2633	4.85371	31	0.19330	10	108
3	43	18.4666	4.80073	22	0.06670	7	30
# Peak Data List							
peak no.	2Theta (deg)	d (Å)	I/I1	FWHM (deg)	Intensity (Counts)	Integrated Int (Counts)	Int
1	2.3300	37.88668	6	0.06000	2	8	
2	2.7500	32.10122	6	0.18000	2	21	
3	3.1900	27.67438	6	0.18000	2	23	
4	3.6800	23.99050	6	0.04000	2	8	
5	3.9800	22.18282	9	0.04000	3	14	
6	4.1900	21.07149	16	0.06000	5	25	
7	4.6000	19.19426	16	0.04000	5	30	
8	4.9650	17.78399	9	0.03000	3	12	
9	5.1800	17.04632	6	0.04000	2	6	
10	5.3800	16.41307	3	0.00000	1	0	
11	5.5900	15.79694	6	0.06000	2	6	
12	6.0200	14.66952	3	0.00000	1	0	
13	6.3200	13.97384	6	0.04000	2	8	
14	6.7600	13.06525	6	0.04000	2	9	
15	6.9400	12.72678	3	0.00000	1	0	
16	7.8900	11.19641	6	0.14000	2	28	
17	8.0800	10.93355	9	0.04000	3	13	
18	8.5000	10.39422	13	0.04000	4	19	
19	8.7150	10.13827	9	0.03000	3	9	
20	9.0900	9.72085	6	0.06000	2	7	
21	9.4733	9.32838	16	0.09330	5	69	
22	9.6200	9.18645	19	0.00000	6	0	
23	9.8550	8.96791	22	0.15000	7	91	
24	10.4600	8.45053	3	0.00000	1	0	
25	10.6500	8.30020	6	0.10000	2	12	
26	10.9200	8.09557	6	0.16000	2	25	
27	11.1150	7.95398	9	0.03000	3	12	
28	11.3800	7.76934	3	0.00000	1	0	
29	13.2600	6.67173	6	0.12000	2	16	
30	13.4800	6.56334	3	0.00000	1	0	
31	14.1650	6.24745	6	0.03000	2	5	
32	14.8200	5.97277	6	0.04000	2	6	
33	15.1850	5.83001	9	0.05000	3	13	
34	15.6550	5.65602	9	0.03000	3	6	
35	15.8650	5.58163	9	0.05000	3	13	
36	16.1100	5.49729	13	0.12000	4	37	
37	16.4300	5.39093	9	0.06000	3	17	
38	16.6800	5.31069	3	0.00000	1	0	
39	17.2400	5.13943	13	0.08000	4	40	
40	17.3800	5.09834	6	0.00000	2	0	
41	17.6500	5.02096	13	0.18000	4	64	
42	18.2633	4.85371	31	0.19330	10	108	
43	18.4666	4.80073	22	0.06670	7	30	
44	18.6950	4.74259	22	0.07000	7	33	
45	18.8400	4.70641	9	0.08000	3	27	
46	19.0800	4.64775	3	0.00000	1	0	
47	19.5400	4.53936	3	0.00000	1	0	
48	20.0000	4.43598	6	0.08000	2	9	
49	20.2400	4.38392	9	0.04000	3	10	
50	20.6000	4.30811	3	0.00000	1	0	

Appendix XVII

Generated XRD Data for Carbonised Coconut Shell at 500°C

Data : CCFP-500C							
# Strongest 3 peaks							
no. peak	2Theta (deg)	d (Å)	I/I1	FWHM (deg)	Intensity (Counts)	Integrated Int (Counts)	
1	28	24.0346	3.69968	100	0.16470	88	819
2	33	25.2067	3.53024	35	0.13850	31	254
3	64	47.5825	1.90949	30	0.12500	26	176
# Peak Data List							
peak no.	2Theta (deg)	d (Å)	I/I1	FWHM (deg)	Intensity (Counts)	Integrated Int (Counts)	
1	3.8200	23.11158	3	0.04000	3	16	
2	4.0400	21.85351	3	0.04000	3	11	
3	4.2750	20.65271	3	0.03000	3	10	
4	4.7000	18.78609	3	0.08000	3	33	
5	5.9800	14.76755	5	0.10000	4	41	
6	6.2300	14.17550	10	0.18000	9	108	
7	6.7400	13.10398	3	0.04000	3	18	
8	7.1500	12.35345	3	0.10000	3	27	
9	7.3800	11.96896	3	0.04000	3	13	
10	7.8650	11.23194	8	0.13000	7	64	
11	8.8400	9.99519	3	0.04000	3	21	
12	9.1350	9.67306	3	0.03000	3	8	
13	10.5200	8.40247	3	0.04000	3	14	
14	10.7750	8.20418	3	0.03000	3	6	
15	10.9900	8.04416	5	0.14000	4	39	
16	11.2600	7.85187	5	0.16000	4	44	
17	15.3400	5.77145	8	0.05340	7	25	
18	15.4633	5.72571	11	0.16670	10	80	
19	15.7400	5.62567	3	0.04000	3	10	
20	18.2667	4.85281	27	0.16000	24	228	
21	19.4250	4.56597	9	0.17000	8	91	
22	19.8150	4.47698	3	0.07000	3	17	
23	20.5800	4.31225	3	0.04000	3	15	
24	21.0166	4.22365	8	0.08670	7	49	
25	21.6700	4.09775	3	0.06000	3	21	
26	22.9400	3.87368	6	0.08000	5	20	
27	23.0550	3.85462	10	0.19000	9	80	
28	24.0346	3.69968	100	0.16470	88	819	
29	24.4600	3.63629	5	0.12000	4	28	
30	24.5600	3.62171	5	0.08000	4	16	
31	24.8400	3.58152	11	0.10660	10	76	
32	25.0200	3.55616	23	0.11000	20	133	
33	25.2067	3.53024	35	0.13850	31	254	
34	25.4400	3.49839	6	0.06660	5	37	
35	26.8266	3.32063	14	0.22670	12	132	
36	27.3300	3.26060	5	0.10000	4	26	
37	27.7450	3.21277	3	0.07000	3	16	
38	27.8650	3.19920	3	0.05000	3	12	
39	28.2316	3.15849	6	0.11670	5	38	
40	28.7050	3.10747	3	0.05000	3	13	
41	28.8800	3.08903	5	0.12000	4	30	
42	29.8300	2.99278	3	0.10000	3	31	
43	31.2400	2.86085	3	0.04000	3	11	
44	31.4933	2.83841	13	0.14670	11	97	
45	31.8000	2.81173	3	0.08000	3	17	
46	32.2500	2.77352	5	0.10000	4	29	
47	32.6200	2.74290	3	0.04000	3	14	
48	33.3800	2.68217	3	0.08000	3	27	
49	33.9566	2.63793	13	0.11330	11	74	
50	34.1333	2.62468	3	0.06670	3	12	

Appendix XVIII

Generated XRD Data for Carbonised Coconut Shell at 600°C

Data : CCFP-600C

# Strongest 3 peaks							
no.	peak no.	2Theta (deg)	d (Å)	I/I1	FWHM (deg)	Intensity (Counts)	Integrated Int (Counts)
1	14	24.0632	3.69535	100	0.13870	239	1779
2	15	24.4973	3.63084	77	0.11330	185	1118
3	16	24.9126	3.57125	26	0.14290	63	523

# Peak Data List							
peak no.	2Theta (deg)	d (Å)	I/I1	FWHM (deg)	Intensity (Counts)	Integrated Int (Counts)	
1	9.4690	9.33260	3	0.08000	8	40	
2	9.6970	9.11368	3	0.05000	7	35	
3	10.2774	8.60026	3	0.10000	7	59	
4	10.7143	8.25053	3	0.08000	7	84	
5	10.9891	8.04482	3	0.07330	8	48	
6	11.1514	7.92809	3	0.06000	7	40	
7	18.2816	4.84889	18	0.15880	43	337	
8	18.4674	4.80052	9	0.13340	21	176	
9	20.5662	4.31512	3	0.09000	8	48	
10	21.3923	4.15031	3	0.09330	7	51	
11	22.8754	3.88447	6	0.08660	15	87	
12	23.0550	3.85462	3	0.12000	8	90	
13	23.8533	3.72739	13	0.09340	30	262	
14	24.0632	3.69535	100	0.13870	239	1779	
15	24.4973	3.63084	77	0.11330	185	1118	
16	24.9126	3.57125	26	0.14290	63	523	
17	26.8453	3.31836	5	0.08500	13	85	
18	27.8812	3.19738	3	0.07000	7	36	
19	28.2557	3.15585	3	0.08000	7	58	
20	28.8199	3.09534	3	0.17000	7	79	
21	29.6338	3.01215	3	0.18000	7	95	
22	31.5115	2.83681	3	0.10000	7	68	
23	32.0184	2.79305	4	0.10500	10	58	
24	32.2839	2.77068	3	0.18000	7	101	
25	33.5886	2.66598	3	0.08530	8	33	
26	33.9617	2.63754	11	0.09440	27	141	
27	35.0578	2.55755	5	0.08000	13	73	
28	35.9620	2.49529	5	0.10000	13	116	
29	36.8613	2.43645	3	0.15000	8	75	
30	37.6856	2.38503	3	0.14000	8	82	
31	43.1751	2.09365	7	0.15330	16	180	
32	44.9174	2.01640	4	0.09330	9	47	
33	47.5337	1.91134	9	0.12860	21	169	
34	48.0233	1.89299	3	0.11830	8	70	
35	52.2572	1.74914	10	0.13000	25	189	
36	52.4621	1.74279	3	0.11000	8	48	
37	52.7300	1.73457	4	0.13400	9	76	
38	56.1157	1.63767	5	0.10000	11	68	
39	56.9587	1.61542	3	0.09330	7	46	
40	57.3519	1.60528	8	0.14670	19	152	
41	61.2372	1.51241	3	0.09330	8	88	
42	65.1602	1.43051	3	0.12500	7	67	
43	65.9367	1.41554	7	0.08470	17	75	
44	70.9476	1.32735	4	0.26670	9	165	

Appendix XIX

Generated XRD Data for Carbonised Coconut Shell at 700°C

Data : CCFP-700C							
# Strongest 3 peaks							
no.	peak no.	2Theta (deg)	d (Å)	I/I1	FWHM (deg)	Intensity (Counts)	Integrated Int (Counts)
1	83	23.9791	3.70812	100	0.14830	37	366
2	81	22.9300	3.87535	30	0.10000	11	66
3	123	34.1283	2.62505	24	0.07670	9	40
# Peak Data List							
peak no.	2Theta (deg)	d (Å)	I/I1	FWHM (deg)	Intensity (Counts)	Integrated Int (Counts)	
1	2.6650	33.12489	5	0.03000	2	5	
2	2.8200	31.30453	3	0.00000	1	0	
3	3.4100	25.88942	11	0.10000	4	22	
4	3.5400	24.93896	5	0.12000	2	13	
5	3.8400	22.99125	5	0.08000	2	14	
6	4.0500	21.79957	5	0.06000	2	10	
7	4.4050	20.04350	8	0.05000	3	9	
8	4.5950	19.21513	8	0.03000	3	12	
9	4.8000	18.39494	14	0.04000	5	19	
10	5.0533	17.47343	8	0.02670	3	7	
11	5.1950	16.99714	8	0.03000	3	6	
12	5.3400	16.53592	8	0.04000	3	12	
13	5.6000	15.76875	8	0.02000	3	5	
14	5.8500	15.09542	8	0.06000	3	18	
15	6.0000	14.71837	11	0.04000	4	12	
16	6.1800	14.29008	8	0.04000	3	20	
17	6.5383	13.50776	11	0.14330	4	37	
18	6.8100	12.96944	5	0.08000	2	13	
19	6.9900	12.63586	11	0.06000	4	13	
20	7.2500	12.18328	8	0.08000	3	14	
21	7.4833	11.80397	8	0.04670	3	12	
22	7.6500	11.54712	16	0.06000	6	28	
23	7.9200	11.15406	8	0.04000	3	14	
24	8.0600	10.96063	3	0.00000	1	0	
25	8.3216	10.61665	14	0.06330	5	29	
26	8.8350	10.00084	5	0.03000	2	4	
27	9.2000	9.60487	3	0.00000	1	0	
28	9.4400	9.36121	5	0.00000	2	0	
29	9.5400	9.26330	11	0.10660	4	27	
30	9.7233	9.08908	14	0.03330	5	21	
31	10.0933	8.75671	8	0.02670	3	5	
32	10.3600	8.53188	3	0.00000	1	0	
33	10.5050	8.41443	5	0.07000	2	14	
34	10.7750	8.20418	8	0.03000	3	6	
35	11.0450	8.00423	5	0.03000	2	3	
36	11.5000	7.68854	5	0.04000	2	5	
37	11.8200	7.48110	5	0.04000	2	7	
38	12.0000	7.36928	3	0.00000	1	0	
39	12.1800	7.26078	8	0.04000	3	12	
40	12.3600	7.15544	5	0.12000	2	13	
41	12.4650	7.09540	8	0.05000	3	9	
42	12.6050	7.01691	8	0.03000	3	15	
43	12.8850	6.86505	11	0.07000	4	30	
44	13.3250	6.63933	5	0.05000	2	6	
45	13.5050	6.55124	8	0.05000	3	12	
46	13.7750	6.42344	11	0.05000	4	21	
47	14.2300	6.21905	5	0.06000	2	11	
48	14.3950	6.14814	11	0.07000	4	17	
49	14.5600	6.07883	3	0.00000	1	0	
50	14.7350	6.00703	11	0.05000	4	13	

Appendix XX

Generated XRD Data for Raw Coconut Fibre

Data : PURE-CSP							
# Strongest 3 peaks	no. peak	2Theta (deg)	d (Å)	I/I1	FWHM (deg)	Intensity (Counts)	Integrated Int (Counts)
1	28	24.0759	3.69343	100	0.15180	87	716
2	33	25.4400	3.49839	46	0.17780	40	290
3	31	24.9466	3.56646	45	0.21330	39	359
# Peak Data List	peak no.	2Theta (deg)	d (Å)	I/I1	FWHM (deg)	Intensity (Counts)	Integrated Int (Counts)
	1	3.9850	22.15500	3	0.03000	3	19
	2	4.8000	18.39494	3	0.08000	3	30
	3	6.2150	14.20968	10	0.19000	9	104
	4	6.7200	13.14293	3	0.04000	3	13
	5	7.2400	12.20009	3	0.04000	3	15
	6	7.5550	11.69211	3	0.03000	3	10
	7	7.9150	11.16110	7	0.11000	6	53
	8	8.4800	10.41869	3	0.04000	3	10
	9	8.5700	10.30948	3	0.06000	3	16
	10	9.1000	9.71019	6	0.08000	5	45
	11	10.0150	8.82500	3	0.03000	3	8
	12	10.4200	8.48288	3	0.04000	3	13
	13	10.6600	8.29243	3	0.08000	3	23
	14	10.8750	8.12897	3	0.09000	3	15
	15	11.0800	7.97902	5	0.24000	4	53
	16	11.3300	7.80352	3	0.04000	3	11
	17	15.4800	5.71957	13	0.14000	11	88
	18	15.9600	5.54862	5	0.08000	4	18
	19	18.1800	4.87576	7	0.10000	6	41
	20	18.3325	4.83554	29	0.14500	25	204
	21	18.6200	4.76152	6	0.02660	5	14
	22	19.4300	4.56481	7	0.10000	6	48
	23	20.5600	4.31640	5	0.08000	4	34
	24	21.0133	4.22430	11	0.13330	10	98
	25	21.8100	4.07176	8	0.06000	7	31
	26	23.0150	3.86123	10	0.13000	9	99
	27	23.9000	3.72021	15	0.04000	13	57
	28	24.0759	3.69343	100	0.15180	87	716
	29	24.5100	3.62899	8	0.10000	7	59
	30	24.8200	3.58436	22	0.08800	19	79
	31	24.9466	3.56646	45	0.21330	39	359
	32	25.3000	3.51744	41	0.16660	36	275
	33	25.4400	3.49839	46	0.17780	40	290
	34	26.8750	3.31476	15	0.13000	13	126
	35	27.2300	3.27235	3	0.10000	3	29
	36	27.3850	3.25418	3	0.07000	3	14
	37	27.7258	3.21495	11	0.12170	10	73
	38	28.2100	3.16086	6	0.10000	5	25
	39	28.3800	3.14231	5	0.08000	4	21
	40	29.6400	3.01153	3	0.08000	3	31
	41	30.0400	2.97234	3	0.04000	3	12
	42	30.2516	2.95203	8	0.08330	7	35
	43	31.4000	2.84663	6	0.10000	5	30
	44	31.5300	2.83519	16	0.14000	14	120
	45	32.2800	2.77101	3	0.04000	3	13
	46	32.4800	2.75440	3	0.04000	3	13
	47	33.4300	2.67827	5	0.10000	4	30
	48	33.6550	2.66087	16	0.11000	14	85
	49	34.0183	2.63328	29	0.11670	25	156
	50	34.4100	2.60420	3	0.06000	3	17

Appendix XXI

Generated XRD Data for Carbonised Coconut Fibre at 300°C

Data : CCSP							
# Strongest 3 peaks							
no.	peak no.	2Theta (deg)	d (Å)	I/I1	FWHM (deg)	Intensity (Counts)	Integrated Int (Counts)
1	37	24.0774	3.69320	100	0.20150	82	929
2	40	24.9834	3.56129	85	0.23970	70	922
3	42	25.4600	3.49569	37	0.17140	30	373
# Peak Data List							
peak no.	2Theta (deg)	d (Å)	I/I1	FWHM (deg)	Intensity (Counts)	Integrated Int (Counts)	
1	2.2700	38.88795	2	0.10000	2	18	
2	4.5800	19.27803	2	0.04000	2	8	
3	5.1900	17.01350	2	0.18000	2	22	
4	6.2400	14.15281	17	0.20000	14	153	
5	6.4200	13.75640	5	0.08000	4	24	
6	7.8333	11.27732	12	0.26670	10	138	
7	9.5550	9.24880	4	0.03000	3	11	
8	9.8800	8.94528	2	0.04000	2	10	
9	10.4650	8.44651	2	0.09000	2	12	
10	10.8000	8.18525	2	0.12000	2	18	
11	11.1000	7.96469	11	0.28000	9	125	
12	11.3000	7.82417	5	0.00000	4	0	
13	12.4500	7.10392	2	0.10000	2	13	
14	13.0500	6.77862	2	0.22000	2	46	
15	13.7900	6.41648	2	0.06000	2	10	
16	14.2900	6.19308	2	0.10000	2	17	
17	14.8500	5.96077	4	0.06000	3	17	
18	15.1300	5.85108	4	0.06000	3	24	
19	15.5000	5.71223	9	0.16000	7	75	
20	15.8700	5.57988	5	0.10000	4	36	
21	16.7700	5.28239	2	0.10000	2	15	
22	17.4000	5.09253	2	0.04000	2	7	
23	18.3300	4.83619	17	0.26000	14	191	
24	18.5200	4.78700	4	0.00000	3	0	
25	19.4666	4.55631	9	0.13330	7	67	
26	19.7400	4.49382	4	0.04000	3	10	
27	19.9200	4.45362	5	0.08000	4	31	
28	20.3450	4.36153	2	0.09000	2	14	
29	20.7000	4.28753	2	0.12000	2	16	
30	20.9900	4.22894	11	0.22000	9	111	
31	21.3500	4.15844	6	0.10000	5	35	
32	21.7950	4.07453	7	0.15000	6	47	
33	22.0600	4.02618	2	0.04000	2	8	
34	22.4600	3.95537	2	0.04000	2	12	
35	23.0700	3.85215	9	0.18000	7	87	
36	23.4100	3.79696	2	0.06000	2	7	
37	24.0774	3.69320	100	0.20150	82	929	
38	24.3600	3.65099	11	0.00000	9	0	
39	24.5200	3.62753	6	0.10000	5	74	
40	24.9834	3.56129	85	0.23970	70	922	
41	25.2600	3.52291	33	0.00000	27	0	
42	25.4600	3.49569	37	0.17140	30	373	
43	25.8250	3.44711	17	0.11000	14	90	
44	26.8900	3.31295	9	0.18000	7	86	
45	27.2200	3.27353	6	0.12000	5	48	
46	27.7000	3.21788	4	0.08000	3	23	
47	27.8800	3.19752	6	0.08000	5	26	
48	28.2650	3.15483	12	0.23000	10	113	
49	28.6350	3.11490	2	0.03000	2	3	
50	28.8650	3.09060	5	0.17000	4	43	

Appendix XXII

Generated XRD Data for Carbonised Coconut Fibre at 400°C

Data : CCSP-400							
#	Strongest peak no.	2Theta (deg)	d (Å)	I/I1	FWHM (deg)	Intensity (Counts)	Integrated Int (Counts)
1	28	24.0465	3.69788	100	0.15970	113	987
2	31	24.9341	3.56822	76	0.12510	86	614
3	33	25.4567	3.49614	72	0.11600	81	515
#	Peak Data List peak no.	2Theta (deg)	d (Å)	I/I1	FWHM (deg)	Intensity (Counts)	Integrated Int (Counts)
1	1	2.4133	36.57913	4	0.09330	5	38
2	2	3.9850	22.15500	3	0.05000	3	17
3	3	4.3150	20.46135	3	0.03000	3	7
4	4	4.4550	19.81866	4	0.07000	4	25
5	5	6.0800	14.52489	4	0.00000	5	0
6	6	6.2633	14.10021	12	0.16670	13	139
7	7	7.5250	11.73865	3	0.09000	3	19
8	8	7.8675	11.22838	13	0.12500	15	115
9	9	8.6350	10.23202	3	0.03000	3	9
10	10	9.1700	9.63622	4	0.06000	4	24
11	11	10.4400	8.46668	3	0.04000	3	8
12	12	10.6450	8.30408	4	0.09000	4	22
13	13	11.0833	7.97665	8	0.11330	9	98
14	14	12.6283	7.00401	3	0.03670	3	7
15	15	13.1500	6.72729	3	0.06000	3	20
16	16	15.0033	5.90021	3	0.04670	3	11
17	17	15.2950	5.78833	4	0.05000	4	14
18	18	15.4860	5.71737	8	0.17200	9	83
19	19	18.1400	4.88642	9	0.08000	10	56
20	20	18.3100	4.84143	40	0.14000	45	304
21	21	18.5108	4.78936	9	0.12830	10	70
22	22	19.4100	4.56947	9	0.14000	10	78
23	23	20.3600	4.35835	4	0.12000	4	44
24	24	20.9575	4.23542	15	0.15500	17	140
25	25	21.3100	4.16615	5	0.08000	6	38
26	26	23.1000	3.84721	6	0.12000	7	61
27	27	23.4400	3.79217	3	0.04000	3	12
28	28	24.0465	3.69788	100	0.15970	113	987
29	29	24.3375	3.65432	5	0.06500	6	20
30	30	24.4850	3.63264	4	0.11000	4	25
31	31	24.9341	3.56822	76	0.12510	86	614
32	32	25.2043	3.53057	27	0.12140	31	218
33	33	25.4567	3.49614	72	0.11600	81	515
34	34	25.8500	3.44383	8	0.10000	9	74
35	35	26.8200	3.32144	4	0.08000	5	26
36	36	26.9450	3.30631	4	0.05000	5	18
37	37	27.0750	3.29073	4	0.07000	4	17
38	38	27.2546	3.26945	10	0.08270	11	53
39	39	27.9366	3.19117	4	0.08670	4	28
40	40	28.2175	3.16003	4	0.08500	5	22
41	41	28.3350	3.14720	3	0.07000	3	14
42	42	28.7150	3.10641	3	0.03000	3	10
43	43	28.9100	3.08590	4	0.06000	5	25
44	44	29.1300	3.06309	4	0.10000	5	30
45	45	29.3200	3.04367	3	0.04000	3	14
46	46	29.7100	3.00460	3	0.06000	3	19
47	47	29.8750	2.98838	3	0.03000	3	8
48	48	30.3100	2.94647	3	0.04000	3	10
49	49	31.5450	2.83388	6	0.17000	7	74
50	50	31.7050	2.81994	4	0.09000	4	25

Appendix XXIII

Generated XRD Data for Carbonised Coconut Fibre at 500°C

Data : CCSP-500C							
# Strongest peaks	no. peak	2Theta (deg)	d (Å)	I/I1	FWHM (deg)	Intensity (Counts)	Integrated Int (Counts)
1	69	24.0464	3.69789	100	0.11820	52	384
2	73	25.3898	3.50520	63	0.12250	33	192
3	56	19.4535	4.55935	62	0.12710	32	205
# Peak Data List							
peak no.	2Theta (deg)	d (Å)	I/I1	FWHM (deg)	Intensity (Counts)	Integrated Int (Counts)	
1	2.0300	43.48497	4	0.06000	2	16	
2	2.7000	32.69557	4	0.04000	2	6	
3	3.0400	29.03955	8	0.10000	4	28	
4	3.2050	27.54489	4	0.13000	2	14	
5	3.4650	25.47859	8	0.11000	4	27	
6	3.6650	24.08866	6	0.07000	3	17	
7	3.7600	23.48024	8	0.12000	4	22	
8	4.0400	21.85351	6	0.08000	3	18	
9	4.1600	21.22338	10	0.04000	5	26	
10	4.5000	19.62057	10	0.08000	5	37	
11	4.8250	18.29968	4	0.03000	2	8	
12	5.1050	17.29659	6	0.03000	3	7	
13	5.3850	16.39784	10	0.09000	5	31	
14	5.5900	15.79694	4	0.08000	2	9	
15	5.7700	15.30454	8	0.06000	4	24	
16	6.0600	14.57278	8	0.00000	4	0	
17	6.4400	13.71372	8	0.12000	4	55	
18	6.7200	13.14293	8	0.10000	4	40	
19	7.4033	11.93134	10	0.07330	5	54	
20	7.7200	11.44258	6	0.04000	3	10	
21	7.8700	11.22482	6	0.10000	3	31	
22	8.2000	10.77381	4	0.00000	2	0	
23	8.6550	10.20842	6	0.03000	3	6	
24	8.9800	9.83968	6	0.04000	3	11	
25	9.2400	9.56338	13	0.12000	7	47	
26	9.4800	9.32180	27	0.28000	14	169	
27	9.6000	9.20554	29	0.00000	15	0	
28	9.8800	8.94528	17	0.13340	9	202	
29	10.1350	8.72078	10	0.07000	5	23	
30	10.4600	8.45053	4	0.04000	2	6	
31	10.6483	8.30152	6	0.07670	3	15	
32	10.9650	8.06245	4	0.03000	2	7	
33	11.1700	7.91493	6	0.06000	3	15	
34	11.7800	7.50641	6	0.04000	3	12	
35	11.9800	7.38154	8	0.04000	4	12	
36	12.4700	7.09257	6	0.06000	3	15	
37	12.6650	6.98380	8	0.11000	4	21	
38	12.7433	6.94107	8	0.04670	4	11	
39	13.0200	6.79417	10	0.08000	5	29	
40	13.7200	6.44906	4	0.04000	2	8	
41	15.0850	5.86843	6	0.03000	3	11	
42	15.2900	5.79021	4	0.06000	2	9	
43	15.4150	5.74354	6	0.05000	3	16	
44	16.2700	5.44359	4	0.06000	2	11	
45	16.4800	5.37469	4	0.04000	2	6	
46	16.7600	5.28552	4	0.04000	2	9	
47	17.2000	5.15129	27	0.16000	14	125	
48	17.3600	5.10417	29	0.20000	15	138	
49	17.5200	5.05792	27	0.11340	14	75	
50	17.7000	5.00688	19	0.12000	10	70	

Appendix XXIV

Generated XRD Data for Carbonised Coconut Fibre at 600°C

Data : CCSP-600C							
# Strongest 3 peaks							
no.	peak no.	2Theta (deg)	d (Å)	I/I1	FWHM (deg)	Intensity (Counts)	Integrated Int (Counts)
1	76	23.9875	3.70684	100	0.16000	44	376
2	68	21.3133	4.16551	70	0.12000	31	194
3	165	47.9480	1.89579	45	0.12800	20	131
# Peak Data List							
peak no.	2Theta (deg)	d (Å)	I/I1	FWHM (deg)	Intensity (Counts)	Integrated Int (Counts)	
1	2.3600	37.40513	5	0.04000	2	6	
2	2.5550	34.55076	5	0.07000	2	11	
3	2.7000	32.69557	2	0.00000	1	0	
4	3.0050	29.37770	5	0.09000	2	15	
5	3.2000	27.58792	2	0.00000	1	0	
6	3.4100	25.88942	7	0.06000	3	19	
7	3.7000	23.86087	7	0.04000	3	10	
8	3.9000	22.63767	2	0.00000	1	0	
9	4.2600	20.72540	2	0.00000	1	0	
10	4.4850	19.68616	5	0.03000	2	7	
11	5.3300	16.56693	9	0.14000	4	31	
12	5.6800	15.54684	2	0.00000	1	0	
13	5.8800	15.01847	5	0.04000	2	4	
14	6.0650	14.56078	5	0.07000	2	10	
15	6.2650	14.09639	16	0.15000	7	54	
16	6.4800	13.62916	9	0.13340	4	31	
17	6.7400	13.10398	9	0.12000	4	27	
18	6.9400	12.72678	7	0.04000	3	12	
19	7.2850	12.12483	11	0.07000	5	27	
20	7.5650	11.67667	9	0.19000	4	40	
21	7.8200	11.29647	7	0.04000	3	13	
22	7.9800	11.07033	7	0.04000	3	18	
23	8.3250	10.61232	7	0.05000	3	16	
24	8.5300	10.35773	5	0.06000	2	11	
25	8.8750	9.95585	11	0.09000	5	34	
26	9.2000	9.60487	14	0.12000	6	42	
27	9.3800	9.42095	23	0.12000	10	51	
28	9.5200	9.28272	23	0.28000	10	112	
29	9.8600	8.96338	16	0.24000	7	96	
30	10.2750	8.60226	5	0.05000	2	7	
31	10.4800	8.43445	7	0.04000	3	7	
32	10.6000	8.33923	9	0.16000	4	45	
33	10.9800	8.05147	11	0.12000	5	64	
34	11.3800	7.76934	9	0.08000	4	21	
35	11.6800	7.57045	2	0.00000	1	0	
36	12.2500	7.21945	7	0.06000	3	14	
37	12.5200	7.06436	2	0.00000	1	0	
38	12.7000	6.96463	5	0.08000	2	10	
39	13.0200	6.79417	5	0.04000	2	7	
40	13.5600	6.52479	5	0.08000	2	16	
41	13.8600	6.38423	2	0.00000	1	0	
42	14.1350	6.26064	5	0.07000	2	7	
43	14.3650	6.16091	5	0.11000	2	13	
44	14.5800	6.07054	2	0.00000	1	0	
45	14.7433	6.00367	7	0.04670	3	11	
46	14.9200	5.93296	7	0.04000	3	11	
47	15.1200	5.85493	2	0.00000	1	0	
48	15.3600	5.76398	7	0.04000	3	14	
49	15.5250	5.70309	7	0.05000	3	15	
50	15.7300	5.62922	7	0.04000	3	11	

Appendix XXV

Generated XRD Data for Carbonised Coconut Fibre at 700°C

Data : CCSP-700C

# Strongest 3 peaks							
no.	peak no.	2Theta (deg)	d (Å)	I/I1	FWHM (deg)	Intensity (Counts)	Integrated Int (Counts)
1	67	23.9441	3.71346	100	0.16520	72	686
2	51	18.2350	4.86117	92	0.13000	66	437
3	154	57.3261	1.60594	86	0.14150	62	441

# Peak Data List							
peak no.	2Theta (deg)	d (Å)	I/I1	FWHM (deg)	Intensity (Counts)	Integrated Int (Counts)	
1	3.2300	27.33175	6	0.10000	4	29	
2	3.4450	25.62647	6	0.13000	4	44	
3	4.0950	21.56011	4	0.03000	3	7	
4	4.3500	20.29680	3	0.10000	2	10	
5	4.7700	18.51056	4	0.06000	3	13	
6	5.0000	17.65958	4	0.04000	3	18	
7	5.2700	16.75541	3	0.06000	2	11	
8	5.6400	15.65701	8	0.16000	6	73	
9	5.9200	14.91709	19	0.24000	14	245	
10	6.1400	14.38308	24	0.00000	17	0	
11	6.2600	14.10764	18	0.20000	13	172	
12	6.6200	13.34124	8	0.08000	6	44	
13	6.8200	12.95044	3	0.08000	2	16	
14	7.1400	12.37073	4	0.04000	3	15	
15	7.3500	12.01775	3	0.06000	2	7	
16	7.5450	11.70758	3	0.07000	2	8	
17	7.6800	11.50208	4	0.04000	3	13	
18	7.8950	11.18933	8	0.09000	6	30	
19	8.0600	10.96063	4	0.04000	3	14	
20	8.4000	10.51774	7	0.04000	5	26	
21	8.5950	10.27955	4	0.03000	3	6	
22	8.8000	10.04053	4	0.04000	3	10	
23	9.2400	9.56338	8	0.14000	6	48	
24	9.3700	9.43098	13	0.10000	9	29	
25	9.5000	9.30222	11	0.40000	8	102	
26	9.7700	9.04574	10	0.10000	7	58	
27	10.0550	8.78998	4	0.03000	3	11	
28	10.5600	8.37073	6	0.12000	4	33	
29	10.8400	8.15514	4	0.04000	3	10	
30	11.1200	7.95041	3	0.10000	2	29	
31	11.4300	7.73547	4	0.06000	3	18	
32	11.7450	7.52870	4	0.03000	3	11	
33	12.0000	7.36928	3	0.12000	2	17	
34	12.2500	7.21945	6	0.06000	4	32	
35	13.3400	6.63190	3	0.04000	2	8	
36	13.6100	6.50094	3	0.06000	2	8	
37	13.9000	6.36595	4	0.04000	3	11	
38	14.8000	5.98079	4	0.08000	3	23	
39	15.1600	5.83957	7	0.08000	5	49	
40	15.3800	5.75653	3	0.00000	2	0	
41	15.7300	5.62922	6	0.06000	4	18	
42	15.8800	5.57639	3	0.08000	2	12	
43	16.1100	5.49729	4	0.06000	3	14	
44	16.3800	5.40728	3	0.04000	2	8	
45	16.6700	5.31386	3	0.06000	2	10	
46	16.9166	5.23695	6	0.12670	4	25	
47	17.1700	5.16022	6	0.06000	4	18	
48	17.3550	5.10563	6	0.09000	4	31	
49	17.5850	5.03937	4	0.03000	3	12	
50	17.8700	4.95963	6	0.06000	4	12	

Appendix XXVI

X-Ray Fluorescence Analysis of Major and Minor Elemental Oxides Composition of Coconut Shell and Fibre

S/N	ELEMENTAL OXIDES	PURE CFP	PURE CSP	CFP 300°C	CSP 300°C	CFP 400°C	CSP 400°C	CFP 500°C	CSP 500°C	CFP 600°C	CSP 600°C	CFP 700°C	CSP 700°C
1.	SiO ₂	20.00	20.89	17.03	16.32	16.75	16.05	15.99	15.30	11.52	10.92	12.04	11.90
2.	K ₂ O	27.30	28.13	42.44	43.01	41.32	40.84	45.44	43.05	58.65	59.01	62.03	60.01
3.	Fe ₂ O ₃	33.11	32.00	13.87	14.53	13.59	14.44	12.94	11.08	2.30	2.70	3.20	3.76
4.	Ti ₂ O	1.50	1.32	2.77	1.04	0.89	0.63	1.91	1.01	0.23	0.34	NILL	0.14
5.	CaO	6.30	6.02	10.09	11.54	12.01	11.97	10.19	10.75	NILL	0.01	NILL	0.01
6.	SO ₃	2.60	1.97	3.57	3.08	3.64	4.01	2.78	3.32	1.23	0.42	2.01	1.73
7.	NiO	0.42	0.35	0.33	0.20	0.24	0.13	0.19	0.10	0.02	NILL	0.05	NILL
8.	P ₂ O ₅	1.70	2.08	2.90	4.02	4.92	4.07	3.09	4.32	2.06	2.63	3.01	4.84
9.	MnO	0.42	0.47	0.45	0.28	0.32	0.45	0.34	0.53	0.03	0.01	NILL	0.01
10.	Al ₂ O ₃	NILL	0.01	NILL	0.01	0.02	NILL	0.01	0.01	NILL	0.01	0.01	NILL
11.	Cl	NILL	NILL	NILL	NILL	NILL	NILL	NILL	NILL	22.60	23.08	17.09	18.03
12.	CuO	1.30	1.22	2.22	1.37	1.61	1.94	0.31	NILL	0.21	0.08	0.11	NILL
13.	Re ₂ O ₇	NILL	0.02	1.65	NILL	1.42	0.48	NILL	0.55	0.14	0.19	0.09	0.05
14.	ZnO	0.10	0.04	2.98	4.44	3.02	4.77	4.56	5.98	0.16	0.20	0.31	0.23
15.	Yb ₂ O ₃	2.01	2.09	NILL	0.21	0.30	0.13	NILL	0.03	0.01	NILL	0.02	0.01
16.	V ₂ O ₅	0.02	NILL	0.01	NILL	NILL	0.01	0.01	0.01	NILL	NILL	NILL	0.02
17.	BaO	NILL	0.01	0.01	NILL	NILL	NILL	0.01	NILL	NILL	0.05	0.02	0.03
18.	MoO ₃	3.03	3.43	0.02	NILL	NILL	0.01	2.01	NILL	0.05	0.07	0.06	0.04

Appendix XXVII

Predictive Analysis and Statistical Modelled Chart for the Mechanical and Chemical Sorption Properties of the Optimised Coconut Fibre Composites used in Model Productions

Analysis of Variance Coconut Fibre

H₀: *There is no significant difference in the Physico-mechanical properties of composites filled with coconut fibre treated at the various carbonisation temperatures.*

Between-Subjects Factors

	Value Label	N
Properties	1.00 Hardness(shore A)	6
	2.00 Abrasion Resistance	6
	3.00 Compression set (%)	6
	4.00 Tensile Strength (MPa)	6
	5.00 EAB (%)	6
	6.00 Modulus (%)	6
	7.00 Flexural Strength (MPa)	6
Sample	1.00 CFP	7
	2.00 300	7
	3.00 400	7
	4.00 500	7
	5.00 600	7
	6.00 700	7

Descriptive Statistics

Dependent Variable: Yield

Properties	Sample	Mean	Std. Deviation	N
Hardness(shore A)	CFP	64.0000	.	1
	300	68.0000	.	1
	400	75.0000	.	1
	500	79.0000	.	1
	600	80.0000	.	1
	700	76.0000	.	1
	Total	73.6667	6.34560	6
Abrasion Resistance	CFP	20.4000	.	1
	300	25.3200	.	1
	400	29.9500	.	1
	500	32.4000	.	1
	600	36.5500	.	1
	700	34.1500	.	1
	Total	29.7950	5.99496	6
Compression set (%)	CFP	26.9200	.	1
	300	24.6500	.	1
	400	20.9600	.	1
	500	19.8500	.	1
	600	19.4600	.	1
	700	22.8500	.	1
	Total	22.4483	2.92920	6
Tensile Strength (MPa)	CFP	5.9600	.	1
	300	7.2500	.	1

	400	7.9700	.	1
	500	8.4500	.	1
	600	8.6800	.	1
	700	7.8500	.	1
	Total	7.6933	.98470	6
	CFP	520.5000	.	1
EAB (%)	300	515.8000	.	1
	400	498.2000	.	1
	500	488.5000	.	1

Descriptive Statistics

Dependent Variable: Yield

Properties	Sample	Mean	Std. Deviation	N
EAB (%)	600	455.7000	.	1
	700	468.8500	.	1
	Total	491.2583	25.61129	6
	CFP	2.8500	.	1
	300	3.2000	.	1
	400	3.8400	.	1
Modulus (%)	500	4.2200	.	1
	600	4.2500	.	1
	700	4.0000	.	1
	Total	3.7267	.57458	6
	CFP	1.9900	.	1
Flexural Strength (MPa)	300	1.6500	.	1
	400	1.4200	.	1

	500	1.4000	.	1
	600	1.3800	.	1
	700	1.4800	.	1
	Total	1.5533	.23526	6
	CFP	91.8029	190.26751	7
	300	92.2671	188.14680	7
	400	91.0486	181.29899	7
Total	500	90.5457	177.49109	7
	600	86.5743	165.02861	7
	700	87.8829	169.95132	7
	Total	90.0202	167.67634	42

Tests of Between-Subjects Effects

Dependent Variable: Yield

Source	Type III Sum of Squares	df	Mean Square	F	Sig.
Corrected Model	1149201.118 ^a	11	104472.829	888.279	.000
Intercept	340353.017	1	340353.017	2893.847	.000
Properties	1149019.098	6	191503.183	1628.253	.000
Samples	182.020	5	36.404	.310	.903
Error	3528.380	30	117.613		
Total	1493082.515	42			
Corrected Total	1152729.497	41			

a. R Squared = .997 (Adjusted R Squared = .996)

Estimated Marginal Means

1. Properties

Dependent Variable: Yield

Properties	Mean	Std. Error	95% Confidence Interval	
			Lower Bound	Upper Bound
Hardness(shore A)	73.667	4.427	64.625	82.709
Abrasion Resistance	29.795	4.427	20.753	38.837
Compression set (%)	22.448	4.427	13.406	31.490
Tensile Strength (MPa)	7.693	4.427	-1.349	16.735
EAB (%)	491.258	4.427	482.216	500.300
Modulus (%)	3.727	4.427	-5.315	12.769
Flexural Strength (MPa)	1.553	4.427	-7.489	10.595

2. Sample

Dependent Variable: Yield

Sample	Mean	Std. Error	95% Confidence Interval	
			Lower Bound	Upper Bound
CFP	91.803	4.099	83.432	100.174
300	92.267	4.099	83.896	100.638
400	91.049	4.099	82.677	99.420
500	90.546	4.099	82.174	98.917
600	86.574	4.099	78.203	94.946
700	87.883	4.099	79.512	96.254

Post Hoc Tests

Properties

Multiple Comparisons

Dependent Variable: Yield

(I) Properties	(J) Properties	Mean Difference (I-J)	Std. Error	Sig.		
LSD	Hardness(shore A)	Abrasion Resistance	43.8717 ⁺	6.26133	.000	
		Compression set (%)	51.2183 ⁺	6.26133	.000	
		Tensile Strength (MPa)	65.9733 ⁺	6.26133	.000	
		EAB (%)	-417.5917 ⁺	6.26133	.000	
		Modulus (%)	69.9400 ⁺	6.26133	.000	
		Flexural Strength (MPa)	72.1133 ⁺	6.26133	.000	
		Hardness(shore A)	-43.8717 ⁺	6.26133	.000	
		Compression set (%)	7.3467	6.26133	.250	
		Abrasion Resistance	Tensile Strength (MPa)	22.1017 ⁺	6.26133	.001
			EAB (%)	-461.4633 ⁺	6.26133	.000
			Modulus (%)	26.0683 ⁺	6.26133	.000
			Flexural Strength (MPa)	28.2417 ⁺	6.26133	.000
	Compression set (%)	Hardness(shore A)	-51.2183 ⁺	6.26133	.000	
		Abrasion Resistance	-7.3467	6.26133	.250	
		Tensile Strength (MPa)	14.7550 ⁺	6.26133	.025	
		EAB (%)	-468.8100 ⁺	6.26133	.000	
		Modulus (%)	18.7217 ⁺	6.26133	.006	
		Flexural Strength (MPa)	20.8950 ⁺	6.26133	.002	
	Tensile Strength (MPa)	Hardness(shore A)	-65.9733 ⁺	6.26133	.000	

EAB (%)	Abrasion Resistance	-22.1017 ⁺	6.26133	.001
	Compression set (%)	-14.7550 ⁺	6.26133	.025
	EAB (%)	-483.5650 ⁺	6.26133	.000
	Modulus (%)	3.9667	6.26133	.531
	Flexural Strength (MPa)	6.1400	6.26133	.335
	Hardness(shore A)	417.5917 ⁺	6.26133	.000
	Abrasion Resistance	461.4633 ⁺	6.26133	.000
	Compression set (%)	468.8100 ⁺	6.26133	.000
	Tensile Strength (MPa)	483.5650 ⁺	6.26133	.000
	Modulus (%)	487.5317 ⁺	6.26133	.000
	Flexural Strength (MPa)	489.7050 ⁺	6.26133	.000

Multiple Comparisons

Dependent Variable: Yield

(I) Properties	(J) Properties	95% Confidence Interval		
		Lower Bound	Upper Bound	
LSD	Abrasion Resistance	31.0843 ⁺	56.6590	
	Compression set (%)	38.4310 ⁺	64.0057	
	Tensile Strength (MPa)	53.1860 ⁺	78.7607	
	Hardness(shore A)	EAB (%)	-430.3790 ⁺	-404.8043
	Modulus (%)	57.1527 ⁺	82.7273	
	Flexural Strength (MPa)	59.3260 ⁺	84.9007	
	Hardness(shore A)	-56.6590 ⁺	-31.0843	
Abrasion Resistance	Compression set (%)	-5.4407	20.1340	
	Tensile Strength (MPa)	9.3143 ⁺	34.8890	

	EAB (%)	-474.2507 [*]	-448.6760
	Modulus (%)	13.2810 [*]	38.8557
	Flexural Strength (MPa)	15.4543 [*]	41.0290
	Hardness(shore A)	-64.0057 [*]	-38.4310
	Abrasion Resistance	-20.1340	5.4407
Compression set (%)	Tensile Strength (MPa)	1.9677 [*]	27.5423
	EAB (%)	-481.5973 [*]	-456.0227
	Modulus (%)	5.9343 [*]	31.5090
	Flexural Strength (MPa)	8.1077 [*]	33.6823
	Hardness(shore A)	-78.7607 [*]	-53.1860
	Abrasion Resistance	-34.8890 [*]	-9.3143
Tensile Strength (MPa)	Compression set (%)	-27.5423 [*]	-1.9677
	EAB (%)	-496.3523 [*]	-470.7777
	Modulus (%)	-8.8207	16.7540
	Flexural Strength (MPa)	-6.6473	18.9273
	Hardness(shore A)	404.8043 [*]	430.3790
	Abrasion Resistance	448.6760 [*]	474.2507
EAB (%)	Compression set (%)	456.0227 [*]	481.5973
	Tensile Strength (MPa)	470.7777 [*]	496.3523
	Modulus (%)	474.7443 [*]	500.3190
	Flexural Strength (MPa)	476.9177 [*]	502.4923

Multiple Comparisons

Dependent Variable: Yield

(I) Properties	(J) Properties	Mean Difference (I-J)	Std. Error	Sig.	
LSD	Hardness(shore A)	-69.9400 [*]	6.26133	.000	
	Abrasion Resistance	-26.0683 [*]	6.26133	.000	
	Modulus (%)	Compression set (%)	-18.7217 [*]	6.26133	.006
	Tensile Strength (MPa)	-3.9667 [*]	6.26133	.531	
	EAB (%)	-487.5317 [*]	6.26133	.000	
	Flexural Strength (MPa)	2.1733 [*]	6.26133	.731	
	Flexural Strength (MPa)	Hardness(shore A)	-72.1133 [*]	6.26133	.000
		Abrasion Resistance	-28.2417	6.26133	.000
		Compression set (%)	-20.8950 [*]	6.26133	.002
		Tensile Strength (MPa)	-6.1400 [*]	6.26133	.335
		EAB (%)	-489.7050 [*]	6.26133	.000
		Modulus (%)	-2.1733 [*]	6.26133	.731

Multiple Comparisons

Dependent Variable: Yield

(I) Properties	(J) Properties	95% Confidence Interval	
		Lower Bound	Upper Bound
LSD	Hardness(shore A)	-82.7273*	-57.1527
	Abrasion Resistance	-38.8557*	-13.2810
	Modulus (%)	-31.5090*	-5.9343
	Tensile Strength (MPa)	-16.7540*	8.8207
	EAB (%)	-500.3190*	-474.7443
	Flexural Strength (MPa)	-10.6140*	14.9607
	Hardness(shore A)	-84.9007*	-59.3260
	Abrasion Resistance	-41.0290	-15.4543
	Flexural Strength (MPa)	-33.6823*	-8.1077
	Tensile Strength (MPa)	-18.9273*	6.6473
	EAB (%)	-502.4923*	-476.9177
	Modulus (%)	-14.9607*	10.6140

Based on observed means.

The error term is Mean Square (Error) = 117.613.

*. The mean difference is significant at the .05 level.

Homogeneous Subsets

Yield

Properties	N	Subset			
		1	2	3	4
Flexural Strength (MPa)	6	1.5533			
Modulus (%)	6	3.7267			
Tensile Strength (MPa)	6	7.6933			
Compression set (%)	6		22.4483		
Abrasion Resistance	6		29.7950		
Hardness(shore A)	6			73.6667	
EAB (%)	6				491.2583
Sig.		.363	.250	1.000	1.000

Means for groups in homogeneous subsets are displayed.

Based on observed means.

The error term is Mean Square (Error) = 117.613.

a. Uses Harmonic Mean Sample Size = 6.000.

b. Alpha = .05.

Sample

Multiple Comparisons

Dependent Variable: Yield

(I) Sample	(J) Sample	Mean Difference (I-J)	Std. Error	Sig.	95% Confidence Interval		
					Lower Bound	Upper Bound	
CFP	300	-.4643	5.79686	.937	-12.3031	11.3745	
	400	.7543	5.79686	.897	-11.0845	12.5931	
	500	1.2571	5.79686	.830	-10.5816	13.0959	
	600	5.2286	5.79686	.374	-6.6102	17.0673	
	700	3.9200	5.79686	.504	-7.9188	15.7588	
LSD	CFP	.4643	5.79686	.937	-11.3745	12.3031	
	400	1.2186	5.79686	.835	-10.6202	13.0573	
	300	500	1.7214	5.79686	.769	-10.1173	13.5602
	600	5.6929	5.79686	.334	-6.1459	17.5316	
	700	4.3843	5.79686	.455	-7.4545	16.2231	
400	CFP	-.7543	5.79686	.897	-12.5931	11.0845	
	300	-1.2186	5.79686	.835	-13.0573	10.6202	
	500	.5029	5.79686	.931	-11.3359	12.3416	
	600	4.4743	5.79686	.446	-7.3645	16.3131	
	700	3.1657	5.79686	.589	-8.6731	15.0045	
500	CFP	-1.2571	5.79686	.830	-13.0959	10.5816	
	300	-1.7214	5.79686	.769	-13.5602	10.1173	
	400	-.5029	5.79686	.931	-12.3416	11.3359	
	600	3.9714	5.79686	.499	-7.8673	15.8102	
	700	2.6629	5.79686	.649	-9.1759	14.5016	

	CFP	-5.2286	5.79686	.374	-17.0673	6.6102
	300	-5.6929	5.79686	.334	-17.5316	6.1459
600	400	-4.4743	5.79686	.446	-16.3131	7.3645
	500	-3.9714	5.79686	.499	-15.8102	7.8673
	700	-1.3086	5.79686	.823	-13.1473	10.5302
	CFP	-3.9200	5.79686	.504	-15.7588	7.9188
	300	-4.3843	5.79686	.455	-16.2231	7.4545
700	400	-3.1657	5.79686	.589	-15.0045	8.6731
	500	-2.6629	5.79686	.649	-14.5016	9.1759
	600	1.3086	5.79686	.823	-10.5302	13.1473

Based on observed means.

The error term is Mean Square (Error) = 117.613.

Homogeneous Subsets

Yield

Sample	N	Subset
		1
600	7	86.5743
700	7	87.8829
500	7	90.5457
Duncan ^{a,b} 400	7	91.0486
CFP	7	91.8029
300	7	92.2671
Sig.		.397

Means for groups in homogeneous subsets are displayed.

Based on observed means.

The error term is Mean Square (Error) = 117.613.

a. Uses Harmonic Mean Sample Size = 7.000.

b. Alpha = .05.

H₀: *There is no significant difference in the chemical sorption behaviours of composites filled with treated coconut fibre at the varying carbonisation temperatures.*

Regression

Descriptive Statistics

	Mean	Std. Deviation	N
Carbonisation Temperature (oC)	422.0000	237.70570	6
Hexane (%)	460.3333	48.99660	6
Xylene (%)	470.1667	39.28571	6
Toluene (%)	401.0000	62.74074	6
Benzene (%)	230.8333	45.90606	6

Correlations

		Carbonisation Temperature (oC)	Hexane (%)	Xylene (%)
Pearson Correlation	Carbonisation Temperature (oC)	1.000	-.937	-.932
	Hexane (%)	-.937	1.000	.924
	Xylene (%)	-.932	.924	1.000
	Toluene (%)	-.917	.967	.892
	Benzene (%)	-.953	.902	.820
Sig. (1-tailed)	Carbonisation Temperature (oC)	.	.003	.003
	Hexane (%)	.003	.	.004
	Xylene (%)	.003	.004	.

N	Toluene (%)	.005	.001	.008
	Benzene (%)	.002	.007	.023
	Carbonisation Temperature (oC)	6	6	6
	Hexane (%)	6	6	6
	Xylene (%)	6	6	6
	Toluene (%)	6	6	6
	Benzene (%)	6	6	6

Correlations

		Toluene (%)	Benzene (%)
Pearson Correlation	Carbonisation Temperature (oC)	-.917	-.953
	Hexane (%)	.967	.902
	Xylene (%)	.892	.820
	Toluene (%)	1.000	.938
	Benzene (%)	.938	1.000
Sig. (1-tailed)	Carbonisation Temperature (oC)	.005	.002
	Hexane (%)	.001	.007
	Xylene (%)	.008	.023
	Toluene (%)	.	.003
	Benzene (%)	.003	.
N	Carbonisation Temperature (oC)	6	6
	Hexane (%)	6	6
	Xylene (%)	6	6
	Toluene (%)	6	6
	Benzene (%)	6	6

Variables Entered/Removed

Model	Variables Entered	Variables Removed	Method
1	Benzene (%), Xylene (%), Hexane (%), Toluene (%) ^b	.	Enter

a. Dependent Variable: Carbonisation Temperature (°C)

b. All requested variables entered.

Model Summary

Model	R	R Square	Adjusted R Square	Std. Error of the Estimate	Change Statistics		
					R Square Change	F Change	df1
1	.999 ^a	.998	.989	24.70458	.998	115.477	4

Model Summary

Model	Change Statistics	
	df2	Sig. F Change
1	1 ^a	.070

a. Predictors: (Constant), Benzene (%), Xylene (%), Hexane (%), Toluene (%)

ANOVA^a

Model		Sum of Squares	df	Mean Square	F	Sig.
1	Regression	281909.684	4	70477.421	115.477	.070 ^b
	Residual	610.316	1	610.316		
	Total	282520.000	5			

a. Dependent Variable: Carbonisation Temperature (oC)

b. Predictors: (Constant), Benzene (%), Xylene (%), Hexane (%), Toluene (%)

Coefficients^a

Model		Unstandardised Coefficients		Standardised Coefficients	t	Sig.
		B	Std. Error	Beta		
1	(Constant)	2664.926	182.791		14.579	.044
	Hexane (%)	-1.673	1.037	-.345	-1.613	.353
	Xylene (%)	-3.180	.737	-.526	-4.318	.145
	Toluene (%)	2.614	.860	.690	3.038	.202
	Benzene (%)	-4.443	.698	-.858	-6.365	.099

a. Dependent Variable: Carbonisation Temperature (oC)

Decisions: Since $F_{cal} > F_{tab}$ in both hypothesis 1 and hypothesis 2 and in all their variances, we therefore accept ***H1***: *The Physico-mechanical properties changes and Chemical sorption properties leading to product reinforcements in the fibre filled formulation as carbonisation treatment at the evaluated varying temperatures were therefore significant.*

Appendix XXVIII

Predictive Analysis and Statistical Modelled Chart for the Mechanical and Chemical Sorption Properties of the Optimised Coconut Shell Composites used in Model Productions

Analysis of Variance Coconut Shell

H₀: *There is no significant difference in the Physico-mechanical properties of composites filled with coconut shell treated at the various carbonisation temperatures.*

Between-Subjects Factors

	Value Label	N
Properties	1.00 Hardness(shore A)	7
	2.00 Abrasion Resistance	7
	3.00 Compression set (%)	7
	4.00 Tensile Strength (MPa)	7
	5.00 Elongation Compression set break (%)	7
	6.00 Modulus (%)	7
	7.00 Flexural Strength (MPa)	7
Sample	1.00 CSP	7
	2.00 300	7
	3.00 400	7
	4.00 500	7
	5.00 600	7

6.00	700	7
7.00	CB(N330)	7

Descriptive Statistics

Dependent Variable: Yield

Properties	Sample	Mean	Std. Deviation	N
Hardness(shore A)	CSP	73.0000	.	1
	300	75.0000	.	1
	400	78.0000	.	1
	500	86.0000	.	1
	600	80.0000	.	1
	700	76.0000	.	1
	CB(N330)	91.0000	.	1
	Total	79.8571	6.46603	7
Abrasion Resistance	CSP	22.5100	.	1
	300	28.4200	.	1
	400	32.1000	.	1
	500	36.9000	.	1
	600	44.8400	.	1
	700	37.4200	.	1
	CB(N330)	48.6300	.	1
	Total	35.8314	9.08237	7
Compression set (%)	CSP	28.9000	.	1
	300	26.4000	.	1
	400	24.8000	.	1

	500	22.3000	.	1
	600	23.0000	.	1
	700	23.2000	.	1
	CB(N330)	10.2000	.	1
	Total	22.6857	5.96222	7
	CSP	3.9100	.	1
	300	4.2100	.	1
	400	4.3000	.	1
	500	5.2000	.	1
Tensile Strength (MPa)	600	4.9000	.	1
	700	4.8000	.	1
	CB(N330)	6.9600	.	1
	Total	4.8971	1.01322	7

Descriptive Statistics

Dependent Variable: Yield

Properties	Sample	Mean	Std. Deviation	N
Elongation Compression set break (%)	CSP	494.5000	.	1
	300	484.6000	.	1
	400	420.0000	.	1
	500	398.2000	.	1
	600	395.0000	.	1
	700	398.2000	.	1
	CB(N330)	298.2000	.	1
	Total	412.6714	65.52121	7
Modulus (%)	CSP	1.9200	.	1

	300	3.1000	.	1
	400	4.3500	.	1
	500	5.4000	.	1
	600	5.3800	.	1
	700	5.1200	.	1
	CB(N330)	6.8000	.	1
	Total	4.5814	1.62539	7
	CSP	.9900	.	1
	300	.3900	.	1
	400	.2800	.	1
	500	.4600	.	1
Flexural Strength (MPa)	600	.3800	.	1
	700	.2100	.	1
	CB(N330)	.6800	.	1
	Total	.4843	.26813	7
	CSP	89.3900	180.41023	7
	300	88.8743	176.40098	7
	400	80.5471	152.07018	7
	500	79.2086	143.73388	7
Total	600	79.0714	142.15701	7
	700	77.8500	143.70263	7
	CB(N330)	66.0671	107.40440	7
	Total	80.1441	141.54205	49

Tests of Between-Subjects Effects

Dependent Variable: Yield

Source	Type I Sum of Squares	df	Mean Square	F	Sig.
Corrected Model	937470.857 ^a	12	78122.571	116.367	.000
Intercept	314730.617	1	314730.617	468.805	.000
Properties	934899.654	6	155816.609	232.095	.000
Samples	2571.203	6	428.534	.638	.699
Error	24168.496	36	671.347		
Total	1276369.970	49			
Corrected Total	961639.353	48			

a. R Squared = .975 (Adjusted R Squared = .966)

Estimated Marginal Means

1. Properties

Dependent Variable: Yield

Properties	Mean	Std. Error	95% Confidence Interval	
			Lower Bound	Upper Bound
Hardness(shore A)	79.857	9.793	59.996	99.719
Abrasion Resistance	35.831	9.793	15.970	55.693
Compression set(%)	22.686	9.793	2.824	42.547
Tensile Strength (Mpa)	4.897	9.793	-14.964	24.759
Elongation Compression set break (%)	412.671	9.793	392.810	432.533
Modulus (%)	4.581	9.793	-15.280	24.443
Flexural Strength (Mpa)	.484	9.793	-19.377	20.346

2. Sample

Dependent Variable: Yield

Sample	Mean	Std. Error	95% Confidence Interval	
			Lower Bound	Upper Bound
CSP	89.390	9.793	69.528	109.252
300	88.874	9.793	69.013	108.736
400	80.547	9.793	60.686	100.409
500	79.209	9.793	59.347	99.070
600	79.071	9.793	59.210	98.933
700	77.850	9.793	57.988	97.712
CB(N330)	66.067	9.793	46.206	85.929

Post Hoc Tests

Properties

Multiple Comparisons

Dependent Variable: Yield

(I) Properties	(J) Properties	Mean Difference (I-J)	Std. Error	Sig.
LSD Hardness(shore A)	Abrasion Resistance	44.0257 [*]	13.84967	.003
	Compression set (%)	57.1714 [*]	13.84967	.000
	Tensile Strength (MPa)	74.9600 [*]	13.84967	.000
	Elongation Compression set break (%)	-332.8143 [*]	13.84967	.000
	Modulus (%)	75.2757 [*]	13.84967	.000
	Flexural Strength (MPa)	79.3729 [*]	13.84967	.000

	Hardness(shore A)	-44.0257 ⁺	13.84967	.003
	Compression set (%)	13.1457	13.84967	.349
	Tensile Strength (MPa)	30.9343 ⁺	13.84967	.032
Abrasion Resistance	Elongation Compression set break (%)	-376.8400 ⁺	13.84967	.000
	Modulus (%)	31.2500 ⁺	13.84967	.030
	Flexural Strength (MPa)	35.3471 ⁺	13.84967	.015
	Hardness(shore A)	-57.1714 ⁺	13.84967	.000
	Abrasion Resistance	-13.1457	13.84967	.349
	Tensile Strength (MPa)	17.7886	13.84967	.207
Compression set (%)	Elongation Compression set break (%)	-389.9857 ⁺	13.84967	.000
	Modulus (%)	18.1043	13.84967	.199
	Flexural Strength (MPa)	22.2014	13.84967	.118
	Hardness(shore A)	-74.9600 ⁺	13.84967	.000
	Abrasion Resistance	-30.9343 ⁺	13.84967	.032
	Compression set (%)	-17.7886	13.84967	.207
Tensile Strength (MPa)	Elongation Compression set break (%)	-407.7743 ⁺	13.84967	.000
	Modulus (%)	.3157	13.84967	.982
	Flexural Strength (MPa)	4.4129	13.84967	.752
	Hardness(shore A)	332.8143 ⁺	13.84967	.000
Elongation Compression set break (%)	Abrasion Resistance	376.8400 ⁺	13.84967	.000
	Compression set (%)	389.9857 ⁺	13.84967	.000

Multiple Comparisons

Dependent Variable: Yield

(I) Properties	(J) Properties	95% Confidence Interval		
		Lower Bound	Upper Bound	
Hardness(shore A)	Abrasion Resistance	15.9373*	72.1142	
	Compression set (%)	29.0830*	85.2599	
	Tensile Strength (MPa)	46.8716*	103.0484	
	Elongation Compression set break (%)	-360.9027*	-304.7258	
	Modulus (%)	47.1873*	103.3642	
	Flexural Strength (MPa)	51.2844*	107.4613	
	Hardness(shore A)	-72.1142*	-15.9373	
	Compression set (%)	-14.9427	41.2342	
	Tensile Strength (MPa)	2.8458*	59.0227	
	LSD Abrasion Resistance	Elongation Compression set break (%)	-404.9284*	-348.7516
Modulus (%)		3.1616*	59.3384	
Flexural Strength (MPa)		7.2587*	63.4356	
Hardness(shore A)		-85.2599*	-29.0830	
Abrasion Resistance		-41.2342	14.9427	
Tensile Strength (MPa)		-10.2999	45.8770	
Compression set (%)		Elongation Compression set break (%)	-418.0742*	-361.8973
		Modulus (%)	-9.9842	46.1927
		Flexural Strength (MPa)	-5.8870	50.2899

	Hardness(shore A)	-103.0484*	-46.8716
	Abrasion Resistance	-59.0227*	-2.8458
	Compression set (%)	-45.8770	10.2999
Tensile Strength (MPa)	Elongation Compression set break (%)	-435.8627*	-379.6858
	Modulus (%)	-27.7727	28.4042
	Flexural Strength (MPa)	-23.6756	32.5013
	Hardness(shore A)	304.7258*	360.9027
Elongation Compression set break (%)	Abrasion Resistance	348.7516*	404.9284
	Compression set (%)	361.8973*	418.0742

Multiple Comparisons

Dependent Variable: Yield

(I) Properties	(J) Properties	Mean Difference (I-J)	Std. Error	Sig.	
LSD	Elongation Compression set break (%)	Tensile Strength (MPa)	407.7743 ⁺	13.84967	.000
		Modulus (%)	408.0900 ⁺	13.84967	.000
		Flexural Strength (MPa)	412.1871 ⁺	13.84967	.000
		Hardness(shore A)	-75.2757 ⁺	13.84967	.000
		Abrasion Resistance	-31.2500 ⁺	13.84967	.030
		Compression set (%)	-18.1043 ⁺	13.84967	.199
Modulus (%)	Tensile Strength (MPa)		-.3157 ⁺	13.84967	.982
		Elongation Compression set break (%)	-408.0900	13.84967	.000
		Flexural Strength (MPa)	4.0971 ⁺	13.84967	.769
Flexural Strength (MPa)	Hardness(shore A)	-79.3729 ⁺	13.84967	.000	

	Abrasion Resistance	-35.3471*	13.84967	.015
	Compression set (%)	-22.2014*	13.84967	.118
	Tensile Strength (MPa)	-4.4129*	13.84967	.752
	Elongation Compression set break (%)	-412.1871	13.84967	.000
	Modulus (%)	-4.0971	13.84967	.769

Multiple Comparisons

Dependent Variable: Yield

(I) Properties		(J) Properties	95% Confidence Interval	
			Lower Bound	Upper Bound
LSD	Elongation Compression set break (%)	Tensile Strength (MPa)	379.6858*	435.8627
		Modulus (%)	380.0016*	436.1784
		Flexural Strength (MPa)	384.0987*	440.2756
		Hardness(shore A)	-103.3642*	-47.1873
		Abrasion Resistance	-59.3384*	-3.1616
	Modulus (%)	Compression set (%)	-46.1927*	9.9842
		Tensile Strength (MPa)	-28.4042*	27.7727
		Elongation Compression set break (%)	-436.1784	-380.0016
		Flexural Strength (MPa)	-23.9913*	32.1856
		Hardness(shore A)	-107.4613*	-51.2844
Flexural Strength (MPa)	Abrasion Resistance	-63.4356*	-7.2587	
	Compression set (%)	-50.2899*	5.8870	
	Tensile Strength (MPa)	-32.5013*	23.6756	

	Elongation Compression set break (%)	-440.2756	-384.0987
	Modulus (%)	-32.1856	23.9913

Based on observed means.

The error term is Mean Square (Error) = 671.347.

*. The mean difference is significant at the .05 level.

Homogeneous Subsets

Yield

Properties	N	Subset			
		1	2	3	4
Flexural Strength (MPa)	7	.4843			
Modulus (%)	7	4.5814			
Tensile Strength (MPa)	7	4.8971			
Compression set (%)	7	22.6857	22.6857		
Abrasion Resistance	7		35.8314		
Hardness(shore A)	7			79.8571	
Elongation Compression set break (%)	7				412.6714
Sig.		.152	.349	1.000	1.000

Means for groups in homogeneous subsets are displayed.

Based on observed means.

The error term is Mean Square (Error) = 671.347.

a. Uses Harmonic Mean Sample Size = 7.000.

b. Alpha = .05.

Sample

Multiple Comparisons

Dependent Variable: Yield

(I) Sample	(J) Sample	Mean Difference (I-J)	Std. Error	Sig.	95% Confidence Interval
					Lower Bound
CSP	300	.5157	13.84967	.971	-27.5727
	400	8.8429	13.84967	.527	-19.2456
	500	10.1814	13.84967	.467	-17.9070
	600	10.3186	13.84967	.461	-17.7699
	700	11.5400	13.84967	.410	-16.5484
	CB(N330)	23.3229	13.84967	.101	-4.7656
	CSP	-.5157	13.84967	.971	-28.6042
LSD 300	400	8.3271	13.84967	.551	-19.7613
	500	9.6657	13.84967	.490	-18.4227
	600	9.8029	13.84967	.484	-18.2856
	700	11.0243	13.84967	.431	-17.0642
	CB(N330)	22.8071	13.84967	.108	-5.2813
	CSP	-8.8429	13.84967	.527	-36.9313
	300	-8.3271	13.84967	.551	-36.4156
400	500	1.3386	13.84967	.924	-26.7499
	600	1.4757	13.84967	.916	-26.6127
	700	2.6971	13.84967	.847	-25.3913
	CB(N330)	14.4800	13.84967	.303	-13.6084

500	CSP	-10.1814	13.84967	.467	-38.2699
	300	-9.6657	13.84967	.490	-37.7542
	400	-1.3386	13.84967	.924	-29.4270
	600	.1371	13.84967	.992	-27.9513
	700	1.3586	13.84967	.922	-26.7299
600	CB(N330)	13.1414	13.84967	.349	-14.9470
	CSP	-10.3186	13.84967	.461	-38.4070
	300	-9.8029	13.84967	.484	-37.8913
	400	-1.4757	13.84967	.916	-29.5642
	500	-.1371	13.84967	.992	-28.2256
	700	1.2214	13.84967	.930	-26.8670
	CB(N330)	13.0043	13.84967	.354	-15.0842

Multiple Comparisons

Dependent Variable: Yield

	(I) Sample	(J) Sample	95% Confidence Interval	
			Upper Bound	
LSD	CSP	300		28.6042
		400		36.9313
		500		38.2699
		600		38.4070
		700		39.6284
		CB(N330)		51.4113
		300	CSP	
		400		36.4156

	500	37.7542
	600	37.8913
	700	39.1127
	CB(N330)	50.8956
	CSP	19.2456
	300	19.7613
400	500	29.4270
	600	29.5642
	700	30.7856
	CB(N330)	42.5684
	CSP	17.9070
	300	18.4227
500	400	26.7499
	600	28.2256
	700	29.4470
	CB(N330)	41.2299
	CSP	17.7699
	300	18.2856
600	400	26.6127
	500	27.9513
	700	29.3099
	CB(N330)	41.0927

Multiple Comparisons

Dependent Variable: Yield

(I) Sample	(J) Sample	Mean Difference (I-J)	Std. Error	Sig.	95% Confidence Interval
					Lower Bound
LSD	CSP	-11.5400	13.84967	.410	-39.6284
	300	-11.0243	13.84967	.431	-39.1127
	400	-2.6971	13.84967	.847	-30.7856
	500	-1.3586	13.84967	.922	-29.4470
	600	-1.2214	13.84967	.930	-29.3099
	CB(N330)	11.7829	13.84967	.401	-16.3056
700	CSP	-23.3229	13.84967	.101	-51.4113
	300	-22.8071	13.84967	.108	-50.8956
	400	-14.4800	13.84967	.303	-42.5684
	500	-13.1414	13.84967	.349	-41.2299
	600	-13.0043	13.84967	.354	-41.0927
	700	-11.7829	13.84967	.401	-39.8713
CB(N330)	CSP	-23.3229	13.84967	.101	-51.4113
	300	-22.8071	13.84967	.108	-50.8956
	400	-14.4800	13.84967	.303	-42.5684
	500	-13.1414	13.84967	.349	-41.2299
	600	-13.0043	13.84967	.354	-41.0927
	700	-11.7829	13.84967	.401	-39.8713

Multiple Comparisons

Dependent Variable: Yield

(I) Sample	(J) Sample	95% Confidence Interval
		Upper Bound
LSD	CSP	16.5484
	700	17.0642
	400	25.3913

	500	26.7299
	600	26.8670
	CB(N330)	39.8713
	CSP	4.7656
	300	5.2813
	400	13.6084
CB(N330)	500	14.9470
	600	15.0842
	700	16.3056

Based on observed means.

The error term is Mean Square (Error) = 671.347.

Homogeneous Subsets

Yield

	Sample	N	Subset
			1
Duncan ^{a,b}	CB(N330)	7	66.0671
	700	7	77.8500
	600	7	79.0714
	500	7	79.2086
	400	7	80.5471
	300	7	88.8743
	CSP	7	89.3900
	Sig.		.153

Means for groups in homogeneous subsets are displayed.

Based on observed means.

The error term is Mean Square (Error) = 671.347.

a. Uses Harmonic Mean Sample Size = 7.000.

b. Alpha = .05.

H₀: *There is no significant difference in the chemical sorption behaviours of composites filled with treated coconut shell at the varying carbonisation temperatures.*

Regression

Descriptive Statistics

	Mean	Std. Deviation	N
Carbonisation Temperature (oC)	422.0000	237.70570	6
Hexane (%)	315.3333	84.64908	6
Xylene (%)	316.0000	79.44558	6
Toluene (%)	328.0000	68.99275	6
Benzene (%)	228.0000	16.54086	6

Correlations

		Carbonisation Temperature (°C)	Hexane (%)	Xylene (%)
Pearson Correlation	Carbonisation Temperature (oC)	1.000	-.959	-.910
	Hexane (%)	-.959	1.000	.977

	Xylene (%)	-0.910	.977	1.000
	Toluene (%)	-0.915	.986	.996
	Benzene (%)	-0.924	.901	.886
	Carbonisation Temperature (°C)	.	.001	.006
	Hexane (%)	.001	.	.000
Sig. (1-tailed)	Xylene (%)	.006	.000	.
	Toluene (%)	.005	.000	.000
	Benzene (%)	.004	.007	.009
	Carbonisation Temperature (°C)	6	6	6
	Hexane (%)	6	6	6
N	Xylene (%)	6	6	6
	Toluene (%)	6	6	6
	Benzene (%)	6	6	6

Correlations

		Toluene (%)	Benzene (%)
	Carbonisation Temperature (°C)	-0.915	-0.924
	Hexane (%)	.986	.901
Pearson Correlation	Xylene (%)	.996	.886
	Toluene (%)	1.000	.880
	Benzene (%)	.880	1.000
	Carbonisation Temperature (°C)	.005	.004
Sig. (1-tailed)	Hexane (%)	.000	.007
	Xylene (%)	.000	.009

N	Toluene (%)	.	.010
	Benzene (%)	.010	.
	Carbonisation Temperature (°C)	6	6
	Hexane (%)	6	6
	Xylene (%)	6	6
	Toluene (%)	6	6
	Benzene (%)	6	6

Variables Entered/Removed^a

Model	Variables Entered	Variables Removed	Method
1	Benzene (%), Toluene (%), Hexane (%), Xylene (%) ^b	.	Enter

a. Dependent Variable: Carbonisation Temperature (°C)

b. All requested variables entered.

Model Summary

Model	R	R Square	Adjusted R Square	Std. Error of the Estimate	Change Statistics		
					R Square Change	F Change	df1
1	.986 ^a	.973	.863	88.02217	.973	8.866	4

Model Summary

Model	Change Statistics	
	df2	Sig. F Change
1	1 ^a	.246

a. Predictors: (Constant), Benzene (%), Toluene (%), Hexane (%), Xylene (%)

ANOVA^a

Model		Sum of Squares	Df	Mean Square	F	Sig.
1	Regression	274772.098	4	68693.024	8.866	.246 ^b
	Residual	7747.902	1	7747.902		
	Total	282520.000	5			

a. Dependent Variable: Carbonisation Temperature (°C)

b. Predictors: (Constant), Benzene (%), Toluene (%), Hexane (%), Xylene (%)

Coefficients^a

Model		Unstandardised Coefficients		Standardised Coefficients	t	Sig.
		B	Std. Error	Beta		
1	(Constant)	1308.959	1395.745		.938	.520
	Hexane (%)	-5.536	3.518	-1.971	-1.573	.360
	Xylene (%)	-2.630	6.702	-.879	-.392	.762
	Toluene (%)	7.176	9.871	2.083	.727	.600
	Benzene (%)	-2.911	6.076	-.203	-.479	.716

a. Dependent Variable: Carbonisation Temperature (°C)

Decisions: Since $F_{cal} > F_{tab}$ in both hypothesis 1 and hypothesis 2 and in all their variances, we therefore accept ***H1: The Physico-mechanical properties changes and Chemical sorption properties leading to product reinforcements in the shell filled formulation as carbonisation treatment at the evaluated varying temperatures were therefore significant.***

PUBLICATIONS

1. Momoh, F.P.; Mamza, P.A.P.; Gimba, C.E. and Nkeonye, P. (2016). Morphological Trends of Modified Coconut Fibre in Natural Rubber Reinforcement. *Journal of Emerging Trends in Engineering and Applied Sciences (JETEAS)* 7(4): 167-172
2. Momoh, F.P.; Mamza, P.A.P.; Gimba, C.E. and Nkeonye, P. (2016). Effects of Carbonization on Coconut Shell as Filler in Natural Rubber Compounding. *Nigerian Journal of Polymer Science and Technology*, (11), PP 115-123
3. Momoh, F.P.; Mamza, P.A.P.; Gimba, C.E. and Nkeonye, P. (2017). Effect of Carbonization Time on the Morphology and Mechanical Properties of Natural Rubber Composites. *International Organization of Scientific Research Journal of Polymer and Textile Engineering*, 4 (2), PP 06-13.
4. Momoh, F.P.; Mamza, P.A.P.; Gimba, C.E. and Nkeonye, P. (2017). Morphology and Crystallinity of Modified Coconut Shell Powder in Natural Rubber Development. *International Journal of Innovative Research and Advanced Studies (IJIRAS)*, (4), PP 257-262.
5. Momoh, F.P.; Mamza, P.A.P.; Gimba, C.E. and Nkeonye, P. (2017). Thermal and Elemental Evaluation of Modified Coconut Shell Fibre in Natural Rubber Reinforcement. *International Journal of Engineering Research and Technology (IJERT)*, 6 (04), PP 663-669.